Research Bank
PhD Thesis

The effects of disrupting AMPK-glycogen binding in mice on glucose homeostasis, glycogen dynamics and exercise metabolism

Janzen, Natalie R.

Janzen, N. R. (2022). The effects of disrupting AMPK-glycogen binding in mice on glucose homeostasis, glycogen dynamics and exercise metabolism [PhD Thesis]. Australian Catholic University. https://doi.org/10.26199/acu.8xzw5

This work © 2021 by Natalie R. Janzen is licensed under Creative Commons Attribution 4.0 International

AUSTRALIAN CATHOLIC UNIVERSITY

The effects of disrupting AMPK-glycogen binding in mice on glucose homeostasis, glycogen dynamics and exercise metabolism

Submitted by:

Natalie R. Janzen

BSc, MSc

A thesis submitted in fulfilment of the requirements of the degree of

Doctor of Philosophy

Ph.D. with Publication

Exercise and Nutrition Research Program

Mary MacKillop Institute for Health Research

Australian Catholic University

Melbourne, Victoria, Australia

September 2021

© Copyright by Natalie Janzen

Statement of Authorship and Sources

This thesis contains no material that has been extracted in whole or in part from a thesis that I have submitted towards the award of any other degree or diploma in any other tertiary institution.

No other person's work has been used without due acknowledgement in the main text of the thesis.

All research procedures reported in the thesis received the approval of the relevant Ethics/Safety Committees (where required).

The extent of collaboration with another person or persons has been acknowledged accordingly where necessary.

Signed: [redacted]

Natalie Janzen Date: 08/09/2021

Acknowledgements

First and foremost, I would like to thank my supervisory team – Dr Nolan Hoffman, Prof John Hawley, and Dr Jamie Whitfield – for giving me the opportunity to take on this research at ACU. Thank you for your patience and for your support and presence throughout my PhD journey. I am deeply grateful for the time and resources that you have invested in me and I have gained so much from your mentorship over the last four years.

Thank you to the past and present members of the Exercise and Nutrition Research Program for creating a fun, supportive and collaborative work environment. A special thank you to Mr Mehdi Belhaj for your constant positive energy and your willingness to help.

I would like to thank all the collaborators whose contributions and generous support have made this thesis possible. I would like to thank everyone at SVI, especially Prof Bruce Kemp and Ms Lisa Murray-Segal, for all of their contributions to the studies in this thesis. From feedback during lab meetings to random hallway chats, your insights have improved the projects and helped me become a better researcher. Thank you to Prof Sean McGee at Deakin for your input on study design and your assistance with the exercise calorimetry experiments.

I would like to thank the assessors for my candidature milestones – Dr Magda Montgomery, Prof Sean McGee, Dr Chris Shaw, and Dr Kim Loh – for their time invested in evaluating my research progress and for their insights that have guided and improved the studies in this thesis.

Finally, my deepest thanks to the friends and family who have made Melbourne home. Your friendship has been invaluable and I love you all.

Life's roughest storms prove the strength of your anchor.

Contents

Statement of Authorship and Sources iii

Acknowledgements v

Contents vii

List of Publications Resulting from Candidature xv

Conference Proceedings xvii

List of Figures xix

List of Tables xxiii

List of Abbreviations xxv

Abstract 1

Chapter 1 Introduction and Overview 5

Chapter 2 Literature Review 9

- 2.1 Abstract 11
- 2.2 Introduction 15
- 2.3 Roles for AMPK and Glycogen in Metabolism 16
  - *2.3.1 AMPK Activation and Signalling* 16
  - *2.3.2 Roles for AMPK in Glucose Uptake* 19
  - *2.3.3 Roles for AMPK in Glycogen Synthesis* 22
  - *2.3.4 Roles for AMPK in Fat Metabolism* 23
  - *2.3.5 Roles for AMPK in Acute Responses to Exercise* 24
  - *2.3.6 Roles for AMPK in Adaptations to Exercise* 27
  - *2.3.7 The AMPK β Subunit and Carbohydrate Binding Module* 29
  - *2.3.8 Glycogen Dynamics* 30

2.3.9 Glycogen Localisation 31

2.3.10 Skeletal Muscle Glycogen Utilisation and Synthesis 33

2.3.11 Hepatic Glycogen Utilisation and Synthesis 36

2.4 Molecular Evidence of AMPK-Glycogen Binding 39

2.5 Regulation of Cellular Energy Sensing by AMPK-Glycogen Binding 41

2.6 Linking AMPK and Glycogen to Exercise Metabolism in Physiological Settings 43

2.6.1 Regulation of Glycogen Storage by AMPK 43

2.6.2 Roles for Glycogen Availability in the Regulation of AMPK Activity .. 46

2.6.3 Metabolic Diseases as Models to Investigate AMPK-Glycogen Binding 48

2.7 Multidisciplinary Techniques and Models to Interrogate Roles for AMPK-Glycogen Interactions 51

2.8 Potential Therapeutic Relevance of Targeting AMPK-Glycogen Binding.......... 54

2.9 Isoform-Specific Consequences of KI Mutations to Disrupt AMPK-Glycogen Binding 56

2.10 Conclusions 58

Chapter 3 Methodology and Design 61

3.1 Study 1 – Phenotypic Effects of the AMPK DKI Mutation on Whole-Body and Tissue Metabolism 61

3.1.1 Animal Models 61

3.1.2 Whole-Body Composition Measurements 63

3.1.3 Metabolic Caging 63

3.1.4 Intraperitoneal Glucose Tolerance and Insulin Tolerance Testing 64

3.1.5 Fasting and Refeeding Protocol 64
3.1.6 Serum Analysis 66
3.1.7 Assessment of Tissue Glycogen Content 66
3.1.8 Immunoblotting 67
3.1.9 RNA Extraction and Gene Expression Analysis 68
3.1.10 Statistical Analyses 69
3.2 Study 2 – Phenotypic Effects of the AMPK DKI Mutation on Exercise Capacity and Substrate Utilisation 70
3.2.1 Animal Models 70
3.2.2 Maximal Running Speed and Time to Exhaustion 71
3.2.3 Exercise Calorimetry 73
3.2.4 Serum Analysis 74
3.2.5 Assessment of Tissue Glycogen Content 74
3.2.6 Immunoblotting 75
3.2.7 Statistical Analyses 79
Chapter 4 Study 1 – Phenotypic Effects of the AMPK DKI Mutation on Whole-Body and Tissue Metabolism 81
4.1 Abstract 87
4.2 Introduction 89
4.3 Results 91
4.3.1 DKI Mice Display Increased Body Mass Associated with Increased Adiposity 91
4.3.2 DKI Mice Have Reduced Voluntary Physical Activity, Increased Rates of CHO Oxidation, and Reduced Rates of Fat Oxidation 93

4.3.3 DKI Mice Display Hyperinsulinemia and Glucose Intolerance but Normal Whole-Body Insulin Sensitivity 95

4.3.4 DKI Mice Have Decreased Voluntary Ambulatory Activity and Decreased Rates of Fat Oxidation during Overnight Fasting 97

4.3.5 DKI Mice Display Reduced Liver Glycogen Concentration in the Fed State and Altered Fasting-Induced Skeletal Muscle Glycogen Depletion 99

4.3.6 Liver and Muscle from DKI Mice Display No Changes in Glycogen Associated Proteins Relative to WT 102

4.3.7 DKI Mice Have Intact AMPK and ACC Phosphorylation in Liver and Skeletal Muscle 104

4.3.8 DKI Mice Have Reduced AMPK Protein Content in Liver and Skeletal Muscle 106

4.4 Discussion 107

4.5 Materials and Methods 115

4.5.1 Animal Models 115

4.5.2 Whole-Body Composition Measurements 116

4.5.3 Metabolic Caging 116

4.5.4 Intraperitoneal Glucose Tolerance and Insulin Tolerance Testing 116

4.5.5 Fasting and Refeeding Protocol 117

4.5.6 Serum Analysis 117

4.5.7 Assessment of Tissue Glycogen Content 117

4.5.8 Immunoblotting 118

4.5.9 RNA Extraction and Gene Expression Analysis 120

4.5.10 Statistical Analyses 121

4.6 Supplementary Material 122

Chapter 5 Linking Chapter 125

Chapter 6 Study 2 – Phenotypic Effects of the AMPK DKI Mutation on Exercise Capacity and Substrate Utilisation During Exercise... 127

6.1 Abstract.. 133

6.2 Introduction 135

6.3 Results 137

6.3.1 DKI Mice Have Reduced Maximal Running Speed 137

6.3.2 DKI Mice Display Increased CHO Utilisation During Submaximal Exercise 137

6.3.3 DKI Mice Have Similar Changes in Circulating Substrates in Response to a Maximal Running Test.. 139

6.3.4 DKI Mice Have Similar Changes in Tissue Glycogen Levels Compared to WT in Response to a Maximal Running Test Despite Less Total Running Time 140

6.3.5 Altered Patterns of Substrate Utilisation in DKI Mice Are Not Due to Changes in GLUT4, CPT1b or Mitochondrial Protein Content in Skeletal Muscle... 144

6.3.6 DKI Mutation Reduces Skeletal Muscle AMPK α and β2 Content But Does Not Impair Relative AMPK Phosphorylation and Downstream Signalling in Response to a Maximal Running Test 146

6.4 Discussion... 148

6.5 Materials and Methods 155

6.5.1 Animal Models 155

6.5.2 Maximal Running Speed and Time to Exhaustion 155

6.5.3. Exercise Calorimetry 157

6.5.4 Serum Analysis 157

6.5.5 Tissue Glycogen Analysis 158

6.5.6 Tissue Protein Analyses 158

6.5.7 Statistical Analyses 159

Chapter 7 Discussion and Conclusion 163

7.1 Introduction 163

7.2 Substrate Utilisation and Whole-Body Composition 166

7.2.1 Fed and Resting Substrate Oxidation and Adiposity 166

7.2.2 Substrate Oxidation in the Fasted State 167

7.2.3 Potential Consequences of the DKI Mutation on Fat Metabolism 168

7.3 Whole-Body Glucose Metabolism 170

7.3.1 Maintenance of Blood Glucose Levels 170

7.3.2 Insulin Sensitivity and Peripheral Glucose Disposal 172

7.3.3 Contraction-Stimulated Glucose Uptake 173

7.4 Exercise Capacity and Rates of Substrate Utilisation 174

7.5 Tissue Glycogen Dynamics 177

7.5.1 Fed and Fasting Liver Glycogen 177

7.5.2 Liver Glycogen Utilisation During Exercise 177

7.5.3 Skeletal Muscle Glycogen Use in Response to Fasting and Synthesis Following Recovery 179

7.5.4 Correlation of Maximal Running Speed and Skeletal Muscle Glycogen Utilisation 180

7.5.5 Characterising Potential Changes in Glycogen Localisation in DKI Mice 181

7.6 Potential Mechanisms for Reduced AMPK Content in DKI Mice 182

7.7 Conclusion 183

Chapter 8 References 185

Chapter 9 Appendices 219

9.1 List of Publications 219

9.2 The Research Portfolio Appendix 221

List of Publications Resulting from Candidature

- **Janzen, NR**, Whitfield, J, & Hoffman, NJ (2018). Interactive Roles for AMPK and Glycogen from Cellular Energy Sensing to Exercise Metabolism. *Int J Mol Sci*, 19(11). doi:10.3390/ijms19113344.
- **Janzen NR**, Whitfield J, Murray-Segal L, Kemp BE, Hawley JA, Hoffman NJ (2021). Mice with Whole-Body Disruption of AMPK-Glycogen Binding Have Increased Adiposity, Reduced Fat Oxidation and Altered Tissue Glycogen Dynamics. *Int J Mol Sci,* 22(17). doi:10.3390/ijms22179616.
- **Janzen NR**, Whitfield J, Murray-Segal L, Kemp BE, Hawley JA, Hoffman NJ (2022). Disrupting AMPK-Glycogen Binding in Mice Increases Carbohydrate Utilisation and Reduces Exercise Capacity. *Front Physiol*, 13:859246. doi:10.3389/fphys.2022.859246.

Conference Proceedings

- "Loss of AMPK-glycogen binding increases total body mass and adiposity associated with hyperinsulinemia and reductions in tissue AMPK content." Australian and New Zealand Obesity Society Annual Meeting (2019). *Poster presentation*.
- "Whole-body disruption of AMPK-glycogen binding increases adiposity and alters liver and skeletal muscle glycogen dynamics via reductions in AMPK content." Victorian Muscle Network Symposium (2020). *Invited oral presentation*.
- "Roles for AMPK-glycogen interactions in exercise capacity and fuel utilisation" 11th Asian Congress on Kinesiology (2021). *Invited oral presentation*.

List of Figures

Figure 1.1 – Acute activation of AMPK in tissues such as skeletal muscle via changes in cellular adenylate charges occuring during energy stress 6

Figure 2.1 – Graphical abstract overviewing current evidence in the literature involving AMPK-glycogen interactions from *in vitro* to *in vivo* studies.. 13

Figure 2.2 – AMPK is a heterotrimeric protein, consisting of a catalytic α subunit, and regulatory β and γ subunits.. 17

Figure 2.3 – Schematic highlighting some of AMPK's substrates and several physiological processes that are linked to AMPK signalling.. 18

Figure 2.4 – Schematic of the signalling mechanisms underlying skeletal muscle glucose uptake.. 20

Figure 2.5 – Proposed mechanism by which increased AMPK activation results in increased glycogen synthesis.. 23

Figure 2.6 – Several proteins involved in regulation of glycogen particle formation and breakdown 31

Figure 2.7 – Schematic representing some of the pathways regulating hepatic glycogen synthesis and breakdown.. 37

Figure 2.8 – Several potential alterations in cellular metabolism and signalling as a consequence of dysregulated AMPK-glycogen interactions.. 47

Figure 2.9 – Summary of findings in single AMPK β subunit isoform knock-in mice with disrupted AMPK-glycogen binding in either the β1 or β2 isoform 57

Figure 3.1 – DKI mouse models with chronic whole-body disruption of AMPK-glycogen binding.. 62

Figure 3.2 – Fasting-induced glycogen depletion and repletion protocol 65

Figure 3.3 – Schematic of exercise testing protocols utilised in Study 2 73

Figure 4.1 – Graphical abstract summarising key findings from Study 1 85

Figure 4.2 – The AMPK DKI mutation utilised to disrupt whole-body AMPK-glycogen binding is associated with increased body mass and adiposity 92

Figure 4.3 – DKI mice have reduced voluntary activity and reduced rates of fat oxidation 95

Figure 4.4 – DKI mice are glucose intolerant but maintain whole-body insulin sensitivity. 97

Figure 4.5 – DKI mice have reduced voluntary activity and rates of fat oxidation during overnight fasting 99

Figure 4.6 – DKI mice display reduced hepatic glycogen concentration in the fed state and increased skeletal muscle glycogen utilisation in response to fasting 101

Figure 4.7 – Liver and skeletal muscle from DKI mice display no alterations in content of glycogen associated proteins... 104

Figure 4.8 – DKI mice have intact AMPK-ACC signalling but reduced AMPK content in liver and skeletal muscle 106

Figure 4.9 – DKI mice display no differences in liver *Prkab1* or muscle *Prkab2* gene expression versus WT, and DKI adipose tissue displays reduced AMPK content............. 122

Figure 6.1 – Graphical abstract summarising key findings from Study 2 131

Figure 6.2 – The AMPK DKI mutation used to disrupt whole-body AMPK-glycogen binding in mice reduces maximal treadmill running speed but does not alter endurance capacity .. 137

Figure 6.3 – DKI mice have increased respiratory exchange ratio and carbohydrate oxidation rates during exercise calorimetry experiments.. 138

Figure 6.4 – DKI and WT mice have similar circulating glucose, lactate, and non-esterified fatty acid levels following a maximal running test 140

Figure 6.5 – DKI and WT mice display similar changes in liver and skeletal muscle glycogen following a maximal running test 141

Figure 6.6 – Maximal running speed is positively correlated with skeletal muscle glycogen utilisation following maximal running in WT but not DKI mice 143

Figure 6.7 – DKI mouse skeletal muscle displays similar content of proteins associated with glucose uptake and protein markers of mitochondrial content relative to WT 145

Figure 6.8 – DKI mice have reduced skeletal muscle AMPK α and β2 content but intact AMPK, ACC and TBC1D1 signalling in response to a maximal running test versus WT .. 147

Figure 7.1 – Summary of the main findings in DKI mice and future research questions stemming from this thesis 165

List of Tables

Table 2.1 – AMPK β subunit isoform distribution in human and mouse tissues 30

Table 3.1 – Antibodies and protocols used for immunoblotting 77

Table 4.1 – Mass of tissues from male WT and AMPK DKI mice 93

Table 4.2 – Antibodies and protocols used for immunoblotting 119

Table 6.1 – Specifics of the four exercise protocols used and corresponding measures. 156

List of Abbreviations

ACC	Acetyl-CoA carboxylase
ACU	Australian Catholic University
ACURF	Australian Catholic University research funding
ADaM	Allosteric drug and metabolite site
ADP	Adenosine diphosphate
AEC	Animal Ethics Committee
AICAR	5-aminoimidazole-4-carboxamide ribonucleotide
AMP	Adenosine monophosphate
AMPK	AMP-activated protein kinase
ANOVA	Analysis of variance
AS160	Akt substrate of 160 kDa
ATP	Adenosine triphosphate
AUC	Area under the curve
BCA	Bicinchoninic acid method
BMI	Body mass index
CaMKK2	Calcium/calmodulin-dependent protein kinase 2
CBM	Carbohydrate binding module
CBS	Cystathionine-β-synthase domains
CD36	Cluster of differentiation 36
CHO	Carbohydrate
CLAMS	Comprehensive lab animal monitoring system
CPT1b	Carnitine palmitoyltransferase Ib
CST	Cell Signaling Technology
DKI	Double knock-in
EDL	Extensor digitorum longus

FA	Fatty acid
Fatmax	Maximal rate of fat oxidation
FOXO1	Forkhead box protein O1
FRET	Fluorescence resonance energy transfer
G6P	Glucose-6-phosphate
GAM	Anti-mouse IgG, horseradish-peroxidase-conjugated secondary antibody
GAR	Anti-rabbit IgG, horseradish-peroxidase-conjugated secondary antibody
GBE	Glycogen branching enzyme
GDE	Glycogen debranching enzyme
GLUT4	Glucose transporter type 4
GP	Glycogen phosphorylase
GS	Glycogen synthase
GSD	Glycogen storage disease
GSK3β	Glycogen synthase kinase 3β
HMGR	HMG-CoA reductase
IntraMF	Intramyofibrillar
IP	Intraperitoneal
IPGTT	Intraperitoneal glucose tolerance test
IPITT	Intraperitoneal insulin tolerance test
InterMF	Intermyofibrillar
KI	Knock-in
KO	Knockout
LKB1	Liver kinase B1
ND	Nondetectable
NEFA	Non-esterified fatty acid
NHMRC	National Health and Medical Research Council of Australia

OXPHOS	Oxidative phosphorylation
PDK1	3-phosphoinositide-dependent protein kinase 1
PFK	Phosphofructokinase
PGC1α	Peroxisome proliferator-activated receptor gamma coactivator 1-α
PKA	Protein kinase A
PTG	Protein targeting glycogen
qPCR	Quantitative polymerase chain reaction
RER	Respiratory exchange ratio
SEM	Standard error of the mean
SREBP1	Sterol regulatory element-binding protein 1
STBD1	Starch-binding domain-containing protein 1
SS	Subsarcolemmal
TBC1D1	Tre-2, BUB2, CDC16, 1 domain family, member 1
TAG	Triglyceride
TBS-T	Tris-buffered saline containing 0.1% Tween 20
TEE	Total energy expenditure
TEM	Transmission electron microscopy
T2D	Type 2 diabetes
UGP2	UDP-glucose pyrophosphorylase 2
VCO_2	Carbon dioxide production
VO_2	Oxygen consumption
$VO_{2\ max}$	Maximal oxygen consumption
$VO_{2\ peak}$	Peak oxygen consumption
WT	Wild type
ZT	Zeitgeber time

Abstract

Background: The AMP-activated protein kinase (AMPK) is a central regulator of cellular energy balance and metabolism. Many of the health benefits of exercise (e.g., improved insulin sensitivity, increased glucose disposal and fat oxidation) are linked to AMPK. AMPK possesses a regulatory β subunit that binds glycogen, the primary storage form of glucose in liver and skeletal muscle. Based on *in vitro* and *in vivo* findings indicating an inverse relationship between glycogen availability and AMPK activity, AMPK's glycogen-binding capacity has been proposed to serve roles in cellular energy sensing. However, *in vivo* models to test the physiological effects of disrupting AMPK-glycogen binding are limited. Previously, murine models with isoform-specific knock-in mutations to disrupt AMPK-glycogen binding in the β1 or β2 subunit isoform demonstrated increased adiposity, glucose intolerance, decreased maximal exercise capacity, and reductions in AMPK protein content and activity in liver and skeletal muscle. However, the consequences of genetic mutations resulting in whole-body disruption of AMPK-glycogen binding and potential compensatory and/or synergistic roles of the β subunits isoforms' glycogen binding capacity remains unknown. Therefore, AMPK β double knock-in (DKI) mice were generated with mutations in tryptophan residues critical for AMPK-glycogen binding in both the β1 (W100A) and β2 (W98A) subunit isoforms, providing the first *in vivo* model to directly assess the consequences of genetic disruption of whole-body AMPK-glycogen binding *in vivo*. The two experimental chapters described in this thesis aimed to elucidate the phenotypic effects of disrupting AMPK-glycogen interactions via AMPK DKI mutation on 1) whole-body substrate utilisation, glucose homeostasis, and tissue glycogen dynamics; and 2) exercise capacity and whole-body substrate utilisation and tissue metabolism during exercise.

Methods: For Study 1, body composition, metabolic caging, glucose and insulin tolerance, serum hormone and lipid profiles, and fed and fasted tissue glycogen and signalling responses were analysed in chow-fed male AMPK DKI and age-matched wild type (WT) mice. For Study 2, maximal treadmill running speed and endurance capacity were determined. Substrate utilisation during submaximal exercise was calculated using indirect calorimetry. Liver and skeletal muscle glycogen content and skeletal muscle AMPK content and signalling were assessed in WT and DKI mice at rest and following maximally exercise.

Results: AMPK DKI mice displayed increased whole-body fat mass, hyperinsulinemia, and whole-body glucose intolerance associated with inactivity and reduced rates of fat oxidation in the fed and fasted states relative to WT mice. DKI mice had reduced liver glycogen content in the fed state and demonstrated increased utilisation and little repletion of skeletal muscle glycogen in response to fasting and refeeding, respectively, despite similar glycogen synthase phosphorylation and content of glycogen associated proteins relative to WT. Liver, skeletal muscle, and adipose tissue from DKI mice displayed reductions in AMPK protein content but no associated impairments in AMPK or acetyl-CoA carboxylase (ACC) phosphorylation in liver or skeletal muscle in response to fasting and refeeding versus WT. DKI mice had reduced maximal running speed, but similar endurance capacity, compared to WT. During submaximal running, DKI mice displayed increased respiratory exchange ratio and increased rates of carbohydrate oxidation. During maximal treadmill running, DKI mice utilised similar absolute levels of liver and skeletal muscle glycogen compared to WT, despite reduced running time. DKI mice displayed no impairments in AMPK or ACC phosphorylation in skeletal muscle following maximal exercise.

Conclusions: Collectively, these findings determine the phenotypic effects of the AMPK DKI mutation utilised to disrupt whole-body glycogen binding capacity *in vivo* in the regulation of whole-body metabolism, liver and skeletal muscle AMPK content, and tissue glycogen utilisation and synthesis. Specifically, the DKI mutation results in reduced maximal running capacity, and high rates of skeletal muscle glycogen utilisation during maximal running that were associated with reduced skeletal muscle AMPK content. This thesis addresses existing knowledge gaps regarding the physiological consequences of disruption of whole-body AMPK-glycogen binding, suggesting that AMPK-glycogen binding may serve physiological roles in cellular, glycogen-storing tissues, and whole-body energy homeostasis. Furthermore, these studies highlight potential unappreciated roles for AMPK in regulating tissue glycogen dynamics and further expand AMPK's known roles in exercise and metabolism. Collectively, the findings in this thesis have broad implications for whole-body, tissue and cellular energy metabolism and homeostasis.

Chapter 1 Introduction and Overview

Energy balance helps maintain metabolic equilibrium, whereby energy intake from food is balanced with energy expenditure, for example during exercise and fasting. Throughout the world and particularly in Western societies, people are more sedentary, less physically active and eating more, thereby tipping the scales toward energy oversupply. Ultimately, this positive energy balance results in dysregulation of the body's ability to sense energy availability and adequately respond to nutrient oversupply, potentially leading to the development of obesity and metabolic diseases, such as insulin resistance and type 2 diabetes (T2D) (Samuel and Shulman 2012). The epidemic of obesity and associated metabolic diseases has placed a tremendous burden on the economic and healthcare systems worldwide, making an improved understanding and development of novel treatments for these conditions an important area for research. While the effectiveness of exercise in countering metabolic diseases associated with energy oversupply is well appreciated, understanding the cellular pathways and molecular mechanisms by which exercise counters pathophysiology of metabolic diseases remains limited.

Central to energy balance sits a metabolic "switch" called the AMP-activated protein kinase (AMPK), a key regulator of cellular energy homeostasis. In response to acute deficits in energy availability, such as those caused by fasting and exercise, changes in cellular adenylate ratio (i.e., adenosine monophosphate [AMP]:adenosine triphosphate [ATP] and adenosine diphosphate [ADP]:ATP) lead to activation of AMPK (**Figure 1.1**). AMPK then phosphorylates several downstream targets to switch on catabolic pathways, such as glycolysis and fat oxidation, while simultaneously switching off anabolic pathways such as fat and protein synthesis, to help restore energy balance. AMPK is a heterotrimer consisting of a catalytic α subunit and regulatory β and γ subunits. The primary phosphorylation site is located at T172 on the α subunit and is phosphorylated by upstream kinases including liver kinase B1 (LKB1) and calcium/calmodulin-dependent protein kinase kinase β (CAMKK2).

Phosphorylation of T172 is required for AMPK activity and phosphorylation of downstream substrates (Hawley, Davison et al. 1996).

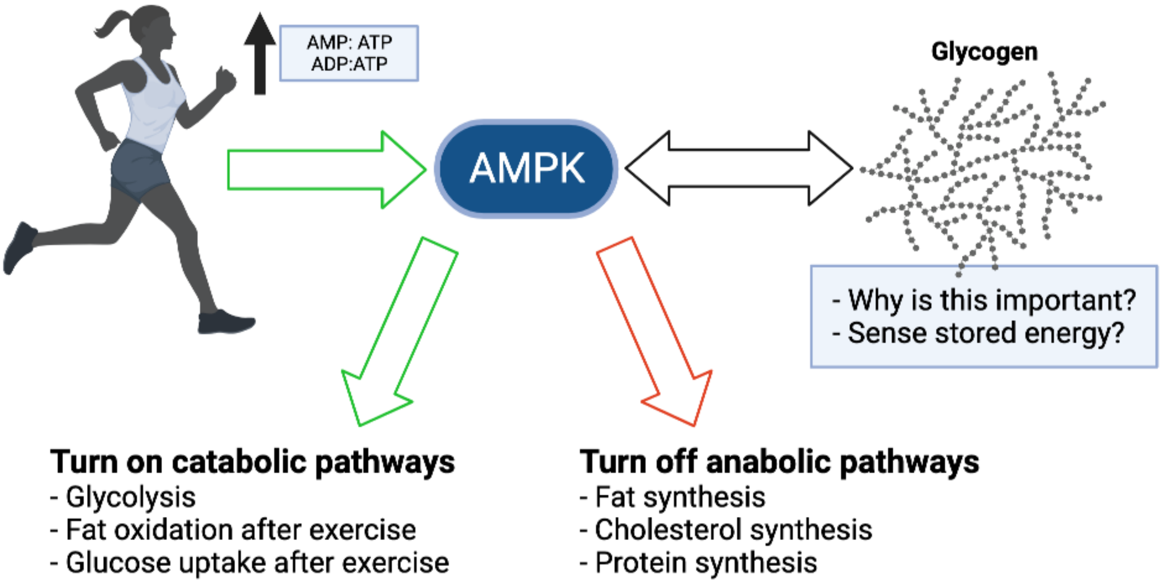
AMP: ATP
ADP:ATP
AMPK
Glycogen
- Why is this important?
- Sense stored energy?
Turn on catabolic pathways
- Glycolysis
- Fat oxidation after exercise
- Glucose uptake after exercise
Turn off anabolic pathways
- Fat synthesis
- Cholesterol synthesis
- Protein synthesis

Figure 1.1 – Acute activation of AMPK in tissues such as skeletal muscle via changes in cellular adenylate charges (i.e., [AMP:ATP] and [ADP:ATP]) occuring during energy stress (e.g. exercise) leads to upregulation of catabolic pathways to promote energy production and inhibition of anabolic pathways to preserve cellular energy availability. AMPK also binds glycogen, the main storage form of glucose. While the physiological roles of these interactions are the topic of current research and warrant further investigation, the prevailing hypothesis is that AMPK-glycogen binding allows AMPK to "sense" available carbohydrate stores. Created with BioRender.com.

In addition to AMPK regulation by various upstream kinases and AMPK's range of downstream substrates regulated by phosphorylation, previous research has established that AMPK binds glycogen via the carbohydrate binding module (CBM) located within the β subunit (Hudson, Pan et al. 2003, Polekhina, Gupta et al. 2003). Glycogen is an important energy substrate and a major contributor to whole-body carbohydrate (CHO) oxidation (Gonzalez, Fuchs et al. 2016). Liver and skeletal muscle are the primary glycogen-storing tissues in mammals; however, glycogen has been detected in a range of other tissues, including adipose tissue (Ceperuelo-Mallafre, Ejarque et al. 2016), brain (Oe, Baba et al. 2016), pancreas

(Brereton, Rohm et al. 2016), and red blood cells (Miwa and Suzuki 2002). AMPK phosphorylates and inhibits glycogen synthase (GS) *in vitro* (Carling and Hardie 1989). AMPK has also been shown to interact with and/or phosphorylate other glycogen-associated proteins, including glycogen phosphorylase (GP) and glycogen debranching enzyme (GDE) (Young, Radda et al. 1996, Sakoda, Fujishiro et al. 2005), suggesting that AMPK is involved in regulating glycogen dynamics.

Since the discovery of the molecular basis of AMPK-glycogen binding nearly twenty years ago, numerous AMPK β knockout (KO) models (Dzamko, van Denderen et al. 2010, Steinberg, O'Neill et al. 2010, O'Neill, Maarbjerg et al. 2011, Dasgupta, Ju et al. 2012) and human interventions manipulating glycogen content (Wojtaszewski, Jorgensen et al. 2002, Wojtaszewski, MacDonald et al. 2003, Steinberg, Watt et al. 2006, Yeo, McGee et al. 2010) have provided insight into potential roles for AMPK-glycogen binding and the reciprocal relationship between AMPK activity and glycogen content. These findings have contributed to the hypothesis that AMPK-glycogen binding allows AMPK to “sense” carbohydrate availability in glycogen stores (McBride, Ghilagaber et al. 2009). However, until recently, there been no *in vivo* model systems available to directly assess the physiological consequences of disrupting these interactions (**Figure 1.1**). We recently determined the phenotypic effects of disrupting AMPK-glycogen binding in two novel mouse models with AMPK single knock-in (KI) mutations in critical residues required for glycogen binding in either the β1 or β2 subunit isoforms – W100A and W98A, respectively. These models established isoform-specific phenotypic effects of chronically disrupting AMPK-glycogen binding *in vivo* via KI mutations, which were associated with reductions in tissue AMPK content (Hoffman, Whitfield et al. 2020). However, these single KI models do not permit investigation of the phenotypic effects of disrupting whole-body AMPK-glycogen binding and potential synergistic and/or compensatory roles of the β1 and β2 subunit isoforms that are concomitantly expressed in many tissues.

Therefore, to address this knowledge gap, single KI mice were bred to generate a mouse model with double knock-in mutations (DKI) to chronically disrupt AMPK-glycogen binding in both β subunit isoforms. This DKI mouse model provides the first *in vivo* model to examine the phenotypic effects of whole-body disruption of AMPK-glycogen binding. The first experimental chapter of this thesis (Study 1) examines the phenotypic effects of the DKI mutation utilised to disrupt AMPK-glycogen binding on whole-body and tissue metabolism, as well as tissue glycogen dynamics in response to fasting, a physiologically relevant stimulus that induces cellular energy stress. It was hypothesised that DKI mice would display increased adiposity, associated with increased CHO oxidation, reduced fat oxidation and reduced tissue AMPK content. Furthermore, it was hypothesised that DKI mice would have increased reliance on liver and skeletal muscle glycogen during overnight fasting due to increased rates of CHO oxidation.

To build on the findings in Study 1 that first established the phenotypic effects of the DKI mutation on fed, resting and fasting metabolism, Study 2 examined the effects of the DKI mutation on responses to acute energy stress through exercise. Both AMPK and glycogen have well-established roles in the regulation of metabolic responses to acute exercise. Therefore, it was expected that the DKI mutation utilised to disrupt AMPK-glycogen binding would result in reduced exercise capacity, altered whole-body substrate utilisation patterns, and increased skeletal muscle glycogen use during exercise. The specific aims and hypotheses of Study 2 are further detailed in **Chapter 5**.

Chapter 2 Literature Review

Publication statement:

This Chapter is based on a review article published in the *International Journal of Molecular Sciences*. For the purpose of this thesis, additional material has been added/updated where appropriate, including new research published since 2018.

Janzen, N. R., Whitfield, J., & Hoffman, N. J. (2018). Interactive Roles for AMPK and Glycogen from Cellular Energy Sensing to Exercise Metabolism. *Int J Mol Sci*, 19(11). doi:10.3390/ijms19113344

2.1 Abstract

The AMP-activated protein kinase (AMPK) is a heterotrimeric complex with central roles in cellular energy sensing, regulation of metabolism, and exercise training-induced adaptations. AMPK regulatory β subunits contain a conserved carbohydrate-binding module (CBM) that binds glycogen, the major tissue storage form of glucose. Research over the past two decades has revealed that regulation of AMPK is impacted by glycogen availability and glycogen storage dynamics are concurrently regulated by AMPK activity. This growing body of research has uncovered new evidence of physical and functional interactive roles for AMPK and glycogen ranging from cellular energy sensing to the regulation of whole-body metabolism and contraction-induced cellular and tissue adaptations. In this literature review, recent advancements in the understanding of molecular, cellular, and physiological processes influenced by AMPK-glycogen interactions are discussed. In addition, novel research technologies and experimental models are appraised that will continue to expand the repertoire of biological processes known to be regulated by AMPK and glycogen. These multidisciplinary research advances will aid discovery of novel pathways and regulatory mechanisms that are central to the AMPK signalling network, beneficial effects of exercise, and maintenance of metabolic homeostasis in health and disease.

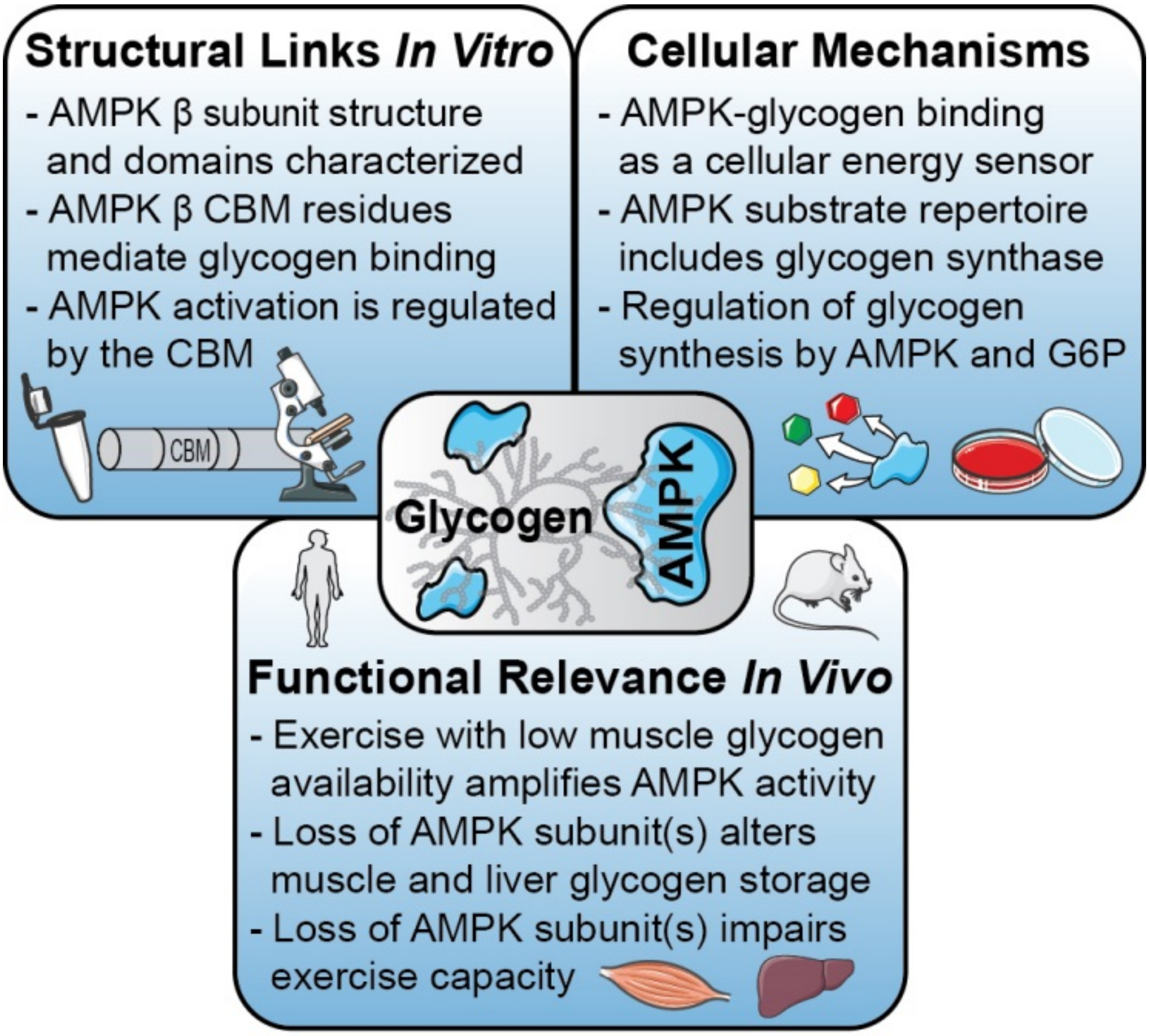

Structural Links *In Vitro*

- AMPK β subunit structure and domains characterized
- AMPK β CBM residues mediate glycogen binding
- AMPK activation is regulated by the CBM

Cellular Mechanisms

- AMPK-glycogen binding as a cellular energy sensor
- AMPK substrate repertoire includes glycogen synthase
- Regulation of glycogen synthesis by AMPK and G6P

Functional Relevance *In Vivo*

- Exercise with low muscle glycogen availability amplifies AMPK activity
- Loss of AMPK subunit(s) alters muscle and liver glycogen storage
- Loss of AMPK subunit(s) impairs exercise capacity

Figure 2.1 – Graphical abstract overviewing the current evidence in the literature involving AMPK-glycogen interactions from structural links *in vitro*, cellular mechanisms, to *in vivo* physiological relevance.

2.2 Introduction

The AMP-activated protein kinase (AMPK) is a heterotrimer composed of a catalytic α subunit and regulatory β and γ subunits which becomes activated in response to decreases in cellular energy availability. Activation of AMPK results in metabolic adaptations such as increases in glucose uptake, glycolytic flux, and fatty acid (FA) oxidation. AMPK activation simultaneously inhibits anabolic processes including protein and FA synthesis. AMPK can also translocate to the nucleus where it regulates transcription factors to increase energy production, meet cellular energy demands, and inhibit cell growth and proliferation. Conversely, when energy levels are replete, AMPK activity returns to basal levels, allowing anabolic processes to resume. Given its central roles in cellular metabolic and growth signalling pathways, AMPK remains an appealing target for treating a range of pathologies associated with obesity and aging, including metabolic diseases such as obesity and T2D.

In response to changes in energy supply and demand, glycogen predominantly stored in the liver and skeletal muscle serves as an important source of energy to maintain metabolic homeostasis. Glycogen is synthesised by the linking of glucose monomers during periods of excess nutrient availability. In response to energy stress and decreased arterial glucose concentration, rising glucagon levels induce increased hepatic glucose output by promoting the breakdown of glycogen and the conversion of non-glucose substrates into glucose (i.e., gluconeogenesis). The newly formed glucose is released into the bloodstream to help restore blood glucose levels. Skeletal muscle glycogen serves as an accessible source of glucose to form ATP and reducing equivalents via glycolytic and oxidative phosphorylation pathways during muscle contraction.

A significant body of evidence demonstrates that AMPK has the capacity to bind glycogen. This physical interaction is mediated by the CBM located within the AMPK β subunit and is thought to allow AMPK to function as a sensor of stored cellular energy. While glycogen is stored in multiple tissues throughout the body, this literature review will primarily focus on the physical interactions underlying the AMPK β subunit binding to glycogen and its potential functional links to glycogen storage dynamics in liver and skeletal muscle, as these tissues are central to metabolic and exercise-regulated biological processes. As the majority of research in these areas has been undertaken in human and mouse model systems, studies in these species will be highlighted. Following a background on the regulation of AMPK and glycogen, this literature review will critically assess recent advances within the past two decades that have added to our understanding of the physical basis of AMPK-glycogen binding and its potential functional interactions in exercise and metabolism. Key remaining biological questions related to the interactive roles of AMPK and glycogen will be raised along with discussion of research advancements that are feasible in the next decade with new technologies and experimental models to determine how AMPK-glycogen binding contributes to and may be therapeutically targeted in health and disease.

2.3 Roles for AMPK and Glycogen in Metabolism

2.3.1 AMPK Activation and Signalling

Structural biology-based studies over the past decade have provided new insights into the molecular mechanisms by which AMPK activation is regulated by nucleotides, including changes in AMP:ATP and ADP:ATP ratios (i.e., adenylate energy charge) that occur in response to cellular energy stress (Garcia and Shaw 2017). Binding of AMP and ADP to the cystathionine-β-synthase (CBS) domains of the γ subunit promotes AMPK activation through several complementary and interdependent mechanisms. Binding of AMP promotes AMPK association with LKB1 and the scaffolding protein axin which enhances the effect of T172 phosphorylation (Oakhill, Chen et al. 2010, Zhang, Guo et al. 2013), the primary phosphorylation and activation site within the AMPK α subunit, while simultaneously preventing its dephosphorylation by protein phosphatases (Garcia-Haro, Garcia-Gimeno et al. 2010, Xiao, Sanders et al. 2011, Gowans, Hawley et al. 2013, Joseph, Liu et al. 2015). This activation is mediated by myristoylation of the G2 site on the N-terminus of the β subunit (**Figure 2.2**), which promotes AMPK association with cellular membranes and LKB1 (Oakhill, Chen et al. 2010). Furthermore, the binding of AMP, but not ADP, can cause allosteric activation of AMPK without T172 phosphorylation (Xiao, Sanders et al. 2011, Gowans, Hawley et al. 2013, Scott, Ling et al. 2014, Li, Wang et al. 2015). The combination of allosteric activation by nucleotides and increased T172 phosphorylation by LKB1 can increase AMPK activity 1000-fold (Kjobsted, Hingst et al. 2018). Additionally, phosphorylation of T172 can be regulated by changes in intracellular Ca^{2+} concentrations via the upstream kinase CaMKK2 in the absence of changes in adenylate energy charge (Hawley, Pan et al. 2005, Woods, Dickerson et al. 2005, Jensen, Rose et al. 2007).

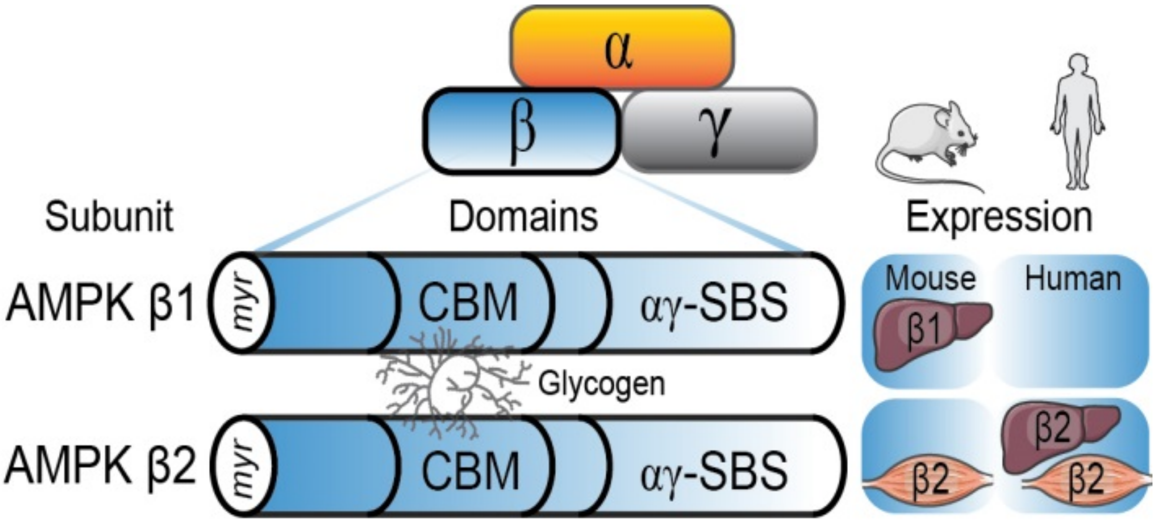

Figure 2.2 – AMPK is a heterotrimeric protein, consisting of a catalytic α subunit, and regulatory β and γ subunits. The β subunit (β1 and β2 isoforms) possesses a glycogen-binding domain (CBM) that mediates AMPK's interaction with glycogen, an N-terminal myristoylation site (myr) and a αγ subunit binding sequence (αγ-SBS) involved in heterotrimeric complex formation. Tissue expression of the β1 and β2 isoforms varies between humans and mice, as the β2 isoform is predominantly expressed in both human liver and skeletal muscle, while mice predominantly express the β1 isoform in liver and β2 isoform in skeletal muscle.

Once activated, AMPK serves as a metabolic "switch" to promote catabolic pathways and inhibit anabolic processes. AMPK is known to have at least 60 downstream substrates and exerts control over a range of cellular pathways regulating glucose and glycogen metabolism, lipid metabolism, protein metabolism, autophagy, and mitochondrial biogenesis (Hardie, Schaffer et al. 2016). **Figure 2.3** highlights several of these targets involved in physiological processes relevant to this thesis.

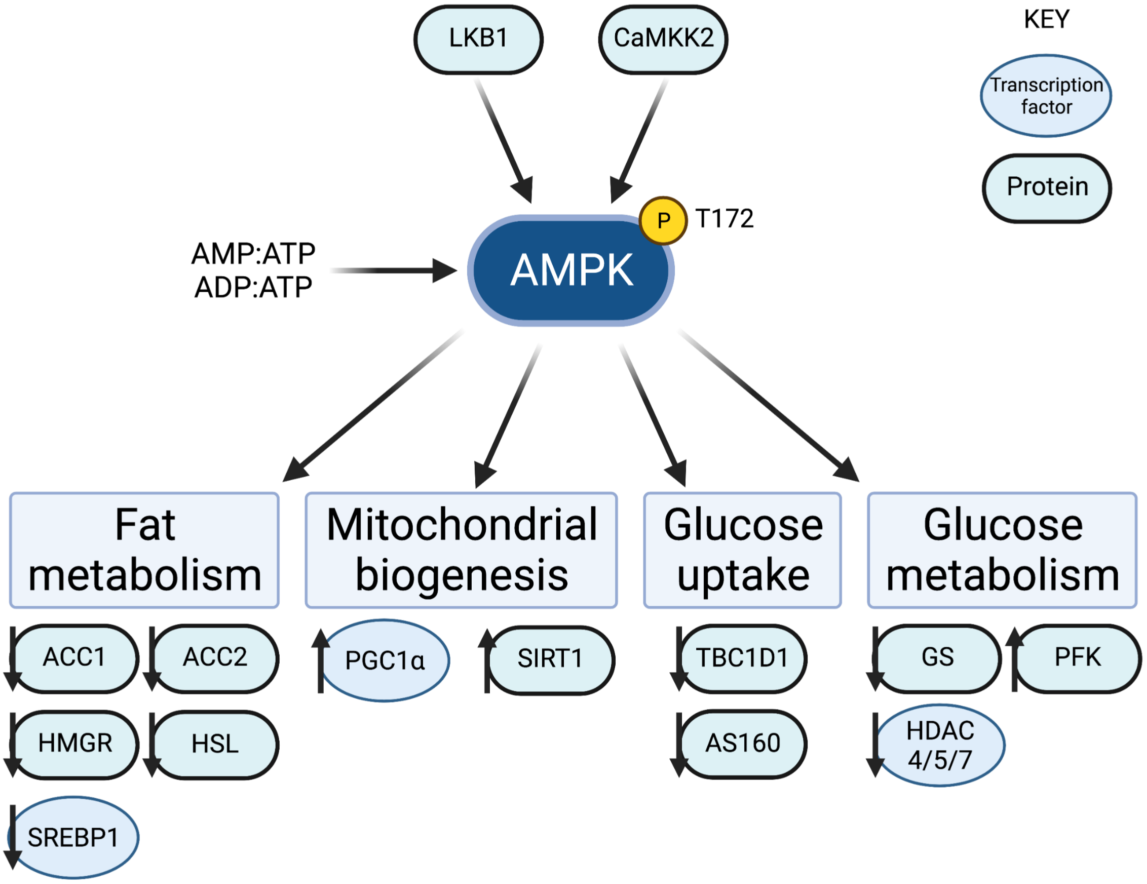
LKB1
CaMKK2
KEY
Transcription factor
Protein
P
T172
AMP:ATP
ADP:ATP
AMPK
Fat metabolism
Mitochondrial biogenesis
Glucose uptake
Glucose metabolism
ACC1
ACC2
PGC1α
SIRT1
TBC1D1
GS
PFK
HMGR
HSL
AS160
HDAC 4/5/7
SREBP1

Figure 2.3 – Schematic highlighting some of AMPK's substrates (i.e., proteins and transcription factors) and several physiological processes that are linked to AMPK signalling. AMPK becomes activated by changes in nucleotides concentrations in response to cellular energy stress and is phosphorylated by upstream kinases LKB1 and CaMKK2 at T172. AMPK then phosphorylates several downstream enzymes and transcription factors to promote or inhibit protein activity and/or up- or downregulate gene expression. Each up or down arrow indicates the effect of AMPK phosphorylation on the respective protein activity or regulation of gene expression by transcription factors. Created with BioRender.com.

2.3.2 Roles for AMPK in Glucose Uptake

Emerging evidence suggests that AMPK is not critical for maintaining skeletal muscle glucose uptake *during* acute exercise in humans or mice. For example, short-term endurance training results in attenuation of human skeletal muscle AMPK activity during an acute bout of cycling without concomitant loss of glucose uptake (McConell, Lee-Young et al. 2005). Additionally, during prolonged exercise at 65% of peak oxygen consumption ($VO_{2\ peak}$), skeletal muscle of well-trained cyclists exhibit significant increases in skeletal muscle glucose uptake without increases in AMPK activity (McConell, Wadley et al. 2020). Chronic muscle-specific AMPK α KO mice have similar glucose uptake during treadmill running compared to wild type (WT) (Fentz, Kjobsted et al. 2015). Additionally, inducible muscle-specific AMPK α1α2 KO mice retain glucose uptake during both treadmill running and *ex vivo* contractions (Kjobsted, Roll et al. 2019, Hingst, Kjobsted et al. 2020).

Following exercise, there is increased glucose uptake into skeletal muscle by contraction-mediated phosphorylation inhibition of Tre-2, BUB2, CDC16, 1 domain family, member 1 (TBC1D1), promoting glucose transporter type 4 (GLUT4) vesicle translocation to the sarcolemmal membrane (**Figure 2.4**) (Sakamoto and Holman 2008, Cartee and Funai 2009). Specifically, phosphorylation of TBC1D1 at sites S231, T596, S660 and/or S700 by AMPK leads to TBC1D1 being sequestered by a 14-3-3 molecular adaptor protein (Pehmoller, Treebak et al. 2009, Vichaiwong, Purohit et al. 2010, Richter and Hargreaves 2013) thereby preventing TBC1D1 from exerting is inhibitory role on GLUT4 translocation to the plasma membrane (Pehmoller, Treebak et al. 2009, Hardie 2013). Loss of TBC1D1 in mice results in decreased glucose uptake in glycolytic muscle fibres in response to both the AMPK activator 5-aminoimidazole-4-carboxamide ribonucleotide (AICAR) and exercise. As a result, TBC1D1 KO mice have reduced running endurance capacity, demonstrating that TBC1D1 plays an important role in exercise-mediated glucose uptake via the AMPK pathway (Stockli, Meoli et al. 2015). These findings have been confirmed in a rat TBC1D1 KO model which had reduced glucose tolerance and GLUT4 translocation in glycolytic muscle in response to stimulated muscle contraction (Whitfield, Paglialunga et al. 2017). Together, these results establish that the AMPK-TBC1D1 signalling axis is necessary for glucose uptake in rodents following exercise.

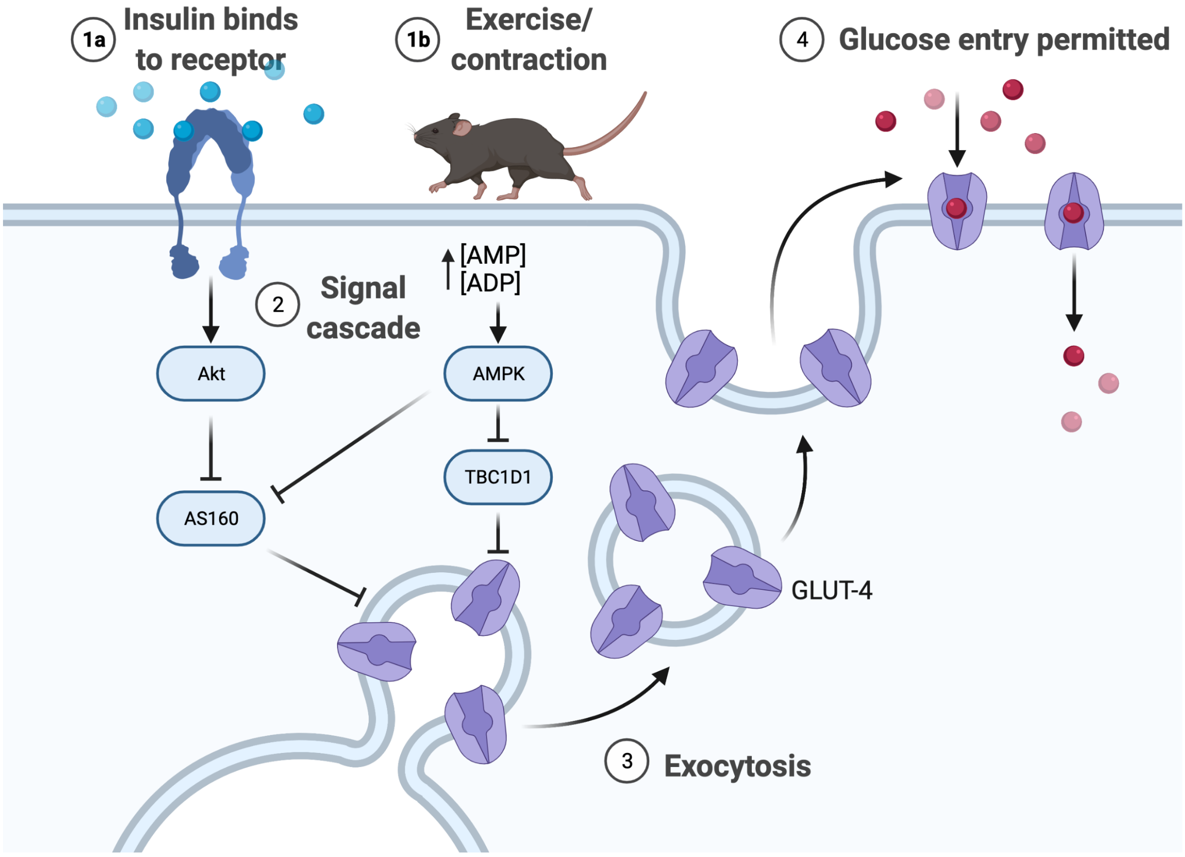
1a
Insulin binds to receptor
1b
Exercise/ contraction
4
Glucose entry permitted
↑[AMP] [ADP]
2
Signal cascade
Akt
AMPK
AS160
TBC1D1
GLUT-4
3
Exocytosis

Figure 2.4 – Schematic of the signalling mechanisms underlying skeletal muscle glucose uptake via insulin-stimulated (1a) and contraction-stimulated (1b) pathways. Muscle contraction increases glucose uptake via both pathways through AMPK's inhibition of both AS160 and TBC1D1 (2), which leads to increased GLUT4 exocytosis and translocation (3) to the sarcolemma and enhances insulin sensitivity in skeletal muscle following exercise (4). Created with BioRender.com.

Along with TBC1D1, the Akt substrate of 160 kDa (AS160), a paralog of TBC1D1, is also involved in contraction-stimulated glucose uptake. When AS160 is sequestered to 14-3-3 proteins by phosphorylation at T642, GLUT4 translocation and detection on the plasma membrane is increased (O'Neill 2013). Phosphorylation of AS160 is attenuated in response to contraction and completely ablated in response to AICAR stimulation in AMPK α2 inactive mice (Kramer, Witczak et al. 2006). A KI mutation of T649A (analogous to the primary T642 in humans) in mice resulted in impaired insulin-stimulated, but unaffected contraction- and AICAR-stimulated glucose uptake in skeletal muscle, suggesting that phosphorylation of this site by AMPK is not necessary for AS160-mediated glucose uptake in response to exercise (Ducommun, Wang et al. 2012). However, it is possible that maintained TBC1D1 phosphorylation could be responsible for the similar contraction-stimulated glucose uptake in AS160 T649A mice. While there are remaining knowledge gaps regarding how the several AMPK phosphorylation sites of AS160 are involved in insulin- and contraction-stimulated glucose uptake, these collective results indicate that contraction-stimulated AS160 phosphorylation is mediated, at least in part, by AMPK.

In addition to contraction-stimulated glucose uptake via the insulin-independent pathway described above, crosstalk between the AMPK and insulin signalling pathways results in improved insulin sensitivity in skeletal muscle following exercise-induced AMPK activation (**Figure 2.4**) (reviewed in further detail in (Steinberg and Kemp 2009, Sylow, Tokarz et al. 2021)). A single bout of exercise can increase insulin-stimulated glucose uptake for several hours, and insulin sensitivity can be increased by exercise training (Richter, Garetto et al. 1982, King, Dalsky et al. 1988). In humans, the increase in insulin sensitivity following an acute bout of exercise is similar in both type I and type II skeletal muscle (Larsen, Steenberg et al. 2020). Meanwhile, acute exercise-induced increases in insulin sensitivity have been observed in mouse type I soleus and type II epitrochlearis muscles, but not in type II extensor digitorum longus (EDL) muscle (Hamada, Arias et al. 2006). While previous findings have been equivocal regarding the role of AMPK in increased insulin sensitivity (O'Neill 2013), a recent study demonstrated that AMPK is involved in increasing insulin sensitivity by phosphorylating and inhibiting AS160 (Kjobsted, Munk-Hansen et al. 2017). Heightened insulin sensitivity following exercise provides increased glucose uptake for rapid glycogen resynthesis in glycogen-depleted skeletal muscle (Richter, Garetto et al. 1982, Richter, Mikines et al. 1989). Collectively, these results indicate that AMPK may be dispensable for increases in glucose uptake during, but not following, acute exercise and muscle contraction.

2.3.3 Roles for AMPK in Glycogen Synthesis

In addition to promoting skeletal muscle glucose uptake, AMPK is also implicated in regulating glycogen synthesis. AMPK phosphorylates and inactivates GS, the rate limiting enzyme of glycogen synthesis, at site 2 (S7) *in vitro* (Carling and Hardie 1989, Roach, Depaoli-Roach et al. 2012). AMPK α2, but not α1, KO mice display blunted phosphorylation of GS at site 2 and higher GS activity in response AICAR simulation (Jorgensen, Nielsen et al. 2004). However, chronic activation of AMPK also results in an accumulation of glycogen in skeletal and cardiac muscle (Hunter, Treebak et al. 2011). It has been proposed that prolonged increases in AMPK activity, with its associated increases in skeletal muscle glucose uptake, results in increased intracellular glucose-6-phosphate (G6P) concentrations, a known allosteric activator of GS. The increase in G6P-stimulated activation of GS eventually overrides the inhibitory influence of AMPK on GS to promote glycogen synthesis (**Figure 2.5**) (Hunter, Treebak et al. 2011). Following acute exercise, AMPK heterotrimers specifically containing the α2 isoform mediate the inhibition of carbohydrate oxidation to promote fat oxidation, which along with increased glucose uptake, allows for optimal glycogen resynthesis and supercompensation in human skeletal muscle (Fritzen, Lundsgaard et al. 2015).

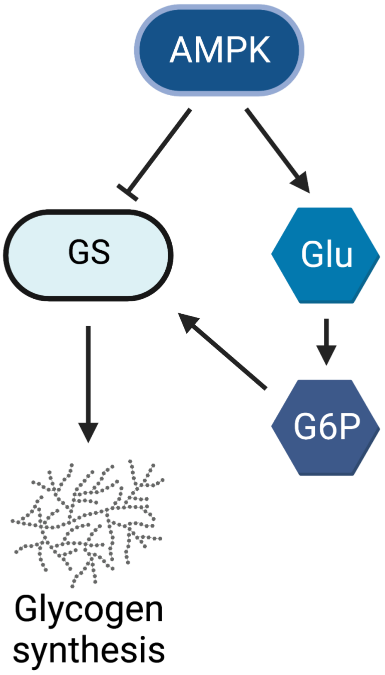

Figure 2.5 – Proposed mechanism by which increased AMPK activation results in increased glycogen synthesis. While AMPK phosphorylates and inhibits GS at S7, AMPK also promotes glucose uptake via phosphorylation and inhibition of AS160 and TBC1D1, leading to increased intracellular concentrations of G6P, a potent allosteric activator of GS. These two competing influences of AMPK on GS activity result in net increases in GS activity and glycogen synthesis. Created with BioRender.com.

2.3.4 Roles for AMPK in Fat Metabolism

AMPK also acutely inhibits FA synthesis (Hardie, Ross et al. 2012) and promotes lipid oxidation (Winder 2001) via phosphorylation of acetyl-CoA carboxylase (ACC) isoforms ACC1 and ACC2 at S79 and S212, respectively (Fullerton, Galic et al. 2013). The AMPK-ACC signalling axis represents an important target for potential treatment of metabolic diseases, such as T2D and nonalcoholic fatty liver disease (Smith, Marcinko et al. 2016), as excessive lipid accumulation in liver and/or skeletal muscle represent major contributors to the development of insulin resistance (Steinberg 2018). Given that ACC is an established AMPK substrate, phosphorylation of ACC at S79 and/or S221 is commonly used as a surrogate measure of AMPK signalling *in vivo* (Steinberg and Kemp 2009). AMPK phosphorylates and inhibits HMG-CoA reductase (HMGR), the rate limiting enzyme in cholesterol synthesis (Singh, Banerjee et al. 2009, Burg and Espenshade 2011). AMPK also phosphorylates and inhibits sterol regulatory element-binding protein 1 (SREBP1), a transcription factor that regulates lipid synthesis (Li, Xu et al. 2011), inducing cells to favour lipid oxidation over lipid synthesis (Li, Xu et al. 2011, Garcia and Shaw 2017). As with ACC, phosphorylation of SREBP1 is an important substrate underlying potential therapeutic treatments targeting AMPK.

2.3.5 Roles for AMPK in Acute Responses to Exercise

Considering its numerous downstream targets, AMPK would be expected to play important roles in responding to settings of energy stress such as exercise. However, despite AMPK's well-established roles in fat and glucose metabolic pathways in response to energy stress *in vitro*, AMPK's involvement in acute and chronic adaptations to exercise *in vivo* is less clear.

As a result of the various isoforms of each of the AMPK subunits, there are 12 possible heterotrimeric combinations of AMPK subunits which are differentially expressed throughout various tissues and respond differently to exercise. For example, only three heterotrimers are expressed in human skeletal muscle ($\alpha1\beta2\gamma1$, $\alpha2\beta2\gamma1$, $\alpha2\beta2\gamma3$) (Wojtaszewski, Birk et al. 2005, Birk and Wojtaszewski 2006), while an additional two ($\alpha1\beta1\gamma1$, $\alpha2\beta1\gamma1$) are found in mouse skeletal muscle (Treebak, Birk et al. 2009). Furthermore, different AMPK isoforms are activated in an exercise intensity- and duration-dependent manner (Chen, Stephens et al. 2003, Kjobsted, Hingst et al. 2018). The AMPK $\alpha2\beta2\gamma3$ complex is activated in response to relatively high intensity exercise (>80% $VO_{2\text{ peak}}$) and is likely responsible for the exercise-induced changes in AMPK signalling in human skeletal muscle (Birk and Wojtaszewski 2006). In contrast, while the $\alpha1\beta2\gamma1$ heterotrimer only contributes ~15% of the total AMPK expression in human quadriceps muscle, it accounts for 65% of total baseline AMPK activity in the fed, resting state (Kjobsted, Hingst et al. 2018). Therefore, AMPK can be relatively unresponsive to further activation by exercise stimuli (Birk and Wojtaszewski 2006), except during prolonged, lower intensity exercise (e.g., >60 min at ~70% $VO_{2\,peak}$) (Treebak, Birk et al. 2007). AMPK is more highly activated in fast twitch muscles than in slow twitch in response to both exercise and electrically induced muscle contraction (Konagaya, Terai et al. 2017). Recent technological applications to assess AMPK activity and localisation have provided additional insight into AMPK heterogeneity across various cell types and species and suggest that AMPK heterotrimeric combinations may have distinct functions (Ross, MacKintosh et al. 2016, Herzig and Shaw 2018).

Acute activation of AMPK results in increased glucose uptake and fat oxidation in non-human primates and rodents, contributing to changes in whole-body substrate oxidation (Merrill, Kurth et al. 1997, Cokorinos, Delmore et al. 2017, Myers, Guan et al. 2017). Muscle-specific AMPK β1/β2 KO mice display a reduction in respiratory exchange ratio (RER) and reduced skeletal muscle glucose clearance compared to WT during treadmill running at 50% of maximal running speed (O'Neill, Maarbjerg et al. 2011). Meanwhile, inducible muscle-specific AMPK α KO models demonstrate no differences in fuel utilisation or skeletal muscle glucose uptake compared to WT (Hingst, Kjobsted et al. 2020). These contrasting findings suggest that AMPK potentially regulates substrate utilisation in an isoform- and tissue-specific manner, which can lead to varied responses in whole-body substrate utilisation.

Skeletal muscle AMPK content appears to be critical for exercise tolerance, as numerous whole-body and skeletal muscle-specific (Steinberg, O'Neill et al. 2010, O'Neill, Maarbjerg et al. 2011, Dasgupta, Ju et al. 2012, Lantier, Fentz et al. 2014, Hingst, Kjobsted et al. 2020), but not liver-specific (Hughey, James et al. 2017), AMPK KO models have reduced maximal running speed during an incremental test to exhaustion and/or time to exhaustion at submaximal running speed. Inducible loss of AMPK α1α2 in skeletal muscle also resulted in reduced maximal running speed in mice (Hingst, Kjobsted et al. 2020). Therefore, the role of

AMPK in the regulation of maximal exercise capacity does not appear to be tied to developmental changes induced by genetic loss of AMPK. Chronic loss of skeletal muscle AMPK α1α2 resulted in attenuated increases in mRNA expression of GLUT4, hexokinase, peroxisome proliferator-activated receptor gamma coactivator 1-alpha (PGC1α), cluster of differentiation 36 (CD36), FA binding protein, FA transport proteins 1 and 4, and oxidative phosphorylation (OXPHOS) complex proteins in response to acute exercise (Fentz, Kjobsted et al. 2015). Meanwhile, mice with chronic loss of α1 or α2 in skeletal muscle had similar exercise-induced responses in mRNA expression of GLUT4, hexokinase, and PGC1α (Jorgensen, Wojtaszewski et al. 2005). Together, these results suggest that, despite potentially different roles of the two AMPK catalytic α isoforms during exercise, both isoforms are capable of isoform compensation to promote exercise-induced mRNA responses.

Obesity has been associated with reduced muscle AMPK protein expression and activation during acute exercise (Mortensen, Poulsen et al. 2009, O'Neill 2013) and therefore, may be associated with exercise intolerance. Lean humans with T2D (body mass index [BMI] <30 kg·m^2) have normal muscle AMPK activity and signalling in response to exercise (Musi, Fujii et al. 2001, Koistinen, Galuska et al. 2003), while AMPK activation is disrupted in obese humans (BMI >30 kg·m^2) with T2D (Sriwijitkamol, Coletta et al. 2007). This results in muscle AMPK activity and signalling responses being significantly lower in obese humans with T2D compared to lean individuals in response to acute high intensity exercise. These findings suggest that obese humans with T2D must exercise at higher relative intensities to achieve the same level of AMPK activation (Sriwijitkamol, Coletta et al. 2007). Collectively, these findings suggest that dysregulation of AMPK is associated with obesity, but not necessarily T2D. However, given the role of AMPK in mediating glucose and fat metabolism, it is unclear whether dysregulation of AMPK precedes and contributes to obesity, or if it occurs as a result of increased tissue fat deposition (Kola, Grossman et al. 2008).

Mice expressing the AMPK γ1 R70Q gain of function mutation, which results in chronically active AMPK in skeletal muscle, have increased exercise endurance capacity, associated with increased resting glycogen content in skeletal muscle (Barre, Richardson et al. 2007). AMPK γ1 H151R mice, expressing another gain of function mutation, display increased skeletal muscle glycogen content, associated with improved insulin sensitivity, and increased energy expenditure (Schonke, Myers et al. 2015). While these gain of function models come with several caveats, including the significant phenotypic differences between humans and murine models and impacts of chronically activated AMPK during developmental stages. Therefore, these findings to date should be interpreted with caution regarding the potential roles of AMPK in energy homeostasis.

2.3.6 Roles for AMPK in Adaptations to Exercise

While AMPK appears critical for exercise capacity, it may not be necessary for exercise training adaptations, at least in rodents. Despite having reduced maximal running speed versus WT, muscle-specific AMPK α1α2 KO mice had similar improvements in exercise capacity following 4 weeks of voluntary running wheel training (Fentz, Kjobsted et al. 2015). This increase in maximal running speed in muscle-specific AMPK α1α2 KO mice following repeated training occurred in spite of ablated increases in content and/or activity of several markers of exercise training, including citrate synthase, GLUT4, hexokinase, and OXPHOS complex proteins. These findings suggest that AMPK α1 and α2 and associated increases in expression of downstream targets are not necessarily critical for training adaptations in mouse skeletal muscle (Fentz, Kjobsted et al. 2015). However, given these mice had chronic loss of AMPK, it is possible that effects on mouse developmental adaptations and/or compensatory adaptations allowed for similar increases in maximal running speed between WT and AMPK α1α2 KO mice. Further research using various transgenic and KO models (i.e., inducible, isoform- and tissue-specific AMPK KO, etc) is necessary to elucidate the precise roles of AMPK in skeletal muscle adaptations to exercise training.

A primary adaptation to endurance training is increased mitochondrial content within skeletal muscle (i.e., mitochondrial biogenesis). AMPK regulates a range of substrates underlying mitochondrial content and remodelling. A recent global phosphoproteomic analysis of exercise and AICAR-stimulated AMPK signalling in human skeletal muscle and rat muscle cells, respectively, identified the mitochondrial scaffolding protein A-kinase anchor protein 1 as an AMPK substrate (Hoffman, Parker et al. 2015). AMPK activity stimulates mitochondrial biogenesis through an increase in PGC1α transcription, thereby promoting oxidative metabolism. This adaptation to exercise training is important, as it allows cells to protect against potential future energy stress, exemplified by the increased mitochondrial content observed in response to the repeated bouts of exercise during training (Hawley, Hargreaves et al. 2014).

Training status appears to have a significant impact on AMPK signalling responses to acute bouts of exercise. AMPK protein expression, particularly the α1 subunit isoform, is increased in skeletal muscle of trained human muscle versus untrained muscle (Nielsen, Mustard et al. 2003, Mortensen, Hingst et al. 2013). While acute exercise results in dramatic increases in AMPK activity and phosphorylation in untrained skeletal muscle in humans (McConell, Lee-Young et al. 2005), exercise training results in similar exercised-induced increases in glucose uptake but without associated increases in AMPK activity and phosphorylation (McConell, Lee-Young et al. 2005, Mortensen, Hingst et al. 2013). Similarly, compared to untrained muscle, trained muscle has attenuated increases in AMPK T172 and ACC S79 phosphorylation in response to acute exercise (Nielsen, Mustard et al. 2003). These findings indicate that endurance training, and the associated mitochondrial adaptations, result in blunted AMPK signalling responses to acute exercise. Therefore, AMPK is not likely directly responsible for metabolic responses to exercise in trained muscle (McConell, Wadley et al. 2020).

2.3.7 The AMPK β Subunit and Carbohydrate Binding Module

The AMPK β subunit exists in two isoforms (β1 and β2) and serves as a scaffolding subunit that binds to the AMPK catalytic α and regulatory γ subunits, playing an important role in the physical stability of the heterotrimer (**Figure 2.2**) (Xiao, Sanders et al. 2013, Li, Wang et al. 2015, Gu, Yan et al. 2017). In human and mouse skeletal muscle, the predominantly expressed isoform is β2 (**Table 2.1**) (Olivier, Foretz et al. 2018). In contrast, liver β subunit isoform expression differs across mammalian species: the β1 isoform is predominantly expressed in mouse liver, while β2 is predominantly expressed in human liver (Stephenne, Foretz et al. 2011, Wu, Puppala et al. 2013). However, despite these isoform differences between species, both β subunit isoforms contain the CBM protein domain which mediates physical AMPK-glycogen interaction and binding. Furthermore, the CBM is highly conserved between species, suggesting that this region possesses evolutionary significance and plays similar roles across species (Polekhina, Gupta et al. 2003, Polekhina, Gupta et al. 2005). The CBM spans residues 68-163 of the β1 subunit isoform and residues 67-163 of the β2 subunit isoform (Polekhina, Gupta et al. 2005, Koay, Woodcroft et al. 2010) and is nearly identical in structure and sequence in both isoforms, with the major difference being the insertion of a threonine at residue 101 in the β2 CBM (Mobbs, Koay et al. 2015, Mobbs, Di Paolo et al. 2017). This insertion is believed to have occurred early in evolutionary history and provides the β2 CBM with higher binding affinity to glycogen (Koay, Woodcroft et al. 2010, Mobbs, Di Paolo et al. 2017). However, the reason for this divergence in β subunit isoforms is unknown.

Table 2.1 – AMPK β subunit isoform distribution in human and mouse tissues

Tissue	β1	β2
Human vastus lateralis	ND	~100%
Human liver	ND	~100%
Mouse extensor digitorum longus	5%	95%
Mouse soleus	18%	78%
Mouse liver	100%	ND

Adapted from (Stephenne, Foretz et al. 2011, O'Neill 2013, Wu, Puppala et al. 2013, Kjobsted, Hingst et al. 2018, Olivier, Foretz et al. 2018). ND, nondetectable.

2.3.8 Glycogen Dynamics

A number of proteins are associated with glycogen particles and function as regulators of glycogen synthesis, breakdown, particle size and degree of branching (**Figure 2.6**). Glycogenin initiates glycogen formation and functions as the central protein of the glycogen particle (Alonso, Lomako et al. 1995). GS is the rate-limiting enzyme in glycogen synthesis responsible for attaching UDP-glucose donors together in α-1,4 linkages, the linear links of the glycogen particle. As G6P is a precursor to UDP-glucose, its accumulation is a potent activator of GS, capable of overriding the inhibitory effects of phosphorylation mediated by proteins such as AMPK, glycogen synthase kinase 3β (GSK3β), and protein kinase A (PKA) (Hunter, Treebak et al. 2011, Roach, Depaoli-Roach et al. 2012). As its name implies, glycogen branching enzyme (GBE) is responsible for introducing α-1,6 branch points to the growing glycogen particle. The rate limiting enzyme of glycogen breakdown is GP, which is known to be activated by elevated intracellular Ca^{2+}, epinephrine and cAMP concentrations (Chasiotis, Sahlin et al. 1982, Richter, Ruderman et al. 1982). In skeletal muscle, GP is also allosterically activated by increases in AMP concentrations and is inhibited by increases in G6P and ATP (Johnson and Barford 1990). When activated, GP degrades the α-1,4 links of glycogen particles and removes glycosyl units from the non-reducing ends of the glycogen particle (Shearer and Graham 2004). GDE assists with the degradation of glycogen and is responsible for breaking the α-1,6 links to allow continued GP activity. Without GDE, GP can only degrade the outer tiers of glycogen particles and stops four glucose residues short of the α-1,6 branch point (Roach, Depaoli-Roach et al. 2012). Further detail regarding glycogen synthesis and breakdown are beyond the scope of this literature review, and readers are referred to other review articles on this specific topic (Roach, Depaoli-Roach et al. 2012, Prats, Graham et al. 2018).

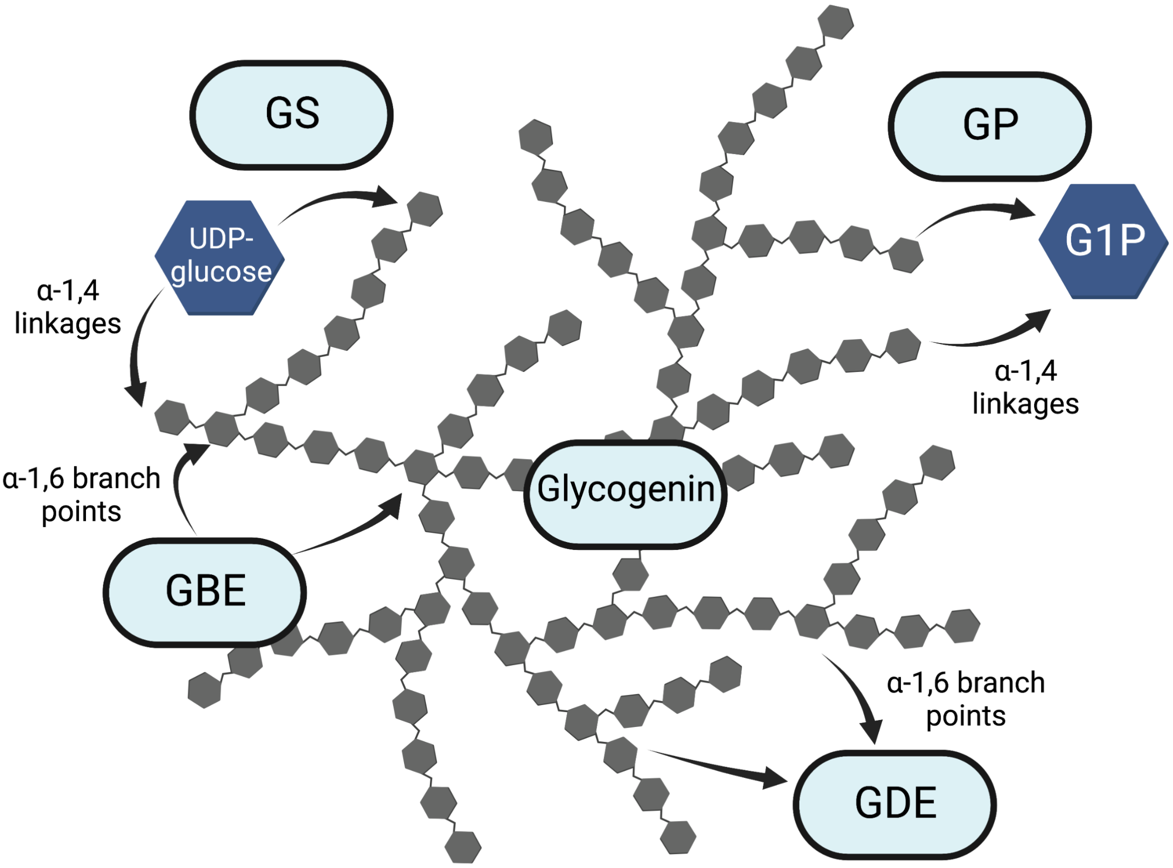

Figure 2.6 – Several proteins involved in regulation of glycogen particle formation and breakdown. Created with BioRender.com.

2.3.9 Glycogen Localisation

Recently, there has been increasing interest regarding the significance of glycogen's subcellular localisation in skeletal muscle (Graham, Yuan et al. 2010, Ortenblad, Nielsen et al. 2011, Philp, Hargreaves et al. 2012, Nielsen and Ortenblad 2013, Ortenblad, Westerblad et al. 2013). Glycogen can be concentrated beneath the sarcolemma (subsarcolemmal; SS), between the myofibers along the I band near the mitochondria and sarcoplasmic reticulum (intermyofibrillar; interMF), or within myofibers near the triad junction (intramyofibrillar; intraMF) (Graham, Yuan et al. 2010, Ortenblad, Nielsen et al. 2011). Recent research has found that intraMF glycogen pools are critical for endurance capacity in humans and that higher glycogen in the SS pool delays utilisation of vital intraMF glycogen (Jensen, Ortenblad et al. 2020). Depletion of these different glycogen pools also impacts muscle function and fatigue profiles, such as impairing Ca^{2+} release and reuptake. Therefore, it has been hypothesised that these different pools of glycogen play significant roles in muscle contraction and fatigue beyond their roles as an energy substrate (Philp, Hargreaves et al. 2012, Nielsen and Ortenblad 2013, Ortenblad, Westerblad et al. 2013).

Human skeletal muscle contains large stores of glycogen, which can exceed 100 mmol glucosyl units·kg^{-1} wet weight (~500 mmol·kg^{-1} dry weight) in the vastus lateralis muscle of humans (Yeo, Paton et al. 2008, Nielsen, Holmberg et al. 2011) and is primarily concentrated in the interMF space (Nielsen, Holmberg et al. 2011). Conversely, rodents tend to have higher stores of glycogen in the liver compared to skeletal muscle. Mice store about 120 µmol·g^{-1} wet weight in liver and 15-20 µmol·g^{-1} wet weight in the type IIA flexor digitorum brevis muscle, with the highest concentrations in the intraMF pool (Nielsen, Cheng et al. 2014). While the relative contributions of intraMF glycogen to total glycogen are different between humans and mice, intraMF content as a percentage of total fibre volume is very similar between species (Nielsen, Holmberg et al. 2011, Nielsen, Cheng et al. 2014). Additionally, substrate utilisation is different between species during exercise, as humans rely predominantly on intramuscular stores and rodents primarily rely on blood-born substrates (Romijn, Coyle et al. 1993, van Loon, Greenhaff et al. 2001, O'Neill, Maarbjerg et al. 2011, Hughey, James et al. 2017). These differences in glycogen storage and utilisation between humans and rodents are important considerations in study design across species when assessing glycogen depletion and/or repletion.

2.3.10 Skeletal Muscle Glycogen Utilisation and Synthesis

Skeletal muscle glycogen utilisation during exercise and its role in exercise capacity has been the focus of decades of research. Early studies reported that skeletal muscle glycogen content was a strong determinant of exercise capacity during higher intensities (>75% maximal oxygen consumption [$VO_{2\ max}$]) of exercise (Bergstrom, Hermansen et al. 1967, Hermansen, Hultman et al. 1967). These findings have recently been replicated using more advanced techniques for quantification of subcellular pools of skeletal muscle glycogen (Jensen, Ortenblad et al. 2020). Preservation of skeletal muscle glycogen (i.e., with carbohydrate supplementation during exercise) delayed exhaustion during prolonged submaximal cycling (Coyle, Coggan et al. 1986). Further studies determined that skeletal muscle glycogen's contribution to total energy expenditure increases with increasing exercise intensity (Romijn, Coyle et al. 1993, van Loon, Greenhaff et al. 2001), establishing glycogen's role in the regulation of exercise capacity, particularly at higher exercise intensities.

The importance of skeletal muscle glycogen content is further underscored by studies examining the effect of exercise on substrate utilisation patterns when skeletal muscle glycogen has been acutely depleted. One hour of cycling at 70% $VO_{2\ peak}$, commenced with low muscle glycogen stores, results in increased arterial FA concentration and reduced arterial blood glucose levels, concomitant with increased FA and glucose uptake in skeletal muscle of trained cyclists (Wojtaszewski, MacDonald et al. 2003). The overall shift to increased reliance on fat oxidation, demonstrated by reduced RER during exercise in the low glycogen state and associated increases in AMPK activity (Wojtaszewski, MacDonald et al. 2003), also indicates that liver glycogen may not be capable of maintaining carbohydrate oxidation during submaximal exercise when exercise is performed with depleted skeletal muscle glycogen. In humans, endurance training results in increased rates of fat oxidation both at rest and during submaximal exercise (Turcotte, Richter et al. 1992, Klein, Coyle et al. 1994), even when training is undertaken at 40% of $VO_{2\ peak}$ (Schrauwen, van Aggel-Leijssen et al. 2002). Endurance training also increases skeletal muscle glycogen synthesis following exercise training in rats (Nakatani, Han et al. 1997), untrained humans (Greiwe, Hickner et al. 1999), and humans with insulin resistance (Perseghin, Price et al. 1996). This shift from CHO to fat oxidation allows glycogen sparing at lower exercise intensities and contributes to improvements in exercise capacity and performance observed following training, further underscoring the importance of preserving skeletal muscle glycogen.

In addition to the established role of glycogen as an important fuel source during exercise, there has been further investigation into how glycogen contributes to exercise capacity and the onset of fatigue. This includes the "glycogen shunt" hypothesis that glycogenolysis, but not glucose uptake, can produce glycosyl units at the rate necessary for glycolysis to produce ATP during muscular contraction, providing an explanation for observations that fatigue occurs when glycogen concentration is low but not yet depleted (Shulman and Rothman 2001). Furthermore, recent studies have indicated an additional role for glycogen, specifically intraMF pools, in regulating Ca^{2+} release from the sarcoplasmic reticulum during muscle contraction (Ortenblad, Nielsen et al. 2011, Nielsen, Cheng et al. 2014). These findings suggest critical roles for glycogen stores in muscle contraction and fatigue beyond the established primary roles as an important source of carbohydrate.

While a large body of research has clarified the role of skeletal muscle glycogen in determining exercise capacity in humans, findings in rodents have been equivocal. Mice lacking muscle glycogen via loss of GS have similar treadmill running endurance capacity to WT mice (Pederson, Cope et al. 2005). Conversely, mice with increased muscle glycogen content as a result of overexpression of GS1 do not have improved endurance compared to WT (Pederson, Cope et al. 2005). In addition to the relatively low levels of glycogen in rodent skeletal muscle compared to liver, these findings indicate that rodents are not necessarily dependent on skeletal muscle glycogen during submaximal endurance exercise. These findings are not likely to be applicable to tests of maximal exercise performance. A recent model with induced loss of muscle GS1 in adult mice displayed significantly reduced maximal and endurance running capacity (Xirouchaki, Mangiafico et al. 2016). These divergent results suggest that surviving mice with chronic loss of GS1 can potentially compensate to maintain exercise endurance capacity (e.g., by increasing oxidative muscle fibres) (Pederson, Cope et al. 2005). This potential discrepancy between humans and rodents is likely explained, at least in part, by the significantly lower relative levels of glycogen stores in rodent versus human skeletal muscle (Kjobsted, Hingst et al. 2018).

Skeletal muscle glycogen resynthesis is a priority during recovery from glycogen-depleting exercise. Complete glycogen resynthesis and/or supercompensation can occur within 3-5 h in humans and rodents with ingestion of CHO to promote resynthesis (Shearer, Wilson et al. 2005, Irimia, Rovira et al. 2012, Irimia, Tagliabracci et al. 2015). However, following extreme, glycogen-depleting exercise, such as prolonged cross-country skiing (Nielsen, Holmberg et al. 2011) and competitive soccer matches (Krustrup, Ortenblad et al. 2011, Nielsen, Krustrup et al. 2012), skeletal muscle glycogen resynthesis and supercompensation of all three subcellular glycogen pools can take up to 24-72 h. Delayed glycogen resynthesis may be attributable to exercise-induced muscle damage and the associated impairments in insulin sensitivity, as well as reductions in muscle GLUT4 content and translocation to the sarcolemma (Tee, Bosch et al. 2007). The usually rapid repletion of skeletal muscle glycogen is possibly due to an increase in fat oxidation, allowing carbohydrates to be spared to promote optimal glycogen repletion (Kiens and Richter 1998, Kimber, Heigenhauser et al. 2003), along with increased glucose uptake via the insulin-independent AMPK pathway. During recovery, skeletal muscle glycogen concentration is increased due to increased number of glycogen particles, rather than via increasing the size of the existing particles (Jensen, Ortenblad et al. 2021).

2.3.11 Hepatic Glycogen Utilisation and Synthesis

Liver glycogen plays a primary role in maintaining glucose availability during periods of fasting in between meals, as skeletal muscle glycogen is not significantly depleted during fasting in either humans (Nieman, Carlson et al. 1987, Vendelbo, Clasen et al. 2012) or rodents (Irimia, Tagliabracci et al. 2015). Glucagon promotes hepatic glycogenolysis to help maintain euglycemia in response to fasting (**Figure 2.7**) (Rothman, Magnusson et al. 1991, Petersen, Price et al. 1996, Hughey, James et al. 2017). Given the role of hepatic glucose output regulation in maintaining blood glucose in the post-prandial and fasting states, liver glycogen is significantly depleted in response to prolonged fasting in humans to help maintain blood glucose levels (Magnusson, Rothman et al. 1992). Given the highly invasive nature of liver biopsy sampling to measure hepatic glycogen content, little is known regarding the roles of liver glycogen in exercise in humans. However, using a combination of methods, including analysis of arteriovenous difference, stable isotope tracers, and ^{13}C magnetic resonance spectroscopy, liver glycogen dynamics can be estimated (Gonzalez, Fuchs et al. 2016).

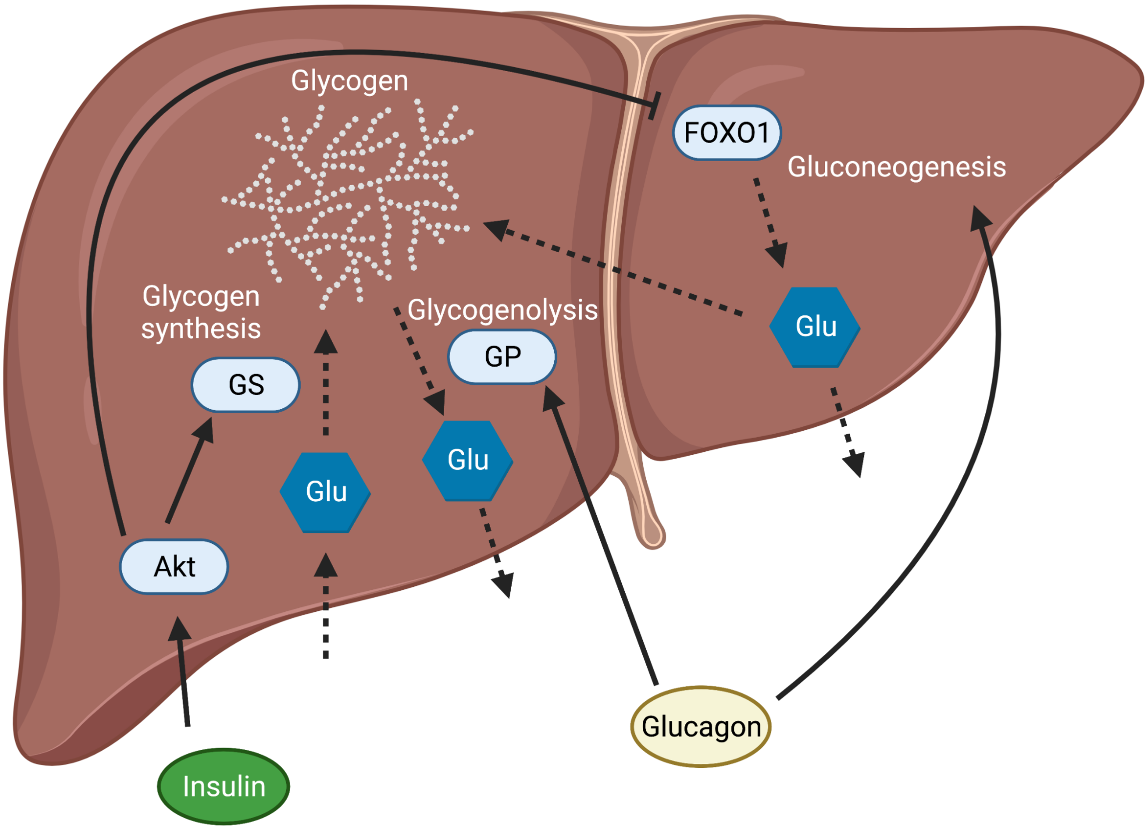

Figure 2.7 – Schematic representing some of the pathways regulating hepatic glycogen synthesis and breakdown. When stimulated by insulin, Akt phosphorylates GS to promote glycogen synthesis while simultaneously inhibiting gluconeogenesis by inhibiting FOXO1. The net result is increased glycogen content and reduced hepatic glucose output. Glucagon promotes glycogen breakdown and gluconeogenesis to upregulate hepatic glucose output. Created with BioRender.com.

Liver glycogen levels are reduced during sustained endurance exercise for 90 min at 70% of $VO_{2\ peak}$ (Stevenson, Thelwall et al. 2009). However, unlike skeletal muscle, where glycogen levels increase as a result of endurance training, fasted liver glycogen levels are similar in untrained and trained humans (Gonzalez, Fuchs et al. 2016). Conversely, trained individuals appear to have reduced hepatic glycogenolysis compared to untrained individuals with increasing exercise intensity (Gonzalez, Fuchs et al. 2016). It is unknown what adaptations in liver glycogen storage accompany exercise training, and, therefore, if hepatic glycogen concentration plays a functional role in regulating exercise endurance. In rodents, it has been hypothesised that liver glycogen plays a more significant role in determining exercise capacity than skeletal muscle (Pederson, Cope et al. 2005), based on the significantly larger stores of glycogen in rodent liver. Mice with elevated liver glycogen have increased endurance capacity while running at submaximal intensity compared with mice with normal liver glycogen (Lopez-Soldado, Guinovart et al. 2021). These findings further underscore potential species-specific roles of liver and skeletal muscle glycogen in exercise.

In liver, insulin stimulation promotes glycogen synthesis both via the Akt signalling pathway and by suppressing hepatic glucose output (**Figure 2.7**) (Cross, Alessi et al. 1995, Ramnanan, Edgerton et al. 2010). Specifically, insulin binds to the insulin receptor (Fruman, Meyers et al. 1998), resulting in a signalling cascade in which Akt is recruited to the plasma membrane (Alessi, Kozlowski et al. 1998, Mora, Komander et al. 2004), where it is phosphorylated by 3-phosphoinositide-dependent protein kinase 1 (PDK1) (Alessi, James et al. 1997). Insulin-mediated phosphorylation of Akt results in suppression of gluconeogenesis in the liver by phosphorylating and inhibiting forkhead box protein O1 (FOXO1) (Li, Monks et al. 2007, Cheng, Tseng et al. 2010, Altarejos and Montminy 2011). While this is the most well-established pathway of insulin-stimulated suppression of gluconeogenesis and hepatic glucose output, there are potentially Akt-independent pathways that downregulate hepatic glucose output in the post-prandial state (Lu, Wan et al. 2012). Following energy stress, glycogen synthesis in the liver also occurs following ingestion of carbohydrates and/or through gluconeogenesis (Woerle, Meyer et al. 2003, Adeva-Andany, Gonzalez-Lucan et al. 2016). Post-prandial increases in insulin stimulate activity of liver GS via dephosphorylation by the PKA, GSK3β, and Akt pathways in order to promote glycogen accumulation (Cross, Alessi et al. 1995, Brady, Nairn et al. 1997, Printen, Brady et al. 1997). Compared to skeletal muscle glycogen, which is relatively stable, the constant turnover of liver glycogen in both the post-prandial and fasting/energy-deficient states makes hepatic glycogen resynthesis relatively difficult to quantify.

2.4 Molecular Evidence of AMPK-Glycogen Binding

In 2003, it was first demonstrated that recombinant AMPK β1 CBM bound glycogen using a cell-free assay system (Polekhina, Gupta et al. 2003). Structural prediction and mutagenesis experiments targeting conserved residues within the CBM thought to mediate glycogen binding demonstrated that W100G and K126Q mutations abolished glycogen binding to the isolated β1 CBM, while W133L, S108E and G147R mutations partially disrupted glycogen binding. Additionally, the AMPK heterotrimeric complex was found to bind glycogen more tightly than the β1 subunit isoform in isolation. The reasons for this differential binding affinity, however, remain unclear (Polekhina, Gupta et al. 2003). Cell-free assays have also revealed that glycogen can have an inhibitory effect on AMPK activity (McBride, Ghilagaber et al. 2009), with mutation of critical residues in the β1 CBM (W100G, W133A, K126A, L148A and T148A) ablating the inhibitory effect of glycogen. In these cell-free assays, glycogen with higher branch points has a greater inhibitory effect on AMPK, indicating that glycogen particle size has the capacity to influence AMPK-glycogen interactions (McBride, Ghilagaber et al. 2009). It was also observed that glycogen particles co-localised with the β subunit of AMPK in the cytoplasm of CCL13 cells (Hudson, Pan et al. 2003). A follow-up structural-based study determined the CBM crystal structure in the presence of β-cyclodextrin and confirmed that AMPK indeed interacts with glycogen (Polekhina, Gupta et al. 2005). Additional experimental approaches such as immunogold cytochemistry have also shown that the AMPK α and β subunits in rat liver tissue are associated with the surface of glycogen particles in situ, providing further molecular evidence supporting this concept of physical AMPK-glycogen interaction (Bendayan, Londono et al. 2009).

In addition to its role in binding glycogen, the CBM of the β subunit also physically interacts with the kinase domain of the catalytic α subunit, forming a pocket, referred to as the allosteric drug and metabolite (ADaM) site. Small molecule AMPK activators such as A-769662, a β1 subunit isoform specific activator, bind to this site and directly activate AMPK

(Scott, van Denderen et al. 2008, Xiao, Sanders et al. 2013). However, to date, any connection of A-769662's subunit specificity in relation to glycogen has been highly speculative and further research is required to establish direct links. The AdaM site is stabilised by autophosphorylation of S108 on the CBM and is dissociated when T172 on the α subunit is dephosphorylated (Li, Wang et al. 2015). Mutation of S108 to a phosphomimetic glutamic acid (S108E) resulted in reduced glycogen binding (Polekhina, Gupta et al. 2003) and increased AMPK activity in response to AMP and A-769662, even in the presence of a non-phosphorylatable T172A mutation (Scott, Ling et al. 2014). Conversely, mutation of S108 to a neutral alanine (S108A) had no effect on glycogen binding (Polekhina, Gupta et al. 2003), but reduced AMPK activity in response to AMP and A-769662 (Scott, Ling et al. 2014). Collectively, these findings suggest that glycogen binding may inhibit AMPK activity by disrupting the interaction between the CBM and the kinase domain of the α subunit (McBride, Ghilagaber et al. 2009, Li, Wang et al. 2015, Garcia and Shaw 2017). The inhibitory role of β subunit T148 autophosphorylation on AMPK-glycogen binding has also been a focus of recent research. Mutation of T148 to a phosphomimetic aspartate (T148D) on the β1 subunit isoform inhibits AMPK-glycogen binding in cellular systems (Oligschlaeger, Miglianico et al. 2015). The results from subsequent experiments in isolated rat skeletal muscle suggest that T148 is constitutively phosphorylated both at rest and following electrical stimulation, therefore preventing glycogen from associating with the AMPK β2 subunit isoform (Xu, Frankenberg et al. 2016). However, further research is necessary to further elucidate the role of T148 in the context of AMPK-glycogen interactions in physiologically relevant *in vivo* settings.

Recent studies provide further structural insights into the affinity of the AMPK β subunit isoforms for carbohydrates. Isolated β2 CBM has a stronger affinity for carbohydrates than the β1 CBM, binding strongly to both branched and unbranched carbohydrates, with a preference for single α-1,6 branched carbohydrates (Mobbs, Di Paolo et al. 2017). One possible explanation for this difference is that a pocket is formed in the CBM by the T101 residue, which is unique to the β2 isoform, therefore allowing binding to branched carbohydrates (Koay, Woodcroft et al. 2010, Mobbs, Di Paolo et al. 2017). In addition, the β1 CBM possesses a threonine at residue 134 which may form a hydrogen bond with the neighbouring W133, restricting the ability of the β1 CBM to accommodate carbohydrates, while the β2 CBM possesses a valine which does not bond with W133 (Mobbs, Di Paolo et al. 2017). This difference may explain the increased affinity of the β2 isoform for branched carbohydrates even though the T134 residue does not directly contact carbohydrates (Mobbs, Di Paolo et al. 2017). These findings indicate that glycogen structure and branching affect AMPK binding, specifically to β1 subunit isoforms, which may dictate the inhibitory effect of glycogen observed in previous studies (McBride, Ghilagaber et al. 2009, Mobbs, Di Paolo et al. 2017). While the role of AMPK β isoform glycogen binding in the contexts of glycogen structure and branching has been investigated *in vitro*, it remains to be determined how these characteristics alter the dynamics of AMPK-glycogen binding *in vivo*.

2.5 Regulation of Cellular Energy Sensing by AMPK-Glycogen Binding

Several independent lines of evidence suggest that these physical AMPK and glycogen interactions also serve mechanistic functional roles in cellular energy sensing. A number of AMPK substrates are known to be directly involved in glycogen storage and breakdown, highlighting AMPK's role as an important regulator of glycogen metabolism. *In vitro*, AMPK regulates glycogen synthesis directly via phosphorylation and inactivation of GS at site 2 (Carling and Hardie 1989). In support of this finding, AMPK α2, but not α1, KO mice display blunted phosphorylation of GS at site 2 and higher GS activity in response to stimulation by the AMPK activator AICAR in skeletal muscle (Jorgensen, Nielsen et al. 2004). Paradoxically, chronic activation of AMPK also results in an accumulation of glycogen in skeletal and cardiac muscle (Hunter, Treebak et al. 2011). While these divergent outcomes appear contradictory, it has been proposed that prolonged AMPK activation leads to glycogen accumulation by increasing glucose uptake, and subsequently increasing intracellular G6P, a known allosteric activator of GS. This hypothesis is further supported by recent independent findings using highly specific and potent pharmacological activators demonstrating that skeletal muscle AMPK activation results in increased skeletal muscle glucose uptake and glycogen synthesis in mice and non-human primates (Cokorinos, Delmore et al. 2017, Myers, Guan et al. 2017). This accumulation of G6P overcomes the inhibition of GS by AMPK, thereby increasing GS activity (Hunter, Treebak et al. 2011). Furthermore, AMPK activation also shifts fuel utilisation towards FA oxidation post-exercise, allowing glucose to be utilised for glycogen resynthesis (Fritzen, Lundsgaard et al. 2015). In addition to regulating GS activity, phosphorylation of GS at site 2 by AMPK causes GS to localise to SS and interMF glycogen pools in humans (Prats, Helge et al. 2009). These findings have been replicated in mouse models, as an R70Q mutation of the AMPK $\gamma1$ subunit results in chronic activation of AMPK and glycogen accumulation in the skeletal muscle interMF region (Barre, Richardson et al. 2007). This has led to the suggestion that AMPK specifically senses and responds to interMF levels of glycogen (Prats, Gomez-Cabello et al. 2011), although further research is warranted to verify this hypothesis.

An increase in GP activity has also been observed to be associated with AMPK activation induced by AICAR treatment of isolated rat soleus muscle (Young, Leighton et al. 1996, Young, Radda et al. 1996). However, the ability to demonstrate a direct relationship between AMPK and GP activity has been limited by the identification of several AMPK-independent targets of AICAR, including phosphofructokinase (PFK), protein kinase C and heat shock protein 90 (Daignan-Fornier and Pinson 2012). Further research is therefore required to determine if such a relationship exists and, if so, elucidate the mechanism by which AMPK may regulate GP. In contrast, there is *in vitro* evidence that GDE binds to residues 68-123 of the AMPK $\beta1$ subunit isoform (Sakoda, Fujishiro et al. 2005). Mutations in this region that disrupt glycogen binding (W100G and K128Q) do not affect binding to GDE, indicating that GDE-AMPK binding is not likely mediated by glycogen (Sakoda, Fujishiro et al. 2005). AMPK's direct positive effect on glycogen accumulation, its known interaction with glycogen-associated proteins, and its ability to promote energy production through glucose uptake and fat oxidation when glycogen levels are low all support AMPK's proposed role as a cellular energy sensor. Given the limited *in vivo* data currently available directly linking AMPK to glycogen-associated proteins, additional studies are necessary to further understand potential direct binding partners and effects of AMPK on the glycogen-associated proteome.

Additional factors may also affect physical and functional AMPK-glycogen interactions. In a proteomic analysis of purified glycogen from rat liver, AMPK was not included in the proteins detected to be associated with glycogen (Stapleton, Nelson et al. 2010), and this has been replicated in a complementary study in adipocytes (Stapleton, Nelson et al. 2013). The authors suggested that this may be due to either AMPK protein being below the level of detection or the predominance of the AMPK β1 isoform expression in the tissues studied, as this isoform has lower affinity for glycogen compared to the β2 subunit isoform (Stapleton, Nelson et al. 2010, Stapleton, Nelson et al. 2013). In future studies interrogating AMPK and glycogen binding and functional interactions, considerations of β subunit isoform expression and glycogen localisation, as well as sample preparation and experimental variables that may limit the preservation and detection of AMPK-glycogen binding, are warranted to build upon this strong foundation of molecular and cellular evidence.

2.6 Linking AMPK and Glycogen to Exercise Metabolism in Physiological Settings

2.6.1 Regulation of Glycogen Storage by AMPK

In the fifteen years following the discovery of glycogen binding to the CBM on the β subunit, several studies utilising AMPK isoform KO mouse models have provided whole-body physiological evidence of AMPK's interactive functional roles with glycogen. Collectively, studies using AMPK α and β subunit KO mouse models have found that ablation of AMPK alters liver and skeletal muscle glycogen content, supporting the role of AMPK in the regulation of tissue glycogen dynamics *in vivo*. Specifically, mice with inducible deletion of muscle AMPK α1α2 have reduced resting glycogen levels (Hingst, Kjobsted et al. 2020), which is accompanied by reduced glycogen synthesis and ablated supercompensation of glycogen content in quadriceps muscle following submaximal exercise, despite similar glucose uptake to WT (Hingst, Bruhn et al. 2018). Whole-body β2 KO mice have reduced glycogen levels in both liver and skeletal muscle in the fed state associated with reduced muscle AMPK activity and attenuated maximal and submaximal running capacity compared to WT mice (Steinberg, O'Neill et al. 2010). AMPK β2 KO mice also display reduced expression and activity of α1 and α2 subunit isoforms as well as compensatory upregulation of the β1 subunit isoform in skeletal muscle (Steinberg, O'Neill et al. 2010). Additional experiments utilising this β2 KO model have demonstrated its negative impact on whole-body and tissue metabolism and exercise capacity associated with attenuated AICAR-induced AMPK phosphorylation and glucose uptake in skeletal muscle (Dasgupta, Ju et al. 2012). As a result of these changes in AMPK subunit expression and activity, it is difficult to elucidate the precise role of AMPK β2 in glycogen dynamics using this model. Similarly, muscle-specific AMPK β1/β2 KO mice display essentially no T172 phosphorylation in EDL and soleus muscle in response to electrical-stimulated contraction, and have reduced exercise capacity, carbohydrate utilisation, and glucose uptake during treadmill running (O'Neill, Maarbjerg et al. 2011). These defects were associated with reduced mitochondrial mRNA expression and reduced mitochondrial protein content (O'Neill, Maarbjerg et al. 2011). Collectively, these findings suggest important roles of the β subunit in regulating AMPK activity and signalling, cellular glucose uptake and glycogen storage, mitochondrial function, and whole-body exercise capacity and metabolism.

In addition to mouse models targeting the AMPK β subunit(s), recent studies utilising tissue-specific α1/α2 KO mice have provided support for the functional interactive roles of

AMPK and glycogen. Liver-specific AMPK α1/α2 KO mice have impaired ability to maintain euglycemia during exercise, as a result of decreased hepatic glucose output due to decreased glycogenolysis (Hughey, James et al. 2017). Specifically, hepatic glycogen content was reduced in these AMPK KO mice following both fasting and exercise. Phosphorylation of GS was unaffected in liver-specific AMPK α1/α2 KO mice, but a decrease in UDP-glucose pyrophosphorylase 2 (UGP2) content was observed, suggesting reduced glycogen synthesis due to decreased glycogen precursors rather than an altered ability to synthesise glycogen (Hughey, James et al. 2017). In addition, when challenged with a long-term (~20 h) fast, these mice had reduced hepatic glycogenolysis and were unable to maintain liver ATP concentration without AMPK activity, providing further support of AMPK's role as an energy sensor (Hasenour, Ridley et al. 2017). Inducible muscle-specific AMPK α1/α2 KO mice have ablated skeletal muscle glycogen resynthesis and rates of FA oxidation following exercise, even though glucose uptake was not affected, suggesting that AMPK functions as a switch to promote fat oxidation in order to preserve glucose for glycogen synthesis (Hingst, Bruhn et al. 2018). These findings indicate that AMPK can influence glycogen dynamics in physiological settings and that ablation of AMPK activity reduces hepatic glucose output in rodents and is critical for skeletal muscle glycogen supercompensation following exercise. Collectively, studies using genetic models and pharmacological activators to date indicate that AMPK activation regulates glycogen synthesis in striated muscle (i.e., skeletal and cardiac muscle) secondary to increased glucose uptake and G6P accumulation, but not in liver. Despite these findings from AMPK transgenic mouse models, the precise role(s) of glycogen binding to the β subunits in the functional regulation of these physiological processes, as opposed to ablation of the entire α subunits or β subunit(s) containing the CBM, remains to be elucidated.

2.6.2 Roles for Glycogen Availability in the Regulation of AMPK Activity

A series of physiological studies have demonstrated that low glycogen availability can amplify AMPK signalling responses and adaptations to exercise. This phenomenon was first described in rat skeletal muscle in which AICAR treatment resulted in increased AMPK α2 activity and markedly reduced GS activity in a glycogen-depleted compared to glycogen-loaded state (Wojtaszewski, Jorgensen et al. 2002). This observation was independent of adenine nucleotide concentrations and has subsequently been replicated in human skeletal muscle following exercise (Wojtaszewski, MacDonald et al. 2003). Additional studies of skeletal muscle have shown reductions in AMPK α1 and α2 association with glycogen, along with increased AMPK α2 activity and translocation to the nucleus following exercise in a glycogen-depleted state (Watt, Steinberg et al. 2004, Steinberg, Watt et al. 2006). This effect does not appear to be dose-dependent, as high intensity interval exercise following graded reductions of skeletal muscle glycogen resulted in similar increases in nuclear AMPK protein content in trained cyclists (Hearris, Owens et al. 2020). Furthermore, consumption of a high-fat, low-carbohydrate diet followed by one day of high-carbohydrate diet increases resting skeletal muscle AMPK α activity in human skeletal muscle compared to high-carbohydrate diet alone (Yeo, Lessard et al. 2008), supporting glycogen's inhibitory role on AMPK observed in cell free assays (McBride, Ghilagaber et al. 2009). In a follow-up study, AMPK T172 phosphorylation was increased by exercise to a greater extent in the glycogen-depleted muscle than normal glycogen repleted state (Yeo, McGee et al. 2010). Similarly, exercise in an overnight carbohydrate-fasted state resulted in increased AMPK T172 phosphorylation and upregulation of signalling pathways involved in FA oxidation (Lane, Camera et al. 2015), while low glycogen stimulated peroxisome proliferator activated receptor δ, a transcription factor that regulates fat utilisation, in rat skeletal muscle following treadmill running (Philp, MacKenzie et al. 2013). Reduced glycogen availability is also associated with increases in regulators of mitochondrial biogenesis, such as p53 and the transcriptional coactivator PGC1α

(Bartlett, Louhelainen et al. 2013, Psilander, Frank et al. 2013). While none of these *in vivo* studies have directly assessed the functional role of AMPK-glycogen physical interaction, together they provide important physiological insights into how AMPK activity, subcellular localisation and signalling may be regulated by glycogen binding (**Figure 2.8**).

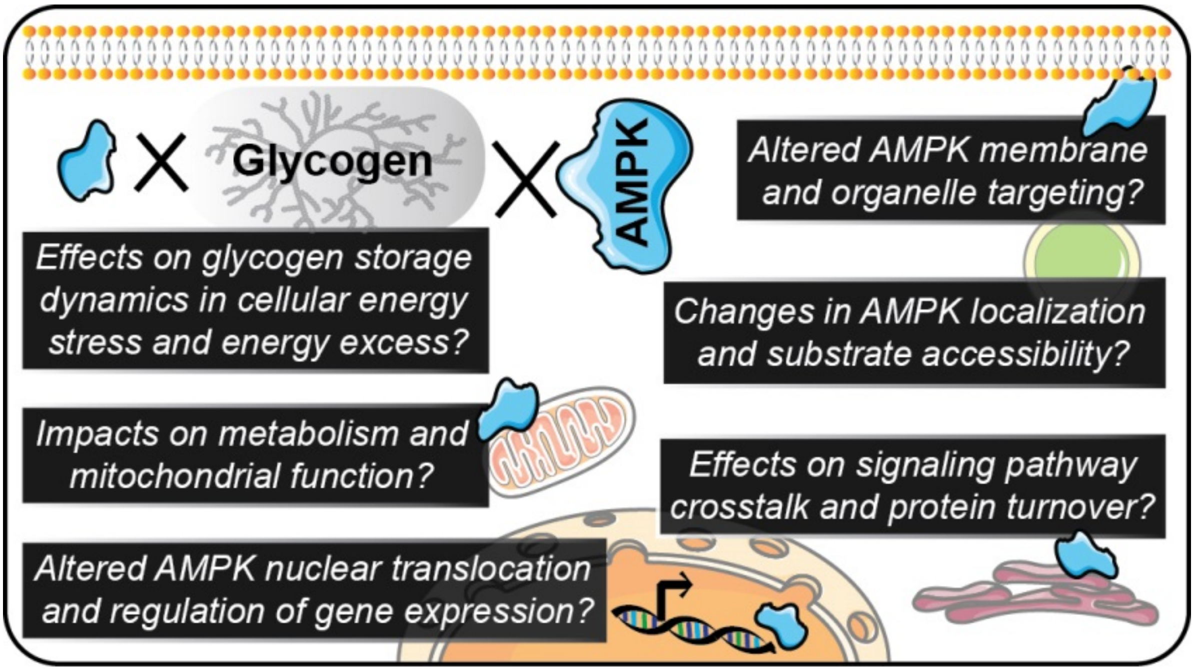

Glycogen
AMPK
Altered AMPK membrane and organelle targeting?
Effects on glycogen storage dynamics in cellular energy stress and energy excess?
Changes in AMPK localization and substrate accessibility?
Impacts on metabolism and mitochondrial function?
Effects on signaling pathway crosstalk and protein turnover?
Altered AMPK nuclear translocation and regulation of gene expression?

Figure 2.8 – There are several potential alterations in cellular metabolism and signalling as a consequence of dysregulated AMPK-glycogen interactions that represent key knowledge gaps in our current understanding and warrant further investigation. These potential alterations include changes in AMPK localisation, translocation, substrates and signalling pathway crosstalk, and subsequently, alterations in gene expression, cellular metabolism, and glycogen storage.

Furthermore, elevated glycogen levels in skeletal muscle of trained individuals can be accompanied by reduced AMPK activation and/or phosphorylation during acute endurance exercise. Comparison of trained versus untrained muscle found that trained muscle has higher fed, resting glycogen and increased glycogen utilisation during exercise associated with attenuated phosphorylation of AMPK T172 and ACC S79 in response to an acute bout of exercise (Nielsen, Mustard et al. 2003). Endurance training results in increased AMPK activity and phosphorylation of AMPK T172 in fed, rested human skeletal muscle, but AMPK activity and phosphorylation are attenuated in response to an acute bout of exercise compared to pretraining (Lee-Young, Canny et al. 2009, Mortensen, Hingst et al. 2013). Reduced AMPK activity and phosphorylation does not alter phosphorylation of GS S7 (Mortensen, Hingst et al. 2013), suggesting that AMPK may influence glycogen dynamics by other direct or indirect means. This reciprocal relationship between glycogen and AMPK activity in the context of exercise training further supports the hypothesis that glycogen binding allows AMPK to "sense" energy stores.

2.6.3 Metabolic Diseases as Models to Investigate AMPK-Glycogen Binding

Metabolic diseases such as insulin resistance and T2D are associated with impairments in AMPK activity, signalling and glycogen storage dynamics. Obese patients with T2D have reduced skeletal muscle AMPK, ACC, and AS160 phosphorylation following an acute bout of exercise (Sriwijitkamol, Coletta et al. 2007). In support of these findings, insulin resistance has been associated with suppressed AMPK activity in humans and mice (Witters and Kemp 1992, Sriwijitkamol, Coletta et al. 2007), although results have been equivocal (Musi, Fujii et al. 2001). Liver-specific AMPK α1/α2 KO mice display an inability to maintain hepatic glucose output during exercise, highlighting the role of AMPK in maintaining euglycemia (Hughey, James et al. 2017). Skeletal muscle GS activity has also been demonstrated to be affected by insulin resistance and T2D, as there is increased phosphorylation of GS at site 2, the site phosphorylated by AMPK, which is not seen in healthy controls, resulting in nearly complete GS inactivation and dysregulation of glycogen synthesis (Hojlund, Staehr et al. 2003). Continued research in metabolic disease populations and rodent models can provide more insight into the significance of dysregulated AMPK and glycogen dynamics.

Skeletal muscle glycogen levels are reduced in insulin resistance, due to the associated reductions in glucose uptake and impairments in glucose metabolism (Shulman, Rothman et al. 1990). While skeletal muscle of people with T2D display normal phosphorylation of GS at sites 3a + 3b, which are mediated by Akt and GSK3β, there is increased phosphorylation and inhibition of GS at sites 2 + 2a, leading to impaired glycogen synthesis (Hojlund, Birk et al. 2009). This corresponds with reduced insulin-stimulated GS activity in patients with obesity and T2D, but not those with only obesity, as demonstrated by euglycemic-hyperinsulinemic clamp (Damsbo, Vaag et al. 1991). Chronic lack of liver glycogen in mice results in whole-body glucose intolerance (Irimia, Meyer et al. 2010) and insulin resistance (Irimia, Meyer et al. 2017), suggesting that hepatic glucose disposal and/or storage is also important for glucose tolerance. Furthermore, hyperglycaemia, associated with impaired insulin secretion, results in accumulation of pancreatic glycogen both *in vivo* in diabetic mice and *in vitro* in diabetic human islets (Brereton, Rohm et al. 2016). Together, these results suggest that peripheral glucose disposal and glycogen synthesis in liver and skeletal muscle serve critical roles in maintaining glucose homeostasis and insulin sensitivity.

Glycogen storage diseases (GSD) provide pathophysiological models that can help provide additional insights into the influence of glycogen dynamics, particularly on AMPK. McArdle's disease is characterised by accumulation of skeletal muscle glycogen due to deficiency of GP (Martin, Rubio et al. 2004, Rubio, Lucia et al. 2006). Individuals with McArdle's disease display higher muscle glycogen both at rest and following exercise compared to healthy controls and increased AMPK α2 activity and reduced GS activity in response to exercise (Nielsen, Wojtaszewski et al. 2002). Patients with McArdle's disease also demonstrate increased glucose clearance and ACC phosphorylation, indicating that AMPK activity is increased in order to maintain ATP concentration by promoting glucose uptake and FA oxidation (Nielsen, Wojtaszewski et al. 2002). The inability to breakdown glycogen, when coupled with retained, albeit reduced, glycogen synthesis, likely results in glycogen accumulation and failure to utilise this energy source during exercise in this setting of disease. In line with this finding, mouse models of McArdle disease demonstrate reduced maximal running capacity (Nogales-Gadea, Pinos et al. 2012, Brull, de Luna et al. 2015). A mouse model of McArdle's disease containing a p.R50X mutation, a nonsense mutation of nucleotide 148 in exon 1 of the GP gene, showed increased fed, resting AMPK phosphorylation in the tibialis anterior and quadricep muscles, associated with increased GLUT4 content and increased AMPK-mediated glucose uptake compared to WT (Krag, Pinos et al. 2016). Following exhaustive exercise, McArdle mice display increased AMPK phosphorylation in the tibialis anterior and EDL muscles, while WT mice display no significant increase in AMPK activity (Nielsen, Pinos et al. 2018). While increased AMPK activity in McArdle patients and rodent models seems contrary to previous findings, the authors hypothesised that since the McArdle disease results in an inability to breakdown glycogen, there is a subsequent increase in AMPK activity in order to maintain energy balance via increased glucose uptake (Krag, Pinos et al. 2016, Nielsen, Pinos et al. 2018). Profoundly, McArdle patients can experience a "second wind" during exercise, which can be amplified with ingestion of CHO, and is likely attributable to this upregulation of glucose metabolism (Haller and Vissing 2002, Vissing and Haller 2003). Therefore, the inability to access carbohydrate stores in the form of skeletal muscle glycogen in McArdle's disease appears to play an important role in exercise capacity; however, the "glycogen shunt" hypothesis discussed above may also contribute to the exercise intolerance observed in McArdle patients and mouse models.

Other rodent models have directly targeted muscle GS, which is affected in patients with GSD 0b (Kollberg, Tulinius et al. 2007). Patients with GSD 0b often experience significant exercise intolerance, and in some cases, fatal cardiac arrest can occur following exercise (Kollberg, Tulinius et al. 2007, Sukigara, Liang et al. 2012). Muscle specific GS KO models display increased AMPK phosphorylation (Pederson, Schroeder et al. 2005) and markedly reduced glycogen content in skeletal muscle in the fed, resting state, likely due to retained capacity to break down but an inability to resynthesise glycogen (Pederson, Chen et al. 2004, Xirouchaki, Mangiafico et al. 2016).

Finally, knockout of glycogenin1 in mice, which models GSD 15, leads to glycogen accumulation in cardiac and skeletal muscle (Malfatti, Nilsson et al. 2014, Visuttijai, Hedberg-Oldfors et al. 2020), suggesting that glycogenin plays a critical role in regulating glycogen synthesis and particle size, but not formation (Testoni, Duran et al. 2017). Glycogenin KO mice have reduced maximal running speed but have dramatic increases in glycogen utilisation during exercise testing, which is driven by increased glycolysis in oxidative fibres without changes in fibre type (Testoni, Duran et al. 2017). This phenotype is consistent with findings in mice with constitutively active GS1 in muscle, which also leads to glycogen accumulation in skeletal muscle and reduced maximal exercise capacity (Testoni, Duran et al. 2017). While these studies did not assess the effect of loss of glycogenin on muscle AMPK content or activity, the glycogenin KO model mirrors most GSD models with impaired exercise capacity, indicating that AMPK activity may be affected. Together, these findings from several glycogen-related disease models challenge the hypothesis that greater muscle glycogen availability would lead to improved exercise performance, at least in rodents. Together, these models of obesity, insulin resistance, and GSD establish that dysregulation of AMPK-glycogen interactions occurs in states of metabolic disease.

2.7 Multidisciplinary Techniques and Models to Interrogate Roles for AMPK-Glycogen Interactions

While much remains to be discovered regarding the molecular and cellular roles and physiological consequences of AMPK-glycogen binding, recent multidisciplinary research in combination with technological advances can be used to help address remaining knowledge gaps. For example, global mass spectrometry-based phosphoproteomics have revealed a repertoire of new AMPK substrates, providing additional evidence regarding the complexity and interconnection of the AMPK signalling network (Hoffman, Parker et al. 2015). These phosphoproteomic analyses mapping the human skeletal muscle exercise signalling network before and immediately following a single bout of intense aerobic exercise, in combination with phosphoproteomic analysis of AICAR-stimulated signalling in rat L6 myotubes, identified several novel AMPK substrates such as AKAP1 (Hoffman, Parker et al. 2015). Other recent efforts have predicted and identified novel AMPK substrate phosphorylation sites via chemical genetic screening combined with peptide capture in whole cells (Schaffer, Levin et al. 2015), as well as via an affinity proteomics-based approach to analyse hepatocyte proteins containing the substrate recognition motif targeted by AMPK phosphorylation (Ducommun, Deak et al. 2015). Together these complementary large-scale approaches have expanded the range of biological functions known to be regulated by AMPK. While additional substrates residing in different subcellular locations and organelles will continue to be uncovered, the mechanisms underlying AMPK subcellular localisation and targeting to substrates residing in these different organelles remains largely unknown. Future global, unbiased studies employing phosphoproteomic approaches can help identify novel glycogen-associated AMPK substrates, post-translational regulation of glycogen regulatory machinery, AMPK subunit-specific regulation and subcellular substrate targeting. Furthermore, omics-based approaches will help reveal how AMPK-glycogen binding may impact other levels of biological regulation, such as the transcriptome, proteome, metabolome and lipidome, in the contexts of exercise, metabolism and beyond (Hoffman 2017).

Novel AMPK fluorescence resonance energy transfer (FRET)-based sensors have revealed heterogeneous activity and tissue-specific roles for AMPK. These sensors have permitted the spatiotemporal and dynamic assessment of AMPK activity in single cells (Tsou, Zheng et al. 2011), 3D cell cultures (Chennell, Willows et al. 2016) and transgenic mice (Konagaya, Terai et al. 2017). These biosensors build upon traditional methods to interrogate AMPK activity such as kinase assays and immunoblotting, which are limited to targeted measures of mean cellular protein phosphorylation and do not allow spatiotemporal and dynamic assessment of AMPK activity. Transmission electron microscopy (TEM) has been recently used to identify subcellular compartments of glycogen within skeletal muscle and establish the differences in utilisation and synthesis in response to exercise and recovery (Jensen, Ortenblad et al. 2020). Electron microscopy-based approaches have also been used to visualise AMPK-glycogen association in fixed rat liver samples (Bendayan, Londono et al. 2009). While improved microscopy technologies and sensors have been used to assess AMPK or glycogen localisation, few studies have directly assessed AMPK-glycogen interactions. Utilising these recent technical advancements will allow interrogation of AMPK-glycogen interactions and dynamics across species and physiologically relevant settings (**Figure 2.8**).

Despite the large body of research using *in vitro* models and physiological evidence indicating potential functional roles for AMPK-glycogen binding, no models are available to disrupt and/or examine this physical binding directly *in vivo*. AMPK subunit KO models, while providing important insights into the functions of AMPK, are limited by potential compensatory upregulation of other subunit isoforms or disrupted stability of the entire AMPK heterotrimer complex (e.g., (Steinberg, O'Neill et al. 2010)). In addition, directly assessing the function of β subunit glycogen binding is challenging when additional functions of AMPK are altered in the presence of subunit deletion, as AMPK activity is impaired when the scaffolding β subunit is removed. Technological advancements in mouse model systems will continue to help clarify the roles of tissue AMPK and glycogen in exercise capacity and whole-body metabolism in the context of health and disease. For example, Cre-LoxP gene editing can be used to generate cell- and tissue-specific transgenic models and, when Cre recombinase is activated by an exogenous inducer such as tamoxifen or tetracycline, can be used to induce gene excision and recombination in a time-controlled manner (Kim, Kim et al. 2018). This temporal and spatial control allows for investigation and differentiation of potential acute versus developmental roles of proteins in specific tissues. CRISPR/Cas9 gene targeting can be programmed to generate precise and specific transgenic modifications, including simultaneous multiple loci and single point mutations (Jinek, Chylinski et al. 2012, Li, Yang et al. 2020). Recent research has adapted CRISPR/Cas9 to a tool for genome editing that is based on transient RNA modification, which can alter protein function without permanently changing the genome (Abudayyeh, Gootenberg et al. 2017, Merkle, Merz et al. 2019). A combination of these transgenic modifications can provide powerful models with tissue-, cell- and/or time-controlled loss of function mutations *in vivo*. Using these techniques, design of novel *in vivo* models in the future will be informed by previous molecular and cellular findings to allow direct interrogation of the functional relevance of the β subunit and CBM. Generation of novel animal models to specifically target physical AMPK-glycogen binding will provide important advances regarding its physiological significance and capability to be targeted *in vivo* to modulate metabolism and the health benefits of exercise.

Finally, previous studies have primarily utilised centrifugation-based assays to detect and quantify physical AMPK-glycogen association. Novel biotechnological platforms and proximity assays will aid this investigation of AMPK-glycogen binding and AMPK's proximity to glycogen with improved sensitivity and specificity across molecular, cellular, and physiological models. Furthermore, newly developed kinase activity reporters (Depry, Mehta et al. 2015) and other non-radioactive activity assays (Yan, Gu et al. 2018) will help provide new measures of intracellular AMPK activity dynamics and complement traditional surrogate measures such as immunoblot analyses of AMPK and ACC phosphorylation. Together these technological advances expand the repertoire of available tools to monitor the range of biological processes regulated by AMPK and further our understanding of the mechanisms and physiological significance underlying AMPK-glycogen interactions.

2.8 Potential Therapeutic Relevance of Targeting AMPK-Glycogen Binding

Consistent with the therapeutic relevance of the CBM, several lines of evidence demonstrate the CBM may play a direct functional role in AMPK conformation and activation. The CBM contains the critical S108 autophosphorylation site required for drug-induced AMPK activation in the absence of AMP (Scott, Ling et al. 2014). Although located on opposite sides of the AMPK heterotrimer, the CBM is conformationally connected to the regulatory AMPK γ subunit and its stabilisation is affected by adenine nucleotide binding (e.g., AMP) to the CBS motifs (Gu, Yan et al. 2017). Despite physical AMPK-glycogen interaction being mediated by the β subunit, mutations in the γ subunit also result in alterations in AMPK activation and glycogen metabolism. The γ2 subunit isoform is known to contain mutations that cause constitutive AMPK activation resulting in glycogen storage diseases in humans. These mutations result in glycogen accumulation with coexisting deleterious effects on cardiac electrical properties that are characteristic of familial hypertrophic cardiomyopathy and Wolff-Parkinson-White syndrome (Arad, Benson et al. 2002). In addition, gain of function mutations in the AMPK γ3 subunit isoform predominantly expressed in skeletal muscle result in excess glycogen storage (Milan, Jeon et al. 2000) as well as improvements in metabolism via increased mitochondrial biogenesis (Garcia-Roves, Osler et al. 2008). Constitutive AMPK activation associated with these γ subunit mutations promotes glycogen synthesis by increasing glucose uptake. As noted previously, the CBM interacts with the α subunit, forming the ADaM site and stabilising the kinase domain of the α subunit in its active formation (Xiao, Sanders et al. 2013, Li, Wang et al. 2015). However, when glycogen binds to the CBM this interaction is destabilised, altering the ADaM site and inhibiting AMPK activity (Li, Wang et al. 2015). For example, isoform-specific allosteric inhibition of AMPK has been shown to be dependent on the β2 isoform CBM in glycogen-containing pancreatic beta cells (Scott, Galic et al. 2015). The CBM therefore functions as both a critical element of AMPK activation as well as a site for allosteric inhibition by glycogen, highlighting the therapeutic potential of new drugs targeting the ADaM site.

2.9 Isoform-Specific Consequences of KI Mutations to Disrupt AMPK-Glycogen Binding

Recent work from our research group using isoform-specific AMPK β subunit knock-in (KI) mouse models, in which AMPK-glycogen binding has been genetically disrupted by a single point mutation in either the β1 (W100A) or β2 (W98A) isoform, has helped establish isoform-specific consequences of KI mutation to disrupt AMPK-glycogen binding (**Figure 2.9**) (Hoffman, Whitfield et al. 2020). The KI mutation to induce loss of AMPK-glycogen binding *in vivo* is accompanied by substantial reduction of AMPK content in liver and skeletal muscle in β1 and β2 KI mice, respectively. The KI mutation in the β1 subunit isoform resulted in increased liver fat mass and increased rates of whole-body carbohydrate oxidation, but little impact on glucose tolerance, maximal exercise capacity, or exercise endurance. Meanwhile, β2 KI mice exhibited increased whole-body fat mass, glucose intolerance, and reduced maximal running speed compared to WT (Hoffman, Whitfield et al. 2020). However, mouse models with chronic whole-body disruption of AMPK-glycogen binding via simultaneous targeting of both β subunit isoforms via KI mutations are warranted to permit investigation of 1) the consequences of disrupting whole-body AMPK-glycogen binding and potential compensatory or synergistic effect of KI of both β subunits; and 2) the effects of disrupting whole-body AMPK-glycogen binding on glycogen dynamics in response to various energy stresses (i.e., fasting and exercise).

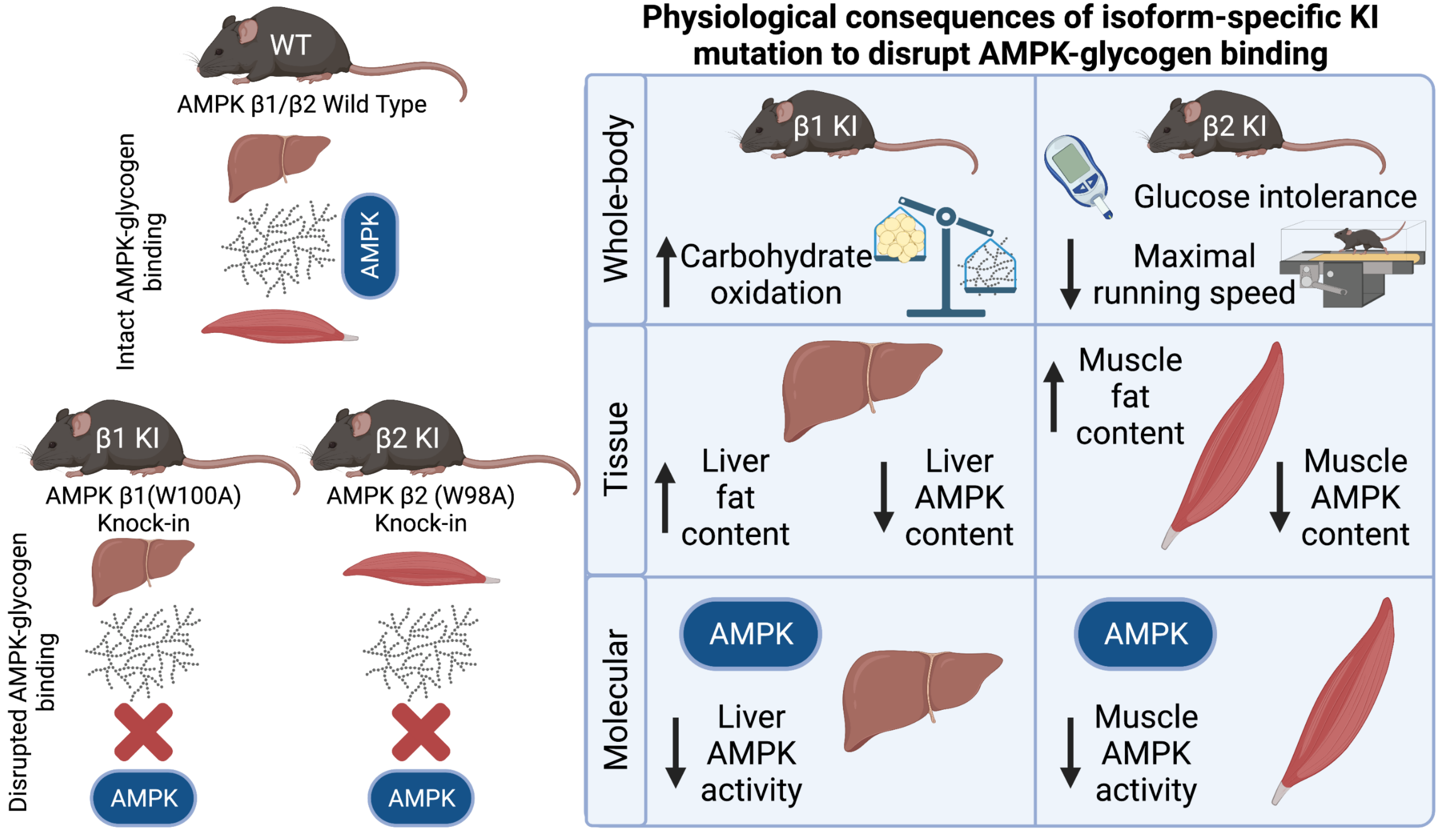
WT
AMPK β1/β2 Wild Type
Intact AMPK-glycogen binding
AMPK
β1 KI
AMPK β1(W100A) Knock-in
β2 KI
AMPK β2 (W98A) Knock-in
Disrupted AMPK-glycogen binding
AMPK
AMPK
Physiological consequences of isoform-specific KI mutation to disrupt AMPK-glycogen binding
Whole-body
β1 KI
↑ Carbohydrate oxidation
β2 KI
Glucose intolerance
↓ Maximal running speed
Tissue
↑ Liver fat content
↓ Liver AMPK content
↑ Muscle fat content
↓ Muscle AMPK content
Molecular
AMPK
↓ Liver AMPK activity
AMPK
↓ Muscle AMPK activity

Figure 2.9 – Summary of findings in single AMPK β subunit isoform knock-in (KI) mice with disrupted AMPK-glycogen binding in either the β1 or β2 isoform. Adapted from Hoffman, Whitfield et al. 2020. Created with BioRender.com.

2.10 Conclusions

AMPK is a central regulator of cellular energy status and plays key cellular roles in metabolism and exercise responses. A growing body of evidence demonstrates that AMPK binds glycogen, and this interaction can alter the conformation of AMPK, and subsequently, its activity and downstream signalling. AMPK activity subsequently regulates glycogen metabolism. Recent research has described experimental and physiological settings that affect AMPK and glycogen interactions, including AMPK β isoform affinity, glycogen availability and particle size. Despite our expanding knowledge of AMPK's relationship with glycogen, much remains to be elucidated regarding the roles of AMPK-glycogen on whole-body metabolism and tissue glycogen dynamics in response to various energy stresses (i.e., fasting and exercise), and potential compensatory or synergistic roles of glycogen-binding via the β subunits. Further research using new technologies and experimental models can help reveal additional mechanisms underlying AMPK and glycogen's interactive roles in cellular energy sensing, exercise, and metabolism. Together these findings will help provide insights into the physiological roles and therapeutic relevance of AMPK and glycogen binding in health and disease. To address some of these questions, the work undertaken in this thesis aimed to determine the phenotypic effects of an AMPK double knock-in (DKI) mutation utilised to chronically disrupt whole-body AMPK-glycogen binding on whole-body and tissue metabolism, including tissue glycogen dynamics in response to energy stress.

Funding: This work was supported by Australian Catholic University (ACU) Faculty of Health Sciences Open Access Publishing Support awarded to NRJ and an ACU research funding (ACURF) Early Career Researcher Grant awarded to NJH.

Acknowledgements: The authors acknowledge that all publications related to AMPK and glycogen could not be discussed in this review article due to word limitations and the primary focus on studies published within the past two decades.

Conflicts of Interest: The authors declare no conflict of interest.

Chapter 3 Methodology and Design

In keeping with Australian Catholic University guidelines, the methods utilised within each study of this thesis are described in full. In **Chapter 4** and **Chapter 6**, the methods section for each study is written per the guidelines of the respective journal.

3.1 Study 1 – Phenotypic Effects of the AMPK DKI Mutation on Whole-Body and Tissue Metabolism

3.1.1 Animal Models

CRISPR/Cas9 gene targeting was used to generate two whole-body single KI mouse models on a C57BL/6J background. Several residues on the respective β isoforms – including W100 within the β1 isoform and the analogous residue W98 in the β2 isoform – have been identified as essential for AMPK-glycogen binding, as mutations in these sites results in inhibition of glycogen binding (Polekhina, Gupta et al. 2003, Polekhina, Gupta et al. 2005, McBride, Ghilagaber et al. 2009). Therefore, these tryptophan residues in the AMPK β1 (W100A) and β2 (W98A) subunit isoforms were mutated to alanine, as described previously (Hoffman, Whitfield et al. 2020).

Heterozygous mice possessing either the β1 W100A or β2 W98A KI mutation were subsequently crossed to generate AMPK β1(W100A)/β2(W98A) DKI mice (**Figure 3.1**). Homozygous carriers of the DKI mutation were used for breeding, and DKI and WT breeders were annually backcrossed to generate heterozygous mice and rederive the homozygous DKI line used for experimentation. Confirmatory genotyping was performed from tail samples by TransnetYX (Cordova, TN, USA).

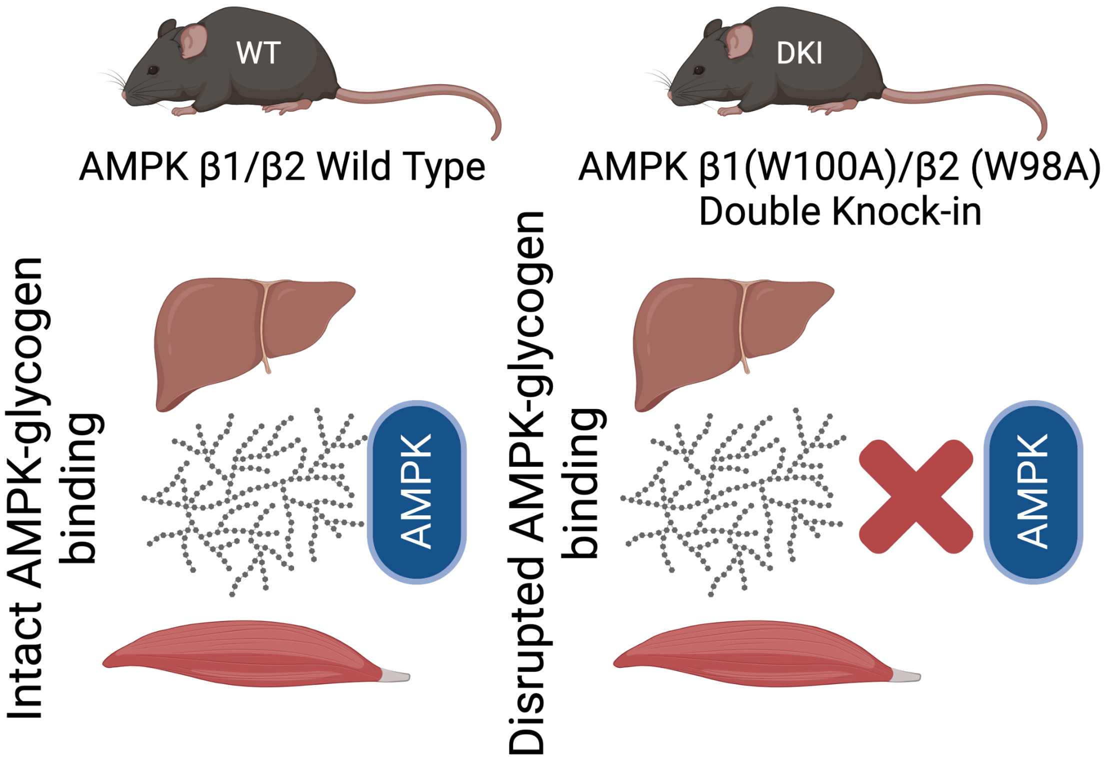

Figure 3.1 – Double knock-in (DKI) mouse models with chronic whole-body disruption of AMPK-glycogen binding. Wild type (WT) mice retain capacity for AMPK and glycogen to bind, while single amino acid mutations within the β1 and β2 isoforms in DKI mice result in disrupted whole-body AMPK-glycogen binding. Liver and skeletal muscle are highlighted as the primary-glycogen storing tissues and for their involvement in metabolic control and exercise responses. Created with BioRender.com.

Experiments were undertaken using age-matched, 8-32 week old male AMPK DKI and WT control mice. Only male mice were used in this study in order to maintain adequate DKI female breeder availability and ensure sufficient age matched DKI mice were readily available for experiments. Mice were group housed in a temperature (22°C) and humidity-controlled facility with a 12:12 h light and dark cycle. Mice were given *ad libitum* access to a standard chow diet (6% fat, 20% protein and 29% starch; Barastoc, Ridley Agriproducts, Pakenham, Victoria, Australia) and water, unless otherwise specified. All mouse procedures were performed under approval of the St. Vincent's Hospital (Melbourne, Victoria, Australia) Animal Ethics Committee (AEC 025-15 and 011-19), conforming to all the requirements of the National Health and Medical Research Council of Australia (NHMRC) and in accordance with the Australian code of practice for the care and use of animals for scientific purposes (8th Edition 2013).

3.1.2 Whole-Body Composition Measurements

Whole-body composition (fat mass and lean mass) was assessed by nuclear magnetic resonance using the EchoMRI Body Composition Analysis system (EchoMRI, Houston, TX, USA). Mice were restrained in opaque tubes during measurements (~90 sec) to minimise stress and movement. Measurements were made in the fed state (0900 h).

3.1.3 Metabolic Caging

Mice underwent metabolic cage analyses using the Comprehensive Lab Animal Monitoring System (CLAMS, Columbus Instruments, Columbus, OH, USA). Mice had either *ad libitum* access to chow or were fasted overnight. Mice with *ad libitum* access to chow were singly housed for ~60 h total at 21°C; food intake, infrared-based ambulatory activity, O_2 consumption (VO_2), CO_2 production (VCO_2), and RER ($VCO_2 \cdot VO_2^{-1}$) were measured continuously every ~18 min per cage. The first ~12 h served as the acclimatisation period and were not included for analysis. Following acclimatisation, hourly, light/dark cycle and 24 h averages were calculated for all measures. Total energy expenditure (TEE) and rates of fat and CHO oxidation were calculated, as previously described (Peronnet and Massicotte 1991). Mice underwent body composition measurements using EchoMRI before and after metabolic cage analysis and were then returned to their home cages with *ad libitum* access to food and water.

For responses to fasting, mice were acclimatised (~6 h) before food was removed at the start of the dark cycle (1800 h). Mice were fasted overnight (~14 h) and ambulatory activity, VO_2, and VCO_2 were measured continuously and used to calculate RER, average

TEE, and substrate oxidation rates. Upon completion of the fast, mice were returned to their home cages with *ad libitum* access to food and water.

3.1.4 Intraperitoneal Glucose Tolerance and Insulin Tolerance Testing

Commencing at 0800 h, mice were fasted for either 6 h (IPGTT) or 4 h (IPITT) and then injected with glucose (1 $g \cdot kg^{-1}$ total lean mass; Sigma-Aldrich, St. Louis, MO, USA) or insulin (0.5 $U \cdot kg^{-1}$ total body mass; Humulin, Eli Lilly and Company, Indianapolis, IN, USA). Blood glucose was monitored via tail tip bleed using a glucometer (Accu-Check Performa, Roche Diagnostics GmbH, Mannheim, Germany). Blood glucose was assessed at 0- (fasted baseline measurement for each test), 20-, 40-, 60-, 90-, and 120-min post glucose or insulin injection. Mice were monitored continuously during the tests and, upon completion, were returned to their home cage with *ad libitum* access to food and water. Mice were allowed at least one week of recovery between tests.

3.1.5 Fasting and Refeeding Protocol

A separate cohort of mice were divided into 4 groups (fed, fasted [0 h post fast], post glucose [5 h post fast], and refed [24 h post fast]) to investigate a time course of glycogen resynthesis (**Figure 3.2**). Fed mice had *ad libitum* access to chow while other cohorts were fasted in separate cages. All mice had *ad libitum* access to water. Mice were fasted overnight (~14 h) to promote significant depletion of liver glycogen stores (Ayala, Bracy et al. 2006). At 0800 h the following morning, blood glucose was measured in all mice via tail tip bleed using a glucometer. Fed and fasted mice were culled via cervical dislocation, and tissues were dissected and immediately snap frozen for subsequent analysis. The remaining fasted mice received a glucose bolus via oral gavage (3.6 g $glucose \cdot kg^{-1}$ body weight). This method of glucose administration was chosen to replicate the normal physiological processes of glucose absorption and metabolism following CHO consumption (Ayala, Samuel et al. 2010). Blood glucose responses were monitored in all remaining mice over a period of 5 h, after which tissues were dissected from the third cohort (post glucose) and snap frozen, as described above. At this point, mice in the final cohort (refed) were given *ad libitum* access to chow to promote optimal glycogen resynthesis and comply with animal ethics requirements regarding mouse fasting duration. The following morning (24 h after the administration of glucose via oral gavage) blood glucose was assessed, mice were culled via cervical dislocation, and tissues were dissected from the final cohort and snap frozen.

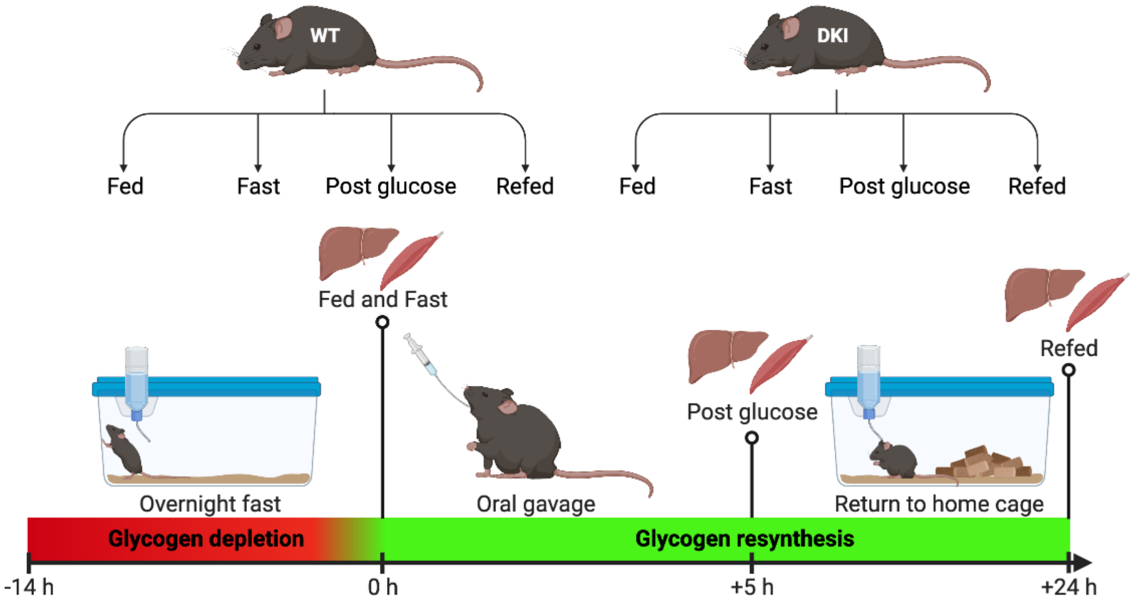
WT
DKI
Fed
Fast
Post glucose
Refed
Fed
Fast
Post glucose
Refed
Fed and Fast
Post glucose
Refed
Overnight fast
Oral gavage
Return to home cage
Glycogen depletion
Glycogen resynthesis
-14 h
0 h
+5 h
+24 h

Figure 3.2 – Fasting-induced glycogen depletion and repletion protocol. WT and DKI mice were each divided into four cohorts. Fasting mice (fast, post glucose, and refed cohorts) underwent an overnight fast (~14 h) to promote liver glycogen depletion, while the fed cohorts had *ad libitum* access to chow. The following morning, blood glucose was assessed in all mice via tail tip bleed. Fed and fast mouse cohorts were culled, and tissues were dissected and snap frozen. Mice in the post glucose and refed cohorts received a glucose bolus via oral gavage (3.6 g glucose·kg^{-1} body weight) to promote glycogen synthesis with no access to chow for 5 h. Blood glucose was assessed periodically and at 5 h-post glucose administration, mice from the post glucose cohorts were culled and tissues were dissected and snap frozen. Mice in the refed cohort were returned to their home cages with *ad libitum* access to chow. At 24 h-post glucose administration, blood glucose was assessed and tissues were dissected from the refed cohort and snap frozen. Created with BioRender.com.

3.1.6 Serum Analysis

Blood samples were collected from the retro-orbital vein and left to clot for 30 min at room temperature in non-coated polypropylene tubes before being placed on ice. Samples were then centrifuged at 10,000 *g* for 5 min at 4°C, and the resulting serum supernatant was aliquoted and stored at -80°C. Hormone and lipid concentrations were assessed in these aliquots using glucagon and ultra-sensitive mouse insulin (Crystal Chem, Elk Grove Village, IL, USA) and leptin (Abcam, Cambridge, UK) ELISA kits, and NEFA-C (Non-esterified fatty acid; Wako Pure Chemical Industries, Osaka, Japan) and triglyceride (TAG; Abcam) colorimetric assay kits according to the respective manufacturer's instructions.

3.1.7 Assessment of Tissue Glycogen Content

Snap-frozen gastrocnemius muscle (~40 mg) and liver (~25 mg) samples were chipped under liquid N_2, freeze-dried overnight, powdered, and dissected free of visible blood and connective tissue. Aliquots of powdered tissue (~2-4 mg) were then alkaline extracted, and the supernatant was used for quantification of glycogen content using spectrophotometry as described previously (Bergmeyer 1974). Briefly, background glucose and hexose monophosphates were destroyed by adding 0.1 M NaOH, then samples were neutralised with a solution containing 0.1 M HCl, 0.2 M citric acid, and 0.2 M Na_2HPO_4. Amyloglucosidase (~1.0 $U \cdot sample^{-1}$) was used to degrade glycogen into glucose and glucose-6-phosphate. Samples were stored at -80°C until further analysis. To promote the production of 6-phosphate-gluconolactone and NADH, 1.0 U hexokinase, 1.0 U glucose-6-phosphate dehydrogenase, 0.75 mM ATP, and 1.0 mM NAD were added to samples in a 96-well plate. Absorbance was measured at 340 nm using a SpectraMax Paradigm plate reader and data was acquired using SoftMax Pro microplate data acquisition software (Molecular Devices, San Jose, CA, USA). Glycogen content was determined using the Bougeur-Lambert-Beer law, as previously described (Bergmeyer 1974). Units of glycogen were expressed as mmol glucosyl $units \cdot kg^{-1}$ dry weight.

3.1.8 Immunoblotting

Snap-frozen liver, gastrocnemius muscle, and adipose tissue samples were lysed in homogenisation buffer containing 50 mM Tris.HCL, pH 7.5, 1 mM EDTA, 1 mM EGTA, 10% glycerol, 1% Triton-X, 50 mM sodium fluoride, 5 mM sodium pyrophosphate with cOmplete Protease Inhibitor Cocktail and PhosSTOP phosphatase inhibitor tablets (Sigma-Aldrich, St. Louis, MO, USA). Lysed tissue samples were centrifuged at 16,000 *g* for 30 min at 4°C, and supernatant protein content was determined using the bicinchoninic acid method (BCA; Pierce, Rockford, IL, USA). Samples were equilibrated with Laemelli's sample buffer, DTT, and bromophenol blue, and lysates were aliquoted, a subset of which were boiled for 5 min at 95°C, and stored at -80°C until blotting. Tissue lysates (10 mg protein$\cdot$well^{-1}) were run on 4-15% or 4-20% precast stain-free gels (Bio-Rad, Hercules, CA, USA) in Tris/Glycine/SDS buffer (Bio-Rad) for approximately 60 min using a Mini PROTEAN Tetra Cell (Bio-Rad). Samples were then transferred to PVDF membranes (Merck Millipore, Burlington, MA, USA) at 60 V for 2 h using a Criterion Blotter (Bio-Rad). Stain-free images were captured before membranes were blocked with 7.5% BSA in Tris-buffered saline containing 0.1% Tween 20 (TBS-T) for 1 h at room temperature, then incubated with primary antibodies with rocking as detailed in **Table 3.1**. After washing with TBS-T, membranes were incubated for 1 h at room temperature in either an anti-rabbit IgG (GAR) or anti-mouse IgG (GAM) horseradish-peroxidase-conjugated secondary antibody from Cell Signaling Technology (CST; Danvers, MA, USA) in TBS-T. Proteins were detected via chemiluminescence using SuperSignal West Femto Maximum Sensitivity Substrate (Thermo Fisher Scientific, Waltham, MA, USA) and imaged using the ChemiDoc Imaging System (Bio-Rad). Band intensities of total proteins and phosphorylation sites were normalised to the total lane protein from the respective stain-free image using Image Lab software (version 6, Bio-Rad), as described previously (Tachtsis, Whitfield et al. 2020), and phosphorylation was expressed relative to respective total protein content. Primary and secondary antibody details are listed in **Table 3.1**.

3.1.9 RNA Extraction and Gene Expression Analysis

RNA was extracted from snap-frozen liver (15 mg) and gastrocnemius muscle (25 mg) from overnight fasted (~14 h) mice using TRIzol LS Reagent (Life Technologies, Carlsbad, CA, USA). Tissues were homogenised in TRIzol LS Reagent in RNase-free, DNase-free polypropylene tubes, then incubated at room temperature for 5 min. Chloroform was added and mixed thoroughly by shaking. Samples were centrifuged at 12,000 *g* for 15 min at 4°C and the clear aqueous layer containing RNA was extracted. The remaining interphase and organic layers were discarded. RNA was precipitated from the aqueous layer with isopropanol. Following a 10 min incubation at 4°C, samples were centrifuged at 12,000 *g* for 10 min at 4°C. The supernatant was removed, and the remaining RNA precipitate was resuspended in 75% EtOH, vortexed briefly, and centrifuged at 7,500 *g* for 5 min at 4°C. After the supernatant was removed, the RNA pellet was airdried for ~10 min. Finally, pellets were resuspended in 50 µl of RNase-free water containing 0.1 mM EDTA. RNA was stored at -80°C until further analysis.

Aliquots of RNA samples were used to determine sample RNA concentration ($ng \cdot \mu l^{-1}$) using the Qubit RNA HS Assay (Invitrogen). RNA quality was determined in randomly selected samples by assessing the ratio of 260:280 nm absorbance using a Nanodrop2000 spectrometer (Thermo Fisher) to ensure the ratio was ~2.

RNA (100-600 ng for skeletal muscle and 400-1000 ng for liver) was treated with Amplification Grade DNase I (Invitrogen). These ranges in RNA concentrations were due to variance in sample extraction efficiency and subsequent availability of RNA. All RNA from each sample was then reverse transcribed using a SuperScript VILO Master Mix (Life Technologies). Total sample volumes were 20 µl and final concentrations of cDNA were 20-

50 ng·μl^{-1} for liver and 5-30 ng·μl^{-1} for skeletal muscle. cDNA samples were stored at -20°C until further analysis. Pre-Amplification was completed with 2 ng (liver) and 1.5 ng (skeletal muscle) cDNA using TaqMan Gene Expression Assays and PreAmp Master Mix (Applied Biosystems, Foster City, CA, USA).

Quantitative polymerase chain reaction (qPCR) was performed in 96-well plate format using a Bio-Rad CFX Connect Real-Time System. Quantification of mRNA for target genes (i.e., *Prkab1* and *Prkab2*) was analysed in triplicate and the normalisation gene (i.e., *Gapdh*) was analysed in duplicate. Gene expression was normalised to GAPDH using TaqMan Fast Advanced Master Mix (Applied Biosystems). *Prkab1* (liver, AMPK β1; Mm01201921_m1), *Prkab2* (skeletal muscle; Mm01257133_m1), and *Gapdh* (liver and skeletal muscle; Mm99999915_g1) TaqMan Gene Expression Assays were used (Applied Biosystems). Expression of *Gapdh* was similar between genotypes in both liver and skeletal muscle. Relative levels of mRNA were assessed using the ΔΔCt method to determine the fold change in mRNA expression between respective WT and DKI tissues (Livak and Schmittgen 2001).

3.1.10 Statistical Analyses

Comparisons between genotypes were analysed using unpaired two-tailed Student's *t* testing (WT versus DKI) or two-way analysis of variance (ANOVA; WT versus DKI comparisons over time or condition). Measurements of body mass and composition were analysed using linear mixed models. If significance was detected using ANOVA or linear mixed models, Bonferroni post hoc testing was applied where appropriate. All statistical analyses were performed using GraphPad Prism software (version 9, GraphPad Software, La Jolla, CA, USA). Significance was set at $p < 0.05$. All data are presented as mean ± standard error of the mean (SEM).

3.2 Study 2 – Phenotypic Effects of the AMPK DKI Mutation on Exercise Capacity and Substrate Utilisation

3.2.1 Animal Models

CRISPR/Cas9 gene targeting was used to generate two whole-body single KI mouse models on a C57BL/6J background. Tryptophan residues in the AMPK β subunit isoforms that are critical for glycogen binding (Polekhina, Gupta et al. 2005, McBride, Ghilagaber et al. 2009) – W100 within the β1 isoform (W100A) and the analogous residue in the β2 isoform (W98A), respectively – were mutated to alanine, as described previously (Hoffman, Whitfield et al. 2020). Heterozygous mice possessing either the β1 W100A or β2 W98A KI mutation were subsequently crossed to generate AMPK β1(W100A)/β2(W98A) DKI mice (**Figure 3.1**). Homozygous carriers of the DKI mutation were used for breeding, and DKI and WT breeders were annually backcrossed to generate heterozygous mice and rederive the homozygous DKI line used for experimentation. Confirmatory genotyping was performed from tail samples by TransnetYX (Cordova, TN, USA).

Experiments were undertaken using age-matched, 17-32 week old male AMPK DKI and WT control mice. Only male mice were used in this study in order to maintain adequate DKI female breeder availability and ensure sufficient age matched DKI mice were available for experiments. Mice were group housed in a temperature (22°C) and humidity-controlled facility with a 12:12 h light and dark cycle. Mice were given *ad libitum* access to a standard chow diet (6% fat, 20% protein and 29% starch; Barastoc, Ridley Agriproducts, Pakenham, Victoria, Australia) and water, unless otherwise specified. All mouse procedures were performed under approval of the St. Vincent's Hospital (Melbourne, Victoria, Australia) Animal Ethics Committee (AEC 025-15 and 011-19), conforming to all the requirements of the NHMRC and in accordance with the Australian code of practice for the care and use of animals for scientific purposes (8th Edition 2013).

3.2.2 Maximal Running Speed and Time to Exhaustion

Maximal and endurance treadmill running were completed on a Columbus Instruments Exer 3/6 rodent treadmill (Columbus Instruments, Columbus, OH, USA). Physical encouragement during treadmill acclimatisation and exercise testing was provided using manual prodding with a bottle brush. Testing was completed in the fed state and at the same time of day to ensure consistency between light/dark cycle and diurnal patterns of feeding and glycogen availability.

Mice underwent 4 days of treadmill acclimatisation prior to completing the maximal exercise test, as described previously (Hoffman, Whitfield et al. 2020). On the first day, mice were familiarised and allowed to rest on the treadmill for 15 min. Mice ran for 5 min on the treadmill at 5 $m \cdot min^{-1}$ on day 2 and 10 $m \cdot min^{-1}$ on day 3. On day 4, mice ran 5 min at 10 $m \cdot min^{-1}$, 5 min at 12 $m \cdot min^{-1}$, and 5 min at 15 $m \cdot min^{-1}$. On day 5, mice completed an incremental maximal exercise capacity test with the treadmill set at a 0° incline, as described in **Figure 3.3**.

For the maximal treadmill test at 0° incline, mice were randomly assigned to groups in order to complete maximal testing in several mice simultaneously. Mice ran for 2 min at 10 $m \cdot min^{-1}$ as a warm-up to help prevent potential injuries, after which speed was increased 1 $m \cdot min^{-1}$ every 2 min until each mouse reached exhaustion, which was defined as an inability to compel the mouse to stay on the treadmill (Steinberg, O'Neill et al. 2010, O'Neill, Maarbjerg et al. 2011). Upon exhaustion, mice were allowed to rest stationary at the back of the treadmill until all other mice had finished testing. Mice were then returned to their home cages with *ad libitum* access to food and water.

After 2-3 days of rest following maximal exercise testing, a subset of mice completed an endurance capacity test. Mice ran for 2 min at 10 $m \cdot min^{-1}$ as a warm-up, after which speed was increased to 70% of individual maximal running speed. Mice with similar maximal running speeds (i.e., within 2 $m \cdot min^{-1}$) were grouped to complete their endurance tests simultaneously. Upon exhaustion, individual mice were allowed to rest stationary at the back of the treadmill until all other mice finished running. Mice were then returned to their home cages with *ad libitum* access to food and water. All treadmill acclimatisation, maximal testing, and endurance testing were completed at a 0° incline commencing at 0900 h.

In order to assess liver and skeletal muscle glycogen use and skeletal muscle AMPK signalling in response to maximal exercise, a separate cohort of mice underwent acclimatisation as described above but completed a maximal running test at a 5° incline (**Figure 3.3**). Blood glucose and lactate were measured via tail tip bleeding the morning before and immediately following the maximal running test using an Accu-Check Performa glucometer (Roche Diagnostics GmbH, Mannheim, Germany) and Lactate Pro analyser (Arkray, Kyoto, Japan). Tail tip bleeding was performed the day before to allow healing and avoid tails bleeding on the treadmill belts during the maximal test. Maximal running tests commenced at 0900 h. Mice were culled via cervical dislocation immediately following the maximal running test, and tissues were excised, immediately snap frozen in liquid N_2, and stored at -80°C until subsequent biochemical analysis. Control rested mice did not undergo the maximal running test and remained in their home cage until being culled via cervical dislocation in the fed state at 0900 h.

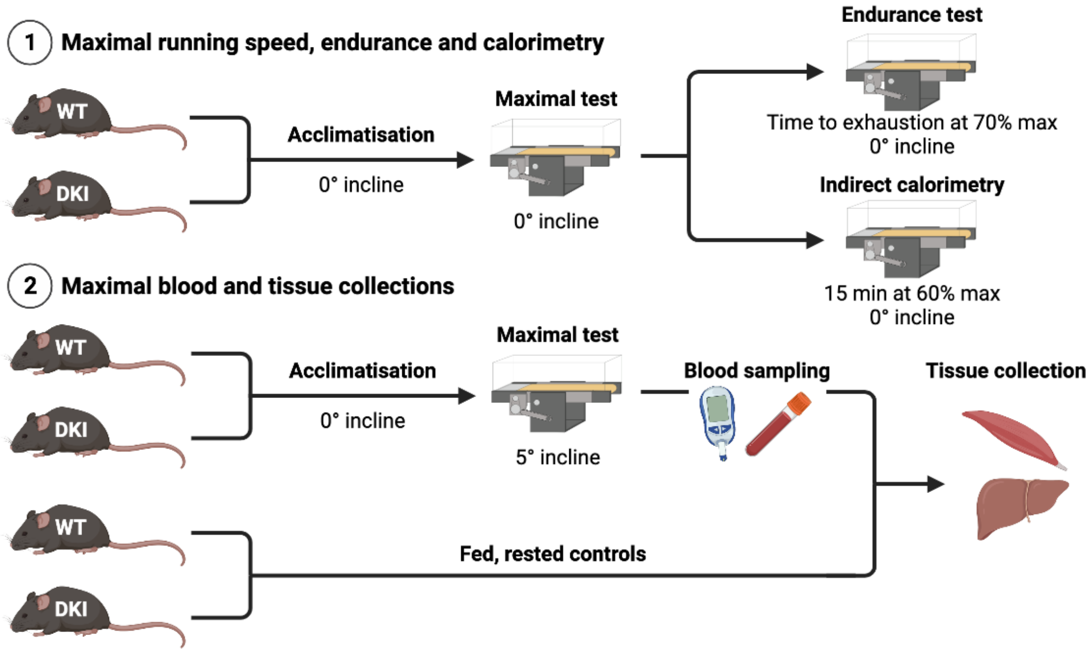
1 Maximal running speed, endurance and calorimetry
WT
DKI
Acclimatisation
0° incline
Maximal test
0° incline
Endurance test
Time to exhaustion at 70% max
0° incline
Indirect calorimetry
15 min at 60% max
0° incline
2 Maximal blood and tissue collections
WT
DKI
Acclimatisation
0° incline
Maximal test
5° incline
Blood sampling
Tissue collection
WT
DKI
Fed, rested controls

Figure 3.3 – Schematic of exercise testing protocols utilised in Study 2. Age-matched WT and DKI mice were randomly allocated to two experimental streams for exercise testing. (1) In the first stream mice completed treadmill acclimatisation and maximal testing at 0° incline. Following 2-3 days of rest, one cohort completed the endurance test described the endurance test described in 3.2.2 and a second cohort completed the treadmill calorimetry experiment described in 3.2.3. (2) Mice in the second stream were randomly divided into experimental and control cohorts. The experimental cohort completed the treadmill acclimatisation at 0° incline and the maximal treadmill test at 5° incline, as described in 3.2.2, with blood sampling and tissue collections immediately following exhaustion. The control cohort did not undergo any treadmill acclimatisation, exercise testing, or blood sampling and tissues were collected from fed, rested mice. Created with BioRender.com.

3.2.3 Exercise Calorimetry

Two to 3 days after completing the acclimatisation and maximal exercise testing at 0° incline, as described above, a subset of mice underwent a submaximal exercise bout to determine substrate utilisation (**Figure 3.3**). For the calorimetry experiments, mice completed a 15 min treadmill exercise bout at 60% of individual maximal speed at 0° incline on a specialised rodent calorimetry treadmill (Omnitech Electronics, Columbus, OH, USA). Mean values for RER were determined using the average VCO_2 and VO_2 from the final 5 min of treadmill running. TEE and fat and CHO oxidation were calculated from average VCO_2 and VO_2 , as previously described (Peronnet and Massicotte 1991). Immediately following the exercise test, mice were culled via cervical dislocation and tissues were dissected and snap frozen.

3.2.4 Serum Analysis

Blood samples were collected from the retro-orbital vein before and immediately after the maximal treadmill test at 5° and left to clot for 30 min at room temperature in non-coated polypropylene tubes before being placed on ice. Samples were then centrifuged at 10,000 *g* for 5 min at 4°C, and the resulting serum supernatant was aliquoted and stored at -80°C. NEFA-C (Wako Pure Chemical Industries, Osaka, Japan) colorimetric assay kits were used according to manufacturer's instructions.

3.2.5 Assessment of Tissue Glycogen Content

Snap-frozen gastrocnemius muscle (~40 mg) and liver (~25 mg) samples from fed, rested and maximally exercised mice were chipped under liquid N_2, freeze-dried overnight, powdered, and dissected free of visible blood and connective tissue. Aliquots of powdered tissue (~2-4 mg) were then alkaline extracted, and the supernatant was used for quantification of glycogen content using spectrophotometry as described previously (Bergmeyer 1974). Briefly, background glucose and hexose monophosphates were destroyed by adding 0.1 M NaOH, then samples were neutralised with a solution containing 0.1 M HCl, 0.2 M citric acid, and 0.2 M Na_2HPO_4. Amyloglucosidase (~1.0 $U \cdot sample^{-1}$) was used to degrade glycogen into glucose and glucose-6-phosphate. Samples were stored at -80°C until further analysis. To promote the production of 6-phosphate-gluconolactone and NADH, 1.0 U hexokinase, 1.0 U glucose-6-phosphate dehydrogenase, 0.75 mM ATP, and 1.0 mM NAD were added to samples in a 96-well plate. Absorbance was measured at 340 nm using a SpectraMax Paradigm plate reader and data was acquired using SoftMax Pro microplate data acquisition software (Molecular

Devices, San Jose, CA, USA). Glycogen content was determined using the Bougeur-Lambert-Beer law, as previously described (Bergmeyer 1974). Units of glycogen were expressed as mmol glucosyl units·kg^{-1} dry weight.

3.2.6 Immunoblotting

Snap-frozen gastrocnemius muscle samples from fed, rested and maximally exercised mice were lysed in homogenisation buffer containing 50 mM Tris.HCL, pH 7.5, 1 mM EDTA, 1 mM EGTA, 10% glycerol, 1% Triton-X, 50 mM sodium fluoride, 5 mM sodium pyrophosphate with cOmplete Protease Inhibitor Cocktail and PhosSTOP phosphatase inhibitor tablets (Sigma-Aldrich, St. Louis, MO, USA). Lysed tissue samples were centrifuged at 16,000 *g* for 30 min at 4°C, and supernatant protein content was determined using the BCA method (Pierce, Rockford, IL, USA). Samples were equilibrated with Laemelli's sample buffer, DTT, and bromophenol blue, and lysates were aliquoted, a subset of which were boiled for 5 min at 95°C, and stored at -80°C until blotting. Tissue lysates (10 mg protein·well^{-1}) were run on 4-15% or 4-20% precast stain-free gels (Bio-Rad, Hercules, CA, USA) in 1X Tris/Glycine/SDS buffer (Bio-Rad) for approximately 60 min using a mini PROTEAN Tetra Cell (Bio-Rad). Samples were then transferred to PVDF membranes (Merck Millipore, Burlington, MA, USA) at 60 V for 2 h using a Criterion Blotter (Bio-Rad). Stain-free images were captured before membranes were blocked with 7.5% BSA in TBS-T for 1 h at room temperature, then incubated with primary antibodies with rocking as detailed in **Table 3.1**. After washing with TBS-T, membranes were incubated for 1 h at room temperature in either a GAR or GAM secondary antibody from CST (Danvers, MA, USA) in TBS-T. Proteins were detected via chemiluminescence using SuperSignal West Femto Maximum Sensitivity Substrate (Thermo Fisher Scientific, Waltham, MA, USA) and imaged using the ChemiDoc Imaging System (Bio-Rad). Band intensities of total proteins and phosphorylation sites were normalised to the total lane protein from the respective stain-free image using Image Lab software (version 6, Bio-Rad), as described previously (Tachtsis, Whitfield et al. 2020), and phosphorylation was expressed relative to respective total protein content. Primary and secondary antibody details are listed in **Table 3.1**.

Table 3.1 – Antibodies and protocols used for immunoblotting

Target	Primary antibody	Incubation	Secondary antibody
AMPK α p-T172	CST 2531 1:1000	Overnight 4°C	GAR CST 7074 1:5000
AMPK α	CST 2532 1:1000	Overnight 4°C	GAR CST 7074 1:5000
AMPK β1 p-S182	CST 4186	Overnight 4°C	GAR CST 7074 1:5000
AMPK β1/β2	CST 4150 1:1000	Overnight 4°C	GAR CST 7074 1:5000
ACC p-S79	CST 11818 1:1000	Overnight 4°C	GAR CST 7074 1:5000
ACC	CST 3662 1:1000	Overnight 4°C	GAR CST 7074 1:5000
Akt p-S473	CST 9271 1:1000	1.5 h Room temperature	GAR CST 7074 1:5000
Akt	CST 4691 1:1000	Overnight 4°C	GAR CST 7074 1:5000
AS160 p-T642	CST 4288 1:1000	Overnight 4°C	GAR CST 7074 1:5000
AS160	Abcam ab24469 1:1000	Overnight 4°C	GAR CST 7074 1:5000
Citrate synthase	Abcam ab96600 1:1000	Overnight 4°C	GAR CST 7074 1:2000

CPT1b	Abcam ab134988 1:1000	Overnight 4°C	GAR CST 7074 1:2000
GLUT4	CST 2213 1:1000	Overnight 4°C	GAM CST 7076 1:2000
GS p-S641	CST 47043 1:1000	Overnight 4°C	GAR CST 7074 1:5000
GS	CST 3886 1:1000	Overnight 4°C	GAR CST 7074 1:5000
Glycogenin1	Abcam ab11171 1:1000	Overnight 4°C	GAR CST 7074 1:2000
GBE1	Abcam ab180596 1:1000	Overnight 4°C	GAR CST 7074 1:2000
GP	Antibody generated by B.E.K. laboratory 1:1000	Overnight 4°C	GAR CST 7074 1:2000
GDE	Antibody generated by B.E.K. laboratory 1:1000	Overnight 4°C	GAR CST 7074 1:2000
OXPHOS cocktail	Abcam ab110413 1:1000	Overnight 4°C	GAM CST 7076 1:2000
TBC1D1 p-S660	CST 66433 1:1000	Overnight 4°C	GAR CST 7074 1:2000

TBC1D1	CST 6928 1:1000	Overnight 4°C	GAR CST 7074 1:2000

3.2.7 Statistical Analyses

Comparisons between genotypes were analysed using unpaired two-tailed Student’s t testing (WT versus DKI) or two-way analysis of variance (ANOVA; WT versus DKI comparisons over time or condition) with Bonferroni post hoc testing applied where appropriate. Pearson’s product moment correlation was used to examine associations between maximal running speed at 5° and change in tissue glycogen content. All statistical analyses were completed using GraphPad Prism software (version 9, GraphPad Software, La Jolla, CA, USA). Significance was set at $p < 0.05$ and all data are presented as mean ± standard error of the mean (SEM).

Chapter 4 Study 1 – Phenotypic Effects of the AMPK DKI Mutation on Whole-Body and Tissue Metabolism

Publication Statement:

This Chapter is comprised of an original research manuscript that was accepted for publication at the *International Journal of Molecular Sciences* on 3 September 2021 and published online on 5 September 2021. This Chapter is presented here as the accepted pre-publication version.

Janzen NR, Whitfield J, Murray-Segal L, Kemp BE, Hawley JA, Hoffman NJ (2021). Mice with Whole-Body Disruption of AMPK-Glycogen Binding Have Increased Adiposity, Reduced Fat Oxidation and Altered Tissue Glycogen Dynamics. *Int J Mol Sci,* 22(17). doi.org/10.3390/ijms22179616.

Mice with Whole-Body Disruption of AMPK-Glycogen Binding Have Increased Adiposity, Reduced Fat Oxidation and Altered Tissue Glycogen Dynamics

Natalie R. Janzen [1], Jamie Whitfield [1], Lisa Murray-Segal [2], Bruce E. Kemp [1,2], John A. Hawley [1], and Nolan J. Hoffman [1,*]

[1] Exercise and Nutrition Research Program, Mary MacKillop Institute for Health Research, Australian Catholic University, Level 5, 215 Spring Street, Melbourne, VIC 3000, Australia; natalie.janzen@acu.edu.au (NRJ); jamie.whitfield@acu.edu.au (JW); bkemp@svi.edu.au (BEK); john.hawley@acu.edu.au (JAH)

[2] St Vincent's Institute of Medical Research and Department of Medicine, University of Melbourne, 9 Princes Street, Fitzroy, Victoria 3065, Australia; lmsegal@svi.edu.au (LM-S)

[*]Correspondence: nolan.hoffman@acu.edu.au; Tel.: +61-3-9230-8277

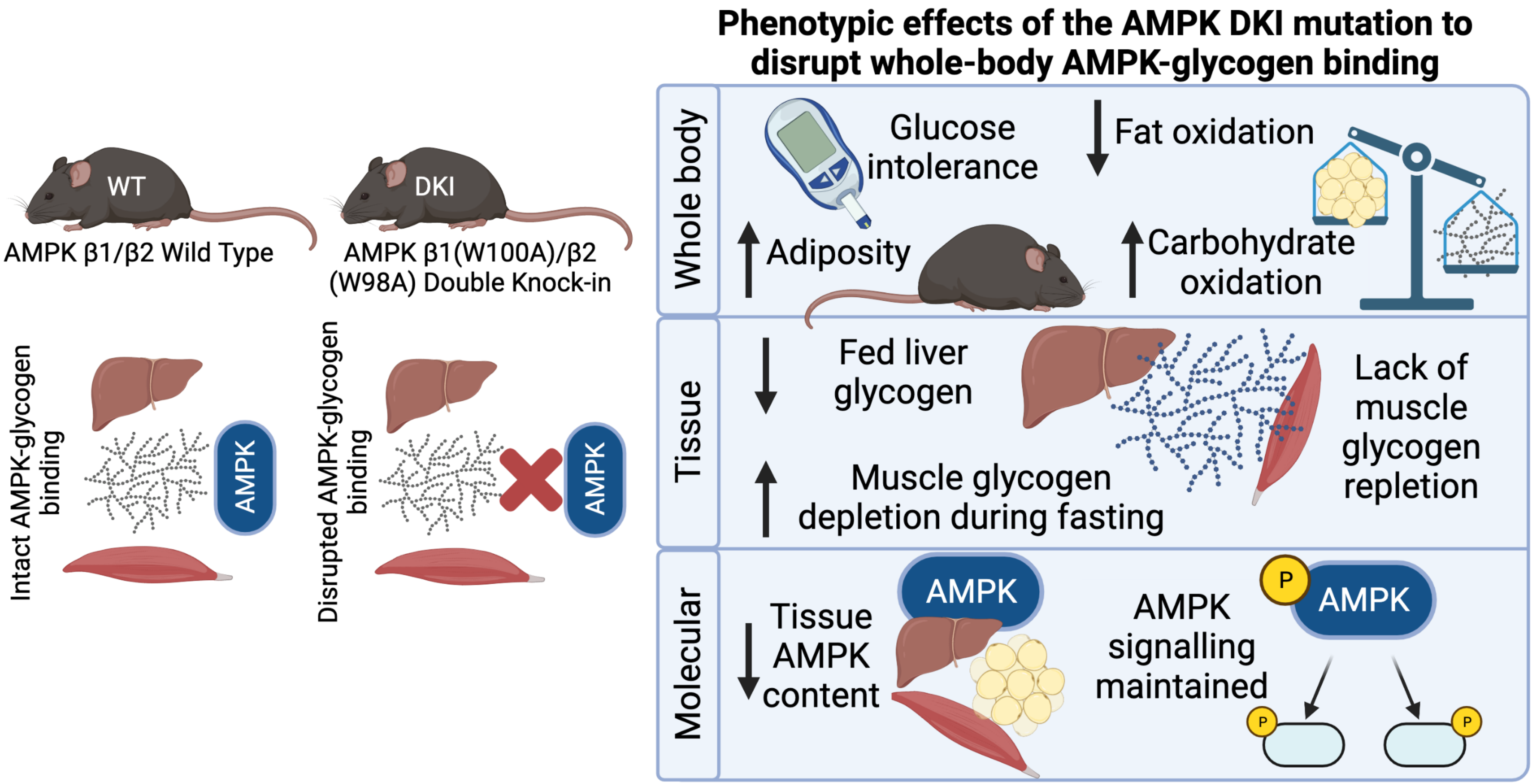
WT
AMPK β1/β2 Wild Type
DKI
AMPK β1(W100A)/β2 (W98A) Double Knock-in
Intact AMPK-glycogen binding
AMPK
Disrupted AMPK-glycogen binding
AMPK
Phenotypic effects of the AMPK DKI mutation to disrupt whole-body AMPK-glycogen binding
Whole body
Glucose intolerance
↓ Fat oxidation
↑ Adiposity
↑ Carbohydrate oxidation
Tissue
↓ Fed liver glycogen
↑ Muscle glycogen depletion during fasting
Lack of muscle glycogen repletion
Molecular
↓ Tissue AMPK content
AMPK
AMPK signalling maintained
P
AMPK
P
P

Figure 4.1 – Graphical abstract summarising key findings from Study 1. Created with BioRender.com.

4.1 Abstract

The AMP-activated protein kinase (AMPK), a central regulator of cellular energy balance and metabolism, binds glycogen via its β subunit. However, the physiological effects of disrupting AMPK-glycogen interactions remain incompletely understood. To chronically disrupt AMPK-glycogen binding, AMPK β double knock-in (DKI) mice were generated with mutations in residues critical for glycogen binding in both the β1 (W100A) and β2 (W98A) subunit isoforms. We examined the effects of this DKI mutation on whole-body substrate utilisation, glucose homeostasis, and tissue glycogen dynamics. Body composition, metabolic caging, glucose and insulin tolerance, serum hormone and lipid profiles, and tissue glycogen and protein content were analysed in chow-fed male DKI and age-matched wild type (WT) mice. DKI mice displayed increased whole-body fat mass and glucose intolerance associated with reduced fat oxidation relative to WT. DKI mice had reduced liver glycogen content in the fed state concomitant with increased utilisation and no repletion of skeletal muscle glycogen in response to fasting and refeeding, respectively, despite similar glycogen-associated protein content relative to WT. DKI liver and skeletal muscle displayed reductions in AMPK protein content versus WT. These findings identify phenotypic effects of the AMPK DKI mutation on whole-body metabolism and tissue AMPK content and glycogen dynamics.

Keywords: AMP-activated protein kinase; carbohydrate-binding module; glucose homeostasis; metabolism; liver; skeletal muscle

4.2 Introduction

The AMP-activated protein kinase (AMPK) is a central regulator of cellular energy balance and metabolism. AMPK becomes activated in response to reductions in cellular energy availability such as those induced by fasting and exercise, which are characterised by increases in ADP and AMP concentrations relative to ATP. When activated, AMPK stimulates several catabolic pathways to promote energy production and inhibits anabolic processes to preserve cellular energy homeostasis (Hardie, Ross et al. 2012). These downstream AMPK-regulated pathways facilitate increases in lipid oxidation, reductions in lipid synthesis, and stimulation of insulin-independent glucose uptake in skeletal muscle to help maintain cellular energy stores (Steinberg and Kemp 2009).

The AMPK αβγ heterotrimer contains a regulatory β subunit that binds the catalytic α and regulatory γ subunits (Iseli, Walter et al. 2005). The AMPK β subunit exists in two isoforms; in rodents, the β1 isoform is predominantly expressed in liver, while the β2 isoform is primarily expressed in skeletal muscle (Janzen, Whitfield et al. 2018). Both AMPK β subunit isoforms possess a carbohydrate binding module (CBM) that allows AMPK to bind glycogen (Hudson, Pan et al. 2003, Polekhina, Gupta et al. 2003, Polekhina, Gupta et al. 2005, McBride, Ghilagaber et al. 2009, Janzen, Whitfield et al. 2018), the primary storage form of glucose in liver and skeletal muscle. In the two decades since AMPK's glycogen-binding capacity was discovered, investigations directly examining the roles of AMPK-glycogen interactions have primarily been limited to *in vitro* studies. Glycogen has been reported to have an inhibitory effect on AMPK activity *in vitr*o (McBride, Ghilagaber et al. 2009), but we (Polekhina, Gupta et al. 2003) and others (Li, Wang et al. 2015) have not detected glycogen-dependent inhibition of AMPK *in vitro*. Experiments in rat skeletal muscle with reduced glycogen concentration have demonstrated a greater increase in AMPK activity in response to 5-aminoimidazole-4-carboxamide ribonucleotide (AICAR) administration compared to glycogen-replete skeletal muscle (Wojtaszewski, Jorgensen et al. 2002). Similarly, human studies have demonstrated greater AMPK phosphorylation and kinase activity when exercise is commenced with low compared to normal or elevated skeletal muscle glycogen availability (Wojtaszewski, MacDonald et al. 2003, Watt, Steinberg et al. 2004, Steinberg, Watt et al. 2006). While these investigations have helped establish the hypothesis that glycogen binding may regulate AMPK activity and allow AMPK to "sense" existing energy stores (McBride, Ghilagaber et al. 2009), the physiological implications of this relationship cannot be fully elucidated by acutely modifying glycogen content *in vivo* (i.e., with exercise and muscle contraction) or examining AMPK and glycogen interactions in isolation *in vitro*. *In vivo* studies investigating the physiological consequences of disrupting AMPK-glycogen interactions are therefore warranted.

We previously generated two isoform-specific AMPK β knock-in (KI) mouse models in which tryptophan residues critical for AMPK-glycogen binding were mutated in either the β1 (W100A) or β2 (W98A) subunit isoform (Hoffman, Whitfield et al. 2020). We demonstrated that mice with a KI mutation to chronically disrupt glycogen-binding capacity in a single AMPK β subunit isoform predominantly expressed in liver or skeletal muscle displayed reduced total AMPK content and kinase activity, which was associated with increased fat content in liver and skeletal muscle of β1 W100A and β2 W98A KI mice, respectively (Hoffman, Whitfield et al. 2020). Additionally, β2 W98A KI mice displayed increased whole-body fat mass and impaired glucose handling (Hoffman, Whitfield et al. 2020). However, these KI mouse models targeted a specific β1 or β2 isoform with predominant tissue expression in either liver or skeletal muscle, respectively. Most rodent tissues, including liver and skeletal muscle, express detectable levels of both isoforms (Janzen, Whitfield et al. 2018). As a result, the phenotypic effects of simultaneous β subunit isoform KI mutations on whole-body and tissue metabolism *in vivo* remain unknown. Furthermore, the consequences of chronically disrupting AMPK-glycogen binding via β subunit KI mutations have not been tested in physiological settings of energy stress and energy excess (i.e., fasting and refeeding).

To investigate these phenotypic effects and the potential for compensatory and/or synergistic consequences of KI of both AMPK β subunit isoforms, we crossed these single β1 W100A KI and β2 W98A KI mouse lines to generate AMPK β1/β2 double knock-in (DKI) mice. We hypothesised that relative to wild type (WT) mice, DKI mice would display increased whole-body fat mass, glucose intolerance, and impaired tissue glycogen utilisation and synthesis.

4.3 Results

4.3.1 DKI Mice Display Increased Body Mass Associated with Increased Adiposity

To first determine how the DKI mutation utilised to chronically disrupt whole-body AMPK-glycogen binding influences body mass and composition, growth was assessed in age-matched WT and AMPK DKI male mice (**Figure 4.2a**) beginning at 9 wk of age. DKI mice displayed increased body mass compared to age-matched WT controls at all ages (**Figure 4.2b**). Increases in total fat mass and total lean mass were observed in DKI mice between 10–15 and 13–17 wk of age, respectively, versus WT mice (**Figure 4.2c, d**). Consistent with the observed increase in total fat mass, DKI mice also exhibited greater epididymal fat pad mass (**Figure 4.2e**). There were modest increases in the mass of glycogen-storing tissues, including skeletal muscle (quadriceps; $p = 0.063$; **Figure 4.2f**) and liver ($p = 0.077$; **Figure 4.2g**), but these were not statistically significant. Finally, DKI mice displayed greater pancreatic tissue mass relative to WT, while tissue mass of heart, gastrocnemius muscle, and soleus muscle were similar between genotypes (**Table 4.1**).

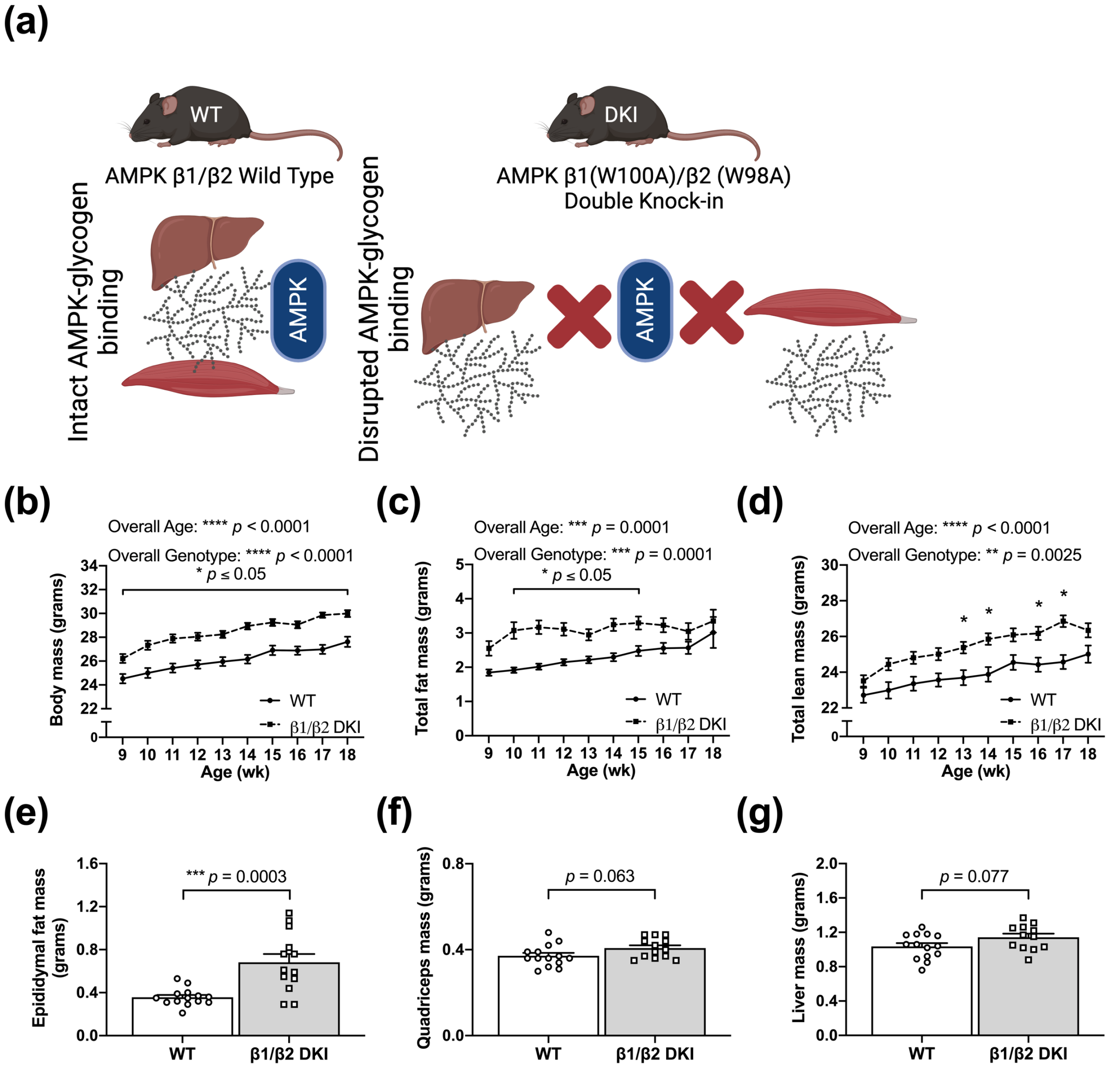

Figure 4.2 – The double knock-in (DKI) mutation utilised to disrupt whole-body AMP-activated protein kinase (AMPK)-glycogen binding is associated with increased body mass and adiposity. (**a**) Schematic of AMPK wild type (WT) versus DKI mouse model in which tryptophan residues critical for AMPK-glycogen binding within the AMPK β1 and β2 subunit isoforms (predominantly expressed in the primary glycogen storing tissues liver and skeletal muscle, respectively) were mutated to alanine, resulting in chronic whole-body disruption of AMPK-glycogen binding. (**b**) Growth was assessed in male DKI and WT mice fed a standard rodent chow diet. EchoMRI analyses revealed that DKI mice had (**c**) greater total fat mass between the ages of 10 and 15 wk and (**d**) increased total lean mass between ages 13 and 17 wk, with the exception of 15 wk. Fed male mice, *n* = 11–30, 9–18 wk. Mice were culled and (**e**) epididymal fat pads, (**f**) quadriceps muscle, (**g**) and liver were excised and weighed. Fed male mice, *n* = 11–14, 17–20 wk. * $p < 0.05$, ** $p < 0.01$, *** $p < 0.001$, **** $p < 0.0001$.

Table 4.1 – Mass of tissues from male WT and AMPK DKI mice

Tissue	WT Tissue Mass (mg)	DKI Tissue Mass (mg)	*p*–Value
Pancreas	120 ± 12.0	167 ± 16.5*	0.029
Heart	159 ± 10.3	176 ± 11.6	0.27
Gastrocnemius	306 ± 12.9	328 ± 17.1	0.11
Soleus	16 ± 1.8	14 ± 1.8	0.35

Pancreas, heart, gastrocnemius muscle, and soleus muscle were collected from mice in the fed state and weighed. Data are presented as mean ± standard error of the mean (SEM); n =8–14, 17–20 wk old mice. * $p < 0.05$.

4.3.2 DKI Mice Have Reduced Voluntary Physical Activity, Increased Rates of CHO Oxidation, and Reduced Rates of Fat Oxidation

To assess potential whole-body metabolic changes underlying the observed differences in body mass and composition, DKI and WT mice were subjected to metabolic cage analysis. Changes in body mass and composition were associated with a main effect for decreased voluntary ambulatory activity in DKI mice versus WT, with significant genotype differences during the dark phase (**Figure 4.3a** and inset). There was a main effect for increased food intake in DKI mice, although post hoc analysis did not identify any genotypic differences during either the light or dark phases (**Figure 4.3b** and inset). There were no associated differences in serum leptin concentration in either the fed or 6 h fasted state compared to WT (**Figure 4.3c**). While there was an overall genotype effect of an increased respiratory exchange ratio (RER) in DKI mice versus WT (**Figure 4.3d**), individual differences in the light phase, dark phase, or 24 h period failed to reach statistical significance (**Figure 4.3e**). Furthermore, there were no differences in total energy expenditure (TEE; **Figure 4.3f**), despite overall genotype effects of decreased rates of fat oxidation (**Figure 4.3g**) and increased carbohydrate (CHO) oxidation (**Figure 4.3h**) in DKI mice versus WT. Consistent with the RER data, individual differences in overall substrate oxidation during light and dark phases or across 24 h did not reach statistical significance (**Figure 4.3g, h**).

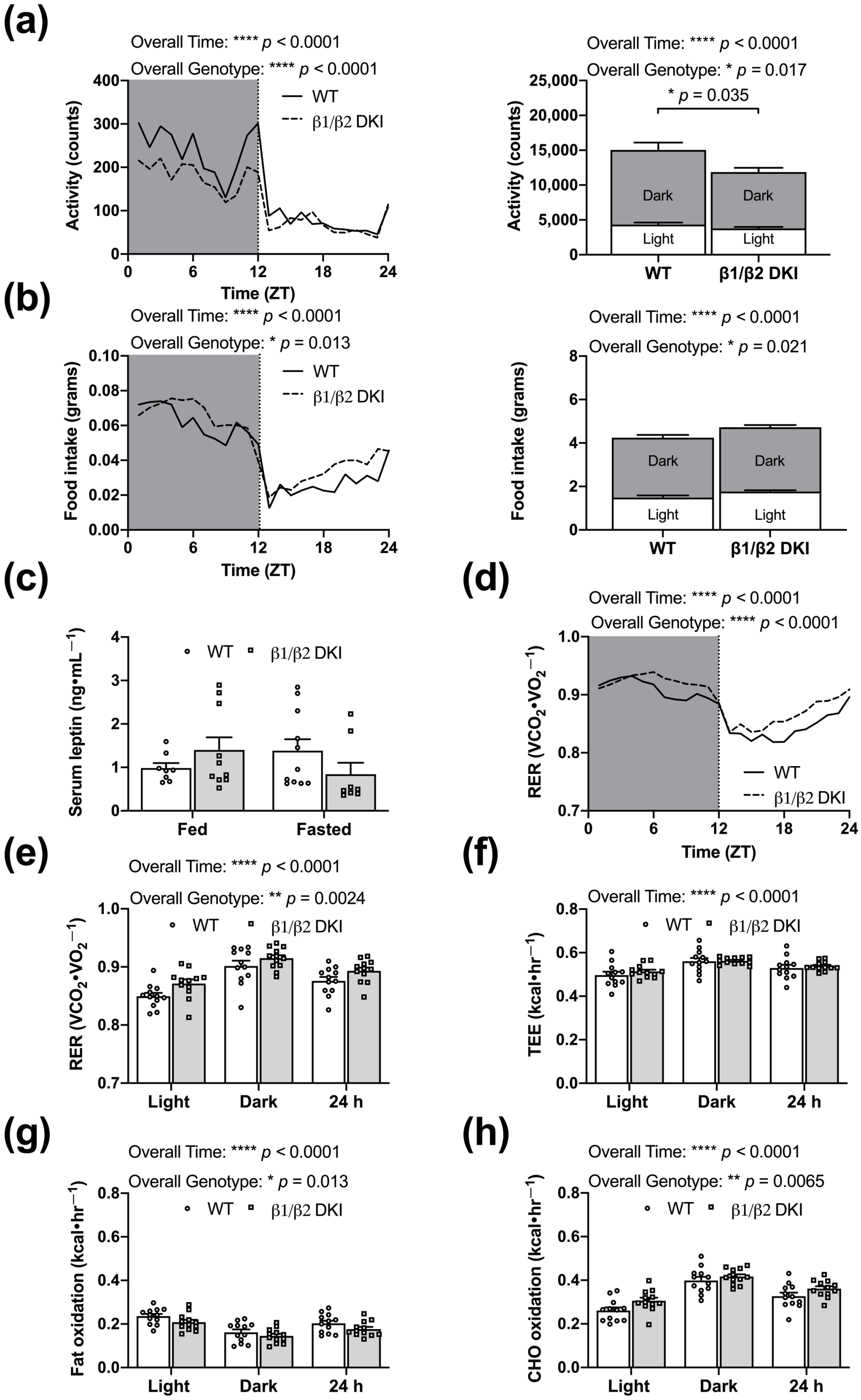

Figure 4.3 – DKI mice have reduced voluntary activity and reduced rates of fat oxidation. Male DKI mice and age-matched WT controls were housed in metabolic cages and activity, food intake, oxygen consumption (VO_2), and carbon dioxide production (VCO_2) were measured every 18 min across ~60 h (after initial ~6 h acclimatisation period). Activity data represent the total beam breaks in the x-ambulatory field. Hourly, 12 h light and dark phases (Zeitgeber time; ZT), and 24 h averages were calculated for activity and food intake. (**a** and inset) DKI had lower ambulatory activity, specifically during the dark phase, and (**b** and inset) a main effect for increased food intake, but no significant differences in either the light or dark cycles. (**c**) The main effect for increased food consumption was not associated with changes in serum leptin concentration in the fed or 6 h fasted states. (**d, e**) Respiratory exchange ratio (RER) was calculated and averaged for hourly, phase, and 24 h measures. (**f**) Total energy expenditure (TEE), (**g**) rates of fat oxidation, and (**h**) rates of carbohydrate (CHO) oxidation were calculated and averaged across the light, dark, and 24 h cycle. Fed male mice, $n = 12$, 12–16 wk. * $p < 0.05$, ** $p < 0.01$, **** $p < 0.0001$.

4.3.3 DKI Mice Display Hyperinsulinemia and Glucose Intolerance but Normal Whole-Body Insulin Sensitivity

To determine the phenotypic effects of the DKI mutation on whole-body glucose homeostasis, a series of blood and serum analyses were performed. Blood glucose concentrations were similar between DKI and WT mice in the 6 h fasted state (**Figure 4.4a**); however, 6 h fasted DKI mice displayed increased serum insulin levels compared to WT (**Figure 4.4b**). DKI mice subjected to intraperitoneal (IP) glucose tolerance testing (IPGTT) displayed increased blood glucose levels 20 min after glucose injection, associated with an elevated blood glucose area under the curve (AUC) compared to WT (**Figure 4.4c** and inset). However, there were no differences in blood glucose responses nor AUC between genotypes during IP insulin tolerance testing (IPITT; **Figure 4.4d** and inset). Tissue analyses were next performed to assess total protein content and phosphorylation status of glucose transport-related proteins in skeletal muscle (**Figure 4.4e**). There were no differences in Akt S473 phosphorylation status and total Akt protein content between DKI and WT skeletal muscle in the fed state (**Figure**

4.4f, g), nor changes in T642 phosphorylation and total protein content of its downstream target Akt substrate of 160 kDa (AS160; **Figure 4.4h, i**). Skeletal muscle GLUT4 protein content was also similar between genotypes (**Figure 4.4j**).

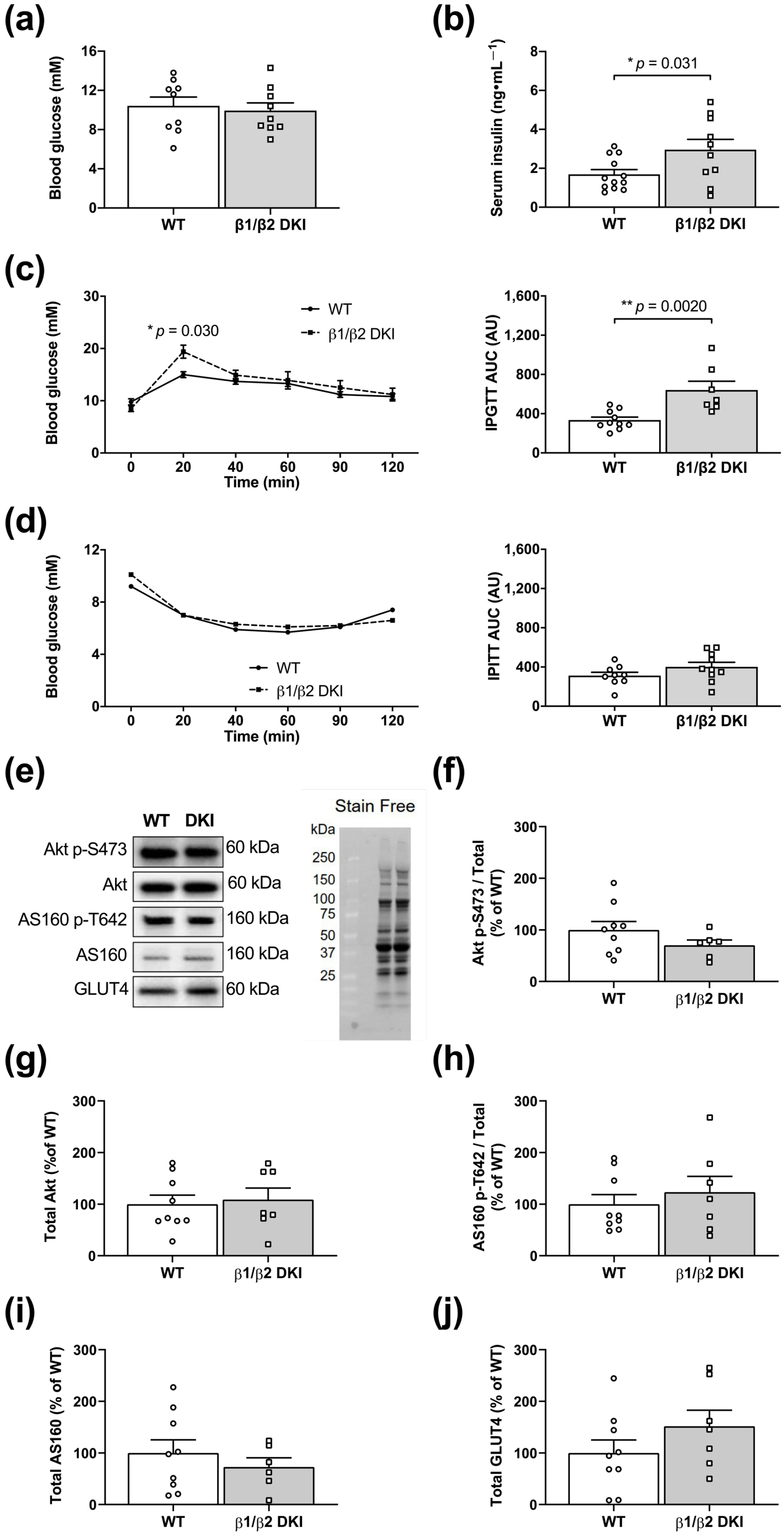

Figure 4.4 – DKI mice are glucose intolerant but maintain whole-body insulin sensitivity. (**a**) Blood glucose was assessed via tail tip bleed in male DKI and WT mice following a 6 h fast. Male mice, *n* = 9, 17–20 wk. (**b**) Blood was collected via retro-orbital bleed from DKI and WT mice following a 6 h fast, and serum samples were analysed for insulin concentration. Male mice, *n* = 10–12, 20–27 wk. (**c** and inset) Following a 6 h fast, DKI and WT mice were injected intraperitoneally with glucose (1 g·kg^{-1} total lean mass), and blood glucose responses were measured over 2 h-post injection and area under the curve (AUC), with baseline as the mean blood glucose at time 0 for each genotype, was calculated to assess glucose handling. Male mice, *n* =7–10, 17–20 wk. (**d** and inset) Following a 4 h fast, DKI and WT mice were injected intraperitoneally with insulin (0.5 units·kg^{-1} total body mass), and blood glucose responses were measured over 2 h and AUC was calculated. Male mice, *n* = 9–10, 17–20 wk. Skeletal muscle was collected from male DKI and WT mice in the fed state, and phosphorylation status and total content of proteins associated with skeletal muscle glucose transport were quantified. (**e**) Representative immunoblots and stain-free image and quantified results of (**f**) Akt p-S573, (**g**) total Akt, (**h**) AS160 p-T642, (**i**) total AS160, and (**j**) total GLUT4 content in DKI versus WT skeletal muscle. Protein quantification was performed by normalising the band intensity of the protein of interest to total lane protein using stain-free imaging, and phosphorylation was expressed relative to respective total protein content. Fed male mice, *n* = 7–9, 20–32 wk. * $p < 0.05$, ** $p < 0.01$.

4.3.4 DKI Mice Have Decreased Voluntary Ambulatory Activity and Decreased Rates of Fat Oxidation during Overnight Fasting

To determine whole-body responses of DKI mice to acute energy stress relative to WT, mice were overnight fasted (~14 h) in metabolic cages. An overall genotype effect was detected for an increased RER in DKI mice compared to WT across the fasting period (**Figure 4.5a**), consistent with an observed increase in average RER (**Figure 4.5b**). DKI mice had reduced total ambulatory activity compared to WT (**Figure 4.5c**); although there were no differences in TEE between genotypes (**Figure 4.5d**). Consistent with overall genotype effects observed in the fed state, DKI mice displayed a decrease in rates of fat oxidation (**Figure 4.5e**) with a reciprocal increase in rates of CHO oxidation (**Figure 4.5f**). While no differences in blood glucose concentration were observed between genotypes in the fed state, there was a greater reduction in blood glucose levels following the overnight fast in WT compared to DKI mice (**Figure 4.5g**). Despite an overall interaction effect of genotype and condition for serum glucagon levels, there were no significant differences observed in WT versus DKI mice in either the fed or overnight fasted states (**Figure 4.5h**). Serum analyses to assess circulating fat availability revealed a genotype effect for increased serum TAG concentration in DKI mice compared to WT; however, post hoc analysis revealed no significant individual differences in either the fed or overnight fasted states (**Figure 4.5i**). WT and DKI mice had similar serum NEFA concentration in the fed state, and NEFA levels increased to a similar extent in response to an overnight fast in both genotypes (**Figure 4.5j**).

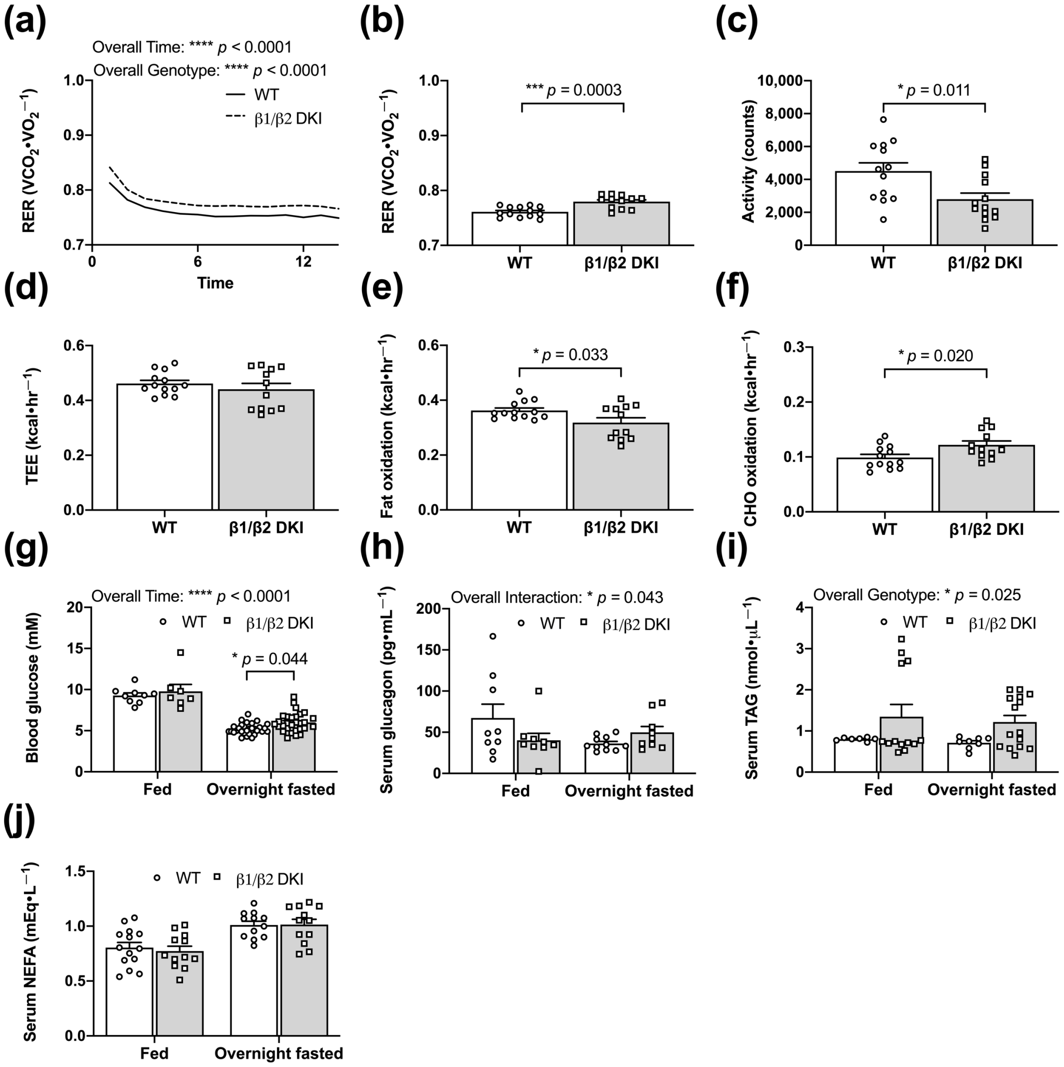

Figure 4.5 – DKI mice have reduced voluntary activity and rates of fat oxidation during overnight fasting (~14 h). Male DKI mice and age-match WT controls were singly housed in metabolic cages and acclimatised for ~6 h. At the beginning of the dark cycle (1800 h), food was removed from cages and respiratory gases and ambulatory activity were measured every 18 min during the overnight fast (~14 h). (**a**) Average hourly RER following induction of fasting. (**b**) Average RER. (**c**) Activity data represented by the total beam breaks in the x-ambulatory field during the fasting period. (**d**) TEE, (**e**) rates of fat oxidation, and (**f**) rates of CHO oxidation were calculated and averaged across the fasting period. Fasting male mice, $n = 12–14$, 17–20 wk. (**g**) Blood glucose was assessed via tail tip bleed in the fed ($n = 7–9$) and overnight fasted ($n = 29–30$) states. Overnight fasted mice in panel (**g**) consists of the three cohorts (overnight fasted, 5 h glucose, and 24 refed) described in Figure 4.6. Male mice, 20–32 wk. Blood was collected via retro-orbital bleed following overnight (~14 h) fast and serum samples were analysed for (**h**) glucagon ($n = 9–11$), (**i**) triglyceride (TAG; $n = 7–15$), and (**j**) non-esterified fatty acid (NEFA; $n = 12–14$) concentrations. Male mice, 17–28 wk. * $p < 0.05$, *** $p < 0.001$, **** $p < 0.0001$.

4.3.5 DKI Mice Display Reduced Liver Glycogen Concentration in the Fed State and Altered Fasting-Induced Skeletal Muscle Glycogen Depletion

Based on genotypic differences observed in patterns of whole-body substrate utilisation in both the fed and fasting states, we next investigated the phenotypic effects of the DKI mutation on physiological regulation of tissue glycogen stores. DKI mice displayed reduced liver glycogen content in the fed state compared to WT (**Figure 4.6a**). Following an overnight fast, liver glycogen levels were depleted to similar levels in both DKI and WT mice; however, the net difference in liver glycogen from the fed to fasted state was 33% lower in DKI mice because of their lower glycogen content in the fed state (**Figure 4.6b**). To assess glycogen repletion, mice received an oral glucose gavage following an overnight fast. Liver glycogen content did not completely return to fed “baseline” levels 5 h-post glucose gavage in either genotype but was restored to fed levels in DKI mice by 24 h-post glucose gavage and refeeding (**Figure 4.6a**). However, WT and DKI mice displayed similar levels of total glycogen repletion from the overnight fasted state to 24 h-post glucose gavage and refeeding (**Figure 4.6c**).

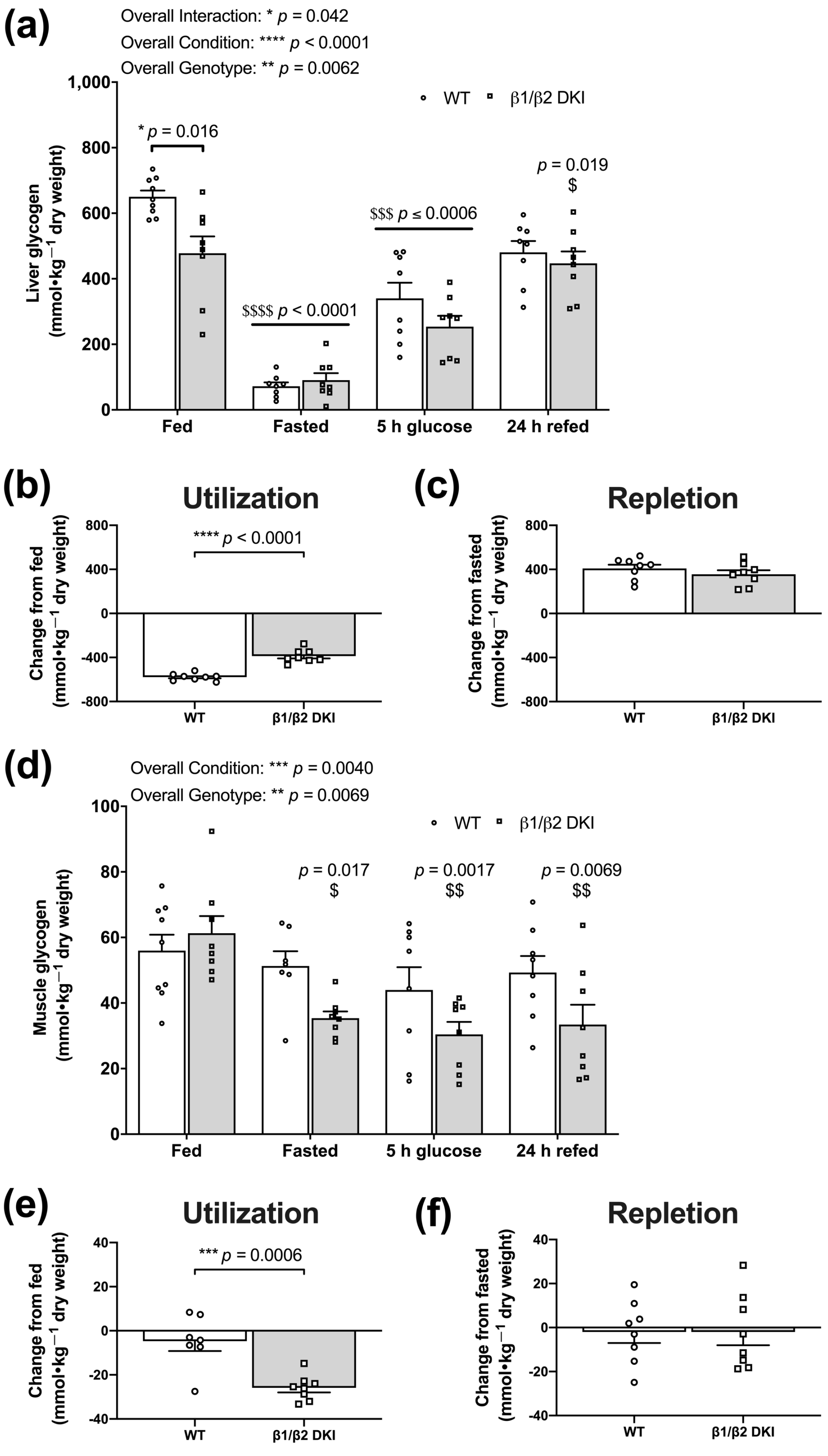

Figure 4.6 – DKI mice display reduced hepatic glycogen concentration in the fed state and increased skeletal muscle glycogen utilisation in response to fasting. Liver and skeletal muscle were collected and snap-frozen from male mice in the fed and overnight fasted states, and 5 h- and 24 h-post administration of a glucose bolus ($3.6\ g \cdot kg^{-1}$ total body mass) via oral gavage. The 24 h-post cohort had *ad libitum* access to chow beginning at 5 h-post glucose gavage. (**a**) Liver glycogen concentration was assessed in the fed state, overnight fasted state, 5 h-post glucose gavage, and 24 h-post glucose gavage and refeeding. (**b**) Utilisation was measured as the difference in total glycogen content between fed and overnight fasted conditions. (**c**) Repletion was measured as the difference in total glycogen content between overnight fasted and 24 h-post glucose gavage and refeeding. (**d**) Fed skeletal muscle glycogen levels were similar between DKI and WT mice but were only significantly reduced in DKI mice following an overnight fast. Glycogen remained suppressed below fed levels at both 5 h-post glucose gavage and 24 h-post glucose gavage and refeeding in DKI mice. (**e**) DKI mice had significantly increased utilisation of skeletal muscle glycogen compared to WT when subjected to an overnight fast. (**f**) There was no significant glycogen repletion observed in either genotype from the overnight fasted state to 24 h-post glucose gavage and refeeding. Due to the large number of mice needed for these experiments, a larger range of mouse ages (20–32 wk) were used, $n = 7–9$. Brackets represent comparison between genotypes within a condition and horizontal bars represent comparison with the fed condition for both genotypes. \$ $p < 0.05$, \$\$ $p < 0.01$, \$\$\$ $p < 0.001$, \$\$\$\$ $p < 0.0001$ versus fed condition from same genotype; * $p < 0.05$, ** $p < 0.01$, *** $p < 0.001$, **** $p < 0.0001$.

In skeletal muscle, glycogen content remained unchanged in WT following the overnight fast (**Figure 4.6d, e**). Meanwhile, there was a significant reduction in glycogen content observed in DKI mice following overnight fasting (**Figure 4.6d**), resulting in ~4-fold greater utilisation of skeletal muscle glycogen from the fed to fasted state in DKI mice compared to WT (**Figure 4.6e**). Given skeletal muscle glycogen content was not altered in WT mice following the overnight fast, there was little estimated repletion 24 h-post glucose gavage and refeeding (**Figure 4.6f**). However, in contrast to liver, skeletal muscle glycogen levels in DKI mice remained suppressed relative to baseline even 24 h-post glucose gavage and refeeding (**Figure 4.6d**), resulting in negligible glycogen repletion (**Figure 4.6f**).

4.3.6 Liver and Muscle from DKI Mice Display No Changes in Glycogen Associated Proteins Relative to WT

To determine if the observed differences in tissue glycogen content were due to changes in proteins associated with the regulation of glycogen breakdown and/or synthesis, glycogen associated proteins were assessed in liver (**Figure 4.7a**) and skeletal muscle (**Figure 4.7c**). Changes in tissue glycogen dynamics observed in fed DKI mice were not accompanied by any differences in total glycogen synthase (GS), glycogen branching enzyme (GBE), glycogenin, glycogen phosphorylase (GP), or glycogen debranching enzyme (GDE) in either liver (**Figure 4.7b**) or skeletal muscle (**Figure 4.7d**). We next measured phosphorylation status of GS, one of the rate-limiting enzymes in glycogen synthesis, in liver (**Figure 4.7e**) and skeletal muscle (**Figure 4.7g**) in the fed, overnight fasted, 5 h-post glucose gavage, and 24 h-post glucose gavage and refeeding states. There were no differences between genotypes nor across conditions observed for phosphorylation of GS S641 in liver (**Figure 4.7f**). There was an overall condition effect observed for phosphorylation of GS S641 in skeletal muscle; however, post hoc analysis did not reveal individual differences between WT and DKI skeletal muscle across conditions (**Figure 4.7h**).

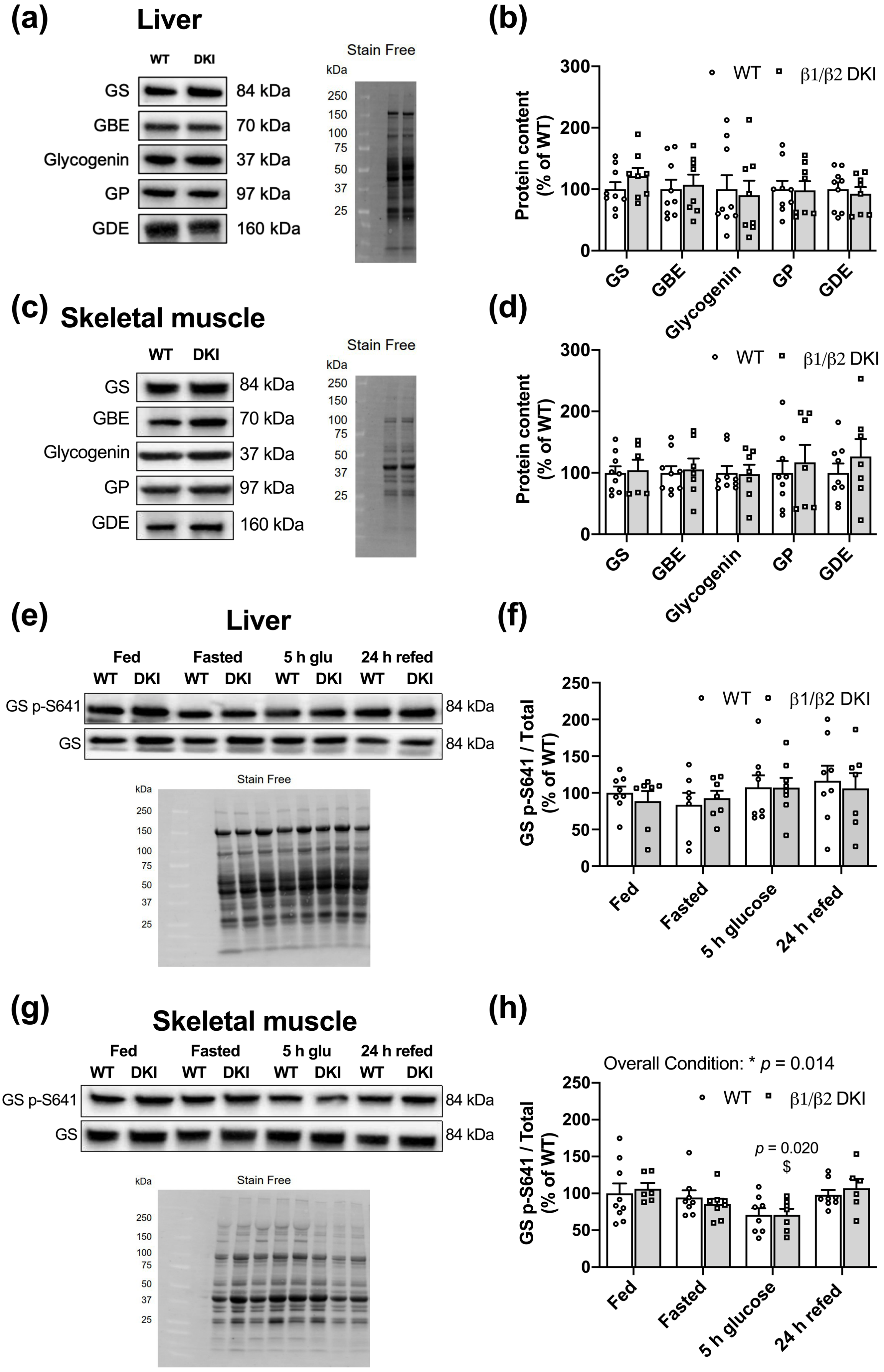
(a)
Liver
WT DKI
GS 84 kDa
GBE 70 kDa
Glycogenin 37 kDa
GP 97 kDa
GDE 160 kDa
Stain Free
kDa 250 150 100 75 50 37 25
(b)
Protein content (% of WT)
0 100 200 300
∘ WT ▫ β1/β2 DKI
GS GBE Glycogenin GP GDE
(c) Skeletal muscle
WT DKI
GS 84 kDa
GBE 70 kDa
Glycogenin 37 kDa
GP 97 kDa
GDE 160 kDa
Stain Free
kDa 250 150 100 75 50 37 25
(d)
Protein content (% of WT)
0 100 200 300
∘ WT ▫ β1/β2 DKI
GS GBE Glycogenin GP GDE
(e)
Liver
Fed Fasted 5 h glu 24 h refed
WT DKI WT DKI WT DKI WT DKI
GS p-S641 84 kDa
GS 84 kDa
Stain Free
kDa 250 150 100 75 50 37 25
(f)
GS p-S641 / Total (% of WT)
0 50 100 150 200 250
∘ WT ▫ β1/β2 DKI
Fed Fasted 5 h glucose 24 h refed
(g)
Skeletal muscle
Fed Fasted 5 h glu 24 h refed
WT DKI WT DKI WT DKI WT DKI
GS p-S641 84 kDa
GS 84 kDa
Stain Free
kDa 250 150 100 75 50 37 25
(h)
Overall Condition: * p = 0.014
GS p-S641 / Total (% of WT)
0 50 100 150 200 250
∘ WT ▫ β1/β2 DKI
p = 0.020
$
Fed Fasted 5 h glucose 24 h refed

Figure 4.7 – Liver and skeletal muscle from DKI mice display no alterations in content of glycogen associated proteins. Tissues were collected from fed male mice and assessed for glycogen associated protein content and phosphorylation status. (**a**) Representative immunoblots and stain-free image for DKI versus WT liver. (**b**) Quantified glycogen synthase (GS), glycogen branching enzyme (GBE), glycogenin, glycogen phosphorylase (GP), and glycogen debranching enzyme (GDE) in liver. (**c**) Representative immunoblots and stain-free image for DKI versus WT skeletal muscle. (**d**) Quantified GS, GBE, glycogenin, GP, and GDE in skeletal muscle. To assess phosphorylation of GS S641, liver and skeletal muscle were collected from male mice in the fed and overnight fasted states, and 5 h- and 24 h-post administration of a glucose bolus (3.6 $g \cdot kg^{-1}$ total body mass) via oral gavage. The 24 h-post cohort had *ad libitum* access to chow beginning at 5 h-post glucose gavage. Representative immunoblots and stain-free images for DKI versus WT (**e**) liver and (**g**) skeletal muscle. Quantified GS p-S641 relative to total protein in (**f**) liver and (**h**) skeletal muscle. Fed male mice, $n = 7–9$, 20–32 wk. \$ $p < 0.05$ versus fed condition from same genotype; * $p < 0.05$.

4.3.7 DKI Mice Have Intact AMPK and ACC Phosphorylation in Liver and Skeletal Muscle

Given the role of AMPK in tissue glycogen storage and dynamics, we measured phosphorylation of AMPK and its downstream substrate acetyl-CoA carboxylase (ACC) in WT and DKI mice in the fed, overnight fasted, 5 h-post glucose gavage, and 24 h-post glucose gavage and refeeding states in liver (**Figure 4.8a**) and skeletal muscle (**Figure 4.8d**). In liver, there was an overall condition effect detected for AMPK α T172 phosphorylation relative to total protein. Specifically, DKI mice displayed increased phosphorylation in the overnight fasted and 5 h-post glucose states compared to the fed state (**Figure 4.8b**). However, no individual genotypic differences were observed between WT and DKI mice (**Figure 4.8b**). There were also no differences detected in ACC S79 phosphorylation between WT and DKI liver observed in any condition (**Figure 4.8c**). In skeletal muscle, there was a trend for a genotypic effect for increased phosphorylation of AMPK α T172 in DKI mice compared to WT that did not reach statistical significance ($p = 0.054$), and post hoc analysis did not identify any significant differences in any individual condition (**Figure 4.8e**). There were also no differences observed in downstream ACC S79 phosphorylation between genotypes or across conditions (**Figure 4.8f**).

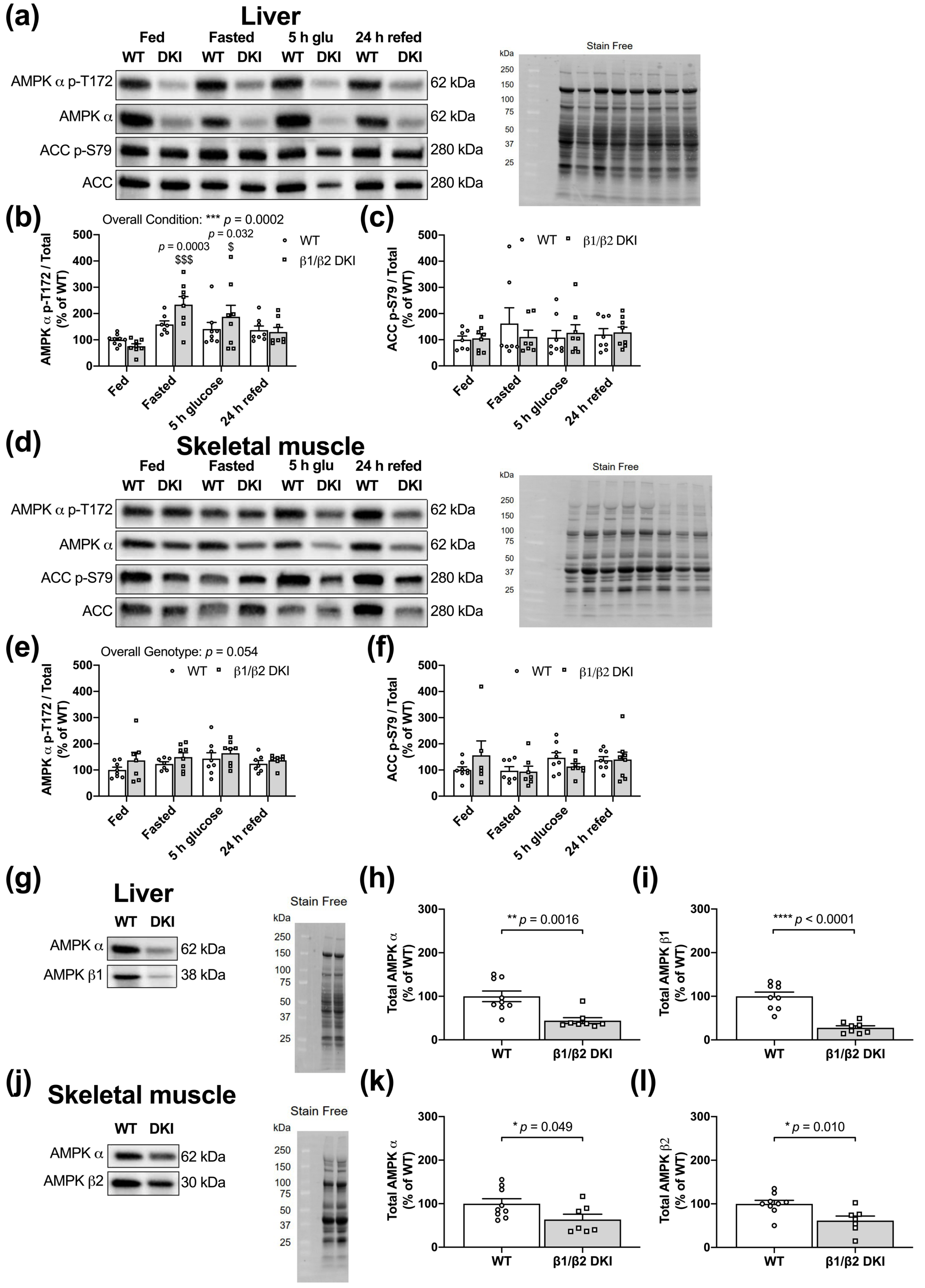

Figure 4.8 – DKI mice have intact AMPK-acetyl-CoA carboxylase (ACC) signalling but reduced AMPK content in liver and skeletal muscle. Tissues were collected from male mice in the fed and overnight fasted states, and 5 h- and 24 h-post administration of a glucose bolus (3.6 $g \cdot kg^{-1}$ total body mass) via oral gavage. The 24 h-post cohort had *ad libitum* access to chow beginning at 5 h-post glucose gavage. Liver and skeletal muscle were collected, snap-frozen and phosphorylation status of AMPK T172 and ACC S79 was assessed. Representative immunoblots and stain-free images for DKI versus WT in (**a**) liver and (**d**) skeletal muscle. Quantified (**b**) AMPK p-T172 and (**c**) ACC p-S79 relative to respective total protein in liver. Quantified (**e**) AMPK p-T172, (**f**) ACC p-S79 relative to respective total protein in skeletal muscle. Given the predominant glycogen stores in liver and skeletal muscle, AMPK content was assessed in these tissues. Representative immunoblots and stain-free images of (**g**) liver and (**j**) skeletal muscle collected from male DKI and WT mice in the fed state. Quantified (**h**) AMPK α and (**i**) AMPK β1 in liver, and (**k**) AMPK α and (**l**) AMPK β2 in skeletal muscle are shown. Male mice, $n = 6–9$, 20–32 wk. \$ $p < 0.05$, \$\$\$ $p < 0.001$ versus fed condition from same genotype; * $p < 0.05$, ** $p < 0.01$, *** $p < 0.001$, **** $p < 0.0001$.

4.3.8 DKI Mice Have Reduced AMPK Protein Content in Liver and Skeletal Muscle

Given the established roles for the AMPK α and β subunits in maintaining cellular energy balance and the observed increases in total body and fat mass as well as alterations in glycogen dynamics in DKI mice, the relative tissue protein content of these AMPK subunits was assessed in the fed state in both liver (**Figure 4.8g**) and skeletal muscle (**Figure 4.8j**). Compared to WT, liver from DKI mice displayed a ~56% reduction in total AMPK α protein content (**Figure 4.8h**). Moreover, DKI liver had a ~72% reduction in AMPK β1 protein content compared to WT (**Figure 4.8i**). In skeletal muscle from DKI mice, total AMPK α was reduced by 36% (**Figure 4.8k**) and total AMPK β2 was reduced by ~38% relative to WT (**Figure 4.8l**). However, decreased tissue AMPK content in DKI mice was not associated with any differences in *Prkab1* and *Prkab2* gene expression in liver and skeletal muscle, respectively, in the overnight fasted state (**Figure 4.9– supplemental**). Finally, given the observed increase in whole-body fat mass and altered patterns of substrate utilisation in DKI mice, AMPK protein content was also assessed in adipose tissue in the fed state. AMPK α, β1, and β2 content were reduced by ~44%, ~53%, and ~47%, respectively, in epididymal fat from DKI mice relative to WT (**Figure 4.9 – supplemental**).

4.4 Discussion

This study aimed to investigate the phenotypic effects of the DKI mutation used to chronically disrupt whole-body AMPK-glycogen binding *in vivo* on whole-body composition, glucose homeostasis, and tissue glycogen dynamics. To address this aim, we utilised a DKI mouse model in which whole-body glycogen binding was disrupted by simultaneously targeting both the AMPK β1 and β2 subunit isoforms. We report that DKI mutation of residues critical for AMPK-glycogen binding in both AMPK β subunit isoforms – AMPK β1 W100A and β2 W98A – leads to 1) increased body mass, associated with increased fat and lean mass; 2) hyperinsulinemia and glucose intolerance; 3) reduced fed liver glycogen levels and altered glycogen dynamics in skeletal muscle; and 4) reductions in AMPK protein content in the primary glycogen-storing tissues liver and skeletal muscle, as well as adipose tissue.

Recent research has identified isoform-specific phenotypic effects in single AMPK β subunit isoform KI mice, including whole-body glucose handling, tissue fat accumulation, and AMPK protein content and kinase activity (Hoffman, Whitfield et al. 2020). The AMPK DKI mouse model generated for the present study displayed robust changes in body mass and body composition, as well as impaired glucose tolerance relative to WT mice when glycogen-binding capacity was disrupted in both β isoforms, similar to the whole-body phenotype observed in AMPK β2 W98A single KI mice. In the present study, we found increased rates of CHO oxidation in DKI mice compared to WT both in the fed, basal state and in response to overnight fasting, concomitant with reduced liver glycogen in the fed state and increased skeletal muscle glycogen depletion following an overnight fast in DKI mice. In response to overnight fasting-induced glycogen depletion, no changes in tissue AMPK content were observed in WT mice and DKI mice with chronic disruption of AMPK-glycogen binding. The lack of changes between tissue AMPK content in the fed state and following overnight fasting

(~14 h) were consistent with previous findings showing no effects of fasting-induced energy stress and accompanying changes in glycogen content on liver and skeletal muscle AMPK content following prolonged 36 h fasting in mice (Lopez-Soldado, Bertini et al. 2020) and 48 h fasting in humans (Wijngaarden, van der Zon et al. 2013), respectively. Despite the observed reductions in tissue AMPK content in DKI relative to WT mice, levels of phosphorylation of AMPK's downstream substrate ACC detected in DKI liver and skeletal muscle were similar to WT in the fed, fasted, and refed states. These data are consistent with observations from AMPK β1 W100A and β2 W98A single KI mice (Hoffman, Whitfield et al. 2020) and suggest that either the remaining AMPK protein is sufficient to maintain downstream signalling to ACC, or the AMPK cellular pool that phosphorylates ACC is distinct from the pool lost with chronic disruption of glycogen binding.

The DKI mutation resulted in increased body mass, whole-body lean and fat mass, decreased ambulatory activity, and a main effect for hyperphagia. Overall genotype effects for increased carbohydrate oxidation and decreased fat oxidation were observed in DKI mice. Furthermore, increased serum TAG levels in DKI compared to WT mice may suggest that the DKI mutation alters fat availability (i.e., lipolysis) and/or reduces tissue fat uptake. Despite leptin's central role in regulating food intake (Minokoshi, Alquier et al. 2004) and increased circulating levels in obesity (Galic, Oakhill et al. 2010), there were no genotype differences detected in serum leptin concentration in either the fed or 6 h fasted states. Furthermore, we observed a reduction in AMPK protein content in adipose tissue in DKI mice compared to WT. While adipose is not a primary glycogen storing tissue, it does contain glycogen (Crosson, Khan et al. 2003, Rahman, Dobrzyn et al. 2005); therefore, this may contribute to the observed reduction in AMPK content similar to that observed in liver and skeletal muscle. While the functional relevance of glycogen in adipose is currently unknown, increased levels of glycogen accumulation in adipose tissue has been associated with obesity (Ceperuelo-Mallafre, Ejarque et al. 2016, Flores-Opazo, Trieu et al. 2020). AMPK is believed to play a role in regulating adipose metabolism and development (Wu, Zhang et al. 2018). Further research is warranted to elucidate the potential roles of AMPK-glycogen binding in the regulation of adipose tissue glycogen metabolism.

AMPK functions as a central regulator of energy utilisation and its dysfunction is associated with the onset of obesity, disruptions in glucose homeostasis, and the development of insulin resistance in insulin-sensitive tissues such as liver and skeletal muscle (Kahn, Hull et al. 2006, Samuel and Shulman 2012). We therefore assessed glucose and insulin tolerance in DKI and WT mice. As hypothesised, DKI mice exhibited elevated blood glucose concentrations in response to IPGTT compared to WT. Glycogen stores, particularly in the liver, play an important role in maintaining euglycemia (Hughey, James et al. 2017, Lopez-Soldado, Bertini et al. 2020) and are critical for maintaining glucose tolerance (Lopez-Soldado, Zafra et al. 2015); therefore, the reduced hepatic glycogen levels observed in DKI mice may contribute to the whole-body glucose intolerance observed in these mice. DKI mice also displayed hyperinsulinemia in the 6 h fasted state, characteristic of the early stages of metabolic abnormalities observed in the progression of insulin resistance (Saad, Knowler et al. 1989). However, we did not observe any impairments in blood glucose responses during an insulin challenge indicating that DKI mice maintain whole-body insulin sensitivity. Additionally, there were no reductions in content nor phosphorylation status of glucose-transport related proteins in skeletal muscle in the fed state. Skeletal muscle is the primary tissue responsible for post prandial glucose disposal (DeFronzo and Tripathy 2009), suggesting that skeletal muscle insulin sensitivity is maintained in DKI mice despite hyperinsulinemia and whole-body glucose intolerance.

Given the role of glycogen as an important source of glucose during energy stress, we examined the phenotypic effects of the DKI mutation on acute whole-body and tissue responses to fasting. At the whole-body level, DKI mice displayed reduced ambulatory activity and reduced rates of fat oxidation compared to WT during an overnight fast, consistent with observations in the fed state. These alterations in substrate utilisation in response to fasting in DKI mice are consistent with reciprocal findings in mice with constitutively active liver AMPK α, which exhibited a more rapid shift to and higher reliance on fat utilisation during fasting compared to WT (Foretz, Even et al. 2018). In contrast, whole-body AMPK β1 knockout (KO) mice display a reduction in RER and increased rates of fat oxidation at the onset of fasting (Shamshoum, Medak et al. 2019). These disparate responses observed in transgenic AMPK models versus the DKI model in the present study suggest the presence of tissue-, subunit-, and/or isoform-specific roles for AMPK in regulating whole-body substrate utilisation patterns in response to acute energy stress.

In the fed state, DKI mice displayed reduced liver glycogen content, in line with findings in fed whole-body AMPK β2 KO mice, which also demonstrate reduced hepatic glycogen levels (Steinberg, O'Neill et al. 2010). DKI mice showed no impairment in the ability to utilise liver glycogen during the overnight fast, as the absolute liver glycogen content following fasting was similar between genotypes. However, when accounting for the lower liver glycogen levels observed in the fed state in DKI mice, the overall glycogen utilisation in DKI mice was significantly reduced relative to WT. At 24 h-post glucose gavage and refeeding, DKI liver glycogen returned to levels observed prior to fasting. Liver glycogen levels can remain suppressed during resynthesis following fasting and exercise, given the greater dependence on liver glycogen to maintain euglycemia in rodents (Conlee, Lawler et al. 1987). The maintenance of liver glycogen synthesis capacity in DKI mice is contrary to observations in liver-specific AMPK α KO mice, which had similar reductions in liver glycogen as WT mice following a 24 h fast, but attenuated resynthesis following 6 h of refeeding (Hughey, James et al. 2017). These results suggest that loss of liver AMPK α reduces glycogen deposition, leading to a limited capacity for glycogenolysis to maintain euglycemia in response to fasting. However, in the current study, DKI mice displayed elevated blood glucose levels and similar serum glucagon levels compared to WT following an overnight fast, as well as increased rates of CHO oxidation and intact signalling proteins underlying glucose uptake in skeletal muscle. These findings suggest that the levels of glucose release from the liver via glycogenolysis and/or gluconeogenesis likely remains intact in DKI mice during energy stress.

DKI mice had lower glycogen accumulation in liver compared to WT. This difference in the glycogen "ceiling" may be due to changes in glycogen particle structure in DKI mice; however, there were no genotypic differences in content of enzymes associated with glycogen particle formation (i.e., GS, GBE, and glycogenin) or degradation (i.e., GP and GDE) in the livers from fed mice. Furthermore, there were no genotypic effects observed for changes in phosphorylation of GS S641 in the fed, fasted, or refed states. GS S641 is a target site of GSK3β (Mora, Sakamoto et al. 2005, Jensen, Tantiwong et al. 2012) and dephosphorylation is associated with increased enzyme activity (Skurat and Roach 1995, Prats, Helge et al. 2009). Similar levels of phosphorylation of AMPK T172 and GS S641 between genotypes suggests that glycogen resynthesis was not impaired in DKI liver, therefore, we did not measure phosphorylation of other GS sites, such as the AMPK site GS S7 (Roach, Depaoli-Roach et al. 2012). It is likely that the lower capacity to store glycogen observed in DKI mice was due to the increased reliance on CHO oxidation in the fed and fasting states compared to WT, limiting the accumulation of hepatic glycogen. Together, these findings suggest that the DKI mutation used to chronically disrupt AMPK-glycogen interactions may not impair glycogenolysis and glycogen repletion in liver but may be responsible for determining peak hepatic glycogen accumulation via altering substrate utilisation.

Given the relatively low levels of glycogen in murine skeletal muscle, mice tend to preserve muscle glycogen stores even during extended periods of fasting (Lopez-Soldado, Bertini et al. 2020). However, considering the lower total availability of liver glycogen in DKI mice, and their increased reliance on CHO both at rest and during energy stress, it is possible that an energy challenge such as an overnight fast could result in DKI mice utilising skeletal muscle glycogen while WT muscle glycogen levels remained unchanged. Therefore, it is plausible that due to an impaired ability to utilise fats and/or a preference for CHO substrates, DKI mice may use more skeletal muscle glycogen during fasting. Alternatively, given the elevated blood glucose concentrations observed in DKI mice compared to WT following overnight fasting, it is also possible that increased skeletal muscle glycogen degradation in DKI mice was due to impaired skeletal muscle uptake of circulating glucose, despite no observed changes in the glucose transport-related proteins in the fed state.

Glycogen resynthesis in skeletal muscle is a metabolic priority following energy stress, and full resynthesis typically occurs within 3-5 hours of recovery and refeeding (Irimia, Rovira et al. 2012, Irimia, Tagliabracci et al. 2015). For example, resynthesis of skeletal muscle glycogen following exercise is promoted by the depletion-induced activation of GS and/or increased glucose uptake via exercise-induced translocation of GLUT4 to the plasma membrane (Prats, Helge et al. 2009, Richter and Hargreaves 2013, Burke, van Loon et al. 2017). Notably, in the current study, skeletal muscle glycogen levels in DKI mice remained suppressed compared to fed levels both 5 h-post glucose gavage to promote glycogen resynthesis and following 24 h with refeeding. A recent study in inducible muscle-specific AMPK α KO mice found that loss of AMPK resulted in reduced glycogen resynthesis rates in skeletal muscle following exercise and glucose administration, leading to blunted glycogen repletion after 5 h of recovery (Hingst, Bruhn et al. 2018), suggesting that skeletal muscle AMPK plays a crucial role in this process. Surprisingly, the inability to resynthesise skeletal muscle glycogen in DKI mice was not accompanied by any reductions in glycogen associated proteins (i.e., GS, GBE, and glycogenin) or changes in phosphorylation of GS S641. Our findings suggest that disruption of AMPK's glycogen binding capacity and/or the associated reductions in AMPK protein content in glycogen storing tissues lead to previously underappreciated consequences on regulation of glycogen dynamics, potentially through AMPK's interactions with glycogen and/or indirectly by shifting substrate utilisation patterns.

Previous studies involving cell-free assays (McBride, Ghilagaber et al. 2009) and acute glycogen-depleting exercise interventions performed in rodents (Wojtaszewski, Jorgensen et al. 2002) and humans (Wojtaszewski, MacDonald et al. 2003, Yeo, McGee et al. 2010) have demonstrated increased AMPK phosphorylation and kinase activity in association with reduced glycogen availability. These findings helped form the hypothesis that AMPK-glycogen binding may serve a role in sensing stored energy (McBride, Ghilagaber et al. 2009), whereby depletion of glycogen releases AMPK, allowing it to become activated and phosphorylate its downstream substrates to promote energy production. While these studies have helped establish the existence of this interaction *in vitro* as well as putative roles of these interactions in acute changes in glycogen availability *in vivo*, the physiological consequences of disrupting AMPK-glycogen binding *in vivo* remained to be elucidated. In the present study, we observed reductions in total AMPK α content in a range of metabolically active tissues and disruptions in metabolism associated with the DKI mutation. This is similar to observations in studies using tissue-specific (O'Neill, Maarbjerg et al. 2011) and isoform-specific (Dzamko, van Denderen et al. 2010, Steinberg, O'Neill et al. 2010, Dasgupta, Ju et al. 2012) AMPK β KO models; however, in DKI tissues we do not observe a complete loss of AMPK protein content that is characteristic of KO models. We cannot distinguish whether the DKI phenotype and associated reductions in tissue AMPK content are due to disruption of AMPK-glycogen binding and/or due to AMPK destabilisation independent of glycogen binding. As these phenotypic effects in DKI mice cannot be attributed directly or exclusively to AMPK-glycogen binding, the possibility of glycogen binding-independent AMPK destabilisation warrants further research. It is well recognised that the β subunit plays an essential role in stabilising the αβγ heterotrimer and the C-terminus (residues 186-270) of the β subunit is sufficient to anchor the α and γ subunits (Iseli, Walter et al. 2005). The C-terminus is structurally distal to the CBM (residues 68-163) responsible for glycogen binding. However, when considered along with findings that mutation of the CBM of the starch or glycogen binding proteins results in loss of protein and/or instability (Chang, Irwin et al. 1998), our results suggest that the CBM and/or glycogen binding capacity of multiple proteins, including AMPK, may be involved in the regulation of protein content and/or stability. In contrast to reductions in expression of *Prkab1* in liver and *Prkab2* in skeletal muscle in AMPK β1 W100A and β2 W98A single KI mice versus WT in the fed state (Hoffman, Whitfield et al. 2020), we did not observe any changes in liver *Prkab1* or muscle *Prkab2* expression in overnight fasted DKI mice, suggesting that changes in gene expression do not contribute to reduced AMPK protein content. However, reduced tissue AMPK content in DKI mice is consistent with results from AMPK β1 W100A and β2 W98A KI models (Hoffman, Whitfield et al. 2020), suggesting that the β subunit CBM may play a role in maintaining pools of cellular AMPK protein and, therefore, metabolic homeostasis.

In summary, we demonstrate that the DKI mutation utilised to chronically disrupt whole-body AMPK-glycogen interactions *in vivo* leads to phenotypic effects including disruptions in whole-body metabolic homeostasis and tissue glycogen dynamics that are associated with reduced AMPK protein content in glycogen-storing tissues including liver, skeletal muscle, and adipose tissue. DKI mice also have increased body mass and adiposity, reduced rates of fat oxidation, as well as impaired glucose handling and hyperinsulinemia. Furthermore, DKI mice display increased rates of CHO oxidation in the fed state and during fasting-induced energy stress, associated with reduced basal liver glycogen levels and altered skeletal muscle glycogen utilisation and repletion. The DKI mutation used to disrupt whole-body AMPK-glycogen binding in mice leads to simultaneous increases in serum insulin levels and adiposity, contributing to the progression of glucose intolerance characteristic of the early stages in the development of insulin resistance. Collectively, these findings highlight roles of AMPK in maintaining energy balance, glucose homeostasis, and glycogen dynamics and suggest that AMPK-glycogen binding may serve potential physiological roles in cellular, glycogen-storing tissue, and whole-body energy homeostasis.

4.5 Materials and Methods

4.5.1 Animal Models

CRISPR/Cas9 gene targeting was used to generate two whole-body single KI mouse models on a C57BL/6J background. Tryptophan residues in the AMPK β subunit isoforms that are critical for glycogen binding (Polekhina, Gupta et al. 2005, McBride, Ghilagaber et al. 2009) – W100 within the β1 isoform (W100A) and the analogous residue in the β2 isoform (W98A), respectively – were mutated to alanine, as described previously (Hoffman, Whitfield et al. 2020). Heterozygous mice possessing either the β1 W100A or β2 W98A KI mutation were subsequently crossed to generate AMPK β1(W100A)/β2(W98A) DKI mice (**Figure 4.2a**) with chronic disruption of AMPK-glycogen binding. Homozygous carriers of the DKI mutations were used for breeding, and DKI and WT breeders were annually backcrossed to generate heterozygous mice and rederive the homozygous DKI line used for experimentation. Confirmatory genotyping was performed from tail samples by TransnetYX (Cordova, TN, USA).

Experiments were undertaken using male AMPK DKI and age-matched WT control mice. Only male mice were used to maintain adequate DKI female breeder availability and ensure sufficient age matched DKI mice were readily available for analyses. Mice were group housed in a temperature (22°C) and humidity-controlled facility with 12:12 h light and dark cycle. Mice were given *ad libitum* access to a standard chow diet (6% fat, 20% protein and 29% starch; Barastoc, Ridley Agriproducts, Pakenham, Victoria, Australia) and water, unless otherwise specified. All mouse procedures were performed under approval of the St. Vincent's Hospital (Melbourne, Victoria, Australia) Animal Ethics Committee (AEC 025-15 and 011-19), conforming to all the requirements of the National Health and Medical Research Council of Australia (NHMRC) and in accordance with the Australian code of practice for the care and use of animals for scientific purposes (8th Edition 2013).

4.5.2 Whole-Body Composition Measurements

Whole-body composition (fat mass, lean mass, and water weight) was assessed by nuclear magnetic resonance using the EchoMRI Body Composition Analysis system (EchoMRI, Houston, TX, USA). Measurements were undertaken in the fed state (0900 h).

4.5.3 Metabolic Caging

Mice underwent metabolic cage analyses using the Comprehensive Lab Animal Monitoring System (CLAMS, Columbus Instruments, Columbus, OH, USA). Mice had either *ad libitum* access to chow or were fasted overnight. Mice with *ad libitum* access to chow were singly housed for ~60 h total at 21°C and food intake, infrared-based ambulatory activity, O_2 consumption (VO_2), CO_2 production (VCO_2), and RER ($VCO_2 \cdot VO_2^{-1}$) were measured continuously. The first ~6 h served as the acclimatisation period and were not included in CLAMS data analyses. Following acclimatisation, hourly, light/dark cycle and 24 h averages were calculated. TEE and rates of fat and CHO oxidation were calculated as previously described (Peronnet and Massicotte 1991). For responses to fasting, mice were acclimatised (~6 h) before food was removed at the start of the dark cycle (1800 h). Mice were fasted overnight (~14 h) and ambulatory activity, VO_2, VCO_2, and RER were measured continuously, and TEE and substrate oxidation rates were calculated. Mice were then returned to their home cages with *ad libitum* access to chow.

4.5.4 Intraperitoneal Glucose Tolerance and Insulin Tolerance Testing

Commencing at 0800 h, mice were fasted either 6 h prior to IPGTT or 4 h prior to IPITT, then injected with glucose (1 $g \cdot kg^{-1}$ total lean mass; Sigma-Aldrich, St. Louis, MO, USA) or insulin (0.5 $U \cdot kg^{-1}$ total body mass; Humulin, Eli Lilly and Company, Indianapolis, IN, USA), respectively. Blood glucose was monitored via tail tip bleed using a glucometer (Accu-Check Performa, Roche Diagnostics GmbH, Mannheim, Germany). Mice were allowed at least one week of recovery between tests.

4.5.5 Fasting and Refeeding Protocol

Mice underwent a fasting and refeeding protocol to assess glycogen depletion and repletion in response to energy stress and availability. A cohort of mice were subjected to an overnight fast (~14 h) while a control fed group had continued *ad libitum* access to food. The following morning shortly after the start of the light cycle (0800 h), blood glucose was measured in all mice via tail tip bleed using a glucometer. Fed mice and a subset of fasted mice were euthanised via cervical dislocation and tissues were collected and immediately snap-frozen for subsequent analysis. The remaining fasted mice received an oral gavage of glucose (3.6 $g \cdot kg^{-1}$ total body mass) and blood glucose responses were monitored over a period of 5 h, after which mice were either euthanised and tissues collected, or were returned to their home cages with *ad libitum* access to food. Blood glucose was measured in the remaining mice 24 h after administration of the glucose gavage, and mice were then euthanised, and tissues were collected.

4.5.6 Serum Analysis

Blood samples collected retro-orbitally were left to clot for 30 min at room temperature in non-coated polypropylene tubes. Samples were then centrifuged at 10,000x *g* for 5 min at 4°C, and the resulting serum supernatant was aliquoted and stored at –80°C. Hormone and lipid concentrations were assessed in these aliquots using leptin (Abcam, Cambridge, UK), glucagon, and ultra-sensitive mouse insulin (Crystal Chem, Elk Grove Village, IL, USA) ELISA kits, and NEFA-C (Wako Pure Chemical Industries, Osaka, Japan) and TAG (Abcam) colorimetric assay kits.

4.5.7 Assessment of Tissue Glycogen Content

Snap-frozen gastrocnemius muscle (~40 mg) and liver (~25 mg) samples were chipped under liquid N_2, freeze-dried overnight, powdered, and dissected free of visible blood and connective tissue. Aliquots of powdered tissue (~2-4 mg) were then alkaline extracted, and the supernatant was used for quantification of glycogen content using spectrophotometry as described previously (Bergmeyer 1974). Absorbance was measured at 340 nm using a SpectraMax Paradigm plate reader (Molecular Devices, San Jose, CA, USA) and data were acquired using SoftMax Pro microplate data acquisition software (Molecular Devices).

4.5.8 Immunoblotting

Snap-frozen liver, gastrocnemius muscle, and adipose tissue samples were lysed in homogenisation buffer containing 50 mM Tris.HCL, pH 7.5, 1 mM EDTA, 1 mM EGTA, 10% glycerol, 1% Triton-X (Sigma-Aldrich), 50 mM sodium fluoride, 5 mM sodium pyrophosphate with cOmplete Protease Inhibitor Cocktail and PhosSTOP phosphatase inhibitor tablets from Sigma-Aldrich. Lysed tissue samples were centrifuged at 16,000x *g* for 30 min at 4°C, and supernatant protein content was determined using the bicinchoninic acid method (BCA; Pierce, Rockford, IL, USA). Tissue lysates (10 mg protein·well^{-1}) were run on 4-15% or 4-20% precast stain-free gels (Bio-Rad, Hercules, CA, USA) and transferred to PVDF membranes (Merck Millipore, Burlington, MA, USA). Membranes were blocked with 7.5% BSA in Tris-buffered saline containing 0.1% Tween 20 from Sigma-Aldrich (TBS-T) for 1 h at room temperature, then incubated with primary antibodies with rocking as detailed in **Table 4.2**. After washing with TBS-T, membranes were incubated for 1 h at room temperature in either an anti-rabbit IgG (GAR) or anti-mouse IgG (GAM) horseradish-peroxidase-conjugated secondary antibody from Cell Signaling Technology (CST; Danvers, MA, USA) in TBS-T. Proteins were detected via chemiluminescence using SuperSignal West Femto Maximum Sensitivity Substrate (Thermo Fisher Scientific, Waltham, MA, USA) and imaged using the ChemiDoc Imaging System (Bio-Rad). Band intensities of total protein content and protein phosphorylation were normalised to the total lane protein from the respective stain-free image using Image Lab software (version 6, Bio-Rad) as described previously (Tachtsis, Whitfield et al. 2020) and phosphorylation was expressed relative to respective total protein content. Primary and secondary antibody details are listed in **Table 4.2**.

Table 4.2 – Antibodies and protocols used for immunoblotting

Target	Primary Antibody	Incubation	Secondary Antibody
AMPK α p-T172	CST 2531 1:1000	Overnight 4°C	GAR CST 7074 1:5000
AMPK α	CST 2532 1:1000	Overnight 4°C	GAR CST 7074 1:5000
AMPK β1/β2	CST 4150 1:1000	Overnight 4°C	GAR CST 7074 1:5000
ACC p-S79	CST 11818 1:1000	Overnight 4°C	GAR CST 7074 1:5000
ACC	CST 3662 1:1000	Overnight 4°C	GAR CST 7074 1:5000
Akt p-S473	CST 9271 1:1000	1.5 h Room temperature	GAR CST 7074 1:5000
Akt	CST 4691 1:1000	Overnight 4°C	GAR CST 7074 1:5000
AS160 p-T642	CST 4288 1:1000	Overnight 4°C	GAR CST 7074 1:5000
AS160	Abcam ab24469 1:1000	Overnight 4°C	GAR CST 7074 1:5000
GLUT4	CST 2213 1:1000	Overnight 4°C	GAM CST 7076 1:2000

GS p-S641	CST 47043 1:1000	Overnight 4°C	GAR CST 7074 1:5000
GS	CST 3886 1:1000	Overnight 4°C	GAR CST 7074 1:5000
Glycogenin1	Abcam ab11171 1:1000	Overnight 4°C	GAR CST 7074 1:2000
GBE1	Abcam ab180596 1:1000	Overnight 4°C	GAR CST 7074 1:2000
GP	Antibody generated by B.E.K. laboratory 1:1000	Overnight 4°C	GAR CST 7074 1:2000
GDE	Antibody generated by B.E.K. laboratory 1:1000	Overnight 4°C	GAR CST 7074 1:2000

4.5.9 RNA Extraction and Gene Expression Analysis

RNA from snap-frozen overnight fasted (~14 h) liver (15 mg) and skeletal muscle (25 mg) was extracted using TRIzol LS Reagent (Life Technologies, Carlsbad, CA, USA). RNA was treated with DNase I (Sigma-Aldrich) and reverse-transcribed using SuperScript VILO Master Mix (Life Technologies). Pre-Amplification was completed using TaqMan Custom PreAmp Pool and PreAmp Master Mix (Applied Biosystems, Foster City, CA, USA). Quantitative polymerase chain reaction (qPCR) was performed using a CFX Connect Real-Time System (Bio-Rad). Gene expression was normalised to GAPDH using TaqMan Fast Advanced Master Mix (Applied Biosystems). *Prkab1* (liver, AMPK β1; Mm01201921_m1), *Prkab2* (skeletal muscle; Mm01257133_m1), and *Gapdh* (liver and skeletal muscle; Mm99999915_g1)

TaqMan Gene Expression Assays were used (Applied Biosystems). Relative levels of mRNA were assessed using the ΔΔCt method.

4.5.10 Statistical Analyses

Comparisons between genotypes were analysed using two-tailed Student's *t* testing (WT versus DKI) or two-way analysis of variance (ANOVA; WT versus DKI comparisons over time or condition). Measurements of body mass and composition were analysed using linear mixed models. If significance was detected using ANOVA or linear mixed models, Bonferroni post hoc testing was applied where appropriate. All statistical analyses were performed using GraphPad Prism software (version 8, GraphPad Software, La Jolla, CA, USA). Significance was set at $p < 0.05$. All data are presented as mean ± standard error of the mean (SEM).

4.6 Supplementary Material

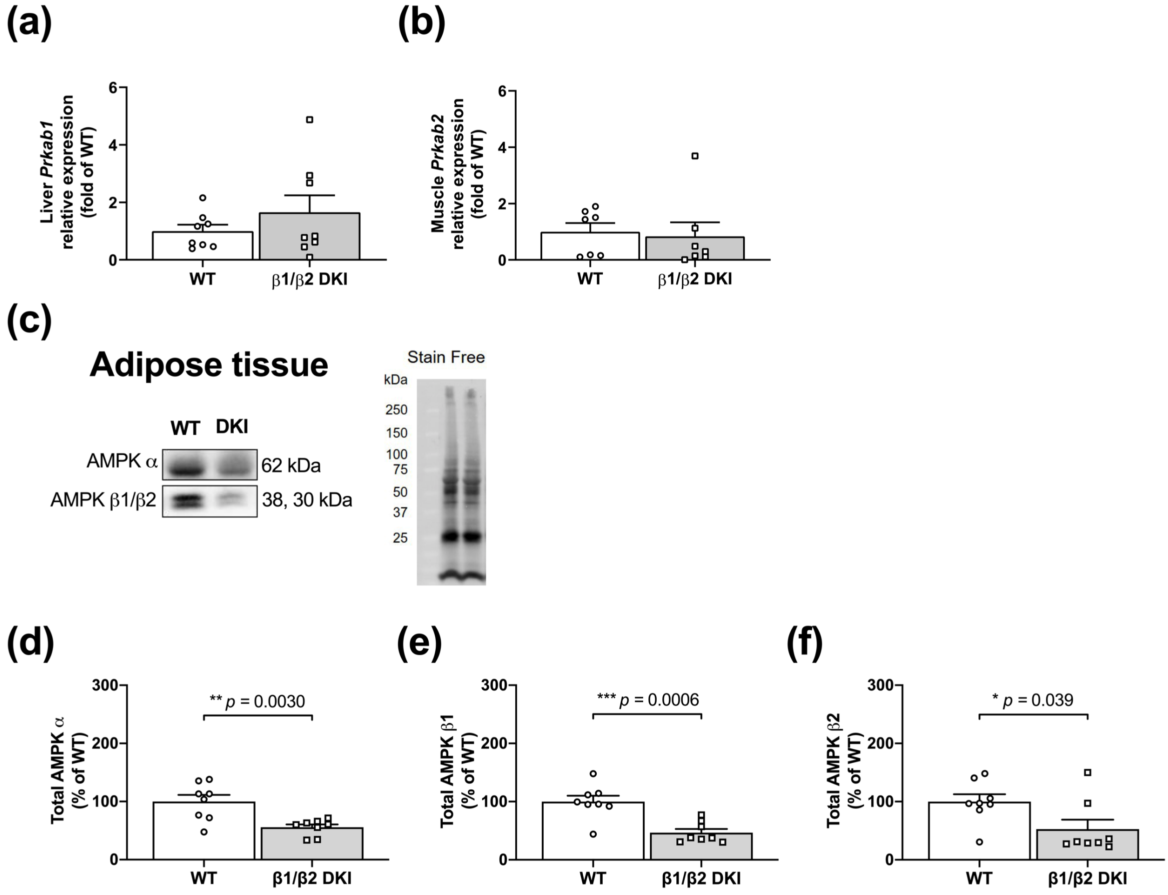

Figure 4.9 – DKI mice display no differences in liver *Prkab1* or muscle *Prkab2* gene expression versus WT, and DKI adipose tissue displays reduced AMPK content. Gene expression was assessed in DKI and WT liver and skeletal muscle using qPCR. (**a**) Relative *Prkab1* (AMPK β1) gene expression in WT and DKI liver and (**b**) relative *Prkab2* (AMPK β2) gene expression in WT and DKI skeletal muscle. Overnight fasted (~14 h), male mice, *n* = 7–8, 20–32 wk. AMPK subunit protein content was assessed in epididymal adipose tissue. (**c**) Representative immunoblots and stain-free images collected from fed DKI and WT mice. Quantified (**d**) AMPK α, (**e**) AMPK β1, and (**f**) AMPK β2. Male mice, *n* = 8, 17–20 wk. * p <0.05, ** $p < 0.01$, *** $p < 0.001$.

Author Contributions: Conceptualisation and methodology, NRJ, JW, LM-S, BEK, JAH, and NJH; investigation and formal analysis, NRJ, JW, and NJH; mouse breeding and husbandry, NRJ, LM-S, and NJH; writing—original draft preparation, NRJ, JW, and NJH; writing—review and editing, NRJ, JW, LM-S, BEK, JAH, and NJH. All authors have read and agreed to the published version of the manuscript.

Funding: This work was supported by Australian Catholic University research funding awarded to NJH, and by a National Health and Medical Research Council of Australia (NHMRC) project grant (1085460) and NHMRC Fellowship (1078752) awarded to BEK. JW is supported by a Natural Sciences and Engineering Research Council of Canada (NSERC) Postdoctoral Fellowship.

Institutional Review Board Statement: The study was approved by the St. Vincent's Hospital (Melbourne, Victoria, Australia) Animal Ethics Committee (AEC 025-15, approved 11/2015, and AEC 011-19, approved 05/2019).

Data Availability Statement: The data that support the findings of this study are available from the corresponding author upon reasonable request.

Acknowledgements: We are grateful to Mehdi Belhaj and Tiego Diniz for assistance with mouse tissue collections, and Vicki Moshovakis for assistance with blood sampling. We thank the St. Vincent's BioResources Centre staff for their assistance with mouse breeding and husbandry. The graphical abstract and Figure 4.2a were created with BioRender.com.

Conflicts of Interest: The authors declare no conflicts of interest.

Chapter 5 Linking Chapter

Findings from Study 1, summarised in **Figure 4.1**, highlighted the phenotypic effects of the DKI mutation utilised to disrupt whole-body AMPK-glycogen binding. These effects were determined in the regulation of energy balance in the fed state and in response to extended, low levels of energy stress induced by overnight fasting. Specifically, DKI mice displayed altered patterns of glycogen utilisation and resynthesis and increased reliance on carbohydrate, associated with reduced tissue AMPK content in metabolically active tissues including liver, skeletal muscle, and adipose tissue.

As a central energy regulator, AMPK is involved in the cellular and tissue responses to acute exercise and contributes to exercise capacity (Kjobsted, Hingst et al. 2018). Previous research utilising whole-body AMPK β2 (Steinberg, O'Neill et al. 2010, Dasgupta, Ju et al. 2012) and muscle-specific AMPK β1/β2 (O'Neill, Maarbjerg et al. 2011) KO mice have demonstrated reduced maximal running speed compared to WT. Furthermore, KI models with disrupted AMPK-glycogen binding in β2, but not β1, subunit isoform have reduced maximal running speed (Hoffman, Whitfield et al. 2020), suggesting potential roles for AMPK-glycogen binding in skeletal muscle and/or the β2 isoform in determining maximal running capacity. The reduced exercise capacity in transgenic AMPK models could be due to changes in substrate utilisation patterns, as AMPK has been implicated in regulating glucose uptake and fat oxidation in non-human primates and rodents (Merrill, Kurth et al. 1997, Cokorinos, Delmore et al. 2017, Myers, Guan et al. 2017). However, findings of whole-body and tissue substate utilisation patterns in AMPK KO mice have been equivocal. As detailed in **Chapter 2**, muscle-specific AMPK β1/β2 KO mice display reduced RER and contraction-stimulated skeletal muscle glucose clearance compared to WT during submaximal treadmill running (O'Neill, Maarbjerg et al. 2011). In contrast, inducible muscle-specific AMPK α1/α2 KO models demonstrate attenuated maximal exercise capacity but no differences in fuel utilisation or skeletal muscle glucose uptake compared to WT (Hingst, Kjobsted et al. 2020). These contrasting findings suggest that AMPK regulates substrate utilisation in an isoform- and tissue-specific manner, which can lead to varied responses in whole-body substrate utilisation in response to exercise. However, given these studies were focused on assessing either the overall function of the catalytic α and regulatory β subunits or the isoform-specific consequences of KI mutation used to disrupt AMPK-glycogen binding, the consequences of whole-body disruption of AMPK-glycogen remain to be elucidated.

Therefore, the overall aim of Study 2 was to determine if the DKI mutation utilised to disrupt whole-body AMPK-glycogen binding also resulted in alterations in exercise capacity and substrate utilisation patterns during exercise. Based on findings in Study 1 showing reduced tissue AMPK content in DKI mice specifically in skeletal muscle, it was hypothesised that maximal running capacity would be reduced in DKI mice. Furthermore, given the finding that DKI mice display increased rates of whole-body CHO utilisation both at rest and during fasting, it was also hypothesised that DKI mice would have increased rates of whole-body carbohydrate oxidation during exercise, due to higher levels of hepatic and skeletal muscle glycogen utilisation during maximal exercise.

Chapter 6 Study 2 – Phenotypic Effects of the AMPK DKI Mutation on Exercise Capacity and Substrate Utilisation During Exercise

Publication Statement:

This Chapter is comprised of an original research manuscript that was accepted for publication at *Frontiers in Physiology* on 3 March 2022 and published online on 22 March 2022. This Chapter is presented here as the accepted pre-publication version.

Janzen NR, Whitfield J, Murray-Segal L, Kemp BE, Hawley JA, Hoffman NJ (2022). Disrupting AMPK-Glycogen Binding in Mice Increases Carbohydrate Utilisation and Reduces Exercise Capacity. *Front Physiol*, 13:859246. doi:10.3389/fphys.2022.859246.

Disrupting AMPK-Glycogen Binding in Mice Increases Carbohydrate Utilisation and Reduces Exercise Capacity

Natalie R. Janzen [1], Jamie Whitfield [1], Lisa Murray-Segal [2], Bruce E. Kemp [1,2], John A. Hawley [1], and Nolan J. Hoffman [1,*]

[1] Exercise and Nutrition Research Program, Mary MacKillop Institute for Health Research, Australian Catholic University, Level 5, 215 Spring Street, Melbourne, VIC 3000, Australia; natalie.janzen@acu.edu.au (NRJ); jamie.whitfield@acu.edu.au (JW); john.hawley@acu.edu.au (JAH)

[2] St Vincent's Institute of Medical Research and Department of Medicine, University of Melbourne, 9 Princes Street, Fitzroy, VIC 3065, Australia; lmsegal@svi.edu.au (LM-S); bkemp@svi.edu.au (BEK)

[*]Correspondence: nolan.hoffman@acu.edu.au

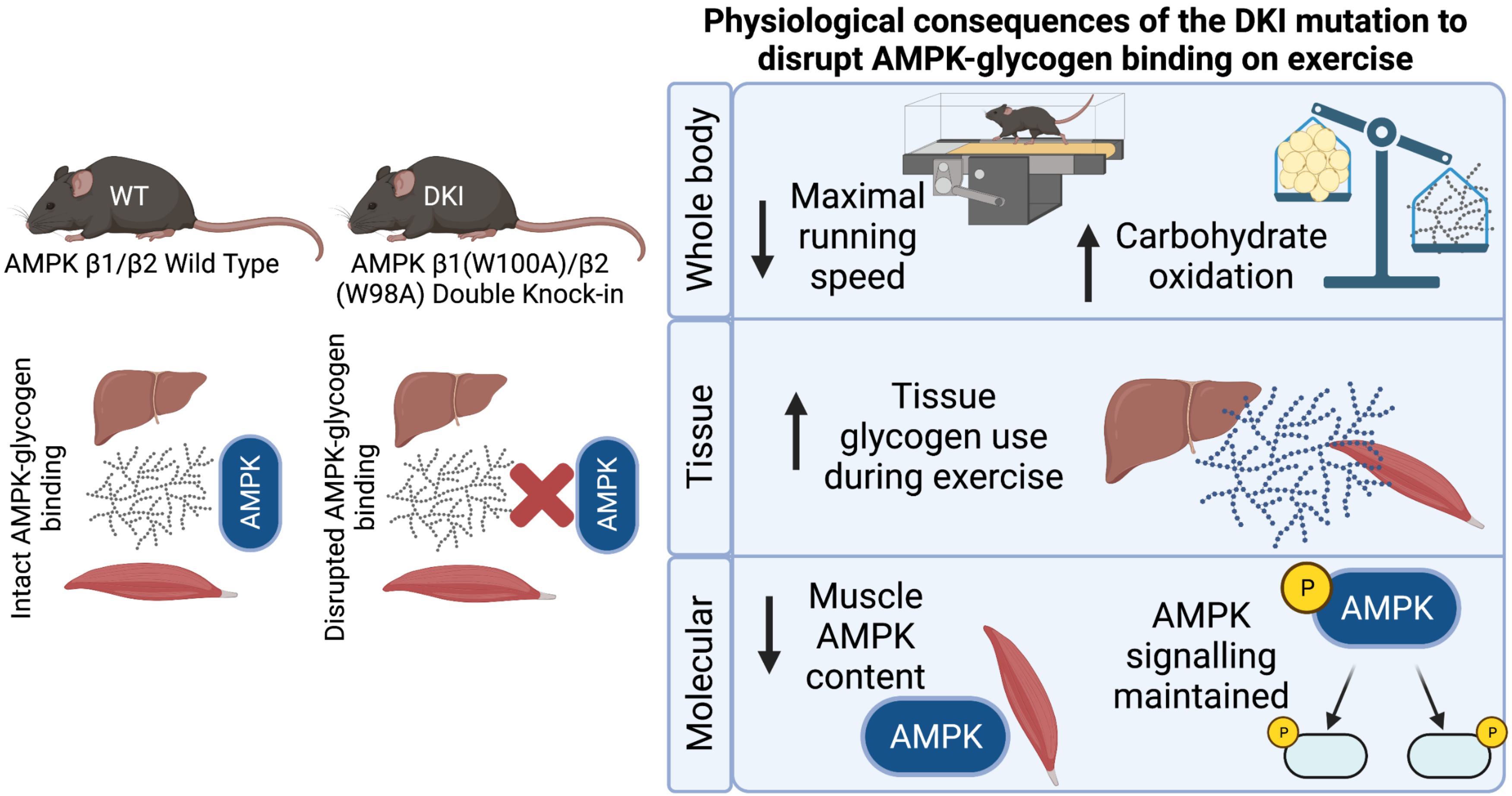
WT
AMPK β1/β2 Wild Type
DKI
AMPK β1(W100A)/β2 (W98A) Double Knock-in
Intact AMPK-glycogen binding
AMPK
Disrupted AMPK-glycogen binding
AMPK
Physiological consequences of the DKI mutation to disrupt AMPK-glycogen binding on exercise
Whole body
Maximal running speed
Carbohydrate oxidation
Tissue
Tissue glycogen use during exercise
Molecular
Muscle AMPK content
AMPK
AMPK signalling maintained
P
AMPK
P
P

Figure 6.1 – Graphical abstract summarising key findings from Study 2. Created with BioRender.com.

6.1 Abstract

The AMP-activated protein kinase (AMPK) is a central regulator of cellular energy balance and metabolism and binds glycogen, the primary storage form of glucose in liver and skeletal muscle. The effects of disrupting whole-body AMPK-glycogen interactions on exercise capacity and substrate utilisation during exercise *in vivo* remain unknown. We used male whole-body AMPK double knock-in (DKI) mice with chronic disruption of AMPK-glycogen binding to determine the effects of DKI mutation on exercise capacity, patterns of whole-body substrate utilisation, and tissue metabolism during exercise. Maximal treadmill running speed and whole-body energy utilisation during submaximal running were determined in wild-type (WT) and DKI mice. Liver and skeletal muscle glycogen and skeletal muscle AMPK α and β2 subunit content and signalling were assessed in rested and maximally exercised WT and DKI mice. Despite a reduced maximal running speed and exercise time, DKI mice utilised similar absolute amounts of liver and skeletal muscle glycogen compared to WT. DKI skeletal muscle displayed reduced AMPK α and β2 content versus WT, but intact relative AMPK phosphorylation and downstream signalling at rest and following exercise. During submaximal running, DKI mice displayed an increased respiratory exchange ratio, indicative of greater reliance on carbohydrate-based fuels. In summary, whole-body disruption of AMPK-glycogen interactions reduces maximal running capacity and skeletal muscle AMPK α and β2 content and is associated with increased skeletal muscle glycogen utilisation. These findings highlight potential unappreciated roles for AMPK in regulating tissue glycogen dynamics and expand AMPK's known roles in exercise and metabolism.

Keywords: AMP-activated protein kinase; carbohydrate binding module; glycogen; skeletal muscle; exercise; energy utilisation; metabolism

6.2 Introduction

The AMP-activated protein kinase (AMPK) is an important regulator of energy utilisation and metabolic homeostasis. AMPK regulates multiple metabolic pathways that help maintain and restore energy balance during energy stress, including glycolysis as well as fatty acid synthesis and oxidation. The AMPK heterotrimeric complex consists of a catalytic α subunit and β and γ regulatory subunits. The β subunit scaffolds the heterotrimer and contains a carbohydrate binding module (CBM) which allows AMPK to bind glycogen (Hudson, Pan et al. 2003, Polekhina, Gupta et al. 2003, Polekhina, Gupta et al. 2005, McBride, Ghilagaber et al. 2009). In rodents, the β1 isoform is predominantly expressed in liver while the β2 isoform, which has the capacity to bind glycogen more tightly (Koay, Woodcroft et al. 2010, Mobbs, Di Paolo et al. 2017), is predominantly expressed in skeletal muscle (Janzen, Whitfield et al. 2018).

Glycogen serves as a critical energy substrate and is predominantly stored in liver and skeletal muscle. In response to energy stress such as exercise, glycogen is mobilised into glycolytic intermediates and resynthesised to help restore liver and/or skeletal muscle energy levels. In rodents, liver glycogen stores are used to maintain euglycemia in both the post-prandial and energy-depleted states, while skeletal muscle stores are preserved for strenuous exercise (Baldwin, Reitman et al. 1973, Reitman, Baldwin et al. 1973, Terjung, Winder et al. 1973). The contribution of glycogen to total energy expenditure becomes higher with increasing exercise intensity (van Loon, Greenhaff et al. 2001), and depletion of skeletal muscle glycogen ultimately results in fatigue (Philp, Hargreaves et al. 2012, Nielsen and Ortenblad 2013, Ortenblad, Westerblad et al. 2013).

Glycogen interactions mediated by the AMPK β subunit CBM have been hypothesised to serve an energy-sensing role, whereby AMPK senses stored glycogen levels and regulates metabolic pathways to maintain cellular energy homeostasis (McBride, Ghilagaber et al. 2009, McBride and Hardie 2009), such as during exercise. In support of this theory, whole-body AMPK β2 knockout (KO) mice have reduced maximal treadmill running speed, and while

WT mice had significant reductions in skeletal muscle glycogen post-exercise, AMPK β2 KO mice had no change in skeletal muscle glycogen content following a maximal test (Dasgupta, Ju et al. 2012). Additionally, skeletal muscle specific AMPK β1/β2 KO mice have reduced maximal running speed, concomitant with increased reliance on fat as an energy substrate (O'Neill, Maarbjerg et al. 2011). AMPK β2 knock-in (W98A KI) mice with disrupted β2 subunit isoform glycogen binding have impaired maximal running speed, although this effect was not observed in β1 (W100A KI) mice (Hoffman, Whitfield et al. 2020). Single AMPK KI mutation utilised to disrupt β1 or β2 AMPK-glycogen binding led to reduced tissue AMPK levels in liver or skeletal muscle, respectively, suggesting that glycogen binding may play a role in maintaining tissue AMPK content (Hoffman, Whitfield et al. 2020). AMPK double knock-in (DKI) mice with chronic whole-body disruption of glycogen binding capacity via simultaneous mutation of both β1 and β2 isoforms display increased adiposity, increased rates of carbohydrate (CHO) oxidation and altered tissue glycogen dynamics in the fed and resting state and in response to fasting, concomitant with reductions in AMPK content in liver and skeletal muscle (Janzen, Whitfield et al. 2021).

Whether reduced tissue AMPK in DKI mice and the accompanying alterations in whole-body substrate utilisation patterns and tissue metabolism affect energy utilisation during exercise and ultimately exercise capacity in these mice remains unknown. Accordingly, we utilised this DKI mouse model with whole-body disruption of AMPK-glycogen binding to determine the effects of the DKI mutation on maximal running speed and fuel utilisation during exercise. We hypothesised that DKI mice would have reduced maximal running speed and increased CHO oxidation rates during treadmill exercise compared to WT.

6.3 Results

6.3.1 DKI Mice Have Reduced Maximal Running Speed

To determine whether the DKI mutation utilised to disrupt whole-body AMPK-glycogen binding alters exercise capacity, DKI and wild type (WT) mice were subjected to treadmill running tests at a 0° incline to determine maximal running speed and time to exhaustion at 70% of individual maximal running speed. DKI mice had significantly lower maximal running speed compared to WT (**Figure 6.2A**), while the time to exhaustion was similar between genotypes (**Figure 6.2B**).

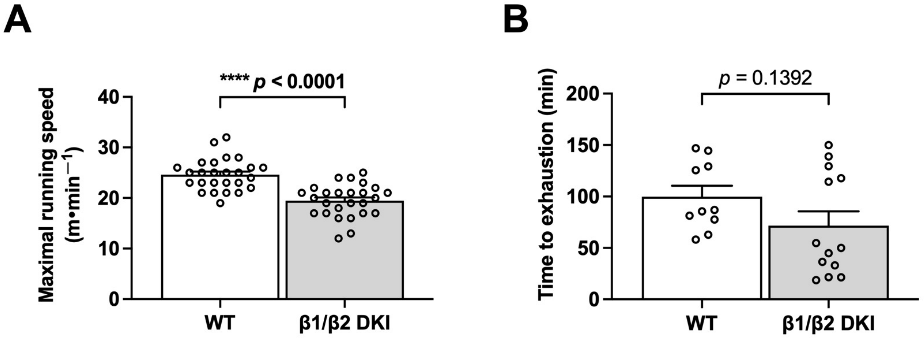

Figure 6.2 – The double knock-in (DKI) mutation used to disrupt whole-body AMPK-glycogen binding in mice reduces maximal running speed but does not alter time to exhaustion at submaximal running speed. (**A**) Maximal running speed at a 0° treadmill incline in wild type (WT) and DKI mice (n = 26); (**B**) Time to exhaustion at 70% of individual maximal running speed at a 0° incline (n = 10-13). Male mice, 17-21 wk. **** $p < 0.0001$.

6.3.2 DKI Mice Display Increased CHO Utilisation During Submaximal Exercise

To determine if differences in patterns of substrate utilisation contribute to the observed reduction in maximal exercise capacity in DKI versus WT mice, a subset of animals underwent exercise calorimetry testing using a treadmill equipped with indirect calorimetry. Continuous running at 60% of maximal running speed was used to ensure mice could complete the running protocol and to promote a mixed utilisation of CHO- and fat-based substrates (Petrosino, Heiss et al. 2016, Ishihara and Taniguchi 2018). While there were no observed differences in relative oxygen consumption (VO_2; **Figure 6.3A**) or total energy expenditure (TEE; **Figure 6.3B**) during submaximal running between genotypes, DKI mice displayed an increase in respiratory exchange ratio (RER; **Figure 6.3C**), indicating increased reliance on CHO fuels during running compared to WT. In line with the observed increase in RER, DKI mice displayed a two-fold increase in calculated rates of CHO oxidation during submaximal running compared to WT mice (**Figure 6.3D**), while there were no differences between genotypes in calculated rates of fat oxidation (**Figure 6.3E**). This resulted in CHO oxidation accounting for nearly 45% of TEE in DKI mice – double the percentage observed in WT (**Figure 6.3F**). Meanwhile, fat oxidation accounted for 56% of TEE in DKI mice, compared to 78% of TEE in WT mice (**Figure 6.3F**).

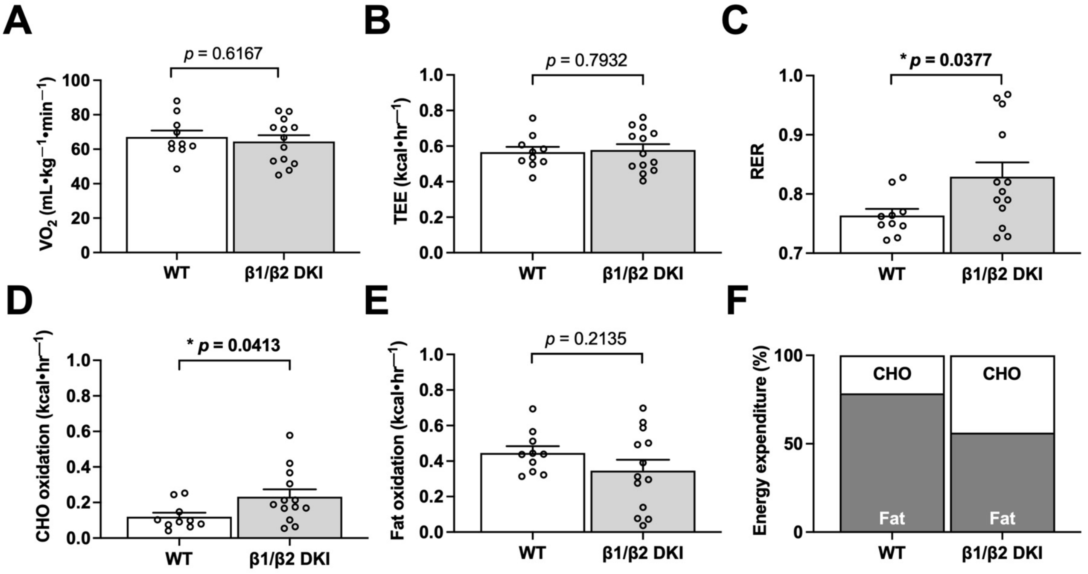

Figure 6.3 – DKI mice have increased respiratory exchange ratio (RER) and carbohydrate (CHO) oxidation rates during exercise calorimetry experiments. Respiratory gases (VO_2 and VCO_2) were measured every min and used to calculate RER, total energy expenditure (TEE), and substrate utilisation during exercise calorimetry treadmill running at 60% of individual maximal running speed. Data presented are the average over the final 5 min of exercise. (**A**) VO_2; (**B**) TEE; (**C**) RER; (**D**); CHO oxidation rates; (**E**) Fat oxidation rates; (**F**) Percent contribution of fat and CHO oxidation rates to TEE. Male mice, 17-20 wk, n = 11-13. * $p < 0.05$.

6.3.3 DKI Mice Have Similar Changes in Circulating Substrates in Response to a Maximal Running Test

To determine if differences in circulating substrates contributed to the observed changes in maximal running speed and substrate oxidation rates during exercise calorimetry experiments in DKI mice, blood glucose, lactate and serum non-esterified fatty acid (NEFA) levels were assessed. Fed, resting blood glucose levels and increases in blood glucose concentration following a maximal running test at a 5° incline were similar between WT and DKI (**Figure 6.4A**). WT and DKI mice also had similar resting lactate levels and similar increases in lactate concentration following the maximal running test at a 5° incline (**Figure 6.4B**) despite differences in absolute maximal running speed at a 0° incline. While circulating NEFA levels were similar between WT and DKI mice in the resting state, only WT mice displayed a significant decrease in NEFA concentrations in response to maximal running at a 5° incline (**Figure 6.4C**). However, NEFA levels following a maximal running test were similar between WT and DKI mice (**Figure 6.4C**). Together, these results suggest that alterations in whole-body substrate availability are not necessarily driving the observed changes in patterns of fuel utilisation during exercise calorimetry.

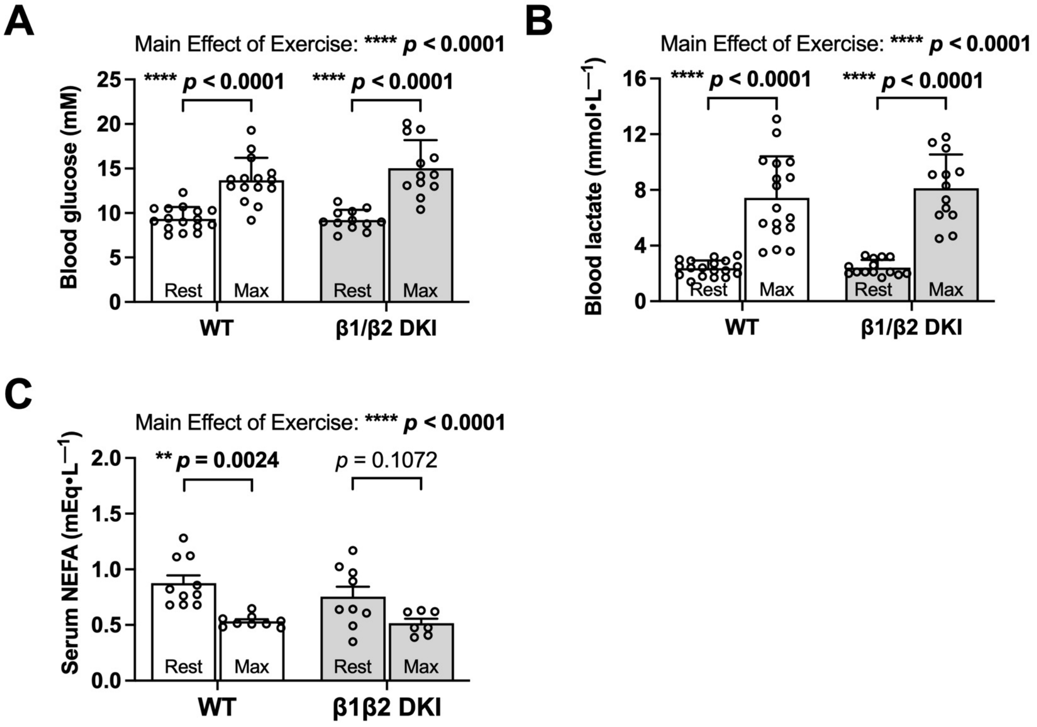

Figure 6.4 – DKI and WT mice have similar circulating glucose, lactate, and non-esterified fatty acid (NEFA) levels following a maximal running test at a 5° incline. (**A**) Blood glucose and (**B**) lactate were measured via tail tip bleeding the morning before and immediately following the maximal exercise test at a 5° incline. Fed male mice, 17-20 wk, n = 12-18. (**C**) Blood was collected via retro-orbital bleed from mice immediately before and after completing the maximal running test, and serum NEFA levels were assessed. Male mice, 17-20 wk, n = 7-10. ** *p* < 0.01, **** *p* < 0.0001.

6.3.4 DKI Mice Have Similar Changes in Tissue Glycogen Levels Compared to WT in Response to a Maximal Running Test Despite Less Total Running Time

Given the increased rates of CHO oxidation observed in DKI mice during exercise calorimetry experiments, we next determined if this increase was associated with a greater utilisation of glycogen during exercise in the primary glycogen-storing tissues liver and skeletal muscle. Liver glycogen concentration in the resting state was similar between WT and DKI mice and declined to similar levels following a maximal running test at a 5° incline in both genotypes (**Figure 6.5A**). Change in glycogen (Δ glycogen content) in liver and skeletal muscle was then determined as the difference between individual glycogen content of maximally exercised mice and the average glycogen content of rested mice from the same genotype. WT and DKI mice had a similar absolute change in liver glycogen content from rest to following a maximal running test (**Figure 6.5B**). In skeletal muscle, resting glycogen concentration was similar between genotypes, but DKI mice displayed a significant reduction in skeletal muscle glycogen following a maximal running test versus rested DKI mice (**Figure 6.5C**). However, there were no differences detected in skeletal muscle glycogen concentration between WT and DKI mice following a maximal running test (**Figure 6.5C**). This similar level of depletion corresponded to a similar absolute change in glycogen content in skeletal muscle (**Figure 6.5D**). However, despite a ~21% reduction in maximal running speed – and therefore, a 10 min reduction in overall treadmill running time – DKI mice had similar levels of muscle glycogen depletion compared to WT following a running test to exhaustion.

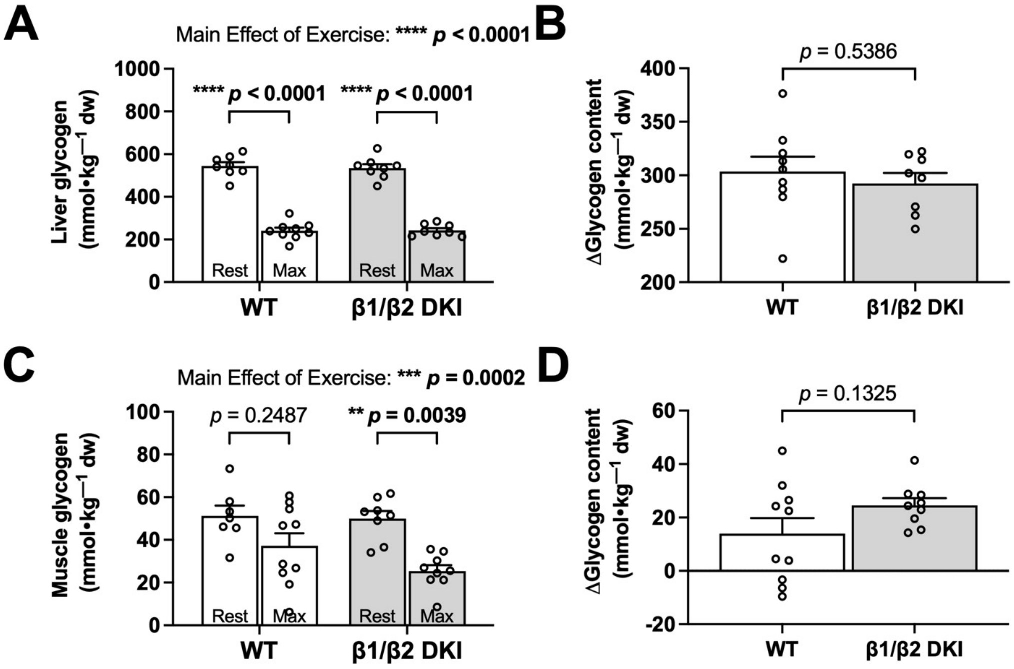

Figure 6.5 – DKI and WT mice display similar changes in liver and skeletal muscle glycogen following a maximal running test at a 5° incline. Glycogen content was assessed in (**A**) liver and (**C**) skeletal muscle from rested mice and maximally exercised mice. Change in glycogen (Δglycogen content) in (**B**) liver and (**D**) skeletal muscle was determined by the difference between individual glycogen content of maximally exercised mice and the average glycogen

content of rested mice from the same genotype. Male mice, 17-20 wk, n = 7-10. ** $p < 0.01$, *** $p < 0.001$, **** $p < 0.0001$.

We next examined the potential relationship between levels of glycogen depletion and onset of fatigue during a maximal running test at a 5° incline. The change between mean tissue glycogen content of resting mice and individual tissue glycogen content of exercised mice following a maximal running test (i.e., Δ glycogen content) was determined and compared with the individual maximal running speed for each mouse. There was no significant correlation observed between change in liver glycogen and maximal running speed for either WT or DKI mice (**Figure 6.6A**).

In contrast, there was a significant positive correlation between change in skeletal muscle glycogen and maximal running speed at a 5° incline in WT mice (**Figure 6.6B**), indicating that WT mice which utilised more skeletal muscle glycogen reached higher maximal running speeds. However, there was no correlation between change in skeletal muscle glycogen and maximal running speed in DKI mice (**Figure 6.6B**), suggesting that higher skeletal muscle glycogen utilisation did not lead to higher maximal running speed in DKI mice.

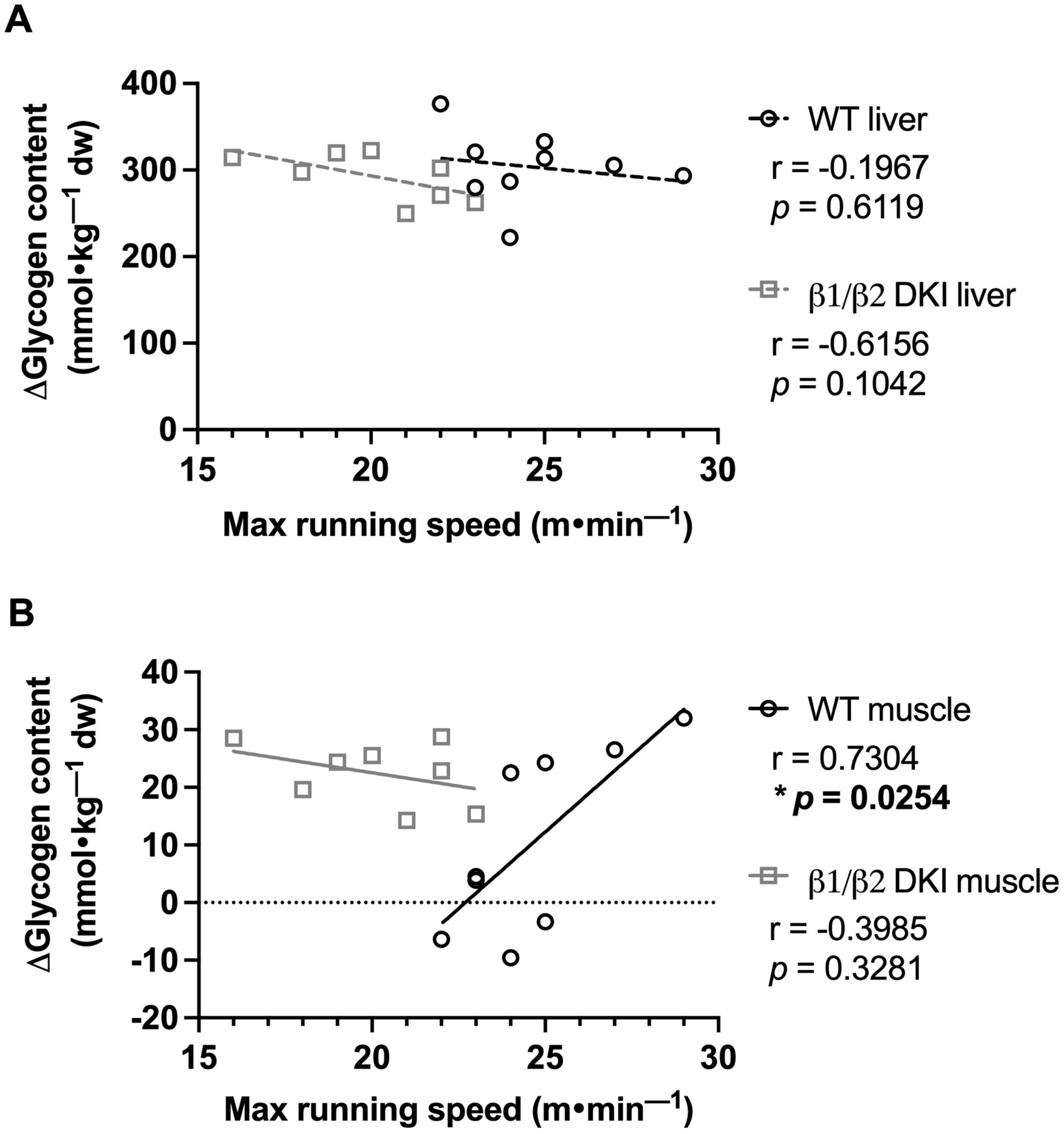

Figure 6.6 – Maximal running speed at a 5° incline is positively correlated with skeletal muscle glycogen utilisation following maximal running in WT but not DKI mice. (**A**) Correlation between maximal running speed and change in liver glycogen was not significant in either WT or DKI mice. (**B**) WT mice display a significant positive correlation between maximal running speed and change in skeletal muscle glycogen between the rested state and following maximal treadmill running, which was not observed in DKI mice. Male mice, 17-20 wk, n = 8-9. * $p < 0.05$.

6.3.5 Altered Patterns of Substrate Utilisation in DKI Mice Are Not Due to Changes in GLUT4, CPT1b or Mitochondrial Protein Content in Skeletal Muscle

To further investigate the observed genotype differences in patterns of substrate utilisation during exercise calorimetry experiments, and the lack of correlation between change in skeletal muscle glycogen content and maximal running speed at a 5° incline in DKI mice, markers of glucose transport (glucose transporter type 4 [GLUT4]), fat transport (carnitine palmitoyltransferase Ib [CPT1b]) and mitochondrial content (citrate synthase and oxidative phosphorylation [OXPHOS] complex proteins) were assessed in skeletal muscle from resting WT and DKI mice (**Figure 6.7A and E**). Skeletal muscle protein content of GLUT4 (**Figure 6.7B**), CPT1b (**Figure 6.7C**), citrate synthase (**Figure 6.7D**) and mitochondrial OXPHOS complexes (Complexes I, II, III, IV and V; **Figure 6.7F**) were similar between genotypes.

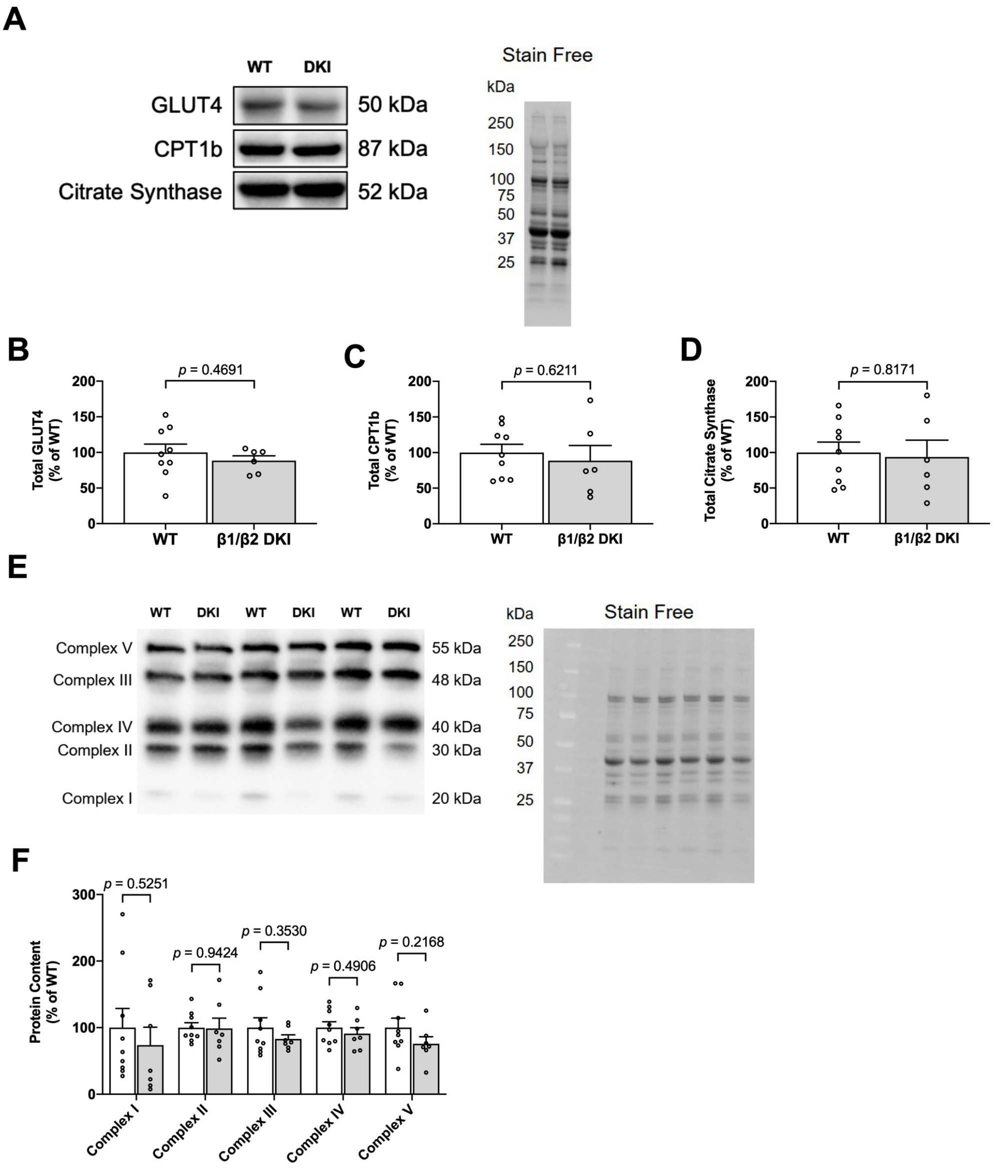

Figure 6.7 – DKI mouse skeletal muscle displays similar content of proteins associated with glucose uptake and protein markers of mitochondrial content relative to WT. (**A**) Representative immunoblots and stain free image of GLUT4, CPT1b, and citrate synthase in WT and DKI skeletal muscle; (**B**) Quantified total GLUT4; (**C**) Quantified total CPT1b; (**D**) Quantified total citrate synthase; (**E**) Representative immunoblots and stain free image of mitochondrial oxidative phosphorylation (OXPHOS) complex proteins in WT and DKI skeletal muscle; (**F**) Quantified OXPHOS complex protein content. Male mice, 20-32 wk, n = 7-9.

6.3.6 DKI Mutation Reduces Skeletal Muscle AMPK α and β2 Content But Does Not Impair Relative AMPK Phosphorylation and Downstream Signalling in Response to a Maximal Running Test

Given AMPK's role as a cellular energy regulator and the energy stress induced in skeletal muscle during exercise, AMPK phosphorylation and downstream signalling was assessed in skeletal muscle at rest and following a maximal running test at a 5° incline to determine if alterations in AMPK α and β2 subunit content and/or downstream signalling contributed to reduced maximal running speed and altered substrate utilisation in DKI mice (**Figure 6.8A**). Phosphorylation status of AMPK T172 relative to total AMPK α content in skeletal muscle was similar between genotypes at rest. While relative AMPK T172 phosphorylation was significantly higher in DKI mice compared to WT following a maximal running test, relative T172 phosphorylation was not significantly increased following exercise relative to the respective resting condition for either genotype (**Figure 6.8B**). Furthermore, exercise did not result in any significant differences in relative phosphorylation of AMPK β1 S182 in either DKI or WT mice (**Figure 6.8C**). There were also no differences in the relative phosphorylation status of AMPK's downstream substrates between genotypes or between the resting versus maximally exercised conditions including phosphorylation of acetyl-CoA carboxylase (ACC) S79 (**Figure 6.8D)** and TBC1 domain family member 1 (TBC1D1) S660 (**Figure 6.8E**), an AMPK substrate involved in contraction-stimulated glucose uptake (Treebak, Pehmoller et al. 2014, Stockli, Meoli et al. 2015). However, total AMPK α (**Figure 6.8F**) and AMPK β2 (**Figure 6.8G**) protein content skeletal muscle from resting DKI mice, was reduced by 38% and 45%, respectively, compared to WT.

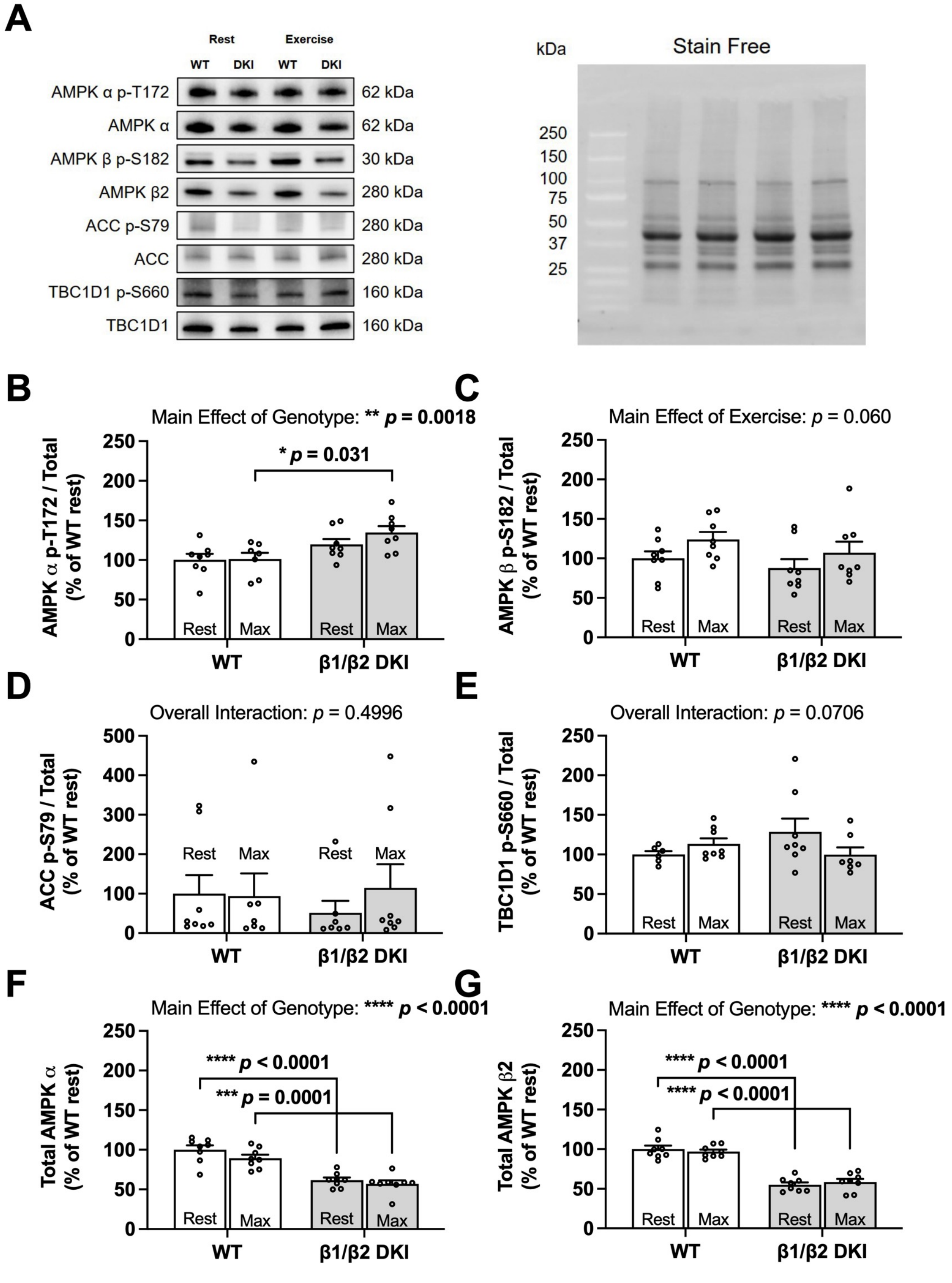

Figure 6.8 – DKI mice have reduced skeletal muscle AMPK α and β2 content but intact AMPK, ACC and TBC1D1 signalling in response to a maximal running test at a 5° incline versus WT. Skeletal muscles were collected from rested and maximally exercised male WT and DKI mice, and phosphorylation of AMPK and downstream substrates was assessed using Western blotting. (**A**) Representative immunoblots of p-T172 and total AMPK, p-S182 and

total AMPK β, p-S79 and total acetyl-CoA carboxylase (ACC) and p-S660 and total TBC1 domain family member 1 (TBC1D1) with representative stain free image. Quantified relative (**B**) AMPK p-T172, (**C**) AMPK β p-S182, (**D**) ACC p-S79, and (**E**) TBC1D1 p-S660; (**F**) Total AMPK α; (**G**) Total AMPK β. Male mice, 17-20 wk, n = 6-8. * $p < 0.05$, ** $p < 0.01$, *** $p < 0.001$, **** $p < 0.0001$.

6.4 Discussion

The primary findings of this study are that the DKI mutation utilised to chronically disrupt whole-body AMPK-glycogen binding reduced maximal running speed and resulted in increased depletion of glycogen levels in skeletal muscle following a maximal running test and was associated with reduced skeletal muscle AMPK α and β2 subunit content. Furthermore, DKI mice displayed increased rates of CHO oxidation during submaximal running, without any accompanying changes in substrate availability, impairments in skeletal muscle relative AMPK phosphorylation and downstream signalling at rest and following a maximal running test, or content of GLUT4, CPT1b and mitochondrial proteins. Collectively, these data suggest that the DKI mutation and the associated reductions in skeletal muscle AMPK α and β2 and/or glycogen content following exercise led to reduced maximal running speed in DKI mice.

It is well established that tissue AMPK α and β2 content, particularly in skeletal muscle, is associated with maximal exercise capacity. Loss of AMPK α in mouse muscle (Lantier, Fentz et al. 2014, Fentz, Kjobsted et al. 2015, Hingst, Kjobsted et al. 2020), but not liver (Hughey, James et al. 2017), resulted in reduced maximal running speed. Furthermore, the β subunit, responsible for scaffolding the AMPK heterotrimer, has also been phenotypically linked with exercise capacity in mice. Muscle-specific β1β2 KO (O'Neill, Maarbjerg et al. 2011) and whole-body β2 KO (Steinberg, O'Neill et al. 2010, Dasgupta, Ju et al. 2012) mouse models exhibited reduced maximal running speed. Similarly, AMPK KI mice with disrupted glycogen binding capacity in the β2 subunit isoform, which is predominantly expressed in skeletal muscle, demonstrated reduced maximal running speed. In contrast, when glycogen binding capacity was disrupted in the β1 subunit isoform, the isoform predominantly expressed in liver, maximal running speed in mice was not impaired (Hoffman, Whitfield et al. 2020). Based on these skeletal muscle- and β2 isoform-specific roles of AMPK in exercise capacity and the positive correlation between change in muscle glycogen content and maximal running speed observed in WT mice in the present study, we focused our analyses of AMPK content and exercise signalling to skeletal muscle. Together with findings from previous studies, our current results suggest that the DKI mutation to disrupt AMPK-glycogen binding, specifically KI mutation of the β2 subunit isoform, reduces maximal running speed but not time to exhaustion at a submaximal speed.

Within skeletal muscle, AMPK phosphorylates a number of downstream targets that can influence tissue substrate utilisation, including ACC and TBC1D1 which promote fat oxidation and contraction-stimulated glucose uptake, respectively (Fullerton, Galic et al. 2013, O'Neill 2013, Stockli, Meoli et al. 2015). Previous studies have found differing exercise-mediated effects on relative AMPK phosphorylation and downstream signalling in WT mice dependent on the exercise protocol employed and/or muscle fibre type studied. For example, submaximal, steady state exercise resulted in significant increases in relative phosphorylation of AMPK T172 in glycolytic quadriceps muscle, which was associated with increases in absolute phosphorylation of both ACC S212 and TBC1D1 S231 (Hingst, Kjobsted et al. 2020). However, no significant increases in relative phosphorylation of AMPK T172 or ACC S79 were observed in mixed gastrocnemius muscle in response to an incremental maximal running test similar to the protocol utilised in the current study (Hoffman, Whitfield et al. 2020). As a result, it is perhaps not surprising that a maximal running test at a 5° incline in the current investigation did not increase the relative phosphorylation of AMPK, ACC or TBC1D1 in WT mixed gastrocnemius muscle in the current investigation. Furthermore, the increased phosphorylation of AMPK T172 relative to total protein in DKI versus WT mice observed following a maximal running test did not result in any detectable changes in downstream phosphorylation of substrates ACC and TBC1D1 between genotypes, suggesting that substrate utilisation patterns were not likely driven by changes in skeletal muscle AMPK phosphorylation and downstream signalling in response to exercise. Longer bouts of high intensity running (e.g., at higher running speed and/or treadmill incline) may be required to detect increases in relative phosphorylation in skeletal muscle of WT and DKI mice and/or elucidate potential impairments in relative AMPK phosphorylation and downstream signalling to other AMPK substrates in DKI skeletal muscle. We have previously shown that DKI mice exhibit increased adiposity concomitant with increased rates of whole-body CHO oxidation in the fed and resting state (Janzen, Whitfield et al. 2021), as well as during submaximal exercise in the present study. Therefore, it is possible that increased rates of CHO oxidation in DKI mice were not due to an acute shift in substrate oxidation patterns in response to exercise, but rather a continuation of chronically increased reliance on CHO substrate. Further study of adipose tissue and fatty acid production/utilisation is warranted to determine if impairments in fat metabolism are contributing to increased rates of CHO oxidation in DKI mice. Alternatively, as the present study focused on mixed gastrocnemius muscle, it is possible that exercise-induced AMPK phosphorylation and signalling to downstream substrates could be differentially affected in other muscle fibre types in DKI mice and/or DKI mice may exhibit a shift in myosin heavy chain expression as a result of the DKI mutation leading to the observed changes in whole-body substrate utilisation patterns. Future studies should evaluate if muscle fibre composition, GLUT4 translocation, or the regulation of other proteins involved in the glycolytic and β-oxidation pathways in various skeletal muscle groups (e.g., the pyruvate dehydrogenase complex and sarcolemmal fatty acid transporters) are affected as a consequence of disrupting whole-body AMPK-glycogen binding.

Findings regarding the role of different AMPK subunits and isoforms in the regulation of substrate utilisation patterns in response to exercise are equivocal. In contrast to our findings of increased rates of CHO oxidation in DKI mice during submaximal running, recent work using an inducible skeletal muscle-specific AMPK α KO model has shown a reduction in maximal exercise capacity and increased ATP depletion, but no changes in rates of whole-body CHO or fat oxidation (Hingst, Kjobsted et al. 2020), suggesting that skeletal muscle AMPK may not directly affect whole-body substrate utilisation patterns. Additionally, mice with chronic KO of AMPK γ3, which is predominately expressed in glycolytic skeletal muscle, have unimpaired glycogen utilisation following swimming exercise and normal contraction-stimulated glucose uptake in glycolytic extensor digitorum longus muscle (Barnes, Marklund et al. 2004). Chronic muscle-specific AMPK β1β2 KO mice displayed increased reliance on fat utilisation (O'Neill, Maarbjerg et al. 2011), while chronic muscle-specific AMPK α KO mice demonstrated an increased RER and impaired FA oxidation (Fentz, Kjobsted et al. 2015) during submaximal treadmill running. DKI mice displayed smaller reductions in muscle AMPK α content than those observed in inducible skeletal muscle-specific AMPK α KO (Hingst, Kjobsted et al. 2020), chronic whole-body AMPK γ3 KO mice (Barnes, Marklund et al. 2004), muscle-specific AMPK β1β2 KO (O'Neill, Maarbjerg et al. 2011) and muscle-specific AMPK α KO mice (Fentz, Kjobsted et al. 2015). Therefore, the relative AMPK α content remaining in DKI mouse skeletal muscle was likely sufficient to sustain rates of whole-body fat oxidation during exercise. The contrary findings in whole-body substrate utilisation observed in DKI mice during energy stress compared to other whole-body, muscle-specific and/or inducible AMPK KO models may also be due either to chronically reduced AMPK α and β2 content in DKI mice and/or reduced AMPK levels observed in additional metabolic tissues, including liver and/or adipose tissue (Janzen, Whitfield et al. 2021). These differences in substrate oxidation patterns during exercise across these various transgenic AMPK mouse models highlight the limitations of current KO and KI models to study respective protein function and underscore the value of developing new inducible and tissue-specific models to elucidate the roles of AMPK and its glycogen binding capacity *in vivo*.

Both WT and DKI mice displayed similar increases in blood glucose concentration following a maximal running test at a 5° incline versus rest, suggesting that hepatic glucose output exceeds skeletal muscle glucose uptake (Camacho, Galassetti et al. 2005) and that DKI mice maintained hepatic glucose output and skeletal muscle glucose uptake during maximal exercise. Given the relatively large stores of liver glycogen, rodents rely predominantly on hepatic glycogenolysis to maintain blood glucose levels in settings of energy stress, such as following fasting or exercise, while the contribution of skeletal muscle glycogen to total energy expenditure becomes higher with increasing exercise intensity and/or duration (Baldwin, Reitman et al. 1973, Pederson, Cope et al. 2005). Therefore, given that DKI mice had a similar change in liver glycogen following a maximal running test - despite a shorter running time compared to WT mice (i.e., ~19 min for DKI versus ~29 min for WT mice) – it was likely that increased liver glycogenolysis was the primary contributor to the increased rates of CHO oxidation in DKI mice. However, there was no correlation observed between change in liver glycogen content and maximal running speed in either WT or DKI mice. The ~60% reduction in liver glycogen observed in both genotypes following a maximal running test was therefore likely not limiting for achieving maximal running speed, suggesting that both WT and DKI mice possessed liver glycogen stores in excess of what could be utilised during an incremental maximal running test. Previous research in AMPK α KO mice has demonstrated impaired liver glycogenolysis, resulting in reduced hepatic glucose output during exercise without altering maximal running speed (Hughey, James et al. 2017). While findings from this previous study suggests that loss of liver AMPK results in impaired glycogenolysis and an associated reduction in hepatic glucose output, our current findings in DKI mice suggest that the hepatic AMPK α content lost as a result of the DKI mutation (Janzen, Whitfield et al. 2021) may not be critical for maintaining liver glycogenolysis and glucose output, and/or the remaining AMPK α content in DKI mice was sufficient to maintain required levels of hepatic glycogenolysis during treadmill running.

Due to the larger total contribution of liver glycogen to total energy expenditure during exhaustive exercise, it has been speculated that skeletal muscle glycogen is not a major determinant of exercise capacity during exhaustive exercise in mice. Previous studies have shown that chronic glycogen synthase KO mice lacking skeletal muscle glycogen did not have impaired running endurance capacity (Pederson, Cope et al. 2005), while elevated skeletal muscle glycogen content via transgenic overexpression of constitutively active glycogen synthase did not enhance running endurance (Pederson, Cope et al. 2005). Furthermore, skeletal muscle glycogen may not play a major role in whole-body rates of CHO oxidation and glucose homeostasis during exercise in mice (Irimia, Meyer et al. 2010). However, in the present study we found a significant positive correlation between change in skeletal muscle glycogen and maximal running speed in WT mice. In contrast, there was no significant correlation between maximal running speed and change in skeletal muscle glycogen in DKI mice, concomitant with reduced muscle AMPK α and β2 content. In the current study we used an incremental maximal treadmill running test at a 5° incline, rather than endurance-based protocols employed in previous studies (Pederson, Cope et al. 2005, Pederson, Cope et al. 2005), and the contrasting results between the current work and previous studies could be explained by differences in exercise intensity and/or duration resulting in different contributions of glycogen to total energy expenditure. Therefore, it is possible that employing exercise protocols similar to the above studies and/or higher intensities could further elicit genotypic differences. Collectively, our results in the present study indicate that the ability to use skeletal muscle glycogen may potentially play an important role in achieving higher maximal running speed in WT mice.

The absence of a significant correlation between estimated levels of skeletal muscle glycogenolysis and maximal running speed at a 5° incline suggests that regulation of skeletal muscle glycogenolysis may be disrupted in DKI mice, particularly in response to energy stress. This contention is supported by previous results using this mouse model, which demonstrated increased skeletal muscle glycogen utilisation during fasting in DKI mice (Janzen, Whitfield et al. 2021). It is possible that glycogen bound to AMPK in skeletal muscle may be protected from glycogenolysis, reciprocal to the proposed hypothesis that glycogen binding anchors cellular AMPK and prevents its degradation (Hoffman, Whitfield et al. 2020). Therefore, it is possible that the reduction in maximal running speed in DKI mice may not be directly related to the observed increases in rates of whole-body CHO oxidation and increased liver and skeletal muscle glycogen utilisation, but rather may be due to indiscriminate utilisation of skeletal muscle glycogen as a result of reduced skeletal muscle AMPK α and β2 content and/or glycogen binding capacity. Alternatively, it is possible that skeletal muscle glycogen utilisation during exercise may be increased in DKI mice due to increased activity or capacity of the glycolytic pathway and/or alterations in muscle fibre type composition. Together, our findings suggest an important role for AMPK in determining acute exercise responses and maximal running speed independent of changes in whole-body substrate utilisation patterns, which is consistent with findings in skeletal muscle AMPK KO mouse models (O'Neill, Maarbjerg et al. 2011, Hingst, Kjobsted et al. 2020).

In conclusion, the results from the present study demonstrate that the DKI mutation used to disrupt AMPK-glycogen binding impairs maximal running speed and alters patterns of substrate utilisation during submaximal exercise. Additionally, reductions in tissue AMPK α and β2 content are associated with increased utilisation of skeletal muscle glycogen, resulting in increased rates of whole-body CHO oxidation. While increased CHO oxidation is not likely to be solely responsible for the observed reduction in maximal running speed, the DKI mutation results in indiscriminate utilisation of skeletal muscle glycogen in mice, likely contributing to premature exhaustion during maximal running tests. These findings further underscore that AMPK serves additional roles in regulating tissue glycogen dynamics and adds another dimension to the known roles of AMPK in regulating substrate utilisations patterns and exercise capacity.

6.5 Materials and Methods

6.5.1 Animal Models

AMPK β1(W100A)/β2(W98A) DKI mice on a C57BL/6J background were generated using CRISPR/Cas9 gene targeting, as described previously (Janzen, Whitfield et al. 2021). Homozygous carriers of both β1 and β2 isoform KI mutations were used for breeding, and DKI and WT breeders were annually backcrossed to generate heterozygous mice and rederive the homozygous DKI line. Confirmatory genotyping was performed from tail samples by Transnetyx (Cordova, TN, USA).

All experiments were undertaken using male DKI mice and age matched WT controls. Male mice were used to maintain adequate female breeders and ensure sufficient age matched litters were available for analyses. Mice were group housed in a temperature (~22°C) and humidity-controlled facility with a 12:12 h light and dark cycle and given *ad libitum* access to a standard chow diet (6% fat, 20% protein and 29% starch; Barastoc, Ridley Agriproducts, Pakenham, Victoria, Australia) and water. All experiments commenced between 0800 and 0900 h when mice were in the fed state, unless otherwise stated. All mouse procedures were reviewed and approved by the St. Vincent's Hospital (Melbourne, Victoria, Australia) Animal Ethics Committee (025-15 and 011-19), conformed to all the requirements of the National Health and Medical Research Council of Australia (NHMRC), and were in accordance with the Australian code of practice for the care and use of animals for scientific purposes (8th Edition 2013).

6.5.2 Maximal Running Speed and Time to Exhaustion

Maximal running speed and time to exhaustion were assessed on a Columbus Instruments Exer 3/6 rodent treadmill (Columbus Instruments, Columbus, OH, USA). Mice underwent 4 days of treadmill acclimatisation, as described previously (Hoffman, Whitfield et al. 2020). On day 5, mice completed an incremental maximal exercise capacity test to determine maximal running speed. Mice ran for 2 min at 10 m·min^{-1}, after which the speed was increased by 1 m·min^{-1} every 2 min until exhaustion, defined as the inability to compel the mouse to remain running despite continued manual prodding. After 2-3 days of recovery, mice either completed the exercise calorimetry experiments (described below) or underwent a time to exhaustion test whereby they ran at 70% of individual maximal speed. Mice with similar maximal running speeds (i.e., within 2 m·min^{-1}) were grouped and completed their time to exhaustion tests simultaneously. These exercise tests were completed at a 0° treadmill incline (**Table 6.1**) and mice were returned to their home cages once testing was completed.

A separate cohort of mice underwent acclimatisation as described above but completed a maximal running test at a 5° incline (**Table 6.1**). Blood glucose and lactate were measured via tail tip bleeding the morning before and immediately following the maximal running test using an Accu-Check Performa glucometer (Roche Diagnostics GmbH, Mannheim, Germany) and Lactate Pro analyser (Arkray, Kyoto, Japan). Mice were culled via cervical dislocation immediately following the maximal running test, and tissues were excised, immediately snap frozen in liquid N_2, and stored at -80°C until subsequent biochemical analysis. Control rested mice did not undergo the maximal running test and remained in their home cage until being culled via cervical dislocation in the fed state at 0900 h.

Table 6.3 – Specifics of the four exercise protocols used and corresponding measures.

Exercise Protocol	Speed	Incline	Duration	Corresponding Measure and Figures
Maximal running speed	2 min at 10 m·min^{-1} then speed increased 1 m·min^{-1} every 2 min	0°	To exhaustion	- Maximal running speed (Figure 6.2A)

Time to exhaustion	70% of individual maximal running speed	0°	To exhaustion	- Time to exhaustion (Figure 6.2B)
Exercise calorimetry	60% of individual maximal running speed	0°	15 min (final 5 min used for calorimetry analysis)	- VO_2, TEE, RER and rates of CHO and fat oxidation (Figure 6.3)
Maximal running test at a 5° incline	2 min at 10 $m \cdot min^{-1}$ then speed increased 1 $m \cdot min^{-1}$ every 2 min	5°	To exhaustion	- Blood glucose, blood lactate and serum NEFA (Figure 6.4) - Change in tissue glycogen (Figure 6.5) - Correlation between maximal running speed and change in tissue glycogen content (Figure 6.6) - Skeletal muscle AMPK α and β2 content and AMPK, ACC and TBC1D1 signalling (Figure 6.8)

6.5.3. Exercise Calorimetry

After completing the acclimatisation and maximal running speed assessment at a 0° incline, a cohort of mice underwent an exercise bout to determine substrate utilisation (**Table 6.1**). For exercise calorimetry experiments, mice completed 15 min running at 60% of their individual maximal speed at a 0° incline on a specialised rodent calorimetry treadmill (Omnitech Electronics, Columbus, OH, USA). Mean values for RER ($VCO_2 \cdot VO_2^{-1}$) were determined. TEE and fat and CHO oxidation rates were calculated as previously described (Peronnet and Massicotte 1991).

6.5.4 Serum Analysis

Blood samples were collected retro-orbitally immediately prior to and upon completion of a maximal running test at a 5° incline. Samples were left to clot for 30 min at room temperature in non-coated polypropylene tubes, then centrifuged at 10,000 *g* for 5 min at 4°C, and the serum supernatant was aliquoted and stored at -80°C. NEFA levels were measured using a

NEFA-C kit (Wako Pure Chemical Industries, Osaka, Japan) according to manufacturer's instructions.

6.5.5 Tissue Glycogen Analysis

Liver and gastrocnemius muscle samples (~25 mg) were chipped under liquid N_2, freeze-dried overnight, powdered, and dissected free of visible blood and connective tissue. Aliquots of powdered tissue (~2-4 mg) were then alkaline extracted and the supernatant was used for quantification of glycogen content using spectrophotometry, as described previously (Bergmeyer 1974). Absorbance was measured at 340 nm using a SpectraMax Paradigm plate reader and SoftMax Pro microplate data acquisition software (Molecular Devices, San Jose, CA, USA).

6.5.6 Tissue Protein Analyses

Gastrocnemius muscle samples were lysed in homogenisation buffer containing 50 mM Tris-HCl (pH 7.5), 1 mM EDTA, 1 mM EGTA, 10% glycerol, 1% Triton-X, 50 mM sodium fluoride, 5 mM sodium pyrophosphate with cOmplete Protease Inhibitor Cocktail and PhosSTOP phosphatase inhibitor (Sigma-Aldrich, St. Louis, MO, USA). Samples were centrifuged at 16,000 *g* for 30 min at 4°C and protein content of the supernatant was determined using bicinchoninic acid (BCA) analysis (Pierce, Rockform, IL, USA). Lysates (10 μg protein$\cdot$well^{-1}) were run on 4-15% or 4-20% precast stain-free gels (Bio-Rad, Hercules, CA, USA) and transferred to PVDF membranes (Merck Milipore, Burlington, MA, USA). Membranes were blocked with 7.5% BSA in Tris-buffered saline containing 0.1% Tween 20 (TBS-T) for 1 h at room temperature then incubated with primary antibodies (1:1000) overnight with rocking at 4°C. After washing with TBS-T, membranes were incubated with secondary antibody for 1 h at room temperature. Proteins were detected via chemiluminescence using SuperSignal West Femto Maximum Sensitivity Substrate (Thermo Fisher Scientific, Waltham, MA, USA) and imaged using the ChemiDoc Imaging System

(Bio-Rad). Band intensities of total proteins and phosphorylation sites were normalised to the total lane protein from the respective stain-free image using Image Lab software (version 6.1, Bio-Rad), as previously described (Tachtsis, Whitfield et al. 2020). Protein phosphorylation was normalised to total content of the respective protein.

Antibodies against total AMPK α (2532), phospho-AMPK T172 (2531), total AMPK β (4150), phospho-AMPK β1 S182 (4186), total ACC (3662), phospho-ACC S79 (11818), GLUT4 (2213), total TBC1D1 (66433), phospho-TBC1D1 S660 (6928) and horseradish peroxidase-conjugated anti-rabbit (7074) and anti-mouse (7076) IgG secondary antibodies were purchased from Cell Signaling Technology (Danvers, MA, USA). Citrate synthase (ab96600), CPT1b (ab134988) and OXPHOS rodent antibody cocktail (ab110413) were purchased from Abcam (Cambridge, United Kingdom).

6.5.7 Statistical Analyses

Comparisons between genotypes were analysed using unpaired two-tailed Student's t testing (WT versus DKI) or two-way analysis of variance (ANOVA; WT versus DKI comparisons over time or condition) with Bonferroni post hoc testing applied where appropriate. Pearson's product moment correlation was used to examine associations between maximal running speed at 5° and change in tissue glycogen content. All statistical analyses were completed using GraphPad Prism software (version 9, GraphPad Software, La Jolla, CA, USA). Significance was set at $p < 0.05$ and all data are presented as mean ± standard error of the mean (SEM).

List of Abbreviations

ACC	Acetyl-CoA carboxylase
AMPK	AMP-activated protein kinase
ANOVA	Analysis of variance
CBM	Carbohydrate binding module
CHO	Carbohydrate
CPT1b	Carnitine palmitoyltransferase Ib
DKI	Double knock-in
GLUT4	Glucose transporter type 4
KI	Knock-in
KO	Knockout
TBC1D1	TBC1 domain family member 1
NEFA	Non-esterified fatty acid
OXPHOS	Oxidative phosphorylation
RER	Respiratory exchange ratio
SEM	Standard error of the mean
TBST-T	Tris-buffered saline containing 0.1% Tween 20
TEE	Total energy expenditure
VCO_2	Carbon dioxide production
VO_2	Oxygen consumption
WT	Wild type

Acknowledgments

We thank Mehdi R. Belhaj for assistance with mouse sample collections and the St. Vincent's BioResources Centre staff for assistance with mouse breeding and husbandry. We are grateful to Sean L. McGee for calorimetry treadmill assistance.

Data Availability Statement

The data that support the findings of this study are available from the corresponding author upon reasonable request.

Ethics Statement

The animal study was reviewed and approved by the St. Vincent's Hospital (Melbourne, Victoria, Australia) Animal Ethics Committee (025-15 and 011-19).

Conflict of Interest

The authors declare that the research was conducted in the absence of any commercial or financial relationships that could be construed as a potential conflict of interest.

Author Contributions

NJ, JW, BK, JH, and NH conceptualised and designed the study. NJ, JW, and NH collected and analysed the data. NJ, LM-S, and NH were responsible for mouse breeding and husbandry. BK and JH provided intellectual input and resources. NJ, JW, and NH wrote the manuscript. All authors have read and agreed to the published version of the manuscript.

Funding

This work was supported by Australian Catholic University research funding awarded to NH. BK was supported by the National Health and Medical Research Council of Australia (NHMRC APP1068813 and APP1085460), the Australian Research Council (ARC DP170101196) and the Victorian Government Operational Infrastructure Support Scheme.

Chapter 7 Discussion and Conclusion

7.1 Introduction

Previous studies investigating AMPK and glycogen binding have generally been limited to *in silico* and *in vitro* model systems. These early studies uncovered the glycogen binding capacity of the CBM within the AMPK β subunit (Hudson, Pan et al. 2003, Polekhina, Gupta et al. 2003, Polekhina, Gupta et al. 2005) and investigated this physical interaction in isolation in molecular and cellular model systems. Therefore, findings from these studies cannot be extrapolated to whole-body and/or tissue physiological systems. Studies using *in vivo* methodologies have examined the relationship between AMPK activity and glycogen either by acutely modifying muscle glycogen content either through exercise and diet intervention(s) and/or by using AMPK KO mouse models in which loss of the regulatory β subunit results in chronic loss of the entire AMPK heterotrimer. Therefore, significant knowledge gaps exist regarding the physiological roles of AMPK-glycogen binding and phenotypic effects of disrupting AMPK-glycogen interactions *in vivo*.

Previous work utilising single AMPK β subunit KI models with disrupted AMPK-glycogen binding capacity in either the β1 or β2 isoform established isoform-specific consequences of the KI mutation *in vivo* (Hoffman, Whitfield et al. 2020). While a specific β subunit isoform can be predominantly expressed in some tissues (i.e., β1 in rodent liver, β2 in rodent skeletal muscle), many rodent tissues express detectable levels of both β isoforms. Furthermore, the specific effects of genetic modifications in many genes, including genes encoding protein kinases such as AMPK, are often unclear due to compensation by other signalling pathways in *in vitro* and *in vivo* models (McGee, Swinton et al. 2014). Therefore, further investigation of potential synergistic and/or compensatory consequences of disrupting AMPK-glycogen interactions in both β subunit isoforms *in vivo* is warranted.

To address some of these knowledge gaps, the overall aim of the experiments conducted for this thesis was to determine the phenotypic effects of the AMPK DKI mutation utilised to chronically disrupt whole-body AMPK-glycogen binding on whole-body and tissue metabolism, including tissue glycogen dynamics in response to energy stress. The findings from this thesis revealed that AMPK DKI mutation in mice led to dysregulation of whole-body metabolism, including increased adiposity, changes in patterns of substrate utilisation, and glucose intolerance; impaired maximal exercise capacity; and increased tissue glycogen utilisation and impaired muscle glycogen resynthesis in DKI mice (as summarised in **Figure 7.1**). Furthermore, these whole-body and tissue consequences of the DKI mutation were associated with reduced tissue AMPK content in the primary glycogen storing tissues liver and skeletal muscle, as well as glycogen-containing and metabolically active adipose tissue. Chapter 7 provides a critical discussion of the main findings of this thesis in the broader context of the current literature and highlights future research questions emerging from these thesis findings (**Figure 7.1**).

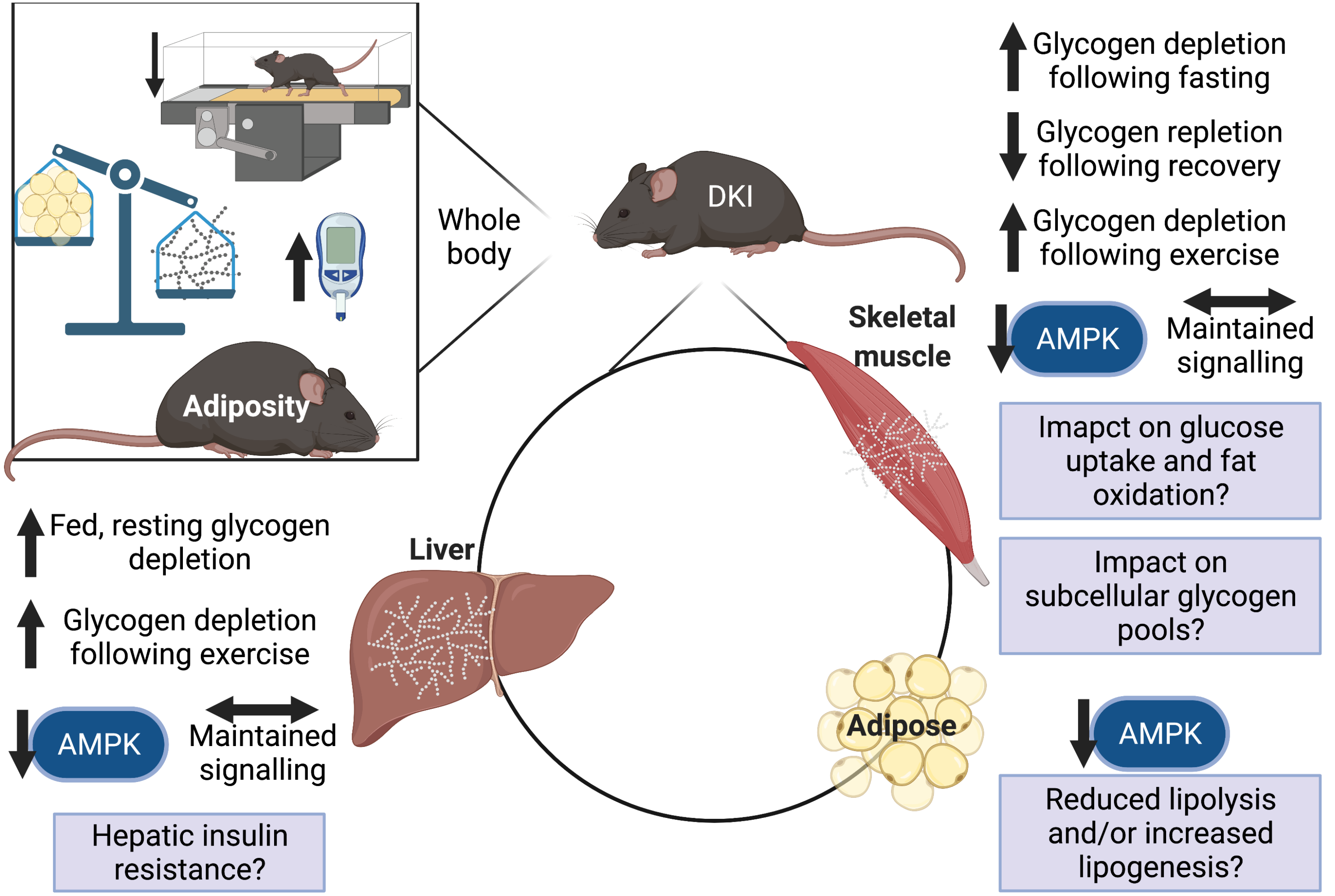
Adiposity
Whole body
DKI
↑ Glycogen depletion following fasting
↓ Glycogen repletion following recovery
↑ Glycogen depletion following exercise
Skeletal muscle
↓ AMPK
↔ Maintained signalling
Imapct on glucose uptake and fat oxidation?
Impact on subcellular glycogen pools?
Liver
↑ Fed, resting glycogen depletion
↑ Glycogen depletion following exercise
↓ AMPK
↔ Maintained signalling
Hepatic insulin resistance?
Adipose
↓ AMPK
Reduced lipolysis and/or increased lipogenesis?

Figure 7.1 – Summary of the main findings in DKI mice and future research questions stemming from this thesis. Created with BioRender.com.

7.2 Substrate Utilisation and Whole-Body Composition

7.2.1 Fed and Resting Substrate Oxidation and Adiposity

At the whole body and tissue levels, AMPK is involved in the control of both glucose and fat metabolism by regulating several cellular signalling pathways involved in oxidation and synthesis of both substrates (Garcia and Shaw 2017). Impairments in AMPK activation have been linked to obesity (Mortensen, Poulsen et al. 2009, Ix and Sharma 2010, Gauthier, O'Brien et al. 2011, O'Neill 2013), suggesting that AMPK plays a role in the maintenance of whole-body and tissue fat metabolism and/or the increased adiposity in obesity. While the majority of findings in AMPK DKI mice in this thesis closely mirror the phenotype of the AMPK β2 KI model, both β1 KI and DKI mice have increased reliance on CHO fuels and reduced rates of fat oxidation in the fed and resting state, while β2 KI mice had similar patterns of substrate oxidation compared to WT (Hoffman, Whitfield et al. 2020). Despite these differences in substrate utilisation patterns, β1 KI mice had similar body mass and fat mass compared to WT. In contrast, the increased adiposity and reduction in muscle AMPK content associated with the AMPK β2 isoform KI mutation did not affect whole-body substrate utilisation patterns. Collectively, these findings across AMPK β1 KI and DKI mouse models suggest that AMPK heterotrimers containing the β1 subunit isoform are likely involved in the regulation of fuel preferences in the fed and resting state, but this does not necessarily affect body mass or adiposity.

To further interrogate the hyperphagia and adiposity observed in DKI mice, fed and fasting serum leptin levels were assessed. Leptin plays a central role in regulating food intake by increasing satiety (Minokoshi, Alquier et al. 2004). Leptin resistance is a potential consequence of obesity and results in elevated circulating leptin levels (Galic, Oakhill et al. 2010, Pan, Guo et al. 2014). Therefore, given increased adiposity and hyperphagia in DKI mice, it was surprising that serum leptin levels were similar between DKI and WT mice. This indicates that the observed hyperphagia and increased adiposity in DKI mice was not necessarily tied to altered leptin circulation and/or sensitivity. The primary leptin-secreting tissues are adipose tissue and the hypothalamus, which also contain AMPK and glycogen (Lima, Lima dos Santos et al. 2010, Stapleton, Nelson et al. 2013). In addition to leptin, there are a number of other neuropeptides, neurotransmitters, and hormones (e.g., pro-opiomelanocortin and cocaine- and amphetamine-regulated transcript secreted by the hypothalamus, and ghrelin, glucagon-like peptide-1, and gastric inhibitory polypeptide secreted by gastric tissue [i.e., stomach and small intestine]) which are involved in regulating hunger and satiety (Austin and Marks 2009, Singla, Bardoloi et al. 2010). Therefore, additional research is required to investigate potential tissue-specific consequences of disrupting AMPK-glycogen binding on secretion of leptin and other factors involved in food intake, and whether these changes underlie the hyperphagia and increased adiposity in DKI mice.

7.2.2 Substrate Oxidation in the Fasted State

As mice tend to have elevated rates of carbohydrate oxidation during the dark, active phase, challenging mice with an overnight fast tested their ability to shift patterns of whole-body substrate oxidation from carbohydrate to fat oxidation (i.e., “metabolic flexibility”). While both DKI and WT mice showed a reduction in RER throughout the fasting period (i.e., an increased reliance on fat as a metabolic substrate), the mean hourly RER in DKI mice was higher than WT throughout the fasting period. This resulted in significantly higher average rates of CHO oxidation and lower rates of fat oxidation in DKI versus WT mice. It therefore appears that DKI mice maintain some metabolic flexibility in response to fasting but demonstrate an overall increased preference for CHO substrates relative to WT. Alternatively, given evidence of isoform-specific roles for AMPK in skeletal muscle responses to exercise (Chen, Stephens et al. 2003, Kjobsted, Hingst et al. 2018), it is possible that the AMPK complexes lost in DKI mice may be involved in these observed changes in patterns of substrate utilisation in the fed state, but not necessarily in regulating substrate utilisation responses to the low energy availability induced by prolonged fasting. However, since the majority of heterotrimeric subunit-specific roles for AMPK identified to date has been related to acute exercise and muscle contraction, further research is warranted to elucidate the precise roles of different AMPK isoforms in other tissues and in response to fasting.

7.2.3 Potential Consequences of the DKI Mutation on Fat Metabolism

Given AMPK's role as a cellular energy sensor, AMPK has been implicated in regulating fat metabolism in insulin-sensitive tissues, including skeletal muscle. AMPK can influence fat metabolism via phosphorylation of ACC and transcription factors involved in regulating lipid synthesis (e.g., SREBP1), and indirectly through AMPK-mediated increases in mitochondrial biogenesis (e.g., via PGC1α) (O'Neill, Holloway et al. 2013, Garcia and Shaw 2017). The experiments conducted for this thesis examined whole-body substrate utilisation and liver and skeletal muscle glycogen concentrations in the fed, resting state and in response to energy stress. Future studies could examine additional tissue-specific consequences of whole-body disruption of AMPK-glycogen binding on fat metabolism (i.e., liver, skeletal muscle, and adipose tissue) by measuring *ex vivo* rates of fat oxidation.

Despite reduced rates of whole-body fat oxidation in the fed and fasting states and reduced liver and skeletal muscle AMPK content, DKI mice maintained liver and skeletal muscle ACC content and phosphorylation status in response to energy stress, suggesting that downstream AMPK signalling to ACC remains intact with the DKI mutation. There were similar levels of protein content of OXPHOS complexes, suggesting no differences in mitochondrial content in skeletal muscle between WT and DKI mice. These findings are in contrast to previous findings from AMPK KO models. Specifically, both chronic AMPK β2 KO (Dasgupta, Ju et al. 2012) and inducible muscle-specific AMPK α KO models (Hingst, Kjobsted et al. 2020) demonstrate reduced skeletal muscle ACC phosphorylation in response to fasting and exercise, respectively. Muscle-specific AMPK β1/β2 KO mice have reduced mitochondrial content as a result of genetic loss of AMPK (O'Neill, Maarbjerg et al. 2011), while inducible muscle-specific AMPK α KO results in no impairments in mitochondrial function nor reductions in OXHOS complex protein content (Hingst, Kjobsted et al. 2020). Based on findings in DKI mice and previous findings in β1 and β2 single KI mice, in which only β1 KI mice had altered substrate utilisation patterns (Hoffman, Whitfield et al. 2020), skeletal muscle fat metabolism and mitochondrial function may not be affected by the DKI mutation utilised to disrupt whole-body AMPK-glycogen binding. To confirm this hypothesis, mitochondrial function and glycolytic and oxidative metabolism should be assessed in DKI permeabilised muscle fibres by respirometry (e.g., using an Oroboros O2k-Respirometer) and analysis of muscle oxygen consumption and extracellular acidification rates (e.g., using a Seahorse XF24 Extracellular Flux Analyser), respectively. Experiments could also be performed to measure the expression and phosphorylation of other AMPK substrates (e.g., HMGR, hormone sensitive lipase, PFK, and GSK3β) involved in skeletal muscle glucose and fat metabolism.

Roles for AMPK have also been implicated in adipose tissue metabolism and adipocyte development (Wu, Zhang et al. 2018). Chronic activation of AMPK in mice protects against obesity through increased rates of whole-body energy expenditure, predominantly attributable to increased energy expenditure of white adipose tissue (Pollard, Martins et al. 2019). Conversely, obesity is associated with reduced AMPK activity in adipose tissue (Gauthier, O'Brien et al. 2011). It has been proposed that AMPK is able to reduce lipolysis via phosphorylation of hormone-sensitive lipase, preventing it from translocating to and hydrolysing lipid droplets, in rodent adipose tissue (Kim, Tang et al. 2016) and adipocytes (Daval, Diot-Dupuy et al. 2005). In contrast, adipose-specific inducible AMPK β1/β2 KO mice showed no AMPK-mediated effects on rates of lipolysis (Mottillo, Desjardins et al. 2016). Therefore, it remains unclear if the DKI mutation and associated reductions in total

AMPK α and β content in adipose tissue in DKI mice would disrupt whole-body or adipose tissue lipolysis. While the results of experiments conducted for this thesis showed reduced total AMPK α and β1 content in DKI adipose tissue compared to WT, future studies are required to assess adipose tissue AMPK and its substrates' phosphorylation status in response to fasting and/or exercise challenges. For example, AMPK β S182 phosphorylation induced either by autophosphorylation or an upstream kinase is involved in AMPK subcellular localisation, and loss of phosphorylation via a S182A mutation results in redistribution of the β subunit to the nucleus in HEK-293 cells (Warden, Richardson et al. 2001). Potential changes in AMPK subcellular distribution in DKI adipocytes could result in altered downstream signalling and/or fat metabolism, including ACC, which, is a major regulator of fat metabolism and plays important regulatory roles in rodent adipose tissue (Bianchi, Evans et al. 1990, Oh, Abu-Elheiga et al. 2005). Alternatively, it is possible that potential impairments in fat utilisation in the fed state are mediated by signalling mechanisms other than AMPK and/or ACC signalling. Future studies can assess adipose tissue signalling pathways, including phosphorylation status of AMPK and a range of its substrates, in response to energy stress to investigate potential underlying impairments in fat metabolism in DKI mice.

7.3 Whole-Body Glucose Metabolism

7.3.1 Maintenance of Blood Glucose Levels

Obesity is a primary contributing factor underpinning metabolic syndrome, which increases the risk of developing chronic diseases such as T2D. Dysfunction in AMPK activity and signalling is associated with the onset of obesity and metabolic disorders, including disruptions in glucose homeostasis and the development of insulin resistance in tissues such as liver and skeletal muscle (Kahn, Hull et al. 2006, Samuel and Shulman 2012). Furthermore, glycogen particle formation and storage can become dysregulated in insulin resistance and T2D (Nikoulina, Ciaraldi et al. 2000). Glycogen stores, particularly in the liver, play an important role in maintaining euglycemia (Hughey, James et al. 2017, Lopez-Soldado, Bertini et al. 2020) and are critical for maintaining glucose tolerance (Lopez-Soldado, Zafra et al. 2015). Based on these central regulatory roles of both AMPK and glycogen and the increased adiposity in DKI mice, potential effects on whole-body glucose handling and insulin tolerance were assessed.

DKI mice displayed hyperinsulinemia in the 6 h fasted state, characteristic of the early stages of insulin resistance (Saad, Knowler et al. 1989). Despite this hyperinsulinemia, DKI mice have similar blood glucose levels in the fed state and following an intraperitoneal insulin challenge compared to WT, suggesting that DKI mice maintain whole-body insulin sensitivity. Chronic hyperinsulinemia in the absence of peripheral insulin resistance can lead to continuous glucose uptake and CHO oxidation in both the post-prandial and energy deprived (i.e., fasting and exercising) states. This continuous peripheral demand for glucose in tissue such as skeletal muscle could drive sustained hepatic glucose output via stimulation of liver glycogenolysis and gluconeogenesis. While insulin suppresses hepatic glucose output (Wasserman 2009), it is possible that an increased demand for glucose in peripheral tissues may be overriding this effect via another hormone or circulating factor (e.g., catecholamines, interleukin-6, or other unknown metabolites and/or hormones). While there were no observed differences in serum glucagon levels between WT and DKI mice in the fed, resting or overnight fasted states, these other circulating factors could promote sustained hepatic glucose output in the absence of increased glucagon (Wasserman 2009). While hepatic glucose output was not directly assessed in this thesis, $^{2}H/^{13}C$ metabolic flux analysis could be utilised to measure the specific contributions of glycogenolysis and gluconeogenesis to hepatic glucose output in response to fasting and administration of glucose (Hughey, James et al. 2017).

While firm conclusions cannot be drawn solely from measurement of blood glucose following insulin and glucose tolerance testing, whole-body glucose intolerance during the IPGTT despite preserved blood glucose levels observed during the IPITT in DKI mice suggests that the underlying impairment in glucose homeostasis may not involve skeletal muscle. Instead, it is possible that hepatic glucose output is unchecked in DKI mice, even when exposed to high concentrations of circulating glucose as seen during the recovery from the overnight fast, which may be coincide with the development of insulin resistance in liver of DKI mice. To test this hypothesis, hyperinsulinemic-euglycemic clamps with radiolabelled glucose could be utilised to determine if DKI mice have whole-body insulin resistance and if suppression of endogenous glucose output in response to insulin is attenuated in DKI mice. Alternatively, glucose-stimulated insulin secretion could be affected in DKI mice.

7.3.2 Insulin Sensitivity and Peripheral Glucose Disposal

While DKI mice display whole-body glucose intolerance in response to IPGTT, no changes in insulin signalling proteins associated with glucose transport (i.e., Akt, AS160, GLUT4) in skeletal muscle were observed in DKI mice in the fed, resting state. Considered along with the findings of hyperinsulinemia and preserved blood glucose levels during the IPITT in DKI mice, these data suggest that glucose intolerance observed in DKI mice may not be due to impaired insulin-stimulated signalling in skeletal muscle. Further experiments could assess the phosphorylation status of these insulin signalling and glucose transport proteins in skeletal muscle collected following *in vivo* inulin stimulation. While the studies in this thesis focused on primary glycogen storing tissues liver and skeletal muscle, it should be acknowledged that adipose tissue metabolic responses could also be affected in DKI mice. For example, hematopoietic AMPK β1 KO mice exhibit insulin resistance in adipose tissue, despite maintaining whole-body glucose disposal during a hyperinsulinemic-euglycemic clamp (Galic, Fullerton et al. 2011). While DKI mice do not display any apparent impairments during the IPITT, this does not exclude the possibility that specific tissues in DKI mice may have impaired insulin sensitivity. To confirm the absence of insulin resistance in DKI mice suggested by the current findings, future studies could use hyperinsulinemic-euglycemic clamps to assess whole-body insulin sensitivity and the possibility of insulin resistance in liver and/or peripheral tissues. If DKI mice do indeed demonstrate impaired insulin sensitivity, *ex vivo* insulin- and/or AICAR-stimulated glucose uptake could be assessed in DKI skeletal muscle and adipose tissue to identify potential tissue-specific impairments.

7.3.3 Contraction-Stimulated Glucose Uptake

During prolonged exercise, there is a reduction in insulin secretion (Wasserman, Williams et al. 1989, Wasserman 2009), as AMPK promotes glucose uptake in skeletal muscle via an insulin-independent signalling pathway (O'Neill 2013, Richter and Hargreaves 2013). This exercise-induced reduction in circulating insulin promotes hepatic glycogenolysis, while concomitant increases in circulating glucagon levels promote both gluconeogenesis and glycogenolysis to maintain blood glucose levels (Wasserman, Spalding et al. 1989, Wasserman, Williams et al. 1989, Lavoie, Ducros et al. 1997). During high intensity exercise (i.e., >85% $VO_{2\ max}$), hepatic glucose output via glycogenolysis and gluconeogenesis can exceed the rate of skeletal muscle glucose uptake, resulting in increases in arterial glucose concentrations (Wasserman 2009). In the current thesis, DKI and WT mice displayed similar increases in blood glucose levels as well as content and phosphorylation of TBC1D1 at rest and following maximal treadmill running. Similar to the finding of preserved blood glucose levels in DKI mice following insulin stimulation, these observations indicate that DKI mice are able to respond to the increased energy demands of exercise and maintain euglycemia. It is possible that DKI mice remain hyperinsulinemic even during exercise, resulting in simultaneous activation of insulin- and contraction-stimulated pathways driving glucose uptake during submaximal and maximal exercise. This may result in increased skeletal muscle and/or adipose tissue glucose uptake during exercise and a preference for CHO substrate oxidation, thereby potentially driving increases in hepatic glucose output. In order to test this hypothesis, serum insulin responses to exercise could be measured. *Ex vivo* contraction-stimulated glucose uptake could then be assessed in DKI skeletal muscle and adipose to confirm if DKI mice display increased glucose uptake in response to exercise.

7.4 Exercise Capacity and Rates of Substrate Utilisation

At rest and during lower intensities of exercise (<40% $VO_{2\ max}$), fat is the primary contributor to energy expenditure, while blood glucose, maintained by hepatic glycogenolysis and gluconeogenesis, supports the majority of CHO requirements (Romijn, Coyle et al. 1993, van Loon, Greenhaff et al. 2001). Rates of fat oxidation continue to increase until the maximal rate of fat oxidation (fatmax) is reached, which occurs at approximately 70% of VO_{2max} in mice (Ishihara and Taniguchi 2018). As exercise intensity increases beyond fatmax, CHO becomes the predominant contributor to total energy expenditure in humans and rodents (Romijn, Coyle et al. 1993, van Loon, Greenhaff et al. 2001, Petrosino, Heiss et al. 2016). To determine if whole-body CHO and fat metabolism were altered in DKI mice, patterns of substrate utilisation were assessed in WT and DKI mice during submaximal treadmill running.

Concurrent with reduced maximal running speed, DKI mice displayed increased rates of CHO oxidation during submaximal running. While there are limited data on the patterns of whole-body substrate oxidation in AMPK KO mice during exercise, previous studies report contrasting results. Some reports indicate increased rates of fat oxidation in muscle-specific AMPK β1/β2 KO (O'Neill, Maarbjerg et al. 2011) while others find no observed differences in inducible muscle-specific AMPK α1/α2 KO (Hingst, Kjobsted et al. 2020) versus respective WT. Therefore, it appears that effects on substrate utilisation may be dependent on whether AMPK KO in the respective KO model was inducible or chronic, and potentially dependent on which AMPK subunit(s) was targeted. Despite these differences, both muscle-specific AMPK β1/β2 and AMPK α1/α2 KO models displayed reduced maximal running speed, suggesting an important role for AMPK in acute exercise responses that is not necessarily due to differences in substrate utilisation patterns (O'Neill, Maarbjerg et al. 2011, Hingst, Kjobsted et al. 2020). These contrasting results limit the ability to interpret the specific role of AMPK in regulating whole-body substrate utilisation patterns and how loss of muscle AMPK impairs maximal exercise capacity.

While substrate utilisation patterns during submaximal endurance testing were not investigated in this thesis, the lack of difference in endurance capacity between DKI and WT genotypes suggests that there may not be a significant and/or functional correlation between substrate utilisation and endurance capacity at submaximal intensities near fatmax (i.e., 60-70% of maximal running speed used in this thesis). Furthermore, while the increased rates of CHO oxidation rates in DKI mice during submaximal exercise contrasts with the results of several previous studies (O'Neill, Maarbjerg et al. 2011, Hingst, Kjobsted et al. 2020), it is possible that the differences in the models used in each study (i.e., the DKI mutation accompanied by ~40% reduction in muscle AMPK versus complete AMPK KO with chronic muscle-specific AMPK β1/β2 KO versus inducible muscle-specific AMPK α1/α2 KO) explain the divergent findings. These differences across the various AMPK mouse models highlight the limitations of using KO models to study respective protein function and underscore the value of developing new inducible and tissue-specific models to elucidate the roles of AMPK and its glycogen binding capacity *in vivo*. While similar levels of phosphorylation of ACC and TBC1D1 following maximal exercise in WT and DKI mice suggest maintained rates of fat metabolism and contraction-stimulated glucose uptake were conserved in skeletal muscle, further studies should evaluate if GLUT4 translocation, sarcolemmal FA transporters (e.g., FA translocase/CD36, FA transport proteins, and plasma membrane FA binding protein) and proteins involved in the glycolytic (e.g., hexokinase, PFK, and pyruvate kinase) and β-oxidation (e.g., long-chain-fatty-acid-CoA synthetase and acyl-CoA dehydrogenase) pathways are affected as a consequence of disrupting whole-body AMPK-glycogen binding.

The concomitant reductions in maximal running speed, increased rates of whole-body CHO oxidation, and increased skeletal muscle glycogen utilisation observed in DKI mice during exercise may possibly be due to shifts in fibre type in DKI skeletal muscle. Chronic activation of AMPK (e.g., as a result of endurance training) has been linked to a shift to a more oxidative phenotype in mouse and human skeletal muscle (Rockl, Hirshman et al. 2007, Egan and Zierath 2013). Chronic increases in AMPK activity via AICAR stimulation results in a shift to type I fibre in EDL muscle in mice (Ljubicic, Miura et al. 2011), while AMPK β2 KO mice have reduced type II muscle fibre size in EDL muscle compared to WT (Steinberg, O'Neill et al. 2010). Conversely, AMPK β1/β2 KO mice demonstrate no differences in fibre type expression in either glycolytic EDL or oxidative soleus muscle compared to WT (O'Neill, Maarbjerg et al. 2011).

AMPK activation in response to exercise appears to be dependent on fibre type in at least some muscle groups. For example, WT mice have increased activity of both AMPK α1 and α2 in oxidative versus glycolytic gastrocnemius muscle following one minute of wheel running (Jorgensen, Treebak et al. 2007). Meanwhile, no differences in increases of phosphorylation of AMPK T172, ACC S221, or TBC1D1 S231 were observed between oxidative and glycolytic human vastus lateralis muscle following 30 min of cycling at 70% of $VO_{2\ peak}$ (Kristensen, Albers et al. 2015). While there were no differences observed in phosphorylation of AMPK or downstream substrates in mixed gastrocnemius muscle following maximal treadmill running in this thesis, it is possible that AMPK phosphorylation and activation may be reduced in response to exercise in oxidative DKI muscles.

While muscle fibre type was not assessed in this thesis, it is possible that chronic reductions in AMPK protein content in DKI muscle could result in a shift toward expression of glycolytic type II fibres. Muscle fibre type shifts could therefore potentially underlie the observed reduction in maximal running speed and patterns of substrate oxidation during exercise. However, as mixed gastrocnemius muscle tissues were used throughout this thesis, it was assumed that samples used for analysis had similar representation of fibre types between genotypes. Therefore, it should be acknowledged that nonhomogeneous representation (i.e., more or less glycolytic or oxidative muscle fibres in a specific muscle sample) could contribute to the differences in glycogen content observed between WT and DKI muscle. While the roles of AMPK-glycogen binding in muscle fibre type expression warrant further investigation, experimental verification of possible shifts muscle fibre type as a result of the DKI mutation and the translation and/or relevance to humans are beyond the scope of this thesis.

7.5 Tissue Glycogen Dynamics

7.5.1 Fed and Fasting Liver Glycogen

Given its role in maintaining hepatic glucose output and euglycemia, liver glycogen content is critical for the regulation and control of glucose homeostasis. In this thesis, DKI mice display lower liver glycogen concentrations in the fed state compared to WT mice, which suggests that liver glycogen is potentially being used to maintain increased rates of CHO oxidation. Hepatic glycogen synthesis is stimulated by insulin (Petersen, Vatner et al. 2017). Furthermore, liver-specific GS KO in mice reduces hepatic glycogen stores and also results in glucose intolerance (Irimia, Meyer et al. 2010) and hepatic insulin resistance (Irimia, Meyer et al. 2017). Therefore, it is possible that the reduced glycogen capacity or "ceiling" in DKI liver, as a result of high glycogen turnover, leads to chronic hyperinsulinemia to promote glycogen resynthesis. This chronic insulin stimulation could potentially result in hepatic insulin resistance and contribute to the observed whole-body glucose intolerance, despite DKI mice retaining their ability to resynthesise and utilise liver glycogen. Therefore, potential associations between hepatic glycogen content and liver-specific glucose intolerance and insulin resistance in DKI mice warrant further investigation.

7.5.2 Liver Glycogen Utilisation During Exercise

Given its role in maintaining blood glucose levels, liver glycogen plays an important role in exercise capacity, particularly in rodents that predominantly rely on utilising circulating substrates during energy stress. However, in comparison to skeletal muscle, the role of liver glycogen during exercise has received little attention. In this thesis, both WT and DKI had a 55% reduction in liver glycogen from rested to maximally exercised, suggesting that liver glycogen levels in mice may exceed what can be oxidised during maximal exercise, and may not be a key determinant of maximal exercise capacity.

Protein targeting glycogen (PTG), a ubiquitously expressed glycogen associated protein, promotes glycogen formation by dephosphorylating GS and GP to increase glycogen synthesis and inhibit glycogen breakdown, respectively (Greenberg, Danos et al. 2006, Ruchti, Roach et al. 2016). Mice overexpressing PTG in liver, which leads to accumulation of glycogen, have improved endurance exercise capacity compared to WT mice (Lopez-Soldado, Guinovart et al. 2021). While the correlation between change in liver glycogen and submaximal endurance capacity was not assessed in this thesis, WT and DKI mice have similar time to exhaustion for the endurance test. This suggests that either liver glycogen use is not different between WT and DKI mice or that potential changes in glycogen use in DKI liver do not have a functional effect on exercise endurance performed at submaximal running speeds. Alternatively, while hepatic glycogen stores are limited (Gonzalez, Fuchs et al. 2016), it is possible that hepatic glucose output exceeds rates of muscle uptake and oxidation during exercise in both WT and DKI mice. Given that submaximal tests in this thesis were performed at 60% and 70% of individual mouse maximal running speed, which typically coincide with fatmax in mice (Ishihara and Taniguchi 2018), it is also possible that rates of fat oxidation in DKI mice are adequate for the energy requirements necessary to preserve endurance capacity. Therefore, other causes of fatigue during endurance exercise (e.g., neuromuscular, chemical and/or cardiovascular factors) may not be affected by chronically disrupting whole-body AMPK-glycogen binding.

7.5.3 Skeletal Muscle Glycogen Use in Response to Fasting and Synthesis Following Recovery

Assessment of tissue glycogen concentration in response to fasting and at multiple time points during recovery revealed that DKI mice have increased levels of skeletal muscle glycogen depletion following an overnight fast. Given the relatively low concentration of glycogen in skeletal muscle compared to liver in mice, prolonged fasting does not usually significantly affect skeletal muscle glycogen concentrations (Irimia, Tagliabracci et al. 2015). The findings in this thesis indicate that increased use of skeletal muscle glycogen potentially contributed to the increased reliance on whole-body CHO oxidation in DKI mice during fasting as well as exercise.

DKI mice have an inability to resynthesise glycogen in skeletal muscle following fasting, even with oral glucose gavage and *ad libitum* access to chow. This finding is in contrast to previous results in either AMPK β1 or β2 single isoform KI mice, which identified no differences in liver or skeletal muscle glycogen depletion in response to overnight fasting. Skeletal muscle glycogen resynthesis is a metabolic priority during recovery and involves the upregulation of fat oxidation to spare glucose so it can be used for glycogen synthesis (Kiens and Richter 1998, Kimber, Heigenhauser et al. 2003, Hunter, Treebak et al. 2011). The inability of DKI mice to synthesise skeletal muscle glycogen suggests an impairment in the function of protein(s) involved in glycogen particle formation, which may occur independently of potential impairment(s) in skeletal muscle fat oxidation or glucose uptake.

The findings in this thesis suggest that alterations in glycogen utilisation and resynthesis observed in DKI tissue are not likely to be associated with changes in content of GS, GBE, glycogenin, GP, or GDE, or phosphorylation of GS S641. Inducible muscle-specific AMPK α1/α2 KO mice demonstrate a maintained ability to utilise skeletal muscle glycogen during exercise, consistent with the findings in DKI mice. However, these AMPK α1/α2 KO mice also display reductions in fed skeletal muscle glycogen content and GS activity, which is associated with reduced expression of UGP2 (Hingst, Kjobsted et al. 2020). UGP2 is responsible for generating UDP-glucose, a precursor of glycogen (Roach, Depaoli-Roach et al. 2012). Therefore, it is possible that DKI mice may have a similar reduction in UGP2 and/or another enzyme involved in glycogen formation that impairs their ability to resynthesise glycogen following fasting. Together, these findings suggest that reduced skeletal muscle AMPK content in DKI mice likely contributes to impaired glycogen dynamics independently of changes in the GS phosphorylation site and the panel of glycogen-associated proteins assessed.

7.5.4 Correlation of Maximal Running Speed and Skeletal Muscle Glycogen Utilisation

In the experiments in this thesis, the change in skeletal muscle glycogen from resting to following maximal running was positively correlated with maximal running speed in WT mice, but not DKI mice. While this interaction cannot be deemed causative, it does suggest that ability to utilise skeletal muscle glycogen is a key component of achieving higher maximal running speed in WT mice. However, the role of skeletal muscle glycogen in determining exercise capacity in mice remains unclear. This is primarily based on the different patterns of tissue glycogen storage and substrate utilisation between humans and rodents (Kjobsted, Hingst et al. 2018). Previous studies have shown that the chronic GS KO mouse model of GSD 0b lacking skeletal muscle glycogen do not have impaired running endurance capacity (Pederson, Cope et al. 2005) and elevated glycogen concentrations do not enhance running endurance (Pederson, Cope et al. 2005). However, it is important to note that these studies used endurance-based protocols, rather than incremental maximal treadmill running challenges similar to the one used in this thesis. Therefore, these contrasting results between this thesis and previous studies could be explained by differences in exercise intensity and/or duration resulting in different contributions of glycogen to total energy expenditure. Future studies could employ endurance-based exercise protocols similar to the above studies and/or higher intensities to determine potential genotypic differences.

7.5.5 Characterising Potential Changes in Glycogen Localisation in DKI Mice

Research in the last decade has established novel and distinct roles for the three subcellular glycogen pools in response to exercise (**Chapter 2**). Experiments in this thesis measured total glycogen content in skeletal muscle but did not investigate potential effects of the DKI mutation on the content, utilisation, and/or synthesis of these distinct glycogen pools. TEM imaging has been used to measure glycogen content and particle size in specific subcellular pools and various muscle fibre types, as well as quantify glycogen depletion in response to exercise, contraction and resynthesis during recovery (Nielsen, Holmberg et al. 2011, Nielsen, Krustrup et al. 2012, Nielsen, Cheng et al. 2014, Jensen, Ortenblad et al. 2020, Jensen, Ortenblad et al. 2021). Therefore, TEM analysis of skeletal muscle glycogen could be performed to determine if disruption of AMPK-glycogen binding differentially affects these glycogen pools. Future investigation could determine subsequent effects on muscle function *ex vivo* (e.g., contractility, fatiguability, Ca^{2+} release and uptake upon contraction).

Future studies could also investigate the mechanism(s) underlying increased skeletal muscle glycogen utilisation in response to energy stress and/or impaired resynthesis in DKI mice. While the content of several glycogen-associated proteins and phosphorylation of GS S641 were measured, activities of these enzymes – specifically GS and GP – were not assessed. It is possible that alterations in the functionality of some glycogen-associated proteins were not identified when assessing only total protein content by Western blotting. Given the allosteric regulation of GP and GS (Johnson and Barford 1990, Bouskila, Hunter et al. 2010), potential changes in adenylate charge ratio and G6P concentrations, as well as the observed changes in insulin concentrations, may impact activity of these proteins in DKI tissue. Protein expression and/or activity of other enzymes involved in glucose uptake, glycogen particle formation, or utilisation therefore could potentially be affected in DKI mice. Alternatively, alterations in glycogen dynamics observed in DKI skeletal muscle may be due to changes in other regulatory pathways. For example, glycophagy, a process which has been linked to glucose metabolism in skeletal muscle during energy stress, is promoted by the starch-binding domain-containing protein 1 (STBD1) (Kaur and Debnath 2015, Zhao, Tang et al. 2018). STBD1 is phosphorylated by AMPK at S175 (Ducommun, Deak et al. 2019), but the functional significance of S175 phosphorylation remains unknown. It is possible that AMPK-mediated phosphorylation of STBD1 S175 may require AMPK to be bound to glycogen and may lead to inhibition of glycophagy. Therefore, the DKI mutation may impair STBD1 phosphorylation by AMPK and lead to increased glycophagy in skeletal muscle, which may contribute to the altered substrate utilisation patterns and tissue glycogen dynamics observed in DKI mice.

7.6 Potential Mechanisms for Reduced AMPK Content in DKI Mice

The overall aim of this thesis was to determine the phenotypic effects of the AMPK DKI mutation on whole-body and tissue metabolism during energy stress and excess, which included findings of reduced tissue AMPK content in DKI mice. A limitation of this thesis is that the specific molecular and/or cellular mechanism(s) by which reduced AMPK content occurs concomitantly with disruption of AMPK-glycogen binding was not determined within the time constraints and the physiological scope of these mouse-based projects. There were no significant differences observed in gene expression of *Prkab1* (β1) or *Prkab2* (β2) between WT and DKI liver and skeletal muscle, suggesting that reduction of AMPK may instead be potentially due to alterations in transcription/translation, protein stability, and/or post-translational modifications. Further work is therefore necessary to pinpoint the precise mechanism(s) responsible for the observed decrease in total AMPK protein content. Previous work has demonstrated that mutations in the CBM of other starch and glycogen-binding proteins (e.g., STBD1 and CGTase) results in loss of stability and/or protein content (Chang, Irwin et al. 1998, Zhu, Zhang et al. 2014). Therefore, the reduction of tissue AMPK protein content associated with the DKI mutation is not exclusive to only the DKI model used in this thesis and is supported by these previous studies indicating that a protein such as AMPK's CBM and/or glycogen binding capacity may contribute to protein content and/or stability.

With advancements in transgenic model systems, it is apparent that chronic versus inducible mutations in genes (e.g., kinases) can produce divergent results between mouse models. The vastly different phenotypes observed between various AMPK KO models indicates that this is also true for AMPK. However, much of our understanding of the function of AMPK has been derived from chronic AMPK KO models. Genetic loss of the AMPK heterotrimer has dramatic effects on development and many biological processes, highlighting a fundamental limitation of KO models, as well as potential KI models with chronic mutations such as the AMPK DKI mutation used in this thesis. Therefore, while outside of the scope and timeframe of this thesis, new inducible, transgenic models will be critical for distinguishing the developmental versus acute effects of disrupting AMPK's diverse cellular roles, including glycogen binding capacity. For example, development of new mouse models with inducible KI mutations to acutely disrupt AMPK-glycogen binding will help build on the findings in this thesis to determine if the observed whole-body and tissue phenotypic effects of the DKI mutation occur as a consequence of loss of AMPK-glycogen binding, reductions in AMPK content, and/or other potential mechanisms.

7.7 Conclusion

The experiments conducted for this thesis have addressed important knowledge gaps regarding the potential physiological roles of AMPK-glycogen binding by identifying phenotypic effects of the DKI mutation utilised to chronically disrupt whole-body AMPK-glycogen binding *in vivo*. These main findings and directions for future research are summarised in **Figure 7.1**. Specifically, this thesis has identified that the AMPK DKI mutation utilised to chronically disrupt whole-body AMPK-glycogen binding in mice results in 1) increased body mass and adiposity, hyperinsulinemia, and whole-body glucose intolerance; 2) increased rates of CHO oxidation and reduced rates of fat oxidation in physiological settings of alterations in energy availability; 3) reduced maximal running capacity; 4) increased utilisation of liver and skeletal muscle glycogen and impaired ability to synthesise skeletal muscle glycogen following energy stress; and 5) associated reductions in tissue AMPK content. The phenotype of DKI mice with whole-body disruption of AMPK-glycogen binding described in this thesis is strikingly similar to that observed in diet-induced obesity and the early development of insulin resistance, suggesting that the interactions between AMPK and glycogen may serve potential physiological roles at the crossroads of metabolic health and disease that warrant future investigation to build upon the findings of this thesis.

Chapter 8 References

Abudayyeh, O. O., J. S. Gootenberg, P. Essletzbichler, S. Han, J. Joung, J. J. Belanto, V. Verdine, D. B. T. Cox, M. J. Kellner, A. Regev, E. S. Lander, D. F. Voytas, A. Y. Ting and F. Zhang (2017). "RNA targeting with CRISPR-Cas13." Nature **550**(7675): 280-284.

Adeva-Andany, M. M., M. Gonzalez-Lucan, C. Donapetry-Garcia, C. Fernandez-Fernandez and E. Ameneiros-Rodriguez (2016). "Glycogen metabolism in humans." BBA Clin **5**: 85-100.

Alessi, D. R., S. R. James, C. P. Downes, A. B. Holmes, P. R. Gaffney, C. B. Reese and P. Cohen (1997). "Characterization of a 3-phosphoinositide-dependent protein kinase which phosphorylates and activates protein kinase Balpha." Curr Biol **7**(4): 261-269.

Alessi, D. R., M. T. Kozlowski, Q. P. Weng, N. Morrice and J. Avruch (1998). "3-Phosphoinositide-dependent protein kinase 1 (PDK1) phosphorylates and activates the p70 S6 kinase in vivo and in vitro." Curr Biol **8**(2): 69-81.

Alonso, M. D., J. Lomako, W. M. Lomako and W. J. Whelan (1995). "A new look at the biogenesis of glycogen." FASEB J **9**(12): 1126-1137.

Altarejos, J. Y. and M. Montminy (2011). "CREB and the CRTC co-activators: sensors for hormonal and metabolic signals." Nat Rev Mol Cell Biol **12**(3): 141-151.

Arad, M., D. W. Benson, A. R. Perez-Atayde, W. J. McKenna, E. A. Sparks, R. J. Kanter, K. McGarry, J. G. Seidman and C. E. Seidman (2002). "Constitutively active AMP kinase mutations cause glycogen storage disease mimicking hypertrophic cardiomyopathy." J Clin Invest **109**(3): 357-362.

Austin, J. and D. Marks (2009). "Hormonal regulators of appetite." Int J Pediatr Endocrinol **2009**: 141753.

Ayala, J. E., D. P. Bracy, O. P. McGuinness and D. H. Wasserman (2006). "Considerations in the design of hyperinsulinemic-euglycemic clamps in the conscious mouse." Diabetes **55**(2): 390-397.

Ayala, J. E., V. T. Samuel, G. J. Morton, S. Obici, C. M. Croniger, G. I. Shulman, D. H. Wasserman, O. P. McGuinness and N. I. H. M. M. P. C. Consortium (2010). "Standard operating procedures for describing and performing metabolic tests of glucose homeostasis in mice." Dis Model Mech **3**(9-10): 525-534.

Baldwin, K. M., J. S. Reitman, R. L. Terjung, W. W. Winder and J. O. Holloszy (1973). "Substrate depletion in different types of muscle and in liver during prolonged running." Am J Physiol **225**(5): 1045-1050.

Barnes, B. R., S. Marklund, T. L. Steiler, M. Walter, G. Hjalm, V. Amarger, M. Mahlapuu, Y. Leng, C. Johansson, D. Galuska, K. Lindgren, M. Abrink, D. Stapleton, J. R. Zierath and L. Andersson (2004). "The 5'-AMP-activated protein kinase gamma3 isoform has a key role in carbohydrate and lipid metabolism in glycolytic skeletal muscle." J Biol Chem **279**(37): 38441-38447.

Barre, L., C. Richardson, M. F. Hirshman, J. Brozinick, S. Fiering, B. E. Kemp, L. J. Goodyear and L. A. Witters (2007). "Genetic model for the chronic activation of skeletal muscle AMP-activated protein kinase leads to glycogen accumulation." Am J Physiol Endocrinol Metab **292**(3): E802-811.

Bartlett, J. D., J. Louhelainen, Z. Iqbal, A. J. Cochran, M. J. Gibala, W. Gregson, G. L. Close, B. Drust and J. P. Morton (2013). "Reduced carbohydrate availability enhances exercise-induced p53 signaling in human skeletal muscle: implications for mitochondrial biogenesis." Am J Physiol Regul Integr Comp Physiol **304**(6): R450-458.

Bendayan, M., I. Londono, B. E. Kemp, G. D. Hardie, N. Ruderman and M. Prentki (2009). "Association of AMP-activated protein kinase subunits with glycogen particles as revealed in situ by immunoelectron microscopy." J Histochem Cytochem **57**(10): 963-971.

Bergmeyer, H. U. (1974). Methods of enzymatic analysis. Weinheim New York, USA, Verlag Chemie; Academic Press.

Bergstrom, J., L. Hermansen, E. Hultman and B. Saltin (1967). "Diet, muscle glycogen and physical performance." Acta Physiol Scand **71**(2): 140-150.

Bianchi, A., J. L. Evans, A. J. Iverson, A. C. Nordlund, T. D. Watts and L. A. Witters (1990). "Identification of an isozymic form of acetyl-CoA carboxylase." J Biol Chem **265**(3): 1502-1509.

Birk, J. B. and J. F. Wojtaszewski (2006). "Predominant alpha2/beta2/gamma3 AMPK activation during exercise in human skeletal muscle." J Physiol **577**(Pt 3): 1021-1032.

Bouskila, M., R. W. Hunter, A. F. Ibrahim, L. Delattre, M. Peggie, J. A. van Diepen, P. J. Voshol, J. Jensen and K. Sakamoto (2010). "Allosteric regulation of glycogen synthase controls glycogen synthesis in muscle." Cell Metab **12**(5): 456-466.

Brady, M. J., A. C. Nairn and A. R. Saltiel (1997). "The regulation of glycogen synthase by protein phosphatase 1 in 3T3-L1 adipocytes. Evidence for a potential role for DARPP-32 in insulin action." J Biol Chem **272**(47): 29698-29703.

Brereton, M. F., M. Rohm, K. Shimomura, C. Holland, S. Tornovsky-Babeay, D. Dadon, M. Iberl, M. V. Chibalina, S. Lee, B. Glaser, Y. Dor, P. Rorsman, A. Clark and F. M. Ashcroft (2016). "Hyperglycaemia induces metabolic dysfunction and glycogen accumulation in pancreatic beta-cells." Nat Commun **7**: 13496.

Brull, A., N. de Luna, A. Blanco-Grau, A. Lucia, M. A. Martin, J. Arenas, R. Marti, A. L. Andreu and T. Pinos (2015). "Phenotype consequences of myophosphorylase dysfunction: insights from the McArdle mouse model." J Physiol **593**(12): 2693-2706.

Burg, J. S. and P. J. Espenshade (2011). "Regulation of HMG-CoA reductase in mammals and yeast." Prog Lipid Res **50**(4): 403-410.

Burke, L. M., L. J. C. van Loon and J. A. Hawley (2017). "Postexercise muscle glycogen resynthesis in humans." J Appl Physiol (1985) **122**(5): 1055-1067.

Camacho, R. C., P. Galassetti, S. N. Davis and D. H. Wasserman (2005). "Glucoregulation during and after exercise in health and insulin-dependent diabetes." Exerc Sport Sci Rev **33**(1): 17-23.

Carling, D. and D. G. Hardie (1989). "The substrate and sequence specificity of the AMP-activated protein kinase. Phosphorylation of glycogen synthase and phosphorylase kinase." Biochim Biophys Acta **1012**(1): 81-86.

Cartee, G. D. and K. Funai (2009). "Exercise and insulin: Convergence or divergence at AS160 and TBC1D1?" Exerc Sport Sci Rev **37**(4): 188-195.

Ceperuelo-Mallafre, V., M. Ejarque, C. Serena, X. Duran, M. Montori-Grau, M. A. Rodriguez, O. Yanes, C. Nunez-Roa, K. Roche, P. Puthanveetil, L. Garrido-Sanchez, E. Saez, F. J. Tinahones, P. M. Garcia-Roves, A. M. Gomez-Foix, A. R. Saltiel, J. Vendrell and S. Fernandez-Veledo (2016). "Adipose tissue glycogen accumulation is associated with obesity-linked inflammation in humans." Mol Metab **5**(1): 5-18.

Chang, H. Y., P. M. Irwin and Z. L. Nikolov (1998). "Effects of mutations in the starch-binding domain of Bacillus macerans cyclodextrin glycosyltransferase." J Biotechnol **65**(2-3): 191-202.

Chasiotis, D., K. Sahlin and E. Hultman (1982). "Regulation of glycogenolysis in human muscle at rest and during exercise." J Appl Physiol Respir Environ Exerc Physiol **53**(3): 708-715.

Chen, Z. P., T. J. Stephens, S. Murthy, B. J. Canny, M. Hargreaves, L. A. Witters, B. E. Kemp and G. K. McConell (2003). "Effect of exercise intensity on skeletal muscle AMPK signaling in humans." Diabetes **52**(9): 2205-2212.

Cheng, Z., Y. Tseng and M. F. White (2010). "Insulin signaling meets mitochondria in metabolism." Trends Endocrinol Metab **21**(10): 589-598.

Chennell, G., R. J. Willows, S. C. Warren, D. Carling, P. M. French, C. Dunsby and A. Sardini (2016). "Imaging of Metabolic Status in 3D Cultures with an Improved AMPK FRET Biosensor for FLIM." Sensors (Basel) **16**(8).

Cokorinos, E. C., J. Delmore, A. R. Reyes, B. Albuquerque, R. Kjobsted, N. O. Jorgensen, J. L. Tran, A. Jatkar, K. Cialdea, R. M. Esquejo, J. Meissen, M. F. Calabrese, J. Cordes, R. Moccia, D. Tess, C. T. Salatto, T. M. Coskran, A. C. Opsahl, D. Flynn, M. Blatnik, W. Li, E. Kindt, M. Foretz, B. Viollet, J. Ward, R. G. Kurumbail, A. S. Kalgutkar, J. F. P. Wojtaszewski, K. O. Cameron and R. A. Miller (2017). "Activation of Skeletal Muscle AMPK Promotes Glucose Disposal and Glucose Lowering in Non-human Primates and Mice." Cell Metab **25**(5): 1147-1159 e1110.

Conlee, R. K., R. M. Lawler and P. E. Ross (1987). "Effects of glucose or fructose feeding on glycogen repletion in muscle and liver after exercise or fasting." Ann Nutr Metab **31**(2): 126-132.

Coyle, E. F., A. R. Coggan, M. K. Hemmert and J. L. Ivy (1986). "Muscle glycogen utilization during prolonged strenuous exercise when fed carbohydrate." J Appl Physiol (1985) **61**(1): 165-172.

Cross, D. A., D. R. Alessi, P. Cohen, M. Andjelkovich and B. A. Hemmings (1995). "Inhibition of glycogen synthase kinase-3 by insulin mediated by protein kinase B." Nature **378**(6559): 785-789.

Crosson, S. M., A. Khan, J. Printen, J. E. Pessin and A. R. Saltiel (2003). "PTG gene deletion causes impaired glycogen synthesis and developmental insulin resistance." J Clin Invest **111**(9): 1423-1432.

Daignan-Fornier, B. and B. Pinson (2012). "5-Aminoimidazole-4-carboxamide-1-beta-D-ribofuranosyl 5'-Monophosphate (AICAR), a Highly Conserved Purine Intermediate with Multiple Effects." Metabolites **2**(2): 292-302.

Damsbo, P., A. Vaag, O. Hother-Nielsen and H. Beck-Nielsen (1991). "Reduced glycogen synthase activity in skeletal muscle from obese patients with and without type 2 (non-insulin-dependent) diabetes mellitus." Diabetologia **34**(4): 239-245.

Dasgupta, B., J. S. Ju, Y. Sasaki, X. Liu, S. R. Jung, K. Higashida, D. Lindquist and J. Milbrandt (2012). "The AMPK beta2 subunit is required for energy homeostasis during metabolic stress." Mol Cell Biol **32**(14): 2837-2848.

Daval, M., F. Diot-Dupuy, R. Bazin, I. Hainault, B. Viollet, S. Vaulont, E. Hajduch, P. Ferre and F. Foufelle (2005). "Anti-lipolytic action of AMP-activated protein kinase in rodent adipocytes." J Biol Chem **280**(26): 25250-25257.

DeFronzo, R. A. and D. Tripathy (2009). "Skeletal muscle insulin resistance is the primary defect in type 2 diabetes." Diabetes Care **32 Suppl 2**: S157-163.

Depry, C., S. Mehta, R. Li and J. Zhang (2015). "Visualization of Compartmentalized Kinase Activity Dynamics Using Adaptable BimKARs." Chem Biol **22**(11): 1470-1479.

Ducommun, S., M. Deak, D. Sumpton, R. J. Ford, A. Nunez Galindo, M. Kussmann, B. Viollet, G. R. Steinberg, M. Foretz, L. Dayon, N. A. Morrice and K. Sakamoto (2015). "Motif affinity and mass spectrometry proteomic approach for the discovery of cellular AMPK targets: identification of mitochondrial fission factor as a new AMPK substrate." Cell Signal **27**(5): 978-988.

Ducommun, S., M. Deak, A. Zeigerer, O. Goransson, S. Seitz, C. Collodet, A. B. Madsen, T. E. Jensen, B. Viollet, M. Foretz, P. Gut, D. Sumpton and K. Sakamoto (2019). "Chemical genetic screen identifies Gapex-5/GAPVD1 and STBD1 as novel AMPK substrates." Cell Signal **57**: 45-57.

Ducommun, S., H. Y. Wang, K. Sakamoto, C. MacKintosh and S. Chen (2012). "Thr649Ala-AS160 knock-in mutation does not impair contraction/AICAR-induced glucose transport in mouse muscle." Am J Physiol Endocrinol Metab **302**(9): E1036-1043.

Dzamko, N., B. J. van Denderen, A. L. Hevener, S. B. Jorgensen, J. Honeyman, S. Galic, Z. P. Chen, M. J. Watt, D. J. Campbell, G. R. Steinberg and B. E. Kemp (2010). "AMPK beta1 deletion reduces appetite, preventing obesity and hepatic insulin resistance." J Biol Chem **285**(1): 115-122.

Egan, B. and J. R. Zierath (2013). "Exercise metabolism and the molecular regulation of skeletal muscle adaptation." Cell Metab **17**(2): 162-184.

Fentz, J., R. Kjobsted, J. B. Birk, A. B. Jordy, J. Jeppesen, K. Thorsen, P. Schjerling, B. Kiens, N. Jessen, B. Viollet and J. F. Wojtaszewski (2015). "AMPKalpha is critical for enhancing skeletal muscle fatty acid utilization during in vivo exercise in mice." FASEB J **29**(5): 1725-1738.

Fentz, J., R. Kjobsted, C. M. Kristensen, J. R. Hingst, J. B. Birk, A. Gudiksen, M. Foretz, P. Schjerling, B. Viollet, H. Pilegaard and J. F. Wojtaszewski (2015). "AMPKalpha is essential for acute exercise-induced gene responses but not for exercise training-induced adaptations in mouse skeletal muscle." Am J Physiol Endocrinol Metab **309**(11): E900-914.

Flores-Opazo, M., J. Trieu, T. Naim, D. Valladares-Ide, H. Zbinden-Foncea and D. Stapleton (2020). "Defective fasting-induced PKA activation impairs adipose tissue glycogen degradation in obese Zucker rats." Int J Obes (Lond) **44**(2): 500-509.

Foretz, M., P. C. Even and B. Viollet (2018). "AMPK Activation Reduces Hepatic Lipid Content by Increasing Fat Oxidation In Vivo." Int J Mol Sci **19**(9).

Fritzen, A. M., A. M. Lundsgaard, J. Jeppesen, M. L. Christiansen, R. Bienso, J. R. Dyck, H. Pilegaard and B. Kiens (2015). "5'-AMP activated protein kinase alpha2 controls substrate metabolism during post-exercise recovery via regulation of pyruvate dehydrogenase kinase 4." J Physiol **593**(21): 4765-4780.

Fruman, D. A., R. E. Meyers and L. C. Cantley (1998). "Phosphoinositide kinases." Annu Rev Biochem **67**: 481-507.

Fullerton, M. D., S. Galic, K. Marcinko, S. Sikkema, T. Pulinilkunnil, Z. P. Chen, H. M. O'Neill, R. J. Ford, R. Palanivel, M. O'Brien, D. G. Hardie, S. L. Macaulay, J. D. Schertzer, J.

R. Dyck, B. J. van Denderen, B. E. Kemp and G. R. Steinberg (2013). "Single phosphorylation sites in Acc1 and Acc2 regulate lipid homeostasis and the insulin-sensitizing effects of metformin." Nat Med **19**(12): 1649-1654.

Galic, S., M. D. Fullerton, J. D. Schertzer, S. Sikkema, K. Marcinko, C. R. Walkley, D. Izon, J. Honeyman, Z. P. Chen, B. J. van Denderen, B. E. Kemp and G. R. Steinberg (2011). "Hematopoietic AMPK beta1 reduces mouse adipose tissue macrophage inflammation and insulin resistance in obesity." J Clin Invest **121**(12): 4903-4915.

Galic, S., J. S. Oakhill and G. R. Steinberg (2010). "Adipose tissue as an endocrine organ." Mol Cell Endocrinol **316**(2): 129-139.

Garcia, D. and R. J. Shaw (2017). "AMPK: Mechanisms of Cellular Energy Sensing and Restoration of Metabolic Balance." Mol Cell **66**(6): 789-800.

Garcia-Haro, L., M. A. Garcia-Gimeno, D. Neumann, M. Beullens, M. Bollen and P. Sanz (2010). "The PP1-R6 protein phosphatase holoenzyme is involved in the glucose-induced dephosphorylation and inactivation of AMP-activated protein kinase, a key regulator of insulin secretion, in MIN6 beta cells." FASEB J **24**(12): 5080-5091.

Garcia-Roves, P. M., M. E. Osler, M. H. Holmstrom and J. R. Zierath (2008). "Gain-of-function R225Q mutation in AMP-activated protein kinase gamma3 subunit increases mitochondrial biogenesis in glycolytic skeletal muscle." J Biol Chem **283**(51): 35724-35734.

Gauthier, M. S., E. L. O'Brien, S. Bigornia, M. Mott, J. M. Cacicedo, X. J. Xu, N. Gokce, C. Apovian and N. Ruderman (2011). "Decreased AMP-activated protein kinase activity is associated with increased inflammation in visceral adipose tissue and with whole-body insulin resistance in morbidly obese humans." Biochem Biophys Res Commun **404**(1): 382-387.

Gonzalez, J. T., C. J. Fuchs, J. A. Betts and L. J. van Loon (2016). "Liver glycogen metabolism during and after prolonged endurance-type exercise." Am J Physiol Endocrinol Metab **311**(3): E543-553.

Gowans, G. J., S. A. Hawley, F. A. Ross and D. G. Hardie (2013). "AMP is a true physiological regulator of AMP-activated protein kinase by both allosteric activation and enhancing net phosphorylation." Cell Metab **18**(4): 556-566.

Graham, T. E., Z. Yuan, A. K. Hill and R. J. Wilson (2010). "The regulation of muscle glycogen: the granule and its proteins." Acta Physiol (Oxf) **199**(4): 489-498.

Greenberg, C. C., A. M. Danos and M. J. Brady (2006). "Central role for protein targeting to glycogen in the maintenance of cellular glycogen stores in 3T3-L1 adipocytes." Mol Cell Biol **26**(1): 334-342.

Greiwe, J. S., R. C. Hickner, P. A. Hansen, S. B. Racette, M. M. Chen and J. O. Holloszy (1999). "Effects of endurance exercise training on muscle glycogen accumulation in humans." J Appl Physiol (1985) **87**(1): 222-226.

Gu, X., Y. Yan, S. J. Novick, A. Kovach, D. Goswami, J. Ke, M. H. E. Tan, L. Wang, X. Li, P. W. de Waal, M. R. Webb, P. R. Griffin, H. E. Xu and K. Melcher (2017). "Deconvoluting AMP-activated protein kinase (AMPK) adenine nucleotide binding and sensing." J Biol Chem **292**(30): 12653-12666.

Haller, R. G. and J. Vissing (2002). "Spontaneous "second wind" and glucose-induced second "second wind" in McArdle disease: oxidative mechanisms." Arch Neurol **59**(9): 1395-1402.

Hamada, T., E. B. Arias and G. D. Cartee (2006). "Increased submaximal insulin-stimulated glucose uptake in mouse skeletal muscle after treadmill exercise." J Appl Physiol (1985) **101**(5): 1368-1376.

Hardie, D. G. (2013). "AMPK: a target for drugs and natural products with effects on both diabetes and cancer." Diabetes **62**(7): 2164-2172.

Hardie, D. G., F. A. Ross and S. A. Hawley (2012). "AMPK: a nutrient and energy sensor that maintains energy homeostasis." Nat Rev Mol Cell Biol **13**(4): 251-262.

Hardie, D. G., B. E. Schaffer and A. Brunet (2016). "AMPK: An Energy-Sensing Pathway with Multiple Inputs and Outputs." Trends Cell Biol **26**(3): 190-201.

Hasenour, C. M., D. E. Ridley, F. D. James, C. C. Hughey, E. P. Donahue, B. Viollet, M. Foretz, J. D. Young and D. H. Wasserman (2017). "Liver AMP-Activated Protein Kinase Is Unnecessary for Gluconeogenesis but Protects Energy State during Nutrient Deprivation." PLoS One **12**(1): e0170382.

Hawley, J. A., M. Hargreaves, M. J. Joyner and J. R. Zierath (2014). "Integrative biology of exercise." Cell **159**(4): 738-749.

Hawley, S. A., M. Davison, A. Woods, S. P. Davies, R. K. Beri, D. Carling and D. G. Hardie (1996). "Characterization of the AMP-activated protein kinase kinase from rat liver and identification of threonine 172 as the major site at which it phosphorylates AMP-activated protein kinase." J Biol Chem **271**(44): 27879-27887.

Hawley, S. A., D. A. Pan, K. J. Mustard, L. Ross, J. Bain, A. M. Edelman, B. G. Frenguelli and D. G. Hardie (2005). "Calmodulin-dependent protein kinase kinase-beta is an alternative upstream kinase for AMP-activated protein kinase." Cell Metab **2**(1): 9-19.

Hearris, M. A., D. J. Owens, J. A. Strauss, S. O. Shepherd, A. P. Sharples, J. P. Morton and J. B. Louis (2020). "Graded reductions in pre-exercise glycogen concentration do not augment exercise-induced nuclear AMPK and PGC-1alpha protein content in human muscle." Exp Physiol.

Hermansen, L., E. Hultman and B. Saltin (1967). "Muscle glycogen during prolonged severe exercise." Acta Physiol Scand **71**(2): 129-139.

Herzig, S. and R. J. Shaw (2018). "AMPK: guardian of metabolism and mitochondrial homeostasis." Nat Rev Mol Cell Biol **19**(2): 121-135.

Hingst, J. R., L. Bruhn, M. B. Hansen, M. F. Rosschou, J. B. Birk, J. Fentz, M. Foretz, B. Viollet, K. Sakamoto, N. J. Faergeman, J. F. Havelund, B. L. Parker, D. E. James, B. Kiens, E. A. Richter, J. Jensen and J. F. P. Wojtaszewski (2018). "Exercise-induced molecular mechanisms promoting glycogen supercompensation in human skeletal muscle." Mol Metab **16**: 24-34.

Hingst, J. R., L. Bruhn, M. B. Hansen, M. F. Rosschou, J. B. Birk, J. Fentz, M. Foretz, B. Viollet, K. Sakamoto, N. J. Faergeman, J. F. Havelund, B. L. Parker, D. E. James, B. Kiens, E. A. Richter, J. Jensen and J. F. P. Wojtaszewski (2018). "Exercise-induced molecular mechanisms promoting glycogen supercompensation in human skeletal muscle." Mol Metab.

Hingst, J. R., R. Kjobsted, J. B. Birk, N. O. Jorgensen, M. R. Larsen, K. Kido, J. K. Larsen, S. A. S. Kjeldsen, J. Fentz, C. Frosig, S. Holm, A. M. Fritzen, T. L. Dohlmann, S. Larsen, M. Foretz, B. Viollet, P. Schjerling, P. Overby, J. F. Halling, H. Pilegaard, Y. Hellsten and J. F. P. Wojtaszewski (2020). "Inducible deletion of skeletal muscle AMPKalpha reveals that AMPK is required for nucleotide balance but dispensable for muscle glucose uptake and fat oxidation during exercise." Mol Metab **40**: 101028.

Hoffman, N. J. (2017). "Omics and Exercise: Global Approaches for Mapping Exercise Biological Networks." Cold Spring Harb Perspect Med **7**(10).

Hoffman, N. J., B. L. Parker, R. Chaudhuri, K. H. Fisher-Wellman, M. Kleinert, S. J. Humphrey, P. Yang, M. Holliday, S. Trefely, D. J. Fazakerley, J. Stockli, J. G. Burchfield, T. E. Jensen, R. Jothi, B. Kiens, J. F. Wojtaszewski, E. A. Richter and D. E. James (2015). "Global Phosphoproteomic Analysis of Human Skeletal Muscle Reveals a Network of Exercise-Regulated Kinases and AMPK Substrates." Cell Metab **22**(5): 922-935.

Hoffman, N. J., J. Whitfield, N. R. Janzen, M. R. Belhaj, S. Galic, L. Murray-Segal, W. J. Smiles, N. X. Y. Ling, T. A. Dite, J. W. Scott, J. S. Oakhill, R. Brink, B. E. Kemp and J. A. Hawley (2020). "Genetic loss of AMPK-glycogen binding destabilizes AMPK and disrupts metabolism." Mol Metab: 101048.

Hojlund, K., J. B. Birk, D. K. Klein, K. Levin, A. J. Rose, B. F. Hansen, J. N. Nielsen, H. Beck-Nielsen and J. F. Wojtaszewski (2009). "Dysregulation of glycogen synthase COOH- and NH2-terminal phosphorylation by insulin in obesity and type 2 diabetes mellitus." J Clin Endocrinol Metab **94**(11): 4547-4556.

Hojlund, K., P. Staehr, B. F. Hansen, K. A. Green, D. G. Hardie, E. A. Richter, H. Beck-Nielsen and J. F. Wojtaszewski (2003). "Increased phosphorylation of skeletal muscle glycogen synthase at NH2-terminal sites during physiological hyperinsulinemia in type 2 diabetes." Diabetes **52**(6): 1393-1402.

Hudson, E. R., D. A. Pan, J. James, J. M. Lucocq, S. A. Hawley, K. A. Green, O. Baba, T. Terashima and D. G. Hardie (2003). "A novel domain in AMP-activated protein kinase causes glycogen storage bodies similar to those seen in hereditary cardiac arrhythmias." Curr Biol **13**(10): 861-866.

Hughey, C. C., F. D. James, D. P. Bracy, E. P. Donahue, J. D. Young, B. Viollet, M. Foretz and D. H. Wasserman (2017). "Loss of hepatic AMP-activated protein kinase impedes the rate of glycogenolysis but not gluconeogenic fluxes in exercising mice." J Biol Chem.

Hunter, R. W., J. T. Treebak, J. F. Wojtaszewski and K. Sakamoto (2011). "Molecular mechanism by which AMP-activated protein kinase activation promotes glycogen accumulation in muscle." Diabetes **60**(3): 766-774.

Irimia, J. M., C. M. Meyer, C. L. Peper, L. Zhai, C. B. Bock, S. F. Previs, O. P. McGuinness, A. DePaoli-Roach and P. J. Roach (2010). "Impaired glucose tolerance and predisposition to the fasted state in liver glycogen synthase knock-out mice." J Biol Chem **285**(17): 12851-12861.

Irimia, J. M., C. M. Meyer, D. M. Segvich, S. Surendran, A. A. DePaoli-Roach, N. Morral and P. J. Roach (2017). "Lack of liver glycogen causes hepatic insulin resistance and steatosis in mice." J Biol Chem **292**(25): 10455-10464.

Irimia, J. M., J. Rovira, J. N. Nielsen, M. Guerrero, J. F. Wojtaszewski and R. Cusso (2012). "Hexokinase 2, glycogen synthase and phosphorylase play a key role in muscle glycogen supercompensation." PLoS One **7**(7): e42453.

Irimia, J. M., V. S. Tagliabracci, C. M. Meyer, D. M. Segvich, A. A. DePaoli-Roach and P. J. Roach (2015). "Muscle glycogen remodeling and glycogen phosphate metabolism following exhaustive exercise of wild type and laforin knockout mice." J Biol Chem **290**(37): 22686-22698.

Iseli, T. J., M. Walter, B. J. van Denderen, F. Katsis, L. A. Witters, B. E. Kemp, B. J. Michell and D. Stapleton (2005). "AMP-activated protein kinase beta subunit tethers alpha and gamma subunits via its C-terminal sequence (186-270)." J Biol Chem **280**(14): 13395-13400.

Ishihara, K. and H. Taniguchi (2018). "Fat max as an index of aerobic exercise performance in mice during uphill running." PLoS One **13**(2): e0193470.

Ix, J. H. and K. Sharma (2010). "Mechanisms linking obesity, chronic kidney disease, and fatty liver disease: the roles of fetuin-A, adiponectin, and AMPK." J Am Soc Nephrol **21**(3): 406-412.

Janzen, N. R., J. Whitfield and N. J. Hoffman (2018). "Interactive Roles for AMPK and Glycogen from Cellular Energy Sensing to Exercise Metabolism." Int J Mol Sci **19**(11).

Janzen, N. R., J. Whitfield, L. Murray-Segal, B. E. Kemp, J. A. Hawley and N. J. Hoffman (2021). "Mice with Whole-Body Disruption of AMPK-Glycogen Binding Have Increased Adiposity, Reduced Fat Oxidation and Altered Tissue Glycogen Dynamics." Int J Mol Sci **22**(17).

Jensen, J., P. Tantiwong, J. T. Stuenaes, M. Molina-Carrion, R. A. DeFronzo, K. Sakamoto and N. Musi (2012). "Effect of acute exercise on glycogen synthase in muscle from obese and diabetic subjects." Am J Physiol Endocrinol Metab **303**(1): E82-89.

Jensen, R., N. Ortenblad, M. H. Stausholm, M. C. Skjaerbaek, D. N. Larsen, M. Hansen, H. C. Holmberg, P. Plomgaard and J. Nielsen (2020). "Heterogeneity in subcellular muscle glycogen utilisation during exercise impacts endurance capacity in men." J Physiol **598**(19): 4271-4292.

Jensen, R., N. Ortenblad, M. H. Stausholm, M. C. Skjaerbaek, D. N. Larsen, M. Hansen, H. C. Holmberg, P. Plomgaard and J. Nielsen (2021). "Glycogen supercompensation is due to increased number, not size, of glycogen particles in human skeletal muscle." Exp Physiol **106**(5): 1272-1284.

Jensen, T. E., A. J. Rose, S. B. Jorgensen, N. Brandt, P. Schjerling, J. F. Wojtaszewski and E. A. Richter (2007). "Possible CaMKK-dependent regulation of AMPK phosphorylation and glucose uptake at the onset of mild tetanic skeletal muscle contraction." Am J Physiol Endocrinol Metab **292**(5): E1308-1317.

Jinek, M., K. Chylinski, I. Fonfara, M. Hauer, J. A. Doudna and E. Charpentier (2012). "A programmable dual-RNA-guided DNA endonuclease in adaptive bacterial immunity." Science **337**(6096): 816-821.

Johnson, L. N. and D. Barford (1990). "Glycogen phosphorylase. The structural basis of the allosteric response and comparison with other allosteric proteins." J Biol Chem **265**(5): 2409-2412.

Jorgensen, S. B., J. N. Nielsen, J. B. Birk, G. S. Olsen, B. Viollet, F. Andreelli, P. Schjerling, S. Vaulont, D. G. Hardie, B. F. Hansen, E. A. Richter and J. F. Wojtaszewski (2004). "The alpha2-5'AMP-activated protein kinase is a site 2 glycogen synthase kinase in skeletal muscle and is responsive to glucose loading." Diabetes **53**(12): 3074-3081.

Jorgensen, S. B., J. T. Treebak, B. Viollet, P. Schjerling, S. Vaulont, J. F. Wojtaszewski and E. A. Richter (2007). "Role of AMPKalpha2 in basal, training-, and AICAR-induced GLUT4, hexokinase II, and mitochondrial protein expression in mouse muscle." Am J Physiol Endocrinol Metab **292**(1): E331-339.

Jorgensen, S. B., J. F. Wojtaszewski, B. Viollet, F. Andreelli, J. B. Birk, Y. Hellsten, P. Schjerling, S. Vaulont, P. D. Neufer, E. A. Richter and H. Pilegaard (2005). "Effects of alpha-AMPK knockout on exercise-induced gene activation in mouse skeletal muscle." FASEB J **19**(9): 1146-1148.

Joseph, B. K., H. Y. Liu, J. Francisco, D. Pandya, M. Donigan, C. Gallo-Ebert, C. Giordano, A. Bata and J. T. Nickels, Jr. (2015). "Inhibition of AMP Kinase by the Protein Phosphatase 2A Heterotrimer, PP2APpp2r2d." J Biol Chem **290**(17): 10588-10598.

Kahn, S. E., R. L. Hull and K. M. Utzschneider (2006). "Mechanisms linking obesity to insulin resistance and type 2 diabetes." Nature **444**(7121): 840-846.

Kaur, J. and J. Debnath (2015). "Autophagy at the crossroads of catabolism and anabolism." Nat Rev Mol Cell Biol **16**(8): 461-472.

Kiens, B. and E. A. Richter (1998). "Utilization of skeletal muscle triacylglycerol during postexercise recovery in humans." Am J Physiol **275**(2): E332-337.

Kim, H., M. Kim, S. K. Im and S. Fang (2018). "Mouse Cre-LoxP system: general principles to determine tissue-specific roles of target genes." Lab Anim Res **34**(4): 147-159.

Kim, S. J., T. Tang, M. Abbott, J. A. Viscarra, Y. Wang and H. S. Sul (2016). "AMPK Phosphorylates Desnutrin/ATGL and Hormone-Sensitive Lipase To Regulate Lipolysis and Fatty Acid Oxidation within Adipose Tissue." Mol Cell Biol **36**(14): 1961-1976.

Kimber, N. E., G. J. Heigenhauser, L. L. Spriet and D. J. Dyck (2003). "Skeletal muscle fat and carbohydrate metabolism during recovery from glycogen-depleting exercise in humans." J Physiol **548**(Pt 3): 919-927.

King, D. S., G. P. Dalsky, W. E. Clutter, D. A. Young, M. A. Staten, P. E. Cryer and J. O. Holloszy (1988). "Effects of exercise and lack of exercise on insulin sensitivity and responsiveness." J Appl Physiol (1985) **64**(5): 1942-1946.

Kjobsted, R., J. R. Hingst, J. Fentz, M. Foretz, M. N. Sanz, C. Pehmoller, M. Shum, A. Marette, R. Mounier, J. T. Treebak, J. F. P. Wojtaszewski, B. Viollet and L. Lantier (2018). "AMPK in skeletal muscle function and metabolism." FASEB J: fj201700442R.

Kjobsted, R., N. Munk-Hansen, J. B. Birk, M. Foretz, B. Viollet, M. Bjornholm, J. R. Zierath, J. T. Treebak and J. F. Wojtaszewski (2017). "Enhanced Muscle Insulin Sensitivity After Contraction/Exercise Is Mediated by AMPK." Diabetes **66**(3): 598-612.

Kjobsted, R., J. L. W. Roll, N. O. Jorgensen, J. B. Birk, M. Foretz, B. Viollet, A. Chadt, H. Al-Hasani and J. F. P. Wojtaszewski (2019). "AMPK and TBC1D1 Regulate Muscle Glucose Uptake After, but Not During, Exercise and Contraction." Diabetes **68**(7): 1427-1440.

Klein, S., E. F. Coyle and R. R. Wolfe (1994). "Fat metabolism during low-intensity exercise in endurance-trained and untrained men." Am J Physiol **267**(6 Pt 1): E934-940.

Koay, A., B. Woodcroft, E. J. Petrie, H. Yue, S. Emanuelle, M. Bieri, M. F. Bailey, M. Hargreaves, J. T. Park, K. H. Park, S. Ralph, D. Neumann, D. Stapleton and P. R. Gooley (2010). "AMPK beta subunits display isoform specific affinities for carbohydrates." FEBS Lett **584**(15): 3499-3503.

Koistinen, H. A., D. Galuska, A. V. Chibalin, J. Yang, J. R. Zierath, G. D. Holman and H. Wallberg-Henriksson (2003). "5-amino-imidazole carboxamide riboside increases glucose transport and cell-surface GLUT4 content in skeletal muscle from subjects with type 2 diabetes." Diabetes **52**(5): 1066-1072.

Kola, B., A. B. Grossman and M. Korbonits (2008). "The role of AMP-activated protein kinase in obesity." Front Horm Res **36**: 198-211.

Kollberg, G., M. Tulinius, T. Gilljam, I. Ostman-Smith, G. Forsander, P. Jotorp, A. Oldfors and E. Holme (2007). "Cardiomyopathy and exercise intolerance in muscle glycogen storage disease 0." N Engl J Med **357**(15): 1507-1514.

Konagaya, Y., K. Terai, Y. Hirao, K. Takakura, M. Imajo, Y. Kamioka, N. Sasaoka, A. Kakizuka, K. Sumiyama, T. Asano and M. Matsuda (2017). "A Highly Sensitive FRET Biosensor for AMPK Exhibits Heterogeneous AMPK Responses among Cells and Organs." Cell Rep **21**(9): 2628-2638.

Krag, T. O., T. Pinos, T. L. Nielsen, J. Duran, M. Garcia-Rocha, A. L. Andreu and J. Vissing (2016). "Differential glucose metabolism in mice and humans affected by McArdle disease." Am J Physiol Regul Integr Comp Physiol **311**(2): R307-314.

Kramer, H. F., C. A. Witczak, N. Fujii, N. Jessen, E. B. Taylor, D. E. Arnolds, K. Sakamoto, M. F. Hirshman and L. J. Goodyear (2006). "Distinct signals regulate AS160 phosphorylation in response to insulin, AICAR, and contraction in mouse skeletal muscle." Diabetes **55**(7): 2067-2076.

Kristensen, D. E., P. H. Albers, C. Prats, O. Baba, J. B. Birk and J. F. Wojtaszewski (2015). "Human muscle fibre type-specific regulation of AMPK and downstream targets by exercise." J Physiol **593**(8): 2053-2069.

Krustrup, P., N. Ortenblad, J. Nielsen, L. Nybo, T. P. Gunnarsson, F. M. Iaia, K. Madsen, F. Stephens, P. Greenhaff and J. Bangsbo (2011). "Maximal voluntary contraction force, SR function and glycogen resynthesis during the first 72 h after a high-level competitive soccer game." Eur J Appl Physiol **111**(12): 2987-2995.

Lane, S. C., D. M. Camera, D. G. Lassiter, J. L. Areta, S. R. Bird, W. K. Yeo, N. A. Jeacocke, A. Krook, J. R. Zierath, L. M. Burke and J. A. Hawley (2015). "Effects of sleeping with reduced carbohydrate availability on acute training responses." J Appl Physiol (1985) **119**(6): 643-655.

Lantier, L., J. Fentz, R. Mounier, J. Leclerc, J. T. Treebak, C. Pehmoller, N. Sanz, I. Sakakibara, E. Saint-Amand, S. Rimbaud, P. Maire, A. Marette, R. Ventura-Clapier, A. Ferry, J. F. Wojtaszewski, M. Foretz and B. Viollet (2014). "AMPK controls exercise endurance, mitochondrial oxidative capacity, and skeletal muscle integrity." FASEB J **28**(7): 3211-3224.

Larsen, M. R., D. E. Steenberg, J. B. Birk, K. A. Sjoberg, B. Kiens, E. A. Richter and J. F. P. Wojtaszewski (2020). "The insulin-sensitizing effect of a single exercise bout is similar in type I and type II human muscle fibres." J Physiol **598**(24): 5687-5699.

Lavoie, C., F. Ducros, J. Bourque, H. Langelier and J. L. Chiasson (1997). "Glucose metabolism during exercise in man: the role of insulin and glucagon in the regulation of hepatic glucose production and gluconeogenesis." Can J Physiol Pharmacol **75**(1): 26-35.

Lee-Young, R. S., B. J. Canny, D. E. Myers and G. K. McConell (2009). "AMPK activation is fiber type specific in human skeletal muscle: effects of exercise and short-term exercise training." J Appl Physiol (1985) **107**(1): 283-289.

Li, H., Y. Yang, W. Hong, M. Huang, M. Wu and X. Zhao (2020). "Applications of genome editing technology in the targeted therapy of human diseases: mechanisms, advances and prospects." Signal Transduct Target Ther **5**(1): 1.

Li, X., B. Monks, Q. Ge and M. J. Birnbaum (2007). "Akt/PKB regulates hepatic metabolism by directly inhibiting PGC-1alpha transcription coactivator." Nature **447**(7147): 1012-1016.

Li, X., L. Wang, X. E. Zhou, J. Ke, P. W. de Waal, X. Gu, M. H. Tan, D. Wang, D. Wu, H. E. Xu and K. Melcher (2015). "Structural basis of AMPK regulation by adenine nucleotides and glycogen." Cell Res **25**(1): 50-66.

Li, Y., S. Xu, M. M. Mihaylova, B. Zheng, X. Hou, B. Jiang, O. Park, Z. Luo, E. Lefai, J. Y. Shyy, B. Gao, M. Wierzbicki, T. J. Verbeuren, R. J. Shaw, R. A. Cohen and M. Zang (2011). "AMPK phosphorylates and inhibits SREBP activity to attenuate hepatic steatosis and atherosclerosis in diet-induced insulin-resistant mice." Cell Metab **13**(4): 376-388.

Lima, S. S., M. C. Lima dos Santos, M. P. Sinder, A. S. Moura, P. C. Barradas and F. Tenorio (2010). "Glycogen stores are impaired in hypothalamic nuclei of rats malnourished during early life." Nutr Neurosci **13**(1): 21-28.

Livak, K. J. and T. D. Schmittgen (2001). "Analysis of relative gene expression data using real-time quantitative PCR and the 2(-Delta Delta C(T)) Method." Methods **25**(4): 402-408.

Ljubicic, V., P. Miura, M. Burt, L. Boudreault, S. Khogali, J. A. Lunde, J. M. Renaud and B. J. Jasmin (2011). "Chronic AMPK activation evokes the slow, oxidative myogenic program and triggers beneficial adaptations in mdx mouse skeletal muscle." Hum Mol Genet **20**(17): 3478-3493.

Lopez-Soldado, I., A. Bertini, A. Adrover, J. Duran and J. J. Guinovart (2020). "Maintenance of liver glycogen during long-term fasting preserves energy state in mice." FEBS Lett **594**(11): 1698-1710.

Lopez-Soldado, I., J. J. Guinovart and J. Duran (2021). "Increased liver glycogen levels enhance exercise capacity in mice." J Biol Chem: 100976.

Lopez-Soldado, I., D. Zafra, J. Duran, A. Adrover, J. Calbo and J. J. Guinovart (2015). "Liver glycogen reduces food intake and attenuates obesity in a high-fat diet-fed mouse model." Diabetes **64**(3): 796-807.

Lu, M., M. Wan, K. F. Leavens, Q. Chu, B. R. Monks, S. Fernandez, R. S. Ahima, K. Ueki, C. R. Kahn and M. J. Birnbaum (2012). "Insulin regulates liver metabolism in vivo in the absence of hepatic Akt and Foxo1." Nat Med **18**(3): 388-395.

Magnusson, I., D. L. Rothman, L. D. Katz, R. G. Shulman and G. I. Shulman (1992). "Increased rate of gluconeogenesis in type II diabetes mellitus. A 13C nuclear magnetic resonance study." J Clin Invest **90**(4): 1323-1327.

Malfatti, E., J. Nilsson, C. Hedberg-Oldfors, A. Hernandez-Lain, F. Michel, C. Dominguez-Gonzalez, G. Viennet, H. O. Akman, C. Kornblum, P. Van den Bergh, N. B. Romero, A. G. Engel, S. DiMauro and A. Oldfors (2014). "A new muscle glycogen storage disease associated with glycogenin-1 deficiency." Ann Neurol **76**(6): 891-898.

Martin, M. A., J. C. Rubio, R. A. Wevers, B. G. Van Engelen, G. C. Steenbergen, O. P. Van Diggelen, M. De Visser, C. De Die-Smulders, A. Blazquez, A. L. Andreu and J. Arenas

(2004). "Molecular analysis of myophosphorylase deficiency in Dutch patients with McArdle's disease." Ann Hum Genet **68**(Pt 1): 17-22.

McBride, A., S. Ghilagaber, A. Nikolaev and D. G. Hardie (2009). "The glycogen-binding domain on the AMPK beta subunit allows the kinase to act as a glycogen sensor." Cell Metab **9**(1): 23-34.

McBride, A. and D. G. Hardie (2009). "AMP-activated protein kinase--a sensor of glycogen as well as AMP and ATP?" Acta Physiol (Oxf) **196**(1): 99-113.

McConell, G. K., R. S. Lee-Young, Z. P. Chen, N. K. Stepto, N. N. Huynh, T. J. Stephens, B. J. Canny and B. E. Kemp (2005). "Short-term exercise training in humans reduces AMPK signalling during prolonged exercise independent of muscle glycogen." J Physiol **568**(Pt 2): 665-676.

McConell, G. K., G. D. Wadley, K. Le Plastrier and K. C. Linden (2020). "Skeletal muscle AMPK is not activated during 2 h of moderate intensity exercise at approximately 65% V O 2 peak in endurance trained men." J Physiol **598**(18): 3859-3870.

McGee, S. L., C. Swinton, S. Morrison, V. Gaur, D. E. Campbell, S. B. Jorgensen, B. E. Kemp, K. Baar, G. R. Steinberg and M. Hargreaves (2014). "Compensatory regulation of HDAC5 in muscle maintains metabolic adaptive responses and metabolism in response to energetic stress." FASEB J **28**(8): 3384-3395.

Merkle, T., S. Merz, P. Reautschnig, A. Blaha, Q. Li, P. Vogel, J. Wettengel, J. B. Li and T. Stafforst (2019). "Precise RNA editing by recruiting endogenous ADARs with antisense oligonucleotides." Nat Biotechnol **37**(2): 133-138.

Merrill, G. F., E. J. Kurth, D. G. Hardie and W. W. Winder (1997). "AICA riboside increases AMP-activated protein kinase, fatty acid oxidation, and glucose uptake in rat muscle." Am J Physiol **273**(6): E1107-1112.

Milan, D., J. T. Jeon, C. Looft, V. Amarger, A. Robic, M. Thelander, C. Rogel-Gaillard, S. Paul, N. Iannuccelli, L. Rask, H. Ronne, K. Lundstrom, N. Reinsch, J. Gellin, E. Kalm, P. L. Roy, P. Chardon and L. Andersson (2000). "A mutation in PRKAG3 associated with excess glycogen content in pig skeletal muscle." Science **288**(5469): 1248-1251.

Minokoshi, Y., T. Alquier, N. Furukawa, Y. B. Kim, A. Lee, B. Xue, J. Mu, F. Foufelle, P. Ferre, M. J. Birnbaum, B. J. Stuck and B. B. Kahn (2004). "AMP-kinase regulates food intake by responding to hormonal and nutrient signals in the hypothalamus." Nature **428**(6982): 569-574.

Miwa, I. and S. Suzuki (2002). "An improved quantitative assay of glycogen in erythrocytes." Ann Clin Biochem **39**(Pt 6): 612-613.

Mobbs, J. I., A. Di Paolo, R. D. Metcalfe, E. Selig, D. I. Stapleton, M. D. W. Griffin and P. R. Gooley (2017). "Unravelling the Carbohydrate-Binding Preferences of the Carbohydrate-Binding Modules of AMP-Activated Protein Kinase." Chembiochem.

Mobbs, J. I., A. Koay, A. Di Paolo, M. Bieri, E. J. Petrie, M. A. Gorman, L. Doughty, M. W. Parker, D. I. Stapleton, M. D. Griffin and P. R. Gooley (2015). "Determinants of oligosaccharide specificity of the carbohydrate-binding modules of AMP-activated protein kinase." Biochem J **468**(2): 245-257.

Mora, A., D. Komander, D. M. van Aalten and D. R. Alessi (2004). "PDK1, the master regulator of AGC kinase signal transduction." Semin Cell Dev Biol **15**(2): 161-170.

Mora, A., K. Sakamoto, E. J. McManus and D. R. Alessi (2005). "Role of the PDK1-PKB-GSK3 pathway in regulating glycogen synthase and glucose uptake in the heart." FEBS Lett **579**(17): 3632-3638.

Mortensen, B., J. R. Hingst, N. Frederiksen, R. W. Hansen, C. S. Christiansen, N. Iversen, M. Friedrichsen, J. B. Birk, H. Pilegaard, Y. Hellsten, A. Vaag and J. F. Wojtaszewski (2013). "Effect of birth weight and 12 weeks of exercise training on exercise-induced AMPK signaling in human skeletal muscle." Am J Physiol Endocrinol Metab **304**(12): E1379-1390.

Mortensen, B., P. Poulsen, L. Wegner, K. L. Stender-Petersen, R. Ribel-Madsen, M. Friedrichsen, J. B. Birk, A. Vaag and J. F. Wojtaszewski (2009). "Genetic and metabolic effects on skeletal muscle AMPK in young and older twins." Am J Physiol Endocrinol Metab **297**(4): E956-964.

Mottillo, E. P., E. M. Desjardins, J. D. Crane, B. K. Smith, A. E. Green, S. Ducommun, T. I. Henriksen, I. A. Rebalka, A. Razi, K. Sakamoto, C. Scheele, B. E. Kemp, T. J. Hawke, J. Ortega, J. G. Granneman and G. R. Steinberg (2016). "Lack of Adipocyte AMPK Exacerbates Insulin Resistance and Hepatic Steatosis through Brown and Beige Adipose Tissue Function." Cell Metab **24**(1): 118-129.

Musi, N., N. Fujii, M. F. Hirshman, I. Ekberg, S. Froberg, O. Ljungqvist, A. Thorell and L. J. Goodyear (2001). "AMP-activated protein kinase (AMPK) is activated in muscle of subjects with type 2 diabetes during exercise." Diabetes **50**(5): 921-927.

Myers, R. W., H. P. Guan, J. Ehrhart, A. Petrov, S. Prahalada, E. Tozzo, X. Yang, M. M. Kurtz, M. Trujillo, D. Gonzalez Trotter, D. Feng, S. Xu, G. Eiermann, M. A. Holahan, D. Rubins, S. Conarello, X. Niu, S. C. Souza, C. Miller, J. Liu, K. Lu, W. Feng, Y. Li, R. E. Painter, J. A. Milligan, H. He, F. Liu, A. Ogawa, D. Wisniewski, R. J. Rohm, L. Wang, M. Bunzel, Y. Qian, W. Zhu, H. Wang, B. Bennet, L. LaFranco Scheuch, G. E. Fernandez, C. Li, M. Klimas, G. Zhou, M. van Heek, T. Biftu, A. Weber, D. E. Kelley, N. Thornberry, M. D. Erion, D. M. Kemp and I. K. Sebhat (2017). "Systemic pan-AMPK activator MK-8722 improves glucose homeostasis but induces cardiac hypertrophy." Science **357**(6350): 507-511.

Nakatani, A., D. H. Han, P. A. Hansen, L. A. Nolte, H. H. Host, R. C. Hickner and J. O. Holloszy (1997). "Effect of endurance exercise training on muscle glycogen supercompensation in rats." J Appl Physiol (1985) **82**(2): 711-715.

Nielsen, J., A. J. Cheng, N. Ortenblad and H. Westerblad (2014). "Subcellular distribution of glycogen and decreased tetanic Ca2+ in fatigued single intact mouse muscle fibres." J Physiol **592**(9): 2003-2012.

Nielsen, J., H. C. Holmberg, H. D. Schroder, B. Saltin and N. Ortenblad (2011). "Human skeletal muscle glycogen utilization in exhaustive exercise: role of subcellular localization and fibre type." J Physiol **589**(Pt 11): 2871-2885.

Nielsen, J., P. Krustrup, L. Nybo, T. P. Gunnarsson, K. Madsen, H. D. Schroder, J. Bangsbo and N. Ortenblad (2012). "Skeletal muscle glycogen content and particle size of distinct subcellular localizations in the recovery period after a high-level soccer match." Eur J Appl Physiol **112**(10): 3559-3567.

Nielsen, J. and N. Ortenblad (2013). "Physiological aspects of the subcellular localization of glycogen in skeletal muscle." Appl Physiol Nutr Metab **38**(2): 91-99.

Nielsen, J. N., K. J. Mustard, D. A. Graham, H. Yu, C. S. MacDonald, H. Pilegaard, L. J. Goodyear, D. G. Hardie, E. A. Richter and J. F. Wojtaszewski (2003). "5'-AMP-activated protein kinase activity and subunit expression in exercise-trained human skeletal muscle." J Appl Physiol (1985) **94**(2): 631-641.

Nielsen, J. N., J. F. Wojtaszewski, R. G. Haller, D. G. Hardie, B. E. Kemp, E. A. Richter and J. Vissing (2002). "Role of 5'AMP-activated protein kinase in glycogen synthase activity and glucose utilization: insights from patients with McArdle's disease." J Physiol **541**(Pt 3): 979-989.

Nielsen, T. L., T. Pinos, A. Brull, J. Vissing and T. O. Krag (2018). "Exercising with blocked muscle glycogenolysis: Adaptation in the McArdle mouse." Mol Genet Metab **123**(1): 21-27.

Nieman, D. C., K. A. Carlson, M. E. Brandstater, R. T. Naegele and J. W. Blankenship (1987). "Running endurance in 27-h-fasted humans." J Appl Physiol (1985) **63**(6): 2502-2509.

Nikoulina, S. E., T. P. Ciaraldi, S. Mudaliar, P. Mohideen, L. Carter and R. R. Henry (2000). "Potential role of glycogen synthase kinase-3 in skeletal muscle insulin resistance of type 2 diabetes." Diabetes **49**(2): 263-271.

Nogales-Gadea, G., T. Pinos, A. Lucia, J. Arenas, Y. Camara, A. Brull, N. de Luna, M. A. Martin, E. Garcia-Arumi, R. Marti and A. L. Andreu (2012). "Knock-in mice for the R50X mutation in the PYGM gene present with McArdle disease." Brain **135**(Pt 7): 2048-2057.

O'Neill, H. M. (2013). "AMPK and Exercise: Glucose Uptake and Insulin Sensitivity." Diabetes Metab J **37**(1): 1-21.

O'Neill, H. M., G. P. Holloway and G. R. Steinberg (2013). "AMPK regulation of fatty acid metabolism and mitochondrial biogenesis: implications for obesity." Mol Cell Endocrinol **366**(2): 135-151.

O'Neill, H. M., S. J. Maarbjerg, J. D. Crane, J. Jeppesen, S. B. Jorgensen, J. D. Schertzer, O. Shyroka, B. Kiens, B. J. van Denderen, M. A. Tarnopolsky, B. E. Kemp, E. A. Richter and G. R. Steinberg (2011). "AMP-activated protein kinase (AMPK) beta1beta2 muscle null mice reveal an essential role for AMPK in maintaining mitochondrial content and glucose uptake during exercise." Proc Natl Acad Sci U S A **108**(38): 16092-16097.

Oakhill, J. S., Z. P. Chen, J. W. Scott, R. Steel, L. A. Castelli, N. Ling, S. L. Macaulay and B. E. Kemp (2010). "beta-Subunit myristoylation is the gatekeeper for initiating metabolic stress sensing by AMP-activated protein kinase (AMPK)." Proc Natl Acad Sci U S A **107**(45): 19237-19241.

Oe, Y., O. Baba, H. Ashida, K. C. Nakamura and H. Hirase (2016). "Glycogen distribution in the microwave-fixed mouse brain reveals heterogeneous astrocytic patterns." Glia **64**(9): 1532-1545.

Oh, W., L. Abu-Elheiga, P. Kordari, Z. Gu, T. Shaikenov, S. S. Chirala and S. J. Wakil (2005). "Glucose and fat metabolism in adipose tissue of acetyl-CoA carboxylase 2 knockout mice." Proc Natl Acad Sci U S A **102**(5): 1384-1389.

Oligschlaeger, Y., M. Miglianico, D. Chanda, R. Scholz, R. F. Thali, R. Tuerk, D. I. Stapleton, P. R. Gooley and D. Neumann (2015). "The recruitment of AMP-activated protein kinase to glycogen is regulated by autophosphorylation." J Biol Chem **290**(18): 11715-11728.

Olivier, S., M. Foretz and B. Viollet (2018). "Promise and challenges for direct small molecule AMPK activators." Biochem Pharmacol.

Ortenblad, N., J. Nielsen, B. Saltin and H. C. Holmberg (2011). "Role of glycogen availability in sarcoplasmic reticulum Ca2+ kinetics in human skeletal muscle." J Physiol **589**(Pt 3): 711-725.

Ortenblad, N., H. Westerblad and J. Nielsen (2013). "Muscle glycogen stores and fatigue." J Physiol **591**(18): 4405-4413.

Pan, H., J. Guo and Z. Su (2014). "Advances in understanding the interrelations between leptin resistance and obesity." Physiol Behav **130**: 157-169.

Pederson, B. A., H. Chen, J. M. Schroeder, W. Shou, A. A. DePaoli-Roach and P. J. Roach (2004). "Abnormal cardiac development in the absence of heart glycogen." Mol Cell Biol **24**(16): 7179-7187.

Pederson, B. A., C. R. Cope, J. M. Irimia, J. M. Schroeder, B. L. Thurberg, A. A. Depaoli-Roach and P. J. Roach (2005). "Mice with elevated muscle glycogen stores do not have improved exercise performance." Biochem Biophys Res Commun **331**(2): 491-496.

Pederson, B. A., C. R. Cope, J. M. Schroeder, M. W. Smith, J. M. Irimia, B. L. Thurberg, A. A. DePaoli-Roach and P. J. Roach (2005). "Exercise capacity of mice genetically lacking muscle glycogen synthase: in mice, muscle glycogen is not essential for exercise." J Biol Chem **280**(17): 17260-17265.

Pederson, B. A., J. M. Schroeder, G. E. Parker, M. W. Smith, A. A. DePaoli-Roach and P. J. Roach (2005). "Glucose metabolism in mice lacking muscle glycogen synthase." Diabetes **54**(12): 3466-3473.

Pehmoller, C., J. T. Treebak, J. B. Birk, S. Chen, C. Mackintosh, D. G. Hardie, E. A. Richter and J. F. Wojtaszewski (2009). "Genetic disruption of AMPK signaling abolishes both contraction- and insulin-stimulated TBC1D1 phosphorylation and 14-3-3 binding in mouse skeletal muscle." Am J Physiol Endocrinol Metab **297**(3): E665-675.

Peronnet, F. and D. Massicotte (1991). "Table of nonprotein respiratory quotient: an update." Can J Sport Sci **16**(1): 23-29.

Perseghin, G., T. B. Price, K. F. Petersen, M. Roden, G. W. Cline, K. Gerow, D. L. Rothman and G. I. Shulman (1996). "Increased glucose transport-phosphorylation and muscle glycogen synthesis after exercise training in insulin-resistant subjects." N Engl J Med **335**(18): 1357-1362.

Petersen, K. F., T. Price, G. W. Cline, D. L. Rothman and G. I. Shulman (1996). "Contribution of net hepatic glycogenolysis to glucose production during the early postprandial period." Am J Physiol **270**(1 Pt 1): E186-191.

Petersen, M. C., D. F. Vatner and G. I. Shulman (2017). "Regulation of hepatic glucose metabolism in health and disease." Nat Rev Endocrinol **13**(10): 572-587.

Petrosino, J. M., V. J. Heiss, S. K. Maurya, A. Kalyanasundaram, M. Periasamy, R. A. LaFountain, J. M. Wilson, O. P. Simonetti and O. Ziouzenkova (2016). "Graded Maximal Exercise Testing to Assess Mouse Cardio-Metabolic Phenotypes." PLoS One **11**(2): e0148010.

Philp, A., M. Hargreaves and K. Baar (2012). "More than a store: regulatory roles for glycogen in skeletal muscle adaptation to exercise." Am J Physiol Endocrinol Metab **302**(11): E1343-1351.

Philp, A., M. G. MacKenzie, M. Y. Belew, M. C. Towler, A. Corstorphine, A. Papalamprou, D. G. Hardie and K. Baar (2013). "Glycogen content regulates peroxisome proliferator activated receptor- partial differential (PPAR- partial differential) activity in rat skeletal muscle." PLoS One **8**(10): e77200.

Polekhina, G., A. Gupta, B. J. Michell, B. van Denderen, S. Murthy, S. C. Feil, I. G. Jennings, D. J. Campbell, L. A. Witters, M. W. Parker, B. E. Kemp and D. Stapleton (2003). "AMPK beta subunit targets metabolic stress sensing to glycogen." Curr Biol **13**(10): 867-871.

Polekhina, G., A. Gupta, B. J. van Denderen, S. C. Feil, B. E. Kemp, D. Stapleton and M. W. Parker (2005). "Structural basis for glycogen recognition by AMP-activated protein kinase." Structure **13**(10): 1453-1462.

Pollard, A. E., L. Martins, P. J. Muckett, S. Khadayate, A. Bornot, M. Clausen, T. Admyre, M. Bjursell, R. Fiadeiro, L. Wilson, C. Whilding, V. N. Kotiadis, M. R. Duchen, D. Sutton, L. Penfold, A. Sardini, Y. M. Bohlooly, D. M. Smith, J. A. Read, M. A. Snowden, A. Woods and D. Carling (2019). "AMPK activation protects against diet induced obesity through Ucp1-independent thermogenesis in subcutaneous white adipose tissue." Nat Metab **1**(3): 340-349.

Prats, C., A. Gomez-Cabello and A. V. Hansen (2011). "Intracellular compartmentalization of skeletal muscle glycogen metabolism and insulin signalling." Exp Physiol **96**(4): 385-390.

Prats, C., T. E. Graham and J. Shearer (2018). "The dynamic life of the glycogen granule." J Biol Chem **293**(19): 7089-7098.

Prats, C., J. W. Helge, P. Nordby, K. Qvortrup, T. Ploug, F. Dela and J. F. Wojtaszewski (2009). "Dual regulation of muscle glycogen synthase during exercise by activation and compartmentalization." J Biol Chem **284**(23): 15692-15700.

Printen, J. A., M. J. Brady and A. R. Saltiel (1997). "PTG, a protein phosphatase 1-binding protein with a role in glycogen metabolism." Science **275**(5305): 1475-1478.

Psilander, N., P. Frank, M. Flockhart and K. Sahlin (2013). "Exercise with low glycogen increases PGC-1alpha gene expression in human skeletal muscle." Eur J Appl Physiol **113**(4): 951-963.

Rahman, S. M., A. Dobrzyn, S. H. Lee, P. Dobrzyn, M. Miyazaki and J. M. Ntambi (2005). "Stearoyl-CoA desaturase 1 deficiency increases insulin signaling and glycogen accumulation in brown adipose tissue." Am J Physiol Endocrinol Metab **288**(2): E381-387.

Ramnanan, C. J., D. S. Edgerton, N. Rivera, J. Irimia-Dominguez, B. Farmer, D. W. Neal, M. Lautz, E. P. Donahue, C. M. Meyer, P. J. Roach and A. D. Cherrington (2010). "Molecular characterization of insulin-mediated suppression of hepatic glucose production in vivo." Diabetes **59**(6): 1302-1311.

Reitman, J., K. M. Baldwin and J. O. Holloszy (1973). "Intramuscular triglyceride utilization by red, white, and intermediate skeletal muscle and heart during exhausting exercise." Proc Soc Exp Biol Med **142**(2): 628-631.

Richter, E. A., L. P. Garetto, M. N. Goodman and N. B. Ruderman (1982). "Muscle glucose metabolism following exercise in the rat: increased sensitivity to insulin." J Clin Invest **69**(4): 785-793.

Richter, E. A. and M. Hargreaves (2013). "Exercise, GLUT4, and skeletal muscle glucose uptake." Physiol Rev **93**(3): 993-1017.

Richter, E. A., K. J. Mikines, H. Galbo and B. Kiens (1989). "Effect of exercise on insulin action in human skeletal muscle." J Appl Physiol (1985) **66**(2): 876-885.

Richter, E. A., N. B. Ruderman, H. Gavras, E. R. Belur and H. Galbo (1982). "Muscle glycogenolysis during exercise: dual control by epinephrine and contractions." Am J Physiol **242**(1): E25-32.

Roach, P. J., A. A. Depaoli-Roach, T. D. Hurley and V. S. Tagliabracci (2012). "Glycogen and its metabolism: some new developments and old themes." Biochem J **441**(3): 763-787.

Rockl, K. S., M. F. Hirshman, J. Brandauer, N. Fujii, L. A. Witters and L. J. Goodyear (2007). "Skeletal muscle adaptation to exercise training: AMP-activated protein kinase mediates muscle fiber type shift." Diabetes **56**(8): 2062-2069.

Romijn, J. A., E. F. Coyle, L. S. Sidossis, A. Gastaldelli, J. F. Horowitz, E. Endert and R. R. Wolfe (1993). "Regulation of endogenous fat and carbohydrate metabolism in relation to exercise intensity and duration." Am J Physiol **265**(3 Pt 1): E380-391.

Ross, F. A., C. MacKintosh and D. G. Hardie (2016). "AMP-activated protein kinase: a cellular energy sensor that comes in 12 flavours." FEBS J **283**(16): 2987-3001.

Rothman, D. L., I. Magnusson, L. D. Katz, R. G. Shulman and G. I. Shulman (1991). "Quantitation of hepatic glycogenolysis and gluconeogenesis in fasting humans with 13C NMR." Science **254**(5031): 573-576.

Rubio, J. C., A. Lucia, I. Fernandez-Cadenas, A. Cabello, A. Blazquez, J. Gamez, A. L. Andreu, M. A. Martin and J. Arenas (2006). "Novel mutation in the PYGM gene resulting in McArdle disease." Arch Neurol **63**(12): 1782-1784.

Ruchti, E., P. J. Roach, A. A. DePaoli-Roach, P. J. Magistretti and I. Allaman (2016). "Protein targeting to glycogen is a master regulator of glycogen synthesis in astrocytes." IBRO Rep **1**: 46-53.

Saad, M. F., W. C. Knowler, D. J. Pettitt, R. G. Nelson, D. M. Mott and P. H. Bennett (1989). "Sequential changes in serum insulin concentration during development of non-insulin-dependent diabetes." Lancet **1**(8651): 1356-1359.

Sakamoto, K. and G. D. Holman (2008). "Emerging role for AS160/TBC1D4 and TBC1D1 in the regulation of GLUT4 traffic." Am J Physiol Endocrinol Metab **295**(1): E29-37.

Sakoda, H., M. Fujishiro, J. Fujio, N. Shojima, T. Ogihara, A. Kushiyama, Y. Fukushima, M. Anai, H. Ono, M. Kikuchi, N. Horike, A. Y. Viana, Y. Uchijima, H. Kurihara and T. Asano (2005). "Glycogen debranching enzyme association with beta-subunit regulates AMP-activated protein kinase activity." Am J Physiol Endocrinol Metab **289**(3): E474-481.

Samuel, V. T. and G. I. Shulman (2012). "Mechanisms for insulin resistance: common threads and missing links." Cell **148**(5): 852-871.

Schaffer, B. E., R. S. Levin, N. T. Hertz, T. J. Maures, M. L. Schoof, P. E. Hollstein, B. A. Benayoun, M. R. Banko, R. J. Shaw, K. M. Shokat and A. Brunet (2015). "Identification of AMPK Phosphorylation Sites Reveals a Network of Proteins Involved in Cell Invasion and Facilitates Large-Scale Substrate Prediction." Cell Metab **22**(5): 907-921.

Schonke, M., M. G. Myers, Jr., J. R. Zierath and M. Bjornholm (2015). "Skeletal muscle AMP-activated protein kinase gamma1(H151R) overexpression enhances whole body energy homeostasis and insulin sensitivity." Am J Physiol Endocrinol Metab **309**(7): E679-690.

Schrauwen, P., D. P. van Aggel-Leijssen, G. Hul, A. J. Wagenmakers, H. Vidal, W. H. Saris and M. A. van Baak (2002). "The effect of a 3-month low-intensity endurance training program on fat oxidation and acetyl-CoA carboxylase-2 expression." Diabetes **51**(7): 2220-2226.

Scott, J. W., S. Galic, K. L. Graham, R. Foitzik, N. X. Ling, T. A. Dite, S. M. Issa, C. G. Langendorf, Q. P. Weng, H. E. Thomas, T. W. Kay, N. C. Birnberg, G. R. Steinberg, B. E. Kemp and J. S. Oakhill (2015). "Inhibition of AMP-Activated Protein Kinase at the Allosteric Drug-Binding Site Promotes Islet Insulin Release." Chem Biol **22**(6): 705-711.

Scott, J. W., N. Ling, S. M. Issa, T. A. Dite, M. T. O'Brien, Z. P. Chen, S. Galic, C. G. Langendorf, G. R. Steinberg, B. E. Kemp and J. S. Oakhill (2014). "Small molecule drug A-769662 and AMP synergistically activate naive AMPK independent of upstream kinase signaling." Chem Biol **21**(5): 619-627.

Scott, J. W., B. J. van Denderen, S. B. Jorgensen, J. E. Honeyman, G. R. Steinberg, J. S. Oakhill, T. J. Iseli, A. Koay, P. R. Gooley, D. Stapleton and B. E. Kemp (2008). "Thienopyridone drugs are selective activators of AMP-activated protein kinase beta1-containing complexes." Chem Biol **15**(11): 1220-1230.

Shamshoum, H., K. D. Medak, L. K. Townsend, K. E. Ashworth, N. D. Bush, M. K. Hahn, B. E. Kemp and D. C. Wright (2019). "AMPK beta1 activation suppresses antipsychotic-induced hyperglycemia in mice." FASEB J **33**(12): 14010-14021.

Shearer, J. and T. E. Graham (2004). "Novel aspects of skeletal muscle glycogen and its regulation during rest and exercise." Exerc Sport Sci Rev **32**(3): 120-126.

Shearer, J., R. J. Wilson, D. S. Battram, E. A. Richter, D. L. Robinson, M. Bakovic and T. E. Graham (2005). "Increases in glycogenin and glycogenin mRNA accompany glycogen resynthesis in human skeletal muscle." Am J Physiol Endocrinol Metab **289**(3): E508-514.

Shulman, G. I., D. L. Rothman, T. Jue, P. Stein, R. A. DeFronzo and R. G. Shulman (1990). "Quantitation of muscle glycogen synthesis in normal subjects and subjects with non-insulin-dependent diabetes by 13C nuclear magnetic resonance spectroscopy." N Engl J Med **322**(4): 223-228.

Shulman, R. G. and D. L. Rothman (2001). "The "glycogen shunt" in exercising muscle: A role for glycogen in muscle energetics and fatigue." Proc Natl Acad Sci U S A **98**(2): 457-461.

Singh, D. K., S. Banerjee and T. D. Porter (2009). "Green and black tea extracts inhibit HMG-CoA reductase and activate AMP kinase to decrease cholesterol synthesis in hepatoma cells." J Nutr Biochem **20**(10): 816-822.

Singla, P., A. Bardoloi and A. A. Parkash (2010). "Metabolic effects of obesity: A review." World J Diabetes **1**(3): 76-88.

Skurat, A. V. and P. J. Roach (1995). "Phosphorylation of sites 3a and 3b (Ser640 and Ser644) in the control of rabbit muscle glycogen synthase." J Biol Chem **270**(21): 12491-12497.

Smith, B. K., K. Marcinko, E. M. Desjardins, J. S. Lally, R. J. Ford and G. R. Steinberg (2016). "Treatment of nonalcoholic fatty liver disease: role of AMPK." Am J Physiol Endocrinol Metab **311**(4): E730-E740.

Sriwijitkamol, A., D. K. Coletta, E. Wajcberg, G. B. Balbontin, S. M. Reyna, J. Barrientes, P. A. Eagan, C. P. Jenkinson, E. Cersosimo, R. A. DeFronzo, K. Sakamoto and N. Musi (2007). "Effect of acute exercise on AMPK signaling in skeletal muscle of subjects with type 2 diabetes: a time-course and dose-response study." Diabetes **56**(3): 836-848.

Stapleton, D., C. Nelson, K. Parsawar, M. Flores-Opazo, D. McClain and G. Parker (2013). "The 3T3-L1 adipocyte glycogen proteome." Proteome Sci **11**(1): 11.

Stapleton, D., C. Nelson, K. Parsawar, D. McClain, R. Gilbert-Wilson, E. Barker, B. Rudd, K. Brown, W. Hendrix, P. O'Donnell and G. Parker (2010). "Analysis of hepatic glycogen-associated proteins." Proteomics **10**(12): 2320-2329.

Steinberg, G. R. (2018). "Cellular Energy Sensing and Metabolism-Implications for Treating Diabetes: The 2017 Outstanding Scientific Achievement Award Lecture." Diabetes **67**(2): 169-179.

Steinberg, G. R. and B. E. Kemp (2009). "AMPK in Health and Disease." Physiol Rev **89**(3): 1025-1078.

Steinberg, G. R., H. M. O'Neill, N. L. Dzamko, S. Galic, T. Naim, R. Koopman, S. B. Jorgensen, J. Honeyman, K. Hewitt, Z. P. Chen, J. D. Schertzer, J. W. Scott, F. Koentgen, G. S. Lynch, M. J. Watt, B. J. van Denderen, D. J. Campbell and B. E. Kemp (2010). "Whole body deletion of AMP-activated protein kinase {beta}2 reduces muscle AMPK activity and exercise capacity." J Biol Chem **285**(48): 37198-37209.

Steinberg, G. R., M. J. Watt, S. L. McGee, S. Chan, M. Hargreaves, M. A. Febbraio, D. Stapleton and B. E. Kemp (2006). "Reduced glycogen availability is associated with increased AMPKalpha2 activity, nuclear AMPKalpha2 protein abundance, and GLUT4 mRNA expression in contracting human skeletal muscle." Appl Physiol Nutr Metab **31**(3): 302-312.

Stephenne, X., M. Foretz, N. Taleux, G. C. van der Zon, E. Sokal, L. Hue, B. Viollet and B. Guigas (2011). "Metformin activates AMP-activated protein kinase in primary human hepatocytes by decreasing cellular energy status." Diabetologia **54**(12): 3101-3110.

Stevenson, E. J., P. E. Thelwall, K. Thomas, F. Smith, J. Brand-Miller and M. I. Trenell (2009). "Dietary glycemic index influences lipid oxidation but not muscle or liver glycogen oxidation during exercise." Am J Physiol Endocrinol Metab **296**(5): E1140-1147.

Stockli, J., C. C. Meoli, N. J. Hoffman, D. J. Fazakerley, H. Pant, M. E. Cleasby, X. Ma, M. Kleinert, A. E. Brandon, J. A. Lopez, G. J. Cooney and D. E. James (2015). "The RabGAP TBC1D1 plays a central role in exercise-regulated glucose metabolism in skeletal muscle." Diabetes **64**(6): 1914-1922.

Sukigara, S., W. C. Liang, H. Komaki, T. Fukuda, T. Miyamoto, T. Saito, Y. Saito, E. Nakagawa, K. Sugai, Y. K. Hayashi, H. Sugie, M. Sasaki and I. Nishino (2012). "Muscle glycogen storage disease 0 presenting recurrent syncope with weakness and myalgia." Neuromuscul Disord **22**(2): 162-165.

Sylow, L., V. L. Tokarz, E. A. Richter and A. Klip (2021). "The many actions of insulin in skeletal muscle, the paramount tissue determining glycemia." Cell Metab **33**(4): 758-780.

Tachtsis, B., J. Whitfield, J. A. Hawley and N. J. Hoffman (2020). "Omega-3 Polyunsaturated Fatty Acids Mitigate Palmitate-Induced Impairments in Skeletal Muscle Cell Viability and Differentiation." Front Physiol **11**: 563.

Tee, J. C., A. N. Bosch and M. I. Lambert (2007). "Metabolic consequences of exercise-induced muscle damage." Sports Med **37**(10): 827-836.

Terjung, R. L., W. W. Winder, K. M. Baldwin and J. O. Holloszy (1973). "Effect of exercise on the turnover of cytochrome c in skeletal muscle." J Biol Chem **248**(21): 7404-7406.

Testoni, G., J. Duran, M. Garcia-Rocha, F. Vilaplana, A. L. Serrano, D. Sebastian, I. Lopez-Soldado, M. A. Sullivan, F. Slebe, M. Vilaseca, P. Munoz-Canoves and J. J. Guinovart (2017). "Lack of Glycogenin Causes Glycogen Accumulation and Muscle Function Impairment." Cell Metab **26**(1): 256-266 e254.

Treebak, J. T., J. B. Birk, B. F. Hansen, G. S. Olsen and J. F. Wojtaszewski (2009). "A-769662 activates AMPK beta1-containing complexes but induces glucose uptake through a PI3-kinase-dependent pathway in mouse skeletal muscle." Am J Physiol Cell Physiol **297**(4): C1041-1052.

Treebak, J. T., J. B. Birk, A. J. Rose, B. Kiens, E. A. Richter and J. F. Wojtaszewski (2007). "AS160 phosphorylation is associated with activation of alpha2beta2gamma1- but not alpha2beta2gamma3-AMPK trimeric complex in skeletal muscle during exercise in humans." Am J Physiol Endocrinol Metab **292**(3): E715-722.

Treebak, J. T., C. Pehmoller, J. M. Kristensen, R. Kjobsted, J. B. Birk, P. Schjerling, E. A. Richter, L. J. Goodyear and J. F. Wojtaszewski (2014). "Acute exercise and physiological insulin induce distinct phosphorylation signatures on TBC1D1 and TBC1D4 proteins in human skeletal muscle." J Physiol **592**(2): 351-375.

Tsou, P., B. Zheng, C. H. Hsu, A. T. Sasaki and L. C. Cantley (2011). "A fluorescent reporter of AMPK activity and cellular energy stress." Cell Metab **13**(4): 476-486.

Turcotte, L. P., E. A. Richter and B. Kiens (1992). "Increased plasma FFA uptake and oxidation during prolonged exercise in trained vs. untrained humans." Am J Physiol **262**(6 Pt 1): E791-799.

van Loon, L. J., P. L. Greenhaff, D. Constantin-Teodosiu, W. H. Saris and A. J. Wagenmakers (2001). "The effects of increasing exercise intensity on muscle fuel utilisation in humans." J Physiol **536**(Pt 1): 295-304.

Vendelbo, M. H., B. F. Clasen, J. T. Treebak, L. Moller, T. Krusenstjerna-Hafstrom, M. Madsen, T. S. Nielsen, H. Stodkilde-Jorgensen, S. B. Pedersen, J. O. Jorgensen, L. J. Goodyear, J. F. Wojtaszewski, N. Moller and N. Jessen (2012). "Insulin resistance after a 72-h fast is associated with impaired AS160 phosphorylation and accumulation of lipid and glycogen in human skeletal muscle." Am J Physiol Endocrinol Metab **302**(2): E190-200.

Vichaiwong, K., S. Purohit, D. An, T. Toyoda, N. Jessen, M. F. Hirshman and L. J. Goodyear (2010). "Contraction regulates site-specific phosphorylation of TBC1D1 in skeletal muscle." Biochem J **431**(2): 311-320.

Vissing, J. and R. G. Haller (2003). "The effect of oral sucrose on exercise tolerance in patients with McArdle's disease." N Engl J Med **349**(26): 2503-2509.

Visuttijai, K., C. Hedberg-Oldfors, C. Thomsen, E. Glamuzina, C. Kornblum, G. Tasca, A. Hernandez-Lain, J. Sandstedt, G. Dellgren, P. Roach and A. Oldfors (2020). "Glycogenin is Dispensable for Glycogen Synthesis in Human Muscle, and Glycogenin Deficiency Causes Polyglucosan Storage." J Clin Endocrinol Metab **105**(2).

Warden, S. M., C. Richardson, J. O'Donnell, Jr., D. Stapleton, B. E. Kemp and L. A. Witters (2001). "Post-translational modifications of the beta-1 subunit of AMP-activated protein kinase affect enzyme activity and cellular localization." Biochem J **354**(Pt 2): 275-283.

Wasserman, D. H. (2009). "Four grams of glucose." Am J Physiol Endocrinol Metab **296**(1): E11-21.

Wasserman, D. H., J. A. Spalding, D. B. Lacy, C. A. Colburn, R. E. Goldstein and A. D. Cherrington (1989). "Glucagon is a primary controller of hepatic glycogenolysis and gluconeogenesis during muscular work." Am J Physiol **257**(1 Pt 1): E108-117.

Wasserman, D. H., P. E. Williams, D. B. Lacy, R. E. Goldstein and A. D. Cherrington (1989). "Exercise-induced fall in insulin and hepatic carbohydrate metabolism during muscular work." Am J Physiol **256**(4 Pt 1): E500-509.

Watt, M. J., G. R. Steinberg, S. Chan, A. Garnham, B. E. Kemp and M. A. Febbraio (2004). "Beta-adrenergic stimulation of skeletal muscle HSL can be overridden by AMPK signaling." FASEB J **18**(12): 1445-1446.

Whitfield, J., S. Paglialunga, B. K. Smith, P. M. Miotto, G. Simnett, H. L. Robson, S. S. Jain, E. A. F. Herbst, E. M. Desjardins, D. J. Dyck, L. L. Spriet, G. R. Steinberg and G. P. Holloway (2017). "Ablating the protein TBC1D1 impairs contraction-induced sarcolemmal glucose transporter 4 redistribution but not insulin-mediated responses in rats." J Biol Chem **292**(40): 16653-16664.

Wijngaarden, M. A., G. C. van der Zon, K. W. van Dijk, H. Pijl and B. Guigas (2013). "Effects of prolonged fasting on AMPK signaling, gene expression, and mitochondrial respiratory chain content in skeletal muscle from lean and obese individuals." Am J Physiol Endocrinol Metab **304**(9): E1012-1021.

Winder, W. W. (2001). "Energy-sensing and signaling by AMP-activated protein kinase in skeletal muscle." J Appl Physiol (1985) **91**(3): 1017-1028.

Witters, L. A. and B. E. Kemp (1992). "Insulin activation of acetyl-CoA carboxylase accompanied by inhibition of the 5'-AMP-activated protein kinase." J Biol Chem **267**(5): 2864-2867.

Woerle, H. J., C. Meyer, J. M. Dostou, N. R. Gosmanov, N. Islam, E. Popa, S. D. Wittlin, S. L. Welle and J. E. Gerich (2003). "Pathways for glucose disposal after meal ingestion in humans." Am J Physiol Endocrinol Metab **284**(4): E716-725.

Wojtaszewski, J. F., J. B. Birk, C. Frosig, M. Holten, H. Pilegaard and F. Dela (2005). "5'AMP activated protein kinase expression in human skeletal muscle: effects of strength training and type 2 diabetes." J Physiol **564**(Pt 2): 563-573.

Wojtaszewski, J. F., S. B. Jorgensen, Y. Hellsten, D. G. Hardie and E. A. Richter (2002). "Glycogen-dependent effects of 5-aminoimidazole-4-carboxamide (AICA)-riboside on AMP-activated protein kinase and glycogen synthase activities in rat skeletal muscle." Diabetes **51**(2): 284-292.

Wojtaszewski, J. F., C. MacDonald, J. N. Nielsen, Y. Hellsten, D. G. Hardie, B. E. Kemp, B. Kiens and E. A. Richter (2003). "Regulation of 5'AMP-activated protein kinase activity and substrate utilization in exercising human skeletal muscle." Am J Physiol Endocrinol Metab **284**(4): E813-822.

Woods, A., K. Dickerson, R. Heath, S. P. Hong, M. Momcilovic, S. R. Johnstone, M. Carlson and D. Carling (2005). "Ca2+/calmodulin-dependent protein kinase kinase-beta acts upstream of AMP-activated protein kinase in mammalian cells." Cell Metab **2**(1): 21-33.

Wu, J., D. Puppala, X. Feng, M. Monetti, A. L. Lapworth and K. F. Geoghegan (2013). "Chemoproteomic analysis of intertissue and interspecies isoform diversity of AMP-activated protein kinase (AMPK)." J Biol Chem **288**(50): 35904-35912.

Wu, L., L. Zhang, B. Li, H. Jiang, Y. Duan, Z. Xie, L. Shuai, J. Li and J. Li (2018). "AMP-Activated Protein Kinase (AMPK) Regulates Energy Metabolism through Modulating Thermogenesis in Adipose Tissue." Front Physiol **9**: 122.

Xiao, B., M. J. Sanders, D. Carmena, N. J. Bright, L. F. Haire, E. Underwood, B. R. Patel, R. B. Heath, P. A. Walker, S. Hallen, F. Giordanetto, S. R. Martin, D. Carling and S. J. Gamblin (2013). "Structural basis of AMPK regulation by small molecule activators." Nat Commun **4**: 3017.

Xiao, B., M. J. Sanders, E. Underwood, R. Heath, F. V. Mayer, D. Carmena, C. Jing, P. A. Walker, J. F. Eccleston, L. F. Haire, P. Saiu, S. A. Howell, R. Aasland, S. R. Martin, D. Carling and S. J. Gamblin (2011). "Structure of mammalian AMPK and its regulation by ADP." Nature **472**(7342): 230-233.

Xirouchaki, C. E., S. P. Mangiafico, K. Bate, Z. Ruan, A. M. Huang, B. W. Tedjosiswoyo, B. Lamont, W. Pong, J. Favaloro, A. R. Blair, J. D. Zajac, J. Proietto and S. Andrikopoulos (2016). "Impaired glucose metabolism and exercise capacity with muscle-specific glycogen synthase 1 (gys1) deletion in adult mice." Mol Metab **5**(3): 221-232.

Xu, H., N. T. Frankenberg, G. D. Lamb, P. R. Gooley, D. I. Stapleton and R. M. Murphy (2016). "When phosphorylated at Thr148, the beta2-subunit of AMP-activated kinase does not associate with glycogen in skeletal muscle." Am J Physiol Cell Physiol **311**(1): C35-42.

Yan, Y., X. Gu, H. E. Xu and K. Melcher (2018). "A Highly Sensitive Non-Radioactive Activity Assay for AMP-Activated Protein Kinase (AMPK)." Methods Protoc **1**(1).

Yeo, W. K., S. J. Lessard, Z. P. Chen, A. P. Garnham, L. M. Burke, D. A. Rivas, B. E. Kemp and J. A. Hawley (2008). "Fat adaptation followed by carbohydrate restoration increases AMPK activity in skeletal muscle from trained humans." J Appl Physiol (1985) **105**(5): 1519-1526.

Yeo, W. K., S. L. McGee, A. L. Carey, C. D. Paton, A. P. Garnham, M. Hargreaves and J. A. Hawley (2010). "Acute signalling responses to intense endurance training commenced with low or normal muscle glycogen." Exp Physiol **95**(2): 351-358.

Yeo, W. K., C. D. Paton, A. P. Garnham, L. M. Burke, A. L. Carey and J. A. Hawley (2008). "Skeletal muscle adaptation and performance responses to once a day versus twice every second day endurance training regimens." J Appl Physiol (1985) **105**(5): 1462-1470.

Young, M. E., B. Leighton and G. K. Radda (1996). "Glycogen phosphorylase may be activated by AMP-kinase in skeletal muscle." Biochem Soc Trans **24**(2): 268S.

Young, M. E., G. K. Radda and B. Leighton (1996). "Activation of glycogen phosphorylase and glycogenolysis in rat skeletal muscle by AICAR--an activator of AMP-activated protein kinase." FEBS Lett **382**(1-2): 43-47.

Zhang, Y. L., H. Guo, C. S. Zhang, S. Y. Lin, Z. Yin, Y. Peng, H. Luo, Y. Shi, G. Lian, C. Zhang, M. Li, Z. Ye, J. Ye, J. Han, P. Li, J. W. Wu and S. C. Lin (2013). "AMP as a low-energy charge signal autonomously initiates assembly of AXIN-AMPK-LKB1 complex for AMPK activation." Cell Metab **18**(4): 546-555.

Zhao, H., M. Tang, M. Liu and L. Chen (2018). "Glycophagy: An emerging target in pathology." Clin Chim Acta **484**: 298-303.

Zhu, Y., M. Zhang, A. R. Kelly and A. Cheng (2014). "The carbohydrate-binding domain of overexpressed STBD1 is important for its stability and protein-protein interactions." Biosci Rep **34**(4).

Chapter 9 Appendices

9.1 List of Publications

Janzen, NR, Whitfield, J, & Hoffman, NJ (2018). Interactive Roles for AMPK and Glycogen from Cellular Energy Sensing to Exercise Metabolism. *Int J Mol Sci*, 19(11). doi:10.3390/ijms19113344

The published review article can be accessed at the link below.

https://www.mdpi.com/1422-0067/19/11/3344

Janzen NR, Whitfield J, Murray-Segal L, Kemp BE, Hawley JA, Hoffman NJ (2021). Mice with Whole-Body Disruption of AMPK-Glycogen Binding Have Increased Adiposity, Reduced Fat Oxidation and Altered Tissue Glycogen Dynamics. *Int J Mol Sci,* 22(17). doi.org/10.3390/ijms22179616.

This published original research manuscript can be accessed at the link below.

https://www.mdpi.com/1422-0067/22/17/9616/htm

Janzen NR, Whitfield J, Murray-Segal L, Kemp BE, Hawley JA, Hoffman NJ (2022). Disrupting AMPK-Glycogen Binding in Mice Increases Carbohydrate Utilization and Reduces Exercise Capacity. *Front Physiol*, 13:859246. doi:10.3389/fphys.2022.859246.

This published original research manuscript can be accessed at the link below.

https://www.frontiersin.org/articles/10.3389/fphys.2022.859246/full

9.2 The Research Portfolio Appendix

In accordance with Australian Catholic University Higher Degree Research policies for the degree of Doctor of Philosophy with publication, the following Research Portfolio has been included to summarise and clearly identify the nature and extent of the intellectual input contributed to research outputs by the Doctor of Philosophy candidate and any co-authors.

Janzen, NR, Whitfield, J, & Hoffman, NJ (2018). Interactive Roles for AMPK and Glycogen from Cellular Energy Sensing to Exercise Metabolism. *Int J Mol Sci*, 19(11). doi:10.3390/ijms19113344

Statement of Contribution: NRJ led the literature search, conceptualisation, drafting the manuscript, and editing the manuscript. JW was involved in conceptualising and editing the manuscript. NJH was involved in conceptualising and editing the manuscript and journal correspondence.

I acknowledge that my contribution to the above paper is 75 percent

[redacted]

Natalie Janzen Date: 08/09/2021

I acknowledge that my contribution to the above paper is 10 percent

[redacted]

Jamie Whitfield Date: 05/09/2021

I acknowledge that my contribution to the above paper is 15 percent

[redacted]

Nolan Hoffman Date: 08/09/2021

Janzen NR, Whitfield J, Murray-Segal L, Kemp BE, Hawley JA, Hoffman NJ (2021). Mice with Whole-Body Disruption of AMPK-Glycogen Binding Have Increased Adiposity, Reduced Fat Oxidation and Altered Tissue Glycogen Dynamics. *Int J Mol Sci,* 22(17). doi.org/10.3390/ijms22179616.

Statement of Contribution: NRJ was involved in the study conceptualisation and led the experimental design, acquisition of ethics approval, colony management, data collection, data analysis, data interpretation, drafting the manuscript, and editing the manuscript. JW was involved in conceptualisation, experimental design, data collection, data analysis, data interpretation, and editing the manuscript. LM-S was involved in mouse colony management and editing the manuscript. BEK was involved in conceptualisation, experimental design, data interpretation, and editing the manuscript. JAH was involved in conceptualisation, experimental design, data interpretation, and editing the manuscript. NJH was involved in conceptualisation, experimental design, acquisition of ethics approval, mouse colony management, data collection, data analysis, data interpretation, editing the manuscript, and journal correspondence.

I acknowledge that my contribution to the above paper is 60 percent

[redacted]

Natalie Janzen Date: 08/09/2021

I acknowledge that my contribution to the above paper is 10 percent

[redacted]

Jamie Whitfield Date: 05/09/2021

I acknowledge that my contribution to the above paper is 5 percent

[redacted]

Lisa Murray Segal Date: 02/09/2021

I acknowledge that my contribution to the above paper is 5 percent

[redacted]

Bruce Kemp Date: 06/09/2021

I acknowledge that my contribution to the above paper is 5 percent

[redacted]

John Hawley Date: 06/09/2021

I acknowledge that my contribution to the above paper is 15 percent

[redacted]

Nolan Hoffman Date: 08/09/2021

Janzen NR, Whitfield J, Murray-Segal L, Kemp BE, Hawley JA, Hoffman NJ (2022). Disrupting AMPK-Glycogen Binding in Mice Increases Carbohydrate Utilization and Reduces Exercise Capacity. *Front Physiol*, 13:859246. doi:10.3389/fphys.2022.859246.

Statement of Contribution: NRJ was involved in the study conceptualisation and led the experimental design, acquisition of ethics approval, mouse colony management, data collection, data analysis, data interpretation, drafting the manuscript, and editing the manuscript. JW was involved in conceptualisation, experimental design, data collection, data analysis, data interpretation, and editing the manuscript. LM-S was involved in mouse colony management and editing the manuscript. BEK was involved in conceptualisation, experimental design, data interpretation, and editing the manuscript. JAH was involved in conceptualisation, experimental design, data interpretation, and editing the manuscript. NJH was involved in conceptualisation, experimental design, acquisition of ethics approval, mouse colony management, data collection, data analysis, data interpretation, and editing the manuscript.

I acknowledge that my contribution to the above paper is 60 percent

[redacted]

Natalie Janzen Date: 08/09/2021

I acknowledge that my contribution to the above paper is 10 percent

[redacted]

Jamie Whitfield Date: 05/09/2021

I acknowledge that my contribution to the above paper is 5 percent

[redacted]

Lisa Murray Segal Date: 02/09/2021

I acknowledge that my contribution to the above paper is 5 percent

[redacted]

Bruce Kemp Date: 06/09/2021

I acknowledge that my contribution to the above paper is 5 percent

[redacted]

John Hawley Date: 06/09/2021

I acknowledge that my contribution to the above paper is 15 percent

[redacted]

Nolan Hoffman Date: 08/09/2021

END OF DOCUMENT